Quantifying the Effects of Uncertainty in Building Simulation

Iain Alexander Macdonald B.Sc., M.Sc.

A thesis submitted for the
Degree of Doctor of Philosophy

Department of Mechanical Engineering
University of Strathclyde

July 2002

In memory of Simon James O'Riordan

Acknowledgements

Foremost I would like to thank Professor Joe Clarke for giving me the opportunity and guidance to complete this work. I am also indebted to my collegues in the Energy Systems Research Unit (especially: Jon Hand, Nick Kelly, Lori McElroy and Paul Strachan) for their advice.

I also wish to thank the University of Strathclyde and the UK Building Research Establishment for providing financial assistance during the early years of this work.

My family deserves thanks for the years of studentship that they have patiently watched me progress through. It all started by rearranging equations - thanks dad!

Finally, thank you Karen for your support and understanding.

Abstract

Uncertainty affects all aspects of building simulation: from the development of algorithms, through the implementation of software, to the use of the resulting systems. This work has focused on the problem of quantifying the effect of uncertainty on the predictions made by simulation tools. Two approaches to quantifying this effect are pursued in this thesis: external and internal methods.

The external approach treats the simulation engine as a 'black box' and alters only the input model. Methods within this approach require multiple simulations of systematically altered models and the subsequent analysis of the differences in the predictions in order to draw conclusions on the effect of uncertainty. Three methods were identified for use in the present work: differential, factorial and Monte Carlo. The differential method alters one parameter at a time to quantify the effect of each parameter and requires $2N+1$ simulations for N uncertain parameters. The factorial method alters groups of parameters simultaneously to determine interactions between effects and requires 2^N simulations. The Monte Carlo method alters all parameters simultaneously to quantify the overall effect of uncertainty. The number of simulations required for the Monte Carlo method is independent of the number of parameters and is typically 80. Each of these methods require a significant number of simulations. To quantify the individual contributions, the interactions between these contributions and the effects overall would require the use of all three methods.

The internal approach represents parameters as a function of uncertainty and alters the underlying algorithms of the simulation tool so that uncertainty is included at all computational stages. Methods within this approach require only a single simulation to quantify the individual and overall effects. Three methods were studied: interval, fuzzy and affine arithmetic. It was found when forming the energy balance equation set, correlations between the source of uncertainty and the equation terms should be maintained. This is necessary so that uncertain parameters have the same value when used in different terms in the equation set. For example, the uncertainty in

conduction into and out of a homogeneous control volume will be correlated because the uncertainty is for the materials properties. Only affine arithmetic accounts for these correlations. To achieve this, uncertainty considerations are embodied within the underlying conservation equations using a first order polynomial representation of uncertainty. This polynomial is formed from the mean value of the parameter with the individual uncertainties defined as separate terms. Each uncertainty term is represented by an interval number. The resulting predictions (state variables) are likewise represented by first order polynomials. The measure of individual effects are the coefficients of these polynomials and the overall effect is the sum of the coefficients. Specific performance instances can then be created in a post-simulation analysis by specifying an exact value for each of the uncertainty terms.

To test the applicability of the two approaches the theory was implemented within the ESP-r system, with the internal approach applied to ESP-r's core thermal model. The advantages and disadvantages of each approach are examined. It is shown that the results of a single internal simulation compare well with the outcomes from the external methods. Although the affine approach does not always produce a converged calculation of the effects of uncertainty, the application represents a novel and integrated approach to the assessment of uncertainty in building simulation. Reasons for the failure are given and approaches to overcoming these are described.

To support the definition of uncertainty at the time of model creation, the uncertainty in key parameters has been quantified. These parameters comprise thermophysical properties, casual heat gains and infiltration rates.

The impact of uncertainty assessment on the design process is explored via three case studies. These examine the use of simulation at the early and detailed design stages and when used to compare design variants. The implications of uncertainty in each case are elaborated.

Finally, recommendations for further research are made. These cover the application of the internal approach to other technical domains, for example air flow modelling, and the quantification of uncertainty in relation to additional parameters such as occupant behaviour.

Contents

List of Symbols

Lower case

a	minimum value
b	maximum value
h	height
k	scale parameter, or thermal conductivity
l	length
m	mass, median
n	sample size
q	heat flux
s	standard deviation of a sample
t	time, or a particular time step
u	% moisture content (kg moisture/kg dry material)
w	width, or moisture content (mass of moisture per unit volume of dry material)
x	uncertain value of parameter, or distance between nodes
$\tilde{x}$	exact value of parameter
$\hat{x}$	an affine number
$\underline{x}$	lowest bounding value of range
$\overline{x}$	highest bounding value of range, or sample average
y	uncertain value of parameter
$\tilde{y}$	exact value of parameter

Upper case

A	area
C	specific heat capacity
N	total number of uncertain parameters
P	probability function
Q	heat energy
R	total number of simulations required
T	total number of time steps
V	volume
W	work
Z	system response for simulation i, *except* differential analysis where the system response is for uncertain parameter i.
$\bar{Z}$	average system response

Subscripts

i	a specific uncertain parameter
$+$	a parameter's on value
$-$	a parameter's off value

Superscripts

p	level of fractionisation in fractional factorial designs

Greek

β	regression coefficient or bound on error in parameter's value
δ	difference
Δ	vector of parameter variations
ϵ	absolute error term or error token in an affine number
ϵ_r	relative error term
μ	population mean
μ'	transformed population mean
Φ	uncertainty coefficient, or probability distribution function
ϕ	uncertainty coefficient, dimensionless
ψ	% moisture content (m^3 moisture/m^3 dry material)
ρ	density
σ	population standard deviation
σ'	transformed population standard deviation
θ	temperature
ξ	efficiency

Chapter 1

Introduction

Uncertainty affects all aspects of simulation. To quantify these effects a well-founded physically based model is needed. Assessing the effects of uncertainties aids understanding of building performance and, therefore, leads to effective decision making.

The built environment comprises a complex set of interactions of heat, mass and momentum transfers. These transfers interact dynamically under the action of occupant and system control. The problem of representing such time varying interactions in a manner suitable for prediction and evaluation of alternate designs has been addressed by many researchers. The work to date, however, has concentrated on the problem of modelling resolution and integration; in the belief that this will improve accuracy and applicability respectively. However, the more complex mathematical models require a greater knowledge of the systems being analysed and an increased quantity of data to describe the different aspects of the modelled system.

For example, the integration of CFD within building simulation requires additional data to define the boundary conditions of the flow domain (thermal, momentum *etc*), the parameters of the equations to be solved (source terms, turbulence model parameters *etc*) and the methods of solution. These aspects increase the burden on the user: a deeper theoretical knowledge is required, more data is necessary and more

results have to be analysed and confirmed.

Although uncertainty and sensitivity analyses have been applied in some validation projects [Jensen 1994, Lomas *et al* 1997], in practice uncertainty is not considered. The limited application of uncertainty analysis would indicate that there are significant barriers to overcome.

Traditionally uncertainty in the performance of a building has been reduced by oversizing the installed heating, cooling or ventilating plant. This resulted in sets of data and calculation methods with *inherent* safety factors. For example, the declared values of thermophysical data necessary for simulation work are to be quoted for the 90% fractile [CEN 1998] (*i.e.* 90% of possible values are less than or equal to this value). This means that tabulated data for conductivity will be artificially high. In addition, calculation methods assume *worst case* scenarios for plant sizing, *e.g.* no occupants, lighting or solar gains in winter for heating plant and full occupant, lighting and solar gains in summer for cooling plant. It has been estimated that the use of such safety factors has resulted in plant sizes being typically double and in some cases treble their necessary size [Parand 1994]. This is clearly an undesirable situation as large plant incurs increased capital and running costs, can adversely affect space utilisation and gives rise to unnecessary emissions of greenhouse gasses. Through the assessment of uncertainties, the natural variation in data is accounted for; thus, the mean value and a measure of variation should be used, allowing more appropriate designs.

1.1 Development of integrated building simulation

The simulation community has, over the last 30 years, attempted to combine the various domain calculations in an attempt to better represent the behaviour of buildings and thereby to produce better designs. As can be seen in figure 1.1, simulation tools have evolved in terms of their detail and applicability. Paradoxically, this increased flexibility has resulted in greater uncertainty in the use of these tools: collating the required data and in understanding the multi-variate results produced. In general terms

1^{st} Generation (1960's and early 1970's)	Handbook oriented Simplified Piecemeal	Indicative Applications limited Difficult to use
2^{nd} Generation (1970's)	Dynamics important Less simplified Still piecemeal	
3^{rd} Generation (1980's)	Field problem approach Numerical methods Integrated energy sub-systems Heat and mass transfer considered Better user interface Partial CABD integration	
4^{th} Generation (1990's)	CABD integration Advanced numerical methods Intelligent Knowledge based Advanced software engineering	Predictive Generalised Easy to use

Figure 1.1: The evolution of building energy simulation tools [Clarke and Maver 1991].

the problem of designing well engineered buildings reduces to ensuring an acceptable indoor environment at an acceptable life cycle cost. This requirement necessitated the integration of modelling techniques (3^{rd} generation tools) to address the complexities of real schemes.

Such detailed models require a considerable amount of detailed information to describe a building to an adequate level of detail. Consider the requirements of simplified and detailed design tools: the LT method [Baker and Steemers 1994], a spreadsheet based 1^{st} generation[1] tool, and the simulation system ESP-r [ESRU 2001], a 3^{rd} generation tool. A typical model in LT requires about 20 data items covering building location, construction, floor and glazing areas. A typical multi-zone model in ESP-r requires over 4000 data items for the geometry, construction and operation descriptions alone! Many of these items are held in system databases from which the user must make a selection. Typically, varying only a few of these parameters will have a significant effect on the predictions made by the system [Saltelli *et al* 2000]. This leaves the users of these systems in a difficult position: the predictions are only sensitive to a few of the input parameters (which ones?) and in the absence of this

[1]The LT method has been classed a 1^{st} generation tool due to its methodology despite the fact that it has been developed throughout the 1990s.

information they have to check all parameters or use their experience to target the correct ones.

A further effect of the developments depicted in figure 1.1 is that 3^{rd} and 4^{th} generation simulation tools are generally used during the later design stages where the necessary information on the building's form, construction and operation are known. Typically the efficacy of simulation tools is less at this late stage because the design decisions with the largest impact on performance occur during the early design stages [Aho 1995, Holm 1993]. As depicted in figure 1.2, the design process progresses from whole building considerations towards specific detailing. This results in the decisions with the largest effect on the performance being made at the beginning of the design process. However, simulation tools require knowledge about the details of surface finishes, orientation *etc.* from which the whole model is created.

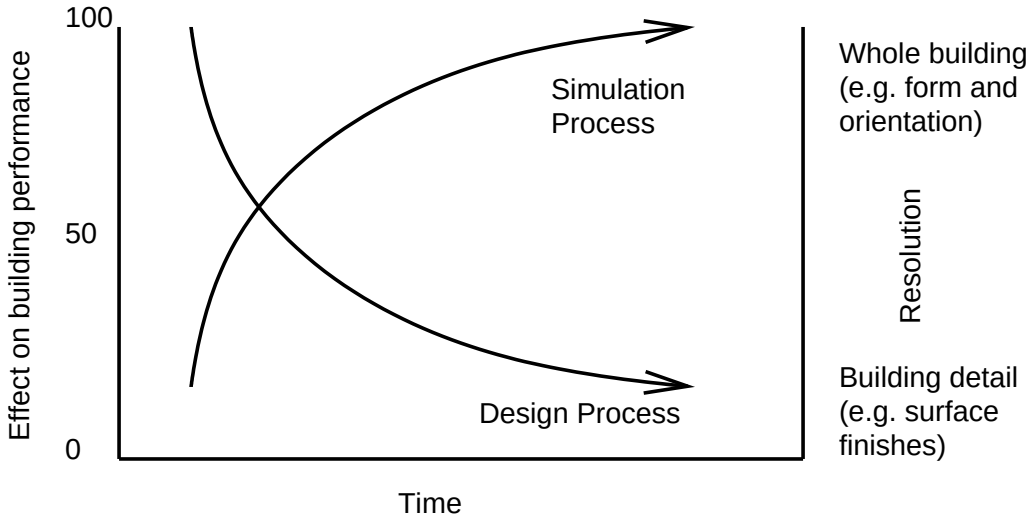

Figure 1.2: Design and simulation processes.

This means that for simulation to be successfully employed at the early design stage (to maximise the benefit) knowledge of building details are needed, which in most cases is unavailable. For the practitioner to progress they must make assumptions about the missing data. These assumptions introduce uncertainty into the model and a method of addressing and quantifying this uncertainty is required. As the design progresses, the uncertainty will generally decrease (as design decisions are made concerning the uncertain data) although it will be impossible to reduce this

uncertainty to zero.

Through assessing the uncertainty in simulation outputs it is possible to identify those parameters that most strongly impact on performance, allowing the appropriate concentration of design effort. Coupled with this, the overall uncertainty in the predictions may also be assessed allowing a design to be refined until the uncertainty reduces to an acceptable level.

Currently there is no building simulation system which allows more than an *ad hoc* approach to the quantification of the effects of uncertainty [CIBSE 1999], despite methods existing in theory for providing a structure for a detailed uncertainty or sensitivity analysis.

1.2 Uncertainty versus sensitivity analysis

A subtle distinction exists between uncertainty and sensitivity analyses. The aim of a sensitivity analysis is to discover the (typically few) input parameters to which the measured output of a model is sensitive, *i.e.* a change in a design parameter (say 1% less infiltration) would result in a relatively larger change in a performance metric (say 10% less heating energy required). A crucial aspect of a sensitivity analysis is that it is unnecessary to quantify the likely variation in the model's parameters. Conversely, in an uncertainty analysis the variation in the input parameters is critical to the analysis, as the aim is to discover the likely variation in the output due to the actual variations in the input. A side effect of this is that the model may be sensitive to a specific parameter but, if the parameter is well known, it is not a critical parameter in an uncertainty analysis.

This work is concerned with calculating the effects of uncertainty on predictions under realistic parameter variations. Therefore the identification of sensitive parameters is not necessary; they may be well known and therefore will not contribute significantly to the overall uncertainty in the predictions. The real variation in input parameters is sought so that the consequences of these uncertainties may be quantified. Coupled with this, the parameters which have the largest contribution to the

overall uncertainty in the predictions are also identified.

1.3 Effects of uncertainties

To demonstrate the effects of uncertainties on building performance, and hence design decisions, consider the single zone office model of figure 1.3.

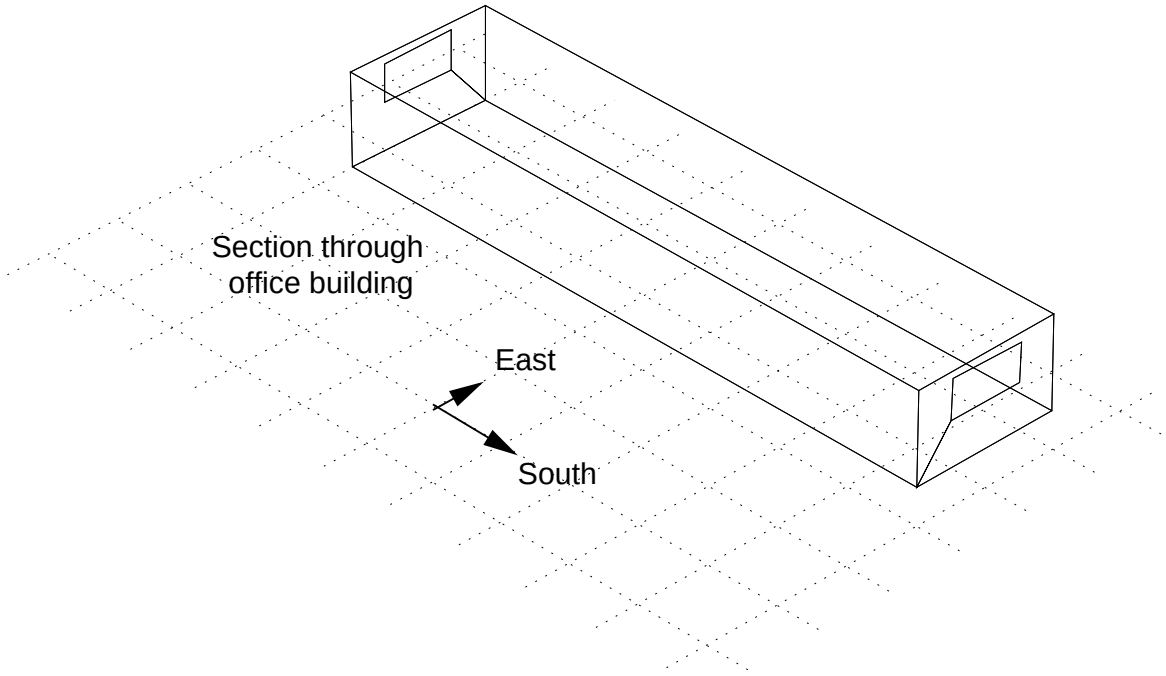

Figure 1.3: Simple office model.

The office has typical construction materials and occupancy gains for this class of building. Consider the following two uncertainty scenarios:

1. The casual gains for the IT equipment were assumed to be $1000W$ ($\approx 15W/m^2$). What if new energy efficient equipment were used with a casual gain of $750W$ ($\approx 11W/m^2$)?

2. The temperature of the ventilation supply to the office is uncertain ($\pm 1°C$). What effect will this have on air quality?

These scenarios have been selected to demonstrate the variety of uncertainty sources and assessment techniques which exist to quantify building performance. Of

note is that an uncertainty can be the magnitude of a parameter (as in these examples) or the location of an object (*e.g.* windows or air supply grills) or the timing of an event (*e.g.* occupancy schedules). The effect of an uncertainty can be assessed by aggregate metrics (*e.g.* energy consumption), temporal measures (*e.g.* number of overheating hours) or spatial measures (*e.g.* radiant temperature variation through a space).

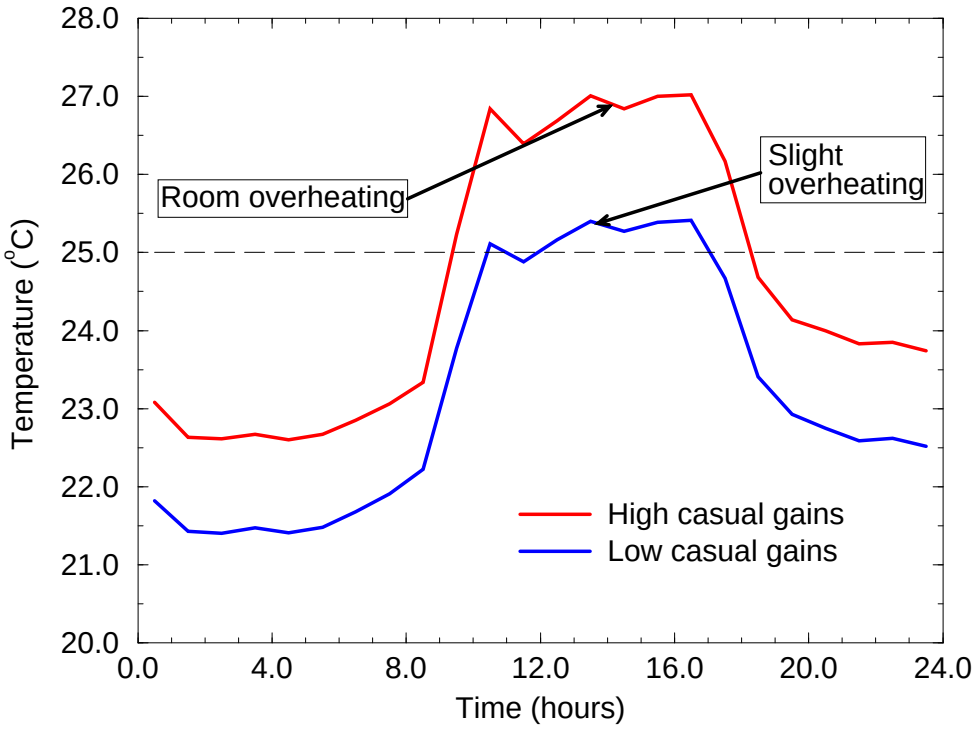

Figure 1.4: Air temperature profile in the simple office.

The air temperature profile of the office for both casual gain scenarios is shown in figure 1.4 for a typical summer day. As can be seen, with the higher gains from the computer equipment the office will overheat ($T > 25°C$), but with the lower gain the overheating would be marginal. Over the summer period the office would overheat for 47% of occupied hours for the higher gain while, for the lower gain, the office would overheat for 11% of the occupied hours. Clearly, the assumption about the casual gains would have a large impact as in the higher gain case a cooling provision would be required to address the overheating problem. This use of cooling plant would require ductwork and space within the building, and increase the capital and running

costs and emissions. For the lower gain case the slight overheating could perhaps be accepted so that there would be no requirement for cooling, thus the above impacts would be avoided.

For the second scenario the intra-zone air flow has to be determined. This requires the use of computational fluid dynamics (CFD) to permit the effectiveness of the ventilation strategy to be assessed in terms of the distribution of the local mean age (LMA) of air. The LMA quantifies the average time taken for the supply air to reach a specific location with respect to the average time air takes to travel from the inlet to the extract in a zone. Thus, if the mean age of air is less than one, then the air in this region is fresh (*i.e.* has entered the domain recently); where greater than one the air is older than average.

Figure 1.5 displays the LMA of air in the office for both scenarios. The upper plot is for the warmest possible air supply temperature where the air flows along the ceiling and circulates back to the low level extract. The lower plot is for a cooler supply temperature ($2°C$ cooler) and shows the supply air flow detaching from the ceiling and falling to the floor within the first half of the room. Two circulation regions are also evident: one of fresh air and one of older air. This example shows the spatial effects of an uncertainty and the possibility that the ventilation system would fail to provide fresh air to the whole office area, thus affecting the comfort of the occupants.

These two examples highlight but two of the myriad uncertainty sources encountered in building energy modelling:

Scenario 1 The magnitude of the casual gain was uncertain. This type of uncertainty applies to many aspects of building energy modelling, *e.g.* material thermophysical properties and building dimensions. The effect of this uncertainty was addressed by examining the maximum temperature in the office. This is a typical analysis metric, others include maximum heating load, total energy consumption and hours above a certain temperature.

Scenario 2 In this case the supply temperature of the air was uncertain and this

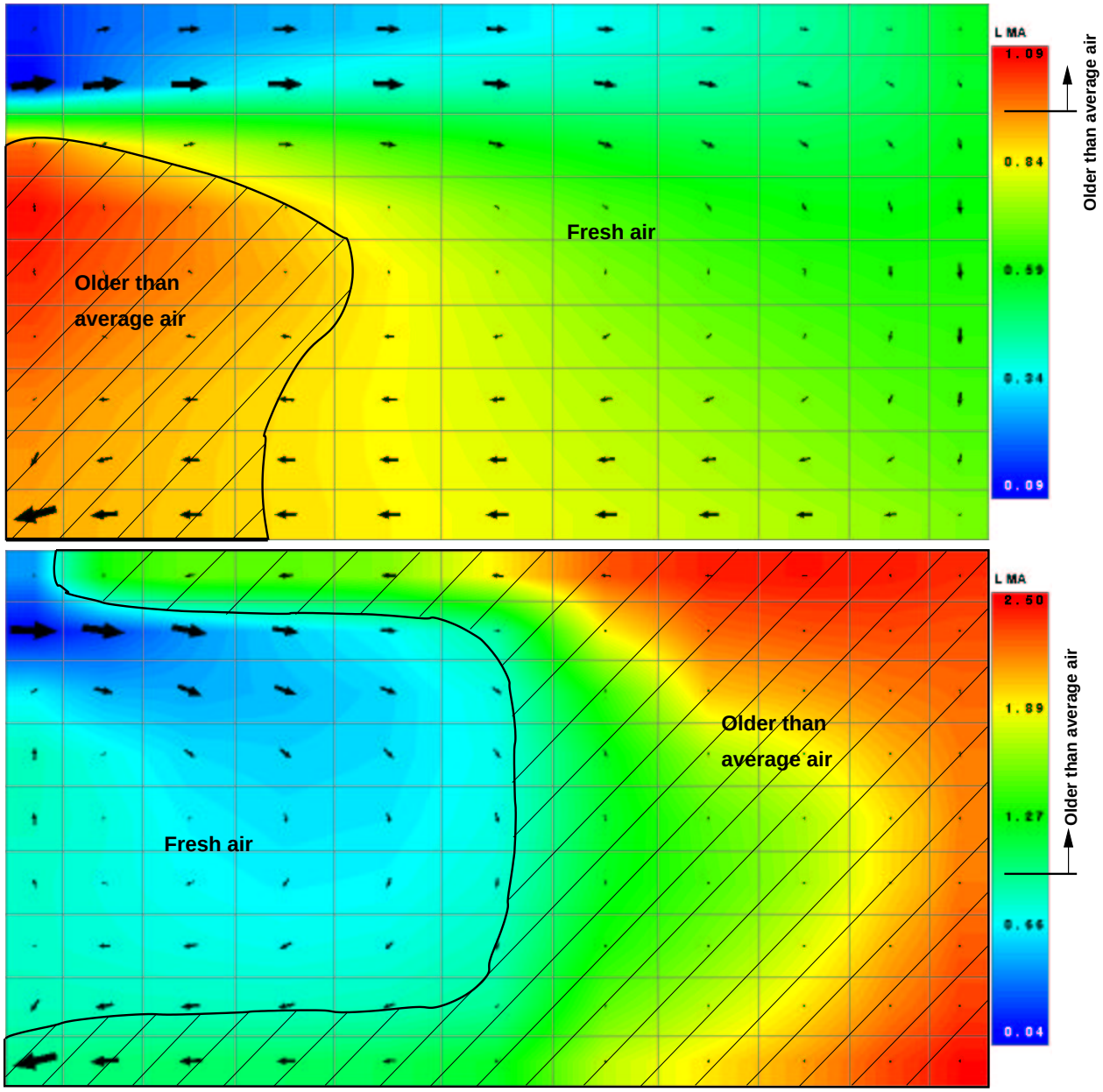

Figure 1.5: Air distribution in the simple office.

affected the spatial distribution of the fresh air. The assessment of the effects of this uncertainty were examined spatially. Other spatial uncertainties include the position of windows in the building and the location of ventilation grills.

These two examples address only the problem of individual uncertainties where a parameter may adopt one value or the other. In practice uncertain parameters may take on any value within a range defined by a probability distribution. The

description of uncertainty in all of the model's parameters would then be required and an assessment of the interactions between these uncertain parameters undertaken.

1.4 Sources of uncertainty

There are many sources of uncertainty and it is important to evaluate the risks that result from these uncertainties. This importance is a direct reflection of the relevance of assessing uncertainty in a physical experiment. Without quantifying the overall error in the predictions, the practitioner has little idea of the accuracy of the result.

Uncertainty analysis is an important experimental technique and can be used in simulation to address the following issues.

- Model realism: How well (and to what resolution) does the model represent reality?
- Input parameters: What values should be used in the absence of measured data?
- Stochastic processes: To what extent do the assumptions made regarding future weather, occupancy and operational factors affect the predictions?
- Simulation program capabilities: What uncertainties are associated with the particular choice of algorithms for the various heat and mass transfer processes?
- Design variations: What will be the effect of changing one aspect of the design?

Being aware of the inherent uncertainties in the modelling techniques is crucial but methods must also be available to evaluate their effects.

1.5 Objectives

The need then is to quantify the uncertainty in the outputs from a simulation program from knowledge of the uncertainties associated with the inputs. To achieve this, suitable methods have to be identified and implemented. This work aims to:

1. Review uncertainty assessment methods.

2. Identify sources of uncertainty as they impact upon building simulation.

3. Identify suitable probability distributions to describe uncertain parameters.

4. Implement quantitative methods for analysing the effect on simulation outputs in ESP-r.

These aims, if realised, will enable simulation users to:

1. Quantify overall uncertainty in model predictions, enabling

   (a) risk based decision making, and

   (b) significance testing between design options.

2. Quantify the uncertainty due to individual parameters for the specific building being analysed, thus enabling

   (a) guided quality assurance (QA) procedures to be adopted, *i.e.* QA can focus upon the parameters in the model with the largest contribution to the output uncertainty, and

   (b) uncertainty based model development, *i.e.* modelling resolution choices can be justified on the basis of reducing the overall uncertainty in predictions.

Such additions to the modelling environment are elaborated in this thesis.

1.6 Summary

Uncertainty impinges on all aspects of building design and particularly in building performance simulation. The two examples given in section 1.3 elaborate this by showing the effects of imperfect knowledge on the output from simulation. However, the examples only show the effect of a single uncertain parameter. How are the effects of more than one uncertain parameter assessed and what are the uncertain parameters?

It should be clear that the quantification of uncertainty is necessary for effective use of building simulation. Furthermore, for the effects to be quantified, and as

uncertainty is present in all aspects of simulation work, the uncertainties cannot be addressed in an *ad hoc* manner.

Before techniques for uncertainty assessment can be applied, the myriad sources of uncertainty need to be identified. This is the subject matter of the next chapter.

References

Aho I, *Transferring Computer Based Energy Analysis Tools to Practice: The Whys and Whats of Simplification*, IBPSA Conference, Building Simulation '95, Madison, Wisconsin USA, pp 493-499, 1995

Baker N V, Steemers K, *The LT Method 2.0*, Cambridge Architectural Research Ltd, 1994

CEN, *Thermal insulation - Building materials and products - Determination of declared and design thermal values*, Final draft prEN ISO 10456, 1998

Chartered Institute of Building Service Engineers, *CIBSE Applications Manual AM11: Building Energy and Environmental Modelling*, London, 1999

Clarke J A, Maver T W, *Advanced Design Tools for Energy Conscious Building Design: Development and Dissemination* Building and Environment, Vol. 26, No 1, 1991

Energy Systems Research Unit, *http://www.esru.strath.ac.uk*, 2001

Holm D, *Building Thermal Analyses: What the Industry Needs: The Architect's Perspective*, Building and Environment, Vol. 28, No 4, 1993

Jensen S O (Editor) *Validation of Building Energy Simulation Programs*, final report, PASSYS project EUR 15115 EN (European Commission), 1994

Lomas K J, Eppel H, Martin C J, Bloomfield D P, *Empirical Validation of Energy Simulation Programs*, Energy and Buildings, Vol 26, 1997

Parand F, *Conversation during visit to Building Research Establishment UK*, 1994

Saltelli A, Chan K, Scott E M, *Sensitivity Analysis*, J Wiley and Sons, 2000

Chapter 2

Modelling buildings

The ESP-r system, the data required for simulation and the mathematical models employed are described. This information is the prerequisite foundation for the work presented in subsequent chapters.

The ESP-r system has been used as the mechanism whereby the uncertainty quantification techniques presented in chapter 3 can be implemented, applied and assessed. The system allows an integrated assessment of building performance and is well described elsewhere [ESRU 2001]. There are two aspects of ESP-r which are germane to the current research:

1. the data model, and
2. the mathematical model.

The purpose of the ESP-r data model is to describe, in a method suitable for simulation, the target system. For example, the target could be a whole building, a part of a building, the HVAC system, the ventilation system, any aggregate of these entities and so on. In practice, the usual approach is to model the different subsystems individually and to then link them and simulate the resulting system in an integrated manner. A particular feature of ESP-r is that few elements of the simulation model are pre-determined. This enables the system to model problems

of arbitrary complexity from traditional buildings to prestige buildings with facade integrated hybrid photovoltaic panels including ventilation pre-heat. In relation to the present research ESP-r's explicit approach permits uncertainty considerations to be applied to all possible design parameters. The data model required to describe such systems is necessarily complex. For example:

- building fabric is described in terms of orientation, area, material thickness, density, conductivity, specific heat capacity, vapour diffusivity, surface short-wave absorptivity and longwave emissivity to enable calculation of heat and moisture transfers,
- electrical networks are described in terms of loads, supplies, generating components and conductors to enable power flow calculations and embedded renewable energy studies, and
- occupant behaviour is described in terms of sensible and latent loads to enable the quantification of heat and moisture gains to a space in support of comfort and indoor air quality studies.

Entities within the data model are subject to varying degrees of uncertainty. Therefore the purpose of describing the ESP-r data model is to elucidate the sources of uncertainty in building simulation.

Section 2.2 of this chapter describes the algorithms employed by ESP-r to solve the described systems. These algorithms use the information provided in the data model to produce meaningful predictions of building performance, given suitable boundary conditions, *e.g.* a climate data set. As will be presented in chapter 3, uncertainty quantification methods can be externally wrapped around these algorithms or integrated within them.

2.1 ESP-r data model

The ESP-r data model exhibits a close relationship between building physics and built reality, *i.e.* the data required by ESP-r are physically measured values (or derived

from measurements) and these data items are used in fundamental physical models of the transport systems in buildings (thermal, moisture, electrical *etc*). As a result, the data model of ESP-r can be viewed as a suitable structure on which to base sources of uncertainty.

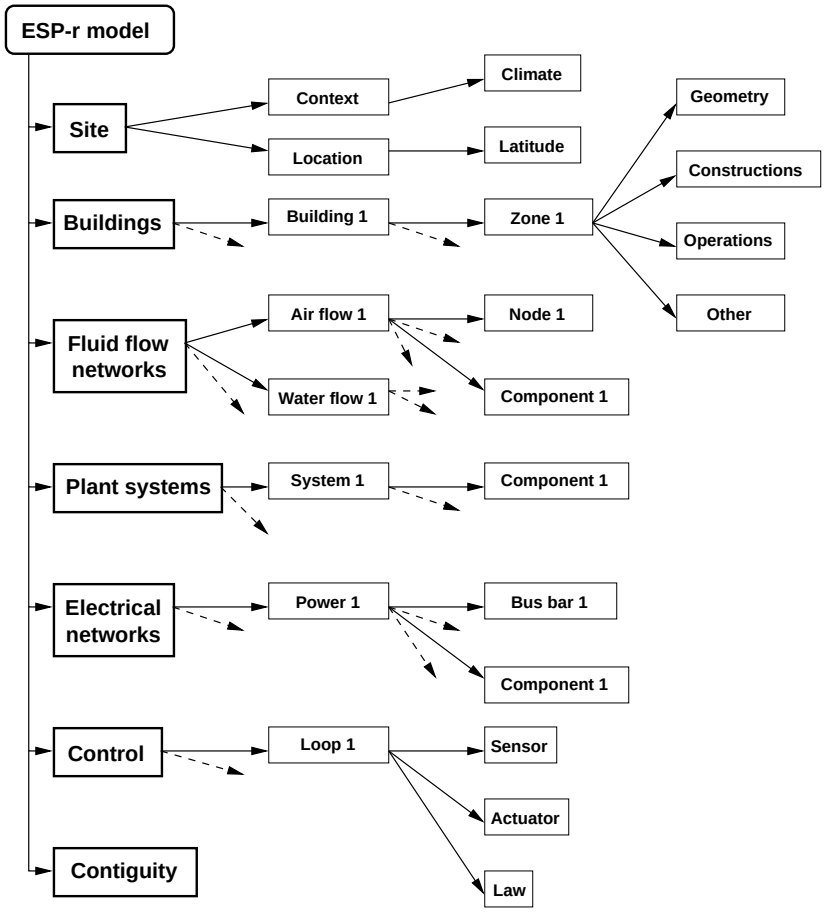

Figure 2.1: ESP-r data model (synopsis).

Figure 2.1 provides a synopsis of the ESP-r data model decomposition. The solid lines represent decompositions of higher level entities: the model has a site, which has a location, which has a latitude and so on. The broken lines represent repetitive aspects of the model: the building's HVAC system may have several constituent parts, which in turn have sub-assemblies. The decomposition does not show an entity's individual data items. These are elaborated in the following sections; it is to these items that uncertainties may be attached.

Uncertainties are described in general terms for the three principle design stages:

outline, scheme and detailed as described in the RIBA plan of work [RIBA 1995]. The three design stages have the following characteristics:

Outline. This stage is extremely time constrained and has the aim of illustrating building form and operation and an indication of building and running costs. Uncertainty is generally large at this stage due to the effectively unconstrained options available.

Scheme. The external form and fabric of the building will be addressed at this stage. Internal space usage will also be organised. Typically uncertainties will be smaller but still significant.

Detailed. The finishes to spaces and equipment to be installed will be specified at this stage. Building form, fabric and function are all well known and operation of control systems can be explored. Although uncertainties are minimal they will still exist as exact building occupation and use is still hypothetical.

The post occupancy operation of a building is generally when uncertainties are least, as built form and fabric can be examined and building use measured. The uncertainties described in the following sections have been classified on a three point scale for each stage described above: well known, uncertain, highly uncertain.

2.1.1 Site

The location of the building is expressed in terms of latitude and longitude as well as an exposure index which is used to determine external view factors for longwave radiation exchanges. The context descriptor is used to describe relevant parameters such as climate patterns and ground albedo.

Uncertainty descriptors are presented in table 2.1. Site parameters are generally well known throughout the design process. However, planned landscaping can affect the ground albedo and site micro climate. Also future operation of the building cannot ignore the possibility of neighbouring buildings being constructed or existing buildings being demolished. These events will effect the site exposure index, micro climate and ground albedo.

Table 2.1: Uncertainty descriptors for site parameters.

Parameter	Outline	Scheme	Detailed
Latitude, longitude	Well known	Well known	Well known
Exposure index	Well known	Well known	Well known
Climate parameters	Uncertain	Uncertain	Uncertain
Ground albedo	Uncertain	Uncertain	Well known

2.1.2 Building

The building model employed by ESP-r is zone based, where a zone is defined as a bounded volume of fluid at a uniform temperature. A zone has geometry to describe the areas of bounding surfaces and the volume of the contained air. Real physical spaces may comprise several zones.

The surfaces which define a zone require constructional information (number of layers and the thickness, conductivity, density, absorptivity, emissivity, vapour resistivity of each) and a boundary condition, which could be another zone, the external climate or a prescribed condition. A surface is defined by a set of vertices from which the area and orientation of the surface may be determined.

Each zone has an associated operations schedule. This describes the internal heat gains and design air change requirements. The heat gains (corresponding to people, lighting and IT equipment) are expressed as time varying sensible and latent heat inputs, with the sensible component characterised by convective and radiant fractions. The design air change rate can be subjected to control action to mimic window opening or other effects of occupants.

Additional and optional definitions can be applied to a zone. For example, a facade or window shading device may be added, surface convection coefficients (time varying) prescribed or a CFD domain attached to enable the simulation of air movement and indoor air quality. Furthermore, the default unidirectional heat conduction model may be elevated to full 3D where, for example, thermal bridges are present. Finally the moisture transfers between the zone air and surfaces and through constructions can be modelled.

Each of these additional definitions require a set of parameters to support the cor-

responding mathematical model. For example, in the case of 3D heat conduction and CFD additional discretisation information is required; while for moisture modelling the hygrothermal properties of the constructional materials must be specified.

Table 2.2 details the uncertainty descriptors for each category of data required in the building model. The general trend is that as the design progresses through to building operation the uncertainty in parameters decreases. This is because as the design progresses more details are specified and uncertainty in geometry and surface attribution will therefore decrease. In the case of casual gains the initial uncertainties will be smaller as zones are generally defined by their usage and hence an indication of likely heat gains will be known from the early design stages. The zone air change rate will remain uncertain as initially design values will be prescribed and when operational the build quality and occupant interactions will effect air flows in the building. The term detailed modelling encompasses the use of CFD domains, multi-dimensional heat flow and moisture flow *etc*, which all require suitably well defined building models before they can be applied. For example, for CFD and multi-dimensional heat flow the geometry of the zone (surface areas, window locations *etc*) must be well defined before meaningful output can be produced.

Table 2.2: Uncertainty descriptors for building parameters.

Parameter	Outline	Scheme	Detailed
Orientation	Highly uncertain	Uncertain	Well known
Zone volume	Highly uncertain	Uncertain	Well known
Surface areas	Highly uncertain	Uncertain	Well known
Construction materials	Highly uncertain	Uncertain	Well known
Casual gains	Uncertain	Uncertain	Well known
Zone air change rate	Uncertain	Uncertain	Uncertain
Shading devices	Highly uncertain	Uncertain	Well known
Detailed modelling	Highly uncertain	Uncertain	Well known

2.1.3 Fluid flow

A fluid flow network consists of a set of pressure points (nodes) connected by components which either resist or induce flow. Boundary nodes are either set to a fixed pressure or are assigned a wind induced pressure at simulation time. Internal nodes

are solved to obtain their pressure as a function of their time-evolving temperature and network boundary pressures. The output from this network can be used in the building model described in the previous subsection in place of the imposed air change rates.

The components in a fluid flow network are described by parameters that depend on their type. For example, a crack is specified by its width and length as required by a related empirical flow equation. A fan, on the other hand, might require the coefficients of an empirical quadratic equation that likewise defines its flow characteristics.

Finally, the connection of nodes via components requires the height difference between each node and the component to be known so that the stack effect can be included in the simulation.

Uncertainty descriptors are presented in table 2.3. Recent work has characterised the uncertainty in pressure coefficients [De Wit 2001], which are used to determine the wind induced pressures of boundary nodes. These coefficients will be highly uncertain while the building form has not been finalised, *i.e.* at the earlier design stages. The temperature of internal nodes will likewise be uncertain until the internal environment is well described. The main source of uncertainty, though, for flow networks is in describing all flow paths. Uncertainty will persist in this area as build quality will affect the ability of air to flow through the building structure. These unintended air flow paths present two problems to the practitioner: they must be identified and then characterised.

Table 2.3: Uncertainty descriptors for flow network parameters.

Parameter	Outline	Scheme	Detailed
Boundary pressures	Highly uncertain	Uncertain	Well known
Node temperatures	Highly uncertain	Uncertain	Well known
Flow paths	Highly uncertain	Highly uncertain	Uncertain

Air flow within the building can also be represented by one or more CFD domains. Each domain represents a volume of air which is discretised and conservation equations for mass, momentum and energy are formed. These equations are solved based on prevailing flow and thermal boundary conditions. Uncertainty affects a CFD do-

main via its geometry and boundary conditions. Therefore, while the building form is uncertain the geometry of the CFD domain will also be uncertain. Boundary conditions will likewise be highly uncertain while the building performance is not well defined, *e.g.* while the flow network is highly uncertain. At the detailed design stage the domain's geometry and boundary conditions will be well known.

2.1.4 Plant systems

A plant network is likewise described by a set of connected components where each component model represents the possible internal heat and fluid flows within the component and the thermal interaction with environment. Plant components are defined via templates, which are parameterised models of specific component types (*e.g.* heat exchangers, or a water heater, or a pump). For a humidifier, for example, the required data includes the design (uncontrolled) water flow rate, the mass and specific heat of the constituent materials and the moisture injection process type.

Uncertainty descriptors are presented in table 2.4. The uncertainties in plant networks are mainly related to the interaction between the network and the building and control system. Thus, as with the flow network the boundary conditions and control signals will be uncertain until the building is well defined.

Table 2.4: Uncertainty descriptors for plant network parameters.

Parameter	Outline	Scheme	Detailed
Boundary temperatures	Highly uncertain	Uncertain	Well known
Boundary flow rates	Highly uncertain	Uncertain	Well known
Control signals	Highly uncertain	Uncertain	Well known
Component data	Uncertain	Uncertain	Well known

2.1.5 Electrical networks

The modelling of electrical power flow in ESP-r is analogous to the modelling of fluid flow. The electrical equivalent of an internal flow node is a busbar and a boundary flow node is equivalent to a power consuming or generating component (*e.g.* a photovoltaic cell or a connection to the public electricity supply). These are connected to each

Table 2.5: Uncertainty descriptors for electrical network parameters.

Parameter	Outline	Scheme	Detailed
Boundary loads	Highly uncertain	Uncertain	Well known
Conductor lengths	Highly uncertain	Uncertain	Well known
Component data	Uncertain	Uncertain	Well known

other via conductors and/or transformers.

Each connection's electrical behaviour has then to be characterised, *e.g.* the data required for a conductor includes its length, resistance and inductance.

Uncertainty descriptors are presented in table 2.5. As with plant networks the main uncertainties are related to the boundary conditions, which will lessen as the design progresses and loads and generating components become better defined. Other uncertainties relate to the length of conductors which again will become smaller as the design progresses and cabling routes through the building are identified.

2.1.6 Control

Control can be applied to any of the parameters within the modelled networks: thermal, flow, plant or electrical. The essence of control is that a property is sensed and an action taken. The magnitude of the action is determined by a control law which relates the sensed condition to the actuated state to attain the required effect. For example, in a flow network for natural ventilation the sensed parameter could be a zone's temperature while the actuator could be applied to the opening of a window. If the temperature is too high such a control law will then open the window.

Uncertainty descriptors are presented in table 2.6. The uncertainties in control systems are mainly related to the sensed property and the actuator performance. It is straightforward to sense the state of a modelled parameter but the relationship between it and a physical sensor is not known *e.g.* a typical thermostat will generally not be solely affected by air temperature but also by radiant exchanges. Likewise, the performance of the actuator is unknown and is often idealised, ignoring hysteresis effects. As with the networks described above the building has to be well described before meaningful control performance information can be ascertained. Finally, the

data associated with the chosen control law will be uncertain until the building is well described, so that for example a PID controller can be tuned.

Table 2.6: Uncertainty descriptors for control parameters.

Parameter	Outline	Scheme	Detailed
Sensed condition	Highly uncertain	Uncertain	Well known
Actuator performance	Highly uncertain	Uncertain	Well known
Control law data	Uncertain	Uncertain	Well known

2.1.7 Contiguity

Contiguity relates to how the various aspects of the model interact with each other. In the control example, above the effect of opening the window will induce more fresh air into the building and thus increase the infiltration rate. Only if the fluid flow and building descriptions have been linked will this interaction be quantified. All interactions between networks are defined in a rigorous manner within ESP-r. For example, if lighting control is active and there is sufficient daylight then the artificial lights will be dimmed or switched off, reducing the power demand in the electrical network and the heat gain to the space. The reduced heat gain in the space would then impact upon the cooling requirement which, in turn, would impact upon the chiller load and fan power. Thus, the simple act of lighting control can affect the thermal, electrical, plant and flow networks.

As with the majority of building parameters, the contiguity will be highly uncertain in the outline design stage, becoming less uncertain as the design progresses, until at the detailed design stage it will be well known, as by this stage the internal layout of the building will be known and the flow networks and control systems defined.

2.2 Control volume conservation equations

The domain models for building simulation comprise a set of conservation equations for energy, mass and momentum with support equations corresponding to source terms.

2.2.1 Thermal modelling

The finite volume approach to building modelling requires the identification of typical control volume (or node) types [Clarke 2001]. Each of these node types is characterised by the energy transfer mechanisms occurring at the node. In a building there are three principal node types:

1. solid;
2. surface (solid/ fluid boundaries);
3. fluid.

There are also special cases of these types, *e.g.* solid nodes can be homogeneous or non-homogeneous, opaque or transparent. However, the energy balances remain essentially the same for each node type. Figure 2.2 summarises the various heat and mass transfer processes that may be included within the conservation equations corresponding to the three node types.

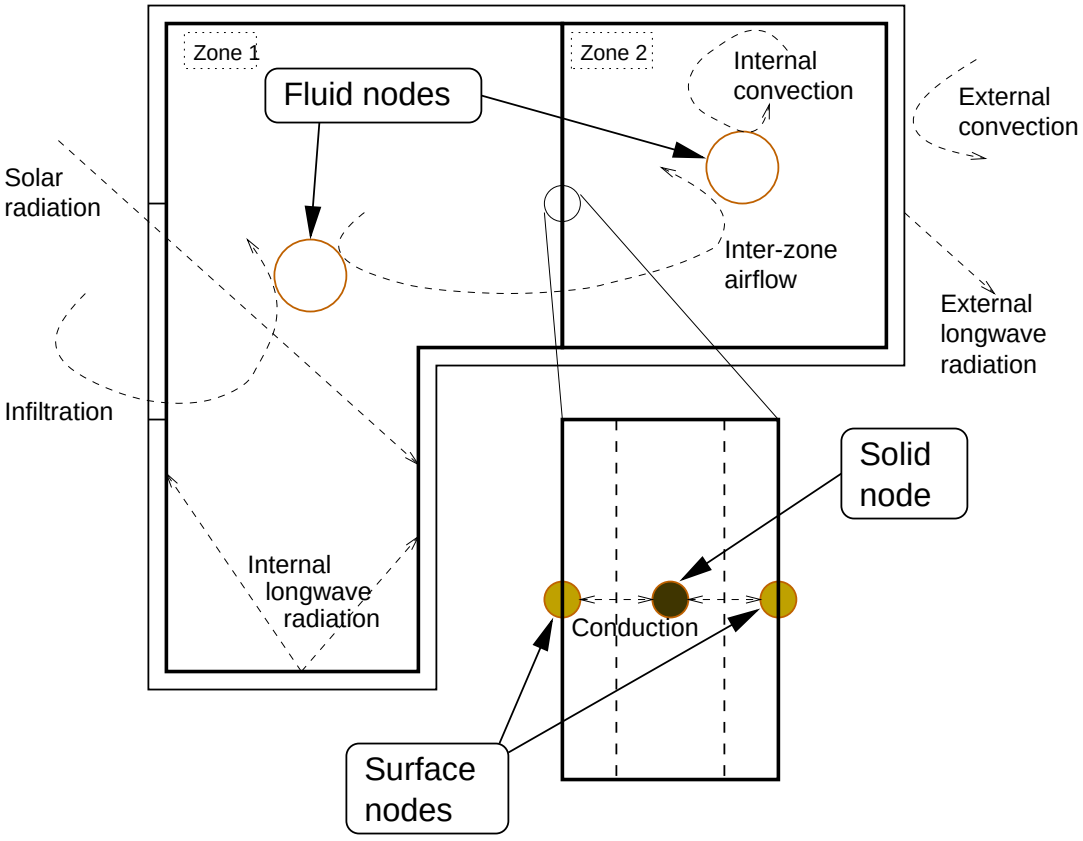

Figure 2.2: Building node types and heat flows.

The energy balances for each of the three node types are described to further exhibit the data requirements for building simulation and as a prerequisite for the inclusive methods of chapter 5.

Energy balance for solid nodes

The available mechanisms for heat transfer in a solid node are shown in figure 2.3. If the solid construction is opaque then the solar flux will be zero.

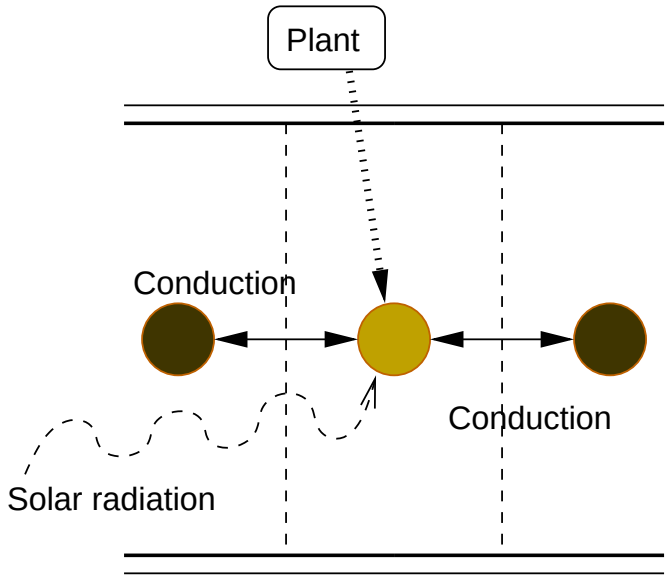

Figure 2.3: Heat transfer mechanisms in a solid node.

The energy balance can be stated as:

$$\begin{bmatrix} \text{Heat} \\ \text{stored} \\ \text{in volume} \end{bmatrix} = \begin{bmatrix} \text{Net heat} \\ \text{conducted} \\ \text{into volume} \end{bmatrix} + \begin{bmatrix} \text{Heat} \\ \text{generated} \\ \text{in volume} \end{bmatrix}.$$

The mathematical representation of these mechanisms is

$$\rho C V \frac{\partial \theta}{\partial t} = \sum_{i=1}^{n} k_i A_i \frac{\partial \theta}{\partial x} + q_{\text{plant}} + q_{\text{solar}} \tag{2.1}$$

where ρ is the density (kg/m^3), C the heat capacity (J/kgK), V the volume of the node (m^3), θ the temperature (K), t time (s), k the thermal conductivity (W/mK),

A the area normal to heat flow (m^2), x the distance between nodes (m) and q_* is an additional heat flux (W) where * is the type of flux[1]. Each of the conductive flow paths (i) is treated separately as there may be different material properties in each direction. For heat flow in one dimension the total number of conductive flow paths is two.

To facilitate numerical solution, equation 2.1 must be approximated. Rearranging the equation and ignoring the additional heat fluxes, (q_*), gives the Fourier equation in one dimension

$$\frac{\partial \theta}{\partial t} = \frac{k}{\rho C}\frac{\partial^2 \theta}{\partial x^2}. \tag{2.2}$$

The partial derivatives of equation 2.2 are represented by a truncated Taylor series for the current time row, t, and the future time row, $t+1$. The expression for the current time row is explicit and conditionally stable, whereas the expression for the future time row is implicit and unconditionally stable. Combining these expressions gives rise to the well known and unconditionally stable Crank-Nicolson difference scheme [Kreyszig 1993], which is given by

$$(2+2r)\theta_{i,t+1} - r(\theta_{i+1,t+1} + \theta_{i-1,t+1}) = (2-2r)\theta_{i,t} + r(\theta_{i+1,t} + \theta_{i-1,t}) \tag{2.3}$$

where $r = \frac{k}{\rho C} \cdot \frac{\delta t}{(\delta x)^2}$, and δt is the size of the temporal discretisation and δx is the size of the spatial discretisation. The terms on the left hand side correspond to the future time row $(t+1)$ and are all unknown, while the terms on the right hand side correspond to the present time row (t) and are all known. Improved stability is gained by multiplying through by ρC to give (after reintroducing plant and solar fluxes)

$$\begin{aligned}\left(2\rho C + \tfrac{2k\delta t}{(\delta x)^2}\right)\theta_{i,t+1} - \tfrac{k\delta t}{(\delta x)^2}(\theta_{i+1,t+1} + \theta_{i-1,t+1}) - \tfrac{q_{\text{plant},t+1}\delta t}{V} - \tfrac{q_{\text{solar},t+1}\delta t}{V} \quad = \\ \left(2\rho C - \tfrac{2k\delta t}{(\delta x)^2}\right)\theta_{i,t} + \tfrac{k\delta t}{(\delta x)^2}(\theta_{i+1,t} + \theta_{i-1,t}) + \tfrac{q_{\text{plant},t}\delta t}{V} + \tfrac{q_{\text{solar},t}\delta t}{V}.\end{aligned} \tag{2.4}$$

This is the general form of the equation for a solid node, where V is the node volume.

[1]Note: q_{solar} is the fraction of the solar flux absorbed at this node, which is a function of the solar transmissivity of the surrounding layers and any shading of the construction.

Energy balance for surface nodes

The available mechanisms for energy transfer at a surface node are as shown in figure 2.4.

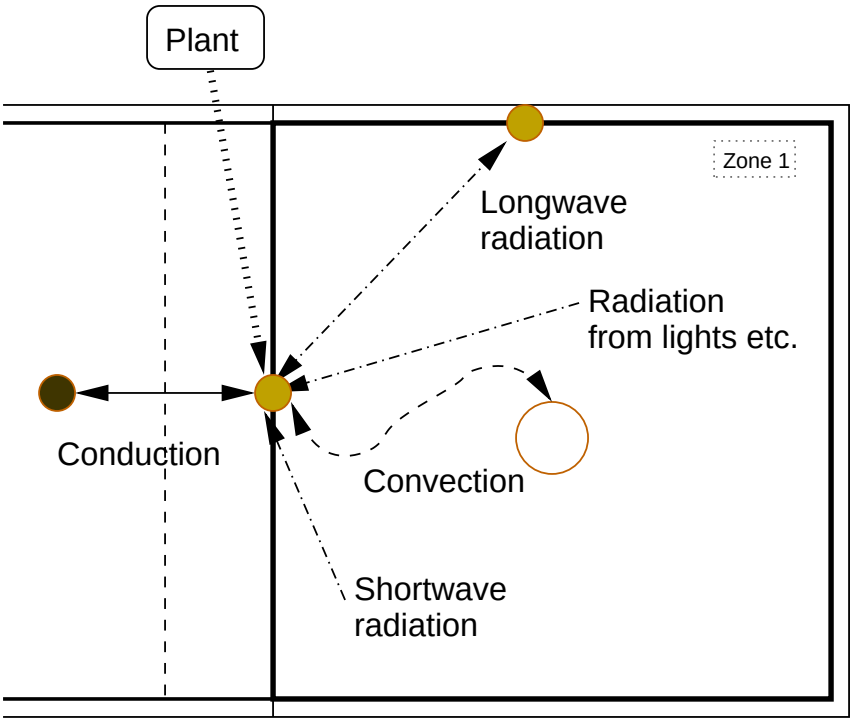

Figure 2.4: Energy transfer mechanisms in a surface node.

The energy balance is given by

$$\begin{bmatrix}\text{Heat}\\ \text{stored}\\ \text{in volume}\end{bmatrix} = \begin{bmatrix}\text{Net heat}\\ \text{conducted}\\ \text{into volume}\end{bmatrix} + \begin{bmatrix}\text{Net heat}\\ \text{radiated}\\ \text{into volume}\end{bmatrix} + \begin{bmatrix}\text{Net heat}\\ \text{convected}\\ \text{into volume}\end{bmatrix} + \begin{bmatrix}\text{Heat}\\ \text{generated}\\ \text{in volume}\end{bmatrix}.$$

The mathematical representation of these mechanisms is given by

$$\rho C V \frac{\partial \theta}{\partial t} = k_i A_i \frac{\partial \theta}{\partial x} + \sum_{s=1}^{m} q_{s,\text{longwave}} + q_{\text{convection}} + q_{\text{plant}} + q_{\text{solar}} \qquad (2.5)$$

where s is the receiving surface for longwave radiation. The longwave radiation and convection terms are additional terms and are expressed as follows for node i. The

longwave radiative flux for each of the m surfaces in longwave contact is given by

$$q = h_r A_i(\theta_s - \theta_i). \tag{2.6}$$

Here the radiative heat transfer coefficient (W/m^2K) has been linearised and is recalculated at each simulation time step. The convective heat flux is expressed likewise:

$$q = h_c A_i(\theta_{fluid} - \theta_i). \tag{2.7}$$

The convective heat transfer coefficients (h_c, W/m^2K) are either time invariant, time varying derived from empirical relationships, or calculated during an explicit simulation of the zone's air movement.

Updating equation 2.4 to account for the additional flow paths gives rise to the following expression

$$\begin{aligned}
&\left(2\rho C + \frac{2k\delta t}{(\delta x)^2} + \sum_{s=1}^{m}\frac{h_{r,s}A_i\delta t}{V} + \frac{h_c A_i \delta t}{V}\right)\theta_{i,t+1} - \frac{2k\delta t}{(\delta x)^2}\theta_{i+1,t+1} - \\
&\frac{q_{\text{plant},t+1}\delta t}{V} - \frac{q_{\text{solar},t+1}\delta t}{V} - \sum_{s=1}^{m}\frac{h_{r,s}A_i\delta t}{V}\theta_{s,t+1} - \frac{h_c A_i\delta t}{V}\theta_{\text{fluid},t+1} = \\
&\left(2\rho C - \frac{2k\delta t}{(\delta x)^2} - \sum_{s=1}^{m}\frac{h_{r,s}A_i\delta t}{V} - \frac{h_c A_i \delta t}{V}\right)\theta_{i,t} + \frac{2k\delta t}{(\delta x)^2}\theta_{i+1,t} + \\
&\frac{q_{\text{plant},t}\delta t}{V} + \frac{q_{\text{solar},t}\delta t}{V} + \sum_{s=1}^{m}\frac{h_{r,s}A_i\delta t}{V}\theta_{s,t} + \frac{h_c A_i\delta t}{V}\theta_{\text{fluid},t}
\end{aligned} \tag{2.8}$$

This is the general form of the equation for a surface node, where V is the volume of the solid section of the control volume[2].

Energy balance for fluid nodes

The available mechanisms for energy transfer at a fluid node are as shown in figure 2.5.

[2]Note that this volume is $A \times \frac{\delta x}{2}$.

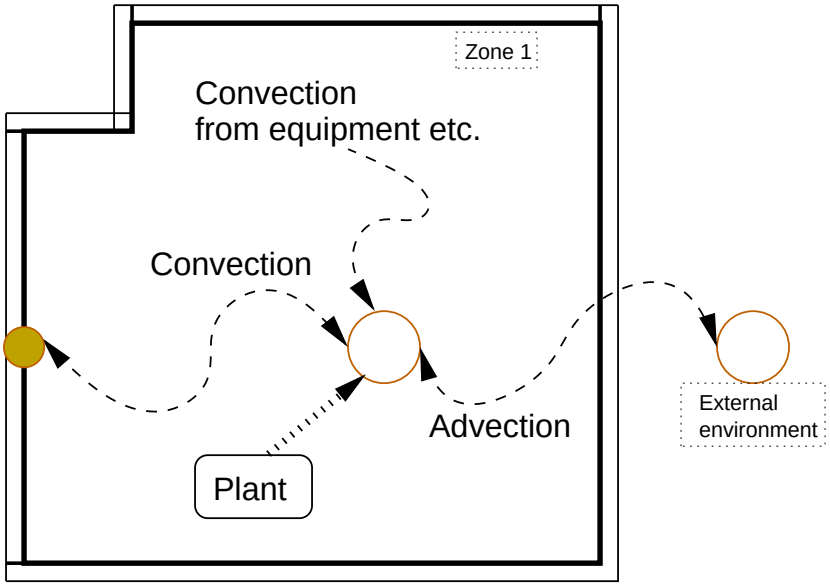

Figure 2.5: Energy transfer mechanisms in a fluid node.

The energy balance can be described as:

$$\begin{bmatrix} \text{Heat} \\ \text{stored} \\ \text{in volume} \end{bmatrix} = \begin{bmatrix} \text{Net heat} \\ \text{convected} \\ \text{into volume} \end{bmatrix} + \begin{bmatrix} \text{Net heat} \\ \text{advected} \\ \text{into volume} \end{bmatrix} + \begin{bmatrix} \text{Heat} \\ \text{generated} \\ \text{in volume} \end{bmatrix}.$$

The mathematical representation of these mechanisms is given by

$$\rho C V \frac{\partial \theta}{\partial t} = \sum_{s=1}^{m} q_{s,\text{convection}} + \sum_{r=1}^{n} q_{\text{advection}} + q_{\text{plant}}. \tag{2.9}$$

The advection term is the only additional term and for each flow path maybe expressed as

$$q = \dot{m}_{\text{srcfluid}} C_{\text{fluid}} (\theta_{\text{srcfluid}} - \theta_{\text{fluid}}). \tag{2.10}$$

The mass flow rate ($\dot{m}_{\text{srcfluid}}$, kg/s) of the source fluid is the rate of fluid entering the fluid volume at a source temperature of θ_{srcfluid}. Note that within a simulation this parameter will be simultaneously available as the solved for variable of state of another finite volume.

Updating equation 2.8 to account for the additional flow paths gives rise to the following difference equation

$$\left(2\rho C + \sum_{s=1}^{m} \frac{h_{c,s} A_s \delta t}{V} + \sum_{r=1}^{n} \frac{\dot{m}_r C \delta t}{V}\right) \theta_{i,t+1} -$$
$$\frac{q_{\text{plant},t+1}\delta t}{V} - \sum_{s=1}^{m} \frac{h_{c,s} A_s \delta t}{V} \theta_{s,t+1} - \sum_{r=1}^{n} \frac{\dot{m}_r C \delta t}{V} \theta_{\text{srcfluid},t+1} =$$
$$\left(2\rho C - \sum_{s=1}^{m} \frac{h_{c,s} A_s \delta t}{V} - \sum_{r=1}^{n} \frac{\dot{m}_r C \delta t}{V}\right) \theta_{i,t} +$$
$$\frac{q_{\text{plant},t+1}\delta t}{V} + \sum_{s=1}^{m} \frac{h_{c,s} A_s \delta t}{V} \theta_{s,t} + \sum_{r=1}^{n} \frac{\dot{m}_r C \delta t}{V} \theta_{\text{srcfluid},t}. \qquad (2.11)$$

This is the general form of the equation for a fluid node, where V is the volume of the fluid contained in the current control volume.

Uncertainty considerations

The parameters in equations 2.4, 2.8 and 2.11 are uncertain. The uncertainties can be attributed to several sources as summarised in table 2.7. In addition to these sources, measurement errors will exist for all physical properties and the magnitude of these uncertainties will vary throughout the design process as described earlier. The effects of temperature and moisture content can be accounted for through more detailed simulation, but the associated models include parameters which are themselves uncertain. Likewise, the uncertainty in the empirical relationships used for the calculation of convective heat transfer coefficients can be reduced through more detailed modelling. The build quality will affect the dimensions of the zones, leading to uncertainty in V and A, and the thicknesses of walls, in turn leading to the

Table 2.7: Uncertainty sources affecting building parameters.

Source	Parameters affected
Temperature	k, ρ, C
Moisture	k, ρ, C
Material age	k, ρ, C, h_r
Dimensions	V, A, δx
Empirical	h_c

uncertainty in δx. Materials degrade with age introducing uncertainty as to the appropriateness of initial properties for older buildings. Finally, the surface finishes will affect the absorptivity and emissivity, and thus the radiative heat transfer coefficient.

The effect of these uncertainties is that the state variables are also uncertain and thus information passed between domains will also be uncertain. In fact the only parameter which is not uncertain is δt, the simulation time step as this is imposed on the modelled domain.

2.2.2 Other domains

As described in section 2.1 an ESP-r model is composed of several domains other than the thermal domain described above. It is unnecessary to describe the theoretical basis of all of these domains. However, to demonstrate the general applicability of the control volume approach the essence of the flow and CFD domains are elaborated. The derived expressions are revisited during the application of the internal method in chapter 5.

Flow modelling

The conservation equations formed in the flow domain are for the preservation of mass. To enable this requires the representation of energy, mass and momentum terms. In the network flow approach the mass and momentum terms are embodied in empirical flow equations, while the energy term is passed from the thermal side. The mass balance for a given volume may be stated as

$$\left[\begin{array}{l}\text{Net mass}\\ \text{transferred}\\ \text{into volume}\end{array}\right] = 0.$$

The mass flow rate between two connected volumes is described by an empirical relationship

$$\dot{m} = f(\Delta P), \tag{2.12}$$

where ΔP is the prevailing pressure difference.

The exact realisation of this function depends on the connection type. Generally the mass flow rate is a non-linear function of the pressure difference. For example, in the case of a crack the function might correspond to a power law:

$$\dot{m} = \rho\kappa(\Delta P)^n, \tag{2.13}$$

where ρ is the density and κ and n are empirical coefficients.

Uncertainty considerations

The main source of uncertainty in the zonal flow equations is in the specification of appropriate empirical relationships and the required parameters, for each connection. The uncertainties in these equations will then affect the predicted mass flow rates between nodes, which will affect the advection terms in the building equation set.

CFD

In computational fluid dynamics there are several sets of inter-related conservation equations for mass, momentum, energy balance. The general conservation equation can be stated as:

$$\begin{bmatrix} \text{Entity} \\ \text{contained} \\ \text{in volume} \end{bmatrix} = \begin{bmatrix} \text{Net entity} \\ \text{diffused/} \\ \text{convected} \\ \text{into volume} \end{bmatrix} + \begin{bmatrix} \text{Net entity} \\ \text{created} \\ \text{in volume} \end{bmatrix}$$

where the entities are: mass, momentum and energy. To represent the effects of turbulence, it is usual practice to add additional equations relating to turbulence intensity and its rate of dissipation. These equations can also be made to conform to the above general form.

The discretisation method employed in ESP-r is the staggered grid approach. With this approach four sets of control volumes are created: a mass balance set and three

momentum balance sets (for the momentum equations in the x, y and z directions). Each momentum control volume is centred on its respective boundary of the mass control volume: the momentum control volumes in the i direction are offset from the mass control volumes by 1/2 a cell in the positive x direction. The conservation equations are then applied to these sets of control volumes, as detailed elsewhere [Negrao 1995, Versteeg and Malalasekera 1995].

Uncertainty considerations

The uncertainty in the solution of a CFD domain is dominated by the definition of the domain's geometry and boundary conditions; a discretisation error exists but is small compared to these two sources. Uncertainty in geometry affects the shape of the domain and the location of any objects (desks, cabinets *etc*) within the domain which will all affect the flow regime. Uncertainty in boundary conditions will likewise affect the flow regime as was demonstrated in chapter 1.

2.2.3 Solution methods

The previous sections have described how the control volume technique can be applied to different parts of a building. The derived equations must now to be arranged in a format suitable for simultaneous solution.

Within ESP-r each technical domain (building, HVAC, electrical *etc*) employs a solution method optimised for the specific domain equation types. For example, in the case of zonal flow modelling the non-linear flow equations are solved by a corrector-predictor iterative method. In the case of CFD, where the solution is complicated by the interactions between the conservation equation sets, a more elaborate iterative scheme is employed based on the SIMPLE-C algorithm [Versteeg and Malalasekera 1995].

Within ESP-r these solution methods are essentially embedded within a higher level solver built to represent the building and its systems. The building domain equation set is generated by repeated application of the node type models described by equations 2.4, 2.8 and 2.11. This domain, along with its constituent domains, is

solved simultaneously at each time increment.

The matrix formulation of the system of conservation equations can be expressed as [Clarke 2001]

$$\mathbf{A}.\theta_{\mathbf{t+1}} = \mathbf{B}.\theta_{\mathbf{t}} + \mathbf{C} = \mathbf{Z} \tag{2.14}$$

where:

A is the future time-row $(t+1)$ coefficients of the nodal temperatures,

B is as **A**, but corresponds to the present time-row (t),

C is a vector of known boundary excitations (relating to present and future time-rows),

θ is a vector of nodal temperatures.

The equations can now be solved directly. In the case of ESP-r a customised solution method is employed due to the sparse nature of the coefficient matrices. Equation sets are derived on a zonal basis: one for each surface and one for the fluid volume. These equation sets are still expressed as described above, but solve more quickly than the complete matrix representation.

Other solution mechanisms exist, for example, an LU decomposition of the matrix **A** to improve the efficiency of the calculation procedure. The equations can also be solved indirectly by an iterative procedure (*e.g.* the Gauss-Seidel method). The choice of solution method is normally determined by efficiency and hence speed. However, when embedding uncertainty within the conservation equations other properties become pertinent to achieving a solution. These are explored in chapter 3.

2.3 Impact of uncertainty

Uncertainty is most evident to practitioners when preparing the data used to describe the system to be modelled. Of no less importance are the uncertainties implicit in the mathematical models and boundary conditions being employed within the program. These two aspects of uncertainty are now expanded to enable the characteristics of an uncertainty assessment method to be elaborated.

2.3.1 Data model

All data entered into a program is subject to uncertainty; the sources of these uncertainties are elaborated and quantified in chapter 4. To allow the impact of uncertainty to be assessed, a method must be provided whereby the practitioner can clearly define the anticipated variation in the input data. At a basic level a typical data item will require a mean value and two additional data items to define this variation, for example a minimum and maximum value or a probability distribution type and a standard deviation. The effect of this could treble the size of the data model. Therefore, significant alterations to existing data structures will be required to hold the definition of uncertainties.

2.3.2 Conservation equations

The uncertainties in the input model directly affect the conservation equations and thus the energy, mass, power, *etc* transfer and storage processes. However, many transfer mechanisms are described by empirical relationships, for example the mass flow rate equations in section 2.2.2, or convective heat transfer coefficients [ETSU 1987]. There will also be discretisation errors associated with the formulation of the control volumes. These errors occur in the spatial and temporal domains and can be minimised by the practitioner. In ESP-r this is achieved through an optimised node placement facility and in the time domain via the user defined simulation time step.

2.3.3 Quantifying the effects

Quantifying the effects of uncertainty is a two stage process: the uncertainties have to be defined and quantification methods employed. The former process involves data manipulation and storage procedures to maintain the data model required for use in the latter. Before this data model can be specified suitable uncertainty quantification methods must be identified. The characteristics of suitable quantification methods are:

1. the method should quantify the individual effect on predictions of each uncertain

data item,

2. the method should be capable of assessing the degree of interaction between the effects caused by multiple uncertainties,

3. the method should be able to quantify the overall effect of all uncertainties.

These three characteristics allow the program user to, in reverse order, state the confidence in the predictions made by the simulation, identify which parameters have synergistic effects and isolate individual parameters that contribute the most to the overall uncertainty.

2.4 Summary

The ESP-r system employs the control volume conservation approach to model the technical domains found in buildings. The data required by the system are directly related to the physical processes being simulated and typically comprise geometry, material and technical parameters. The building is typically divided into several technical domains, each described by its own set of conservation equations. The technical domains are then solved using co-operating solver algorithms.

Uncertainty impacts on all aspects of the simulation, from the input data through to the solution methods. The magnitude of uncertainties varies through the design process, generally reducing as the design progresses. To enable effective simulations at early design stages requires uncertainty to be assessed.

References

Clarke J A, *Energy Simulation in Building Design*, Butterworth Heinemann, 2nd ed, 2001

Energy Systems Research Unit, *http://www.esru.strath.ac.uk*, 2001

ETSU *Report on Heat Transfer at Internal Building Surfaces*, Energy Technology Support Unit, UK Department of Energy, June 1987

Kreyszig E, *Advanced Engineering Mathematics*, J Wiley and Sons, 7th ed, 1993

Negrao C O R, *Conflation of computational fluid dynamics and building thermal simulation*, PhD thesis, ESRU, University of Strathclyde, 1995

Royal Institute of British Architects, *Architect's job book*, RIBA publications, 1995

Versteeg H K and Malalasekera W, *An introduction to computational fluid dynamics: the finite volume method*, Longman, 1995

Wit S de, *Uncertainty in predictions of thermal comfort in buildings*, PhD thesis, Delft University, 2001

Chapter 3

Uncertainty quantification techniques

Two approaches to uncertainty quantification are explored: external and internal. Methods within each approach are described.

The quantification of the error in experimental results has long been a standard procedure: primarily to increase confidence in the reproducibility of the experimental method and hence the results. These techniques were further refined [Box *et al* 1978] to enable the quantification of those controllable aspects of an experiment that had the largest effect on the results, e.g. to enable increased yields from a chemical experiment. This refinement is known as sensitivity analysis. The techniques of experimental analysis have been further refined in the latter half of the 20th century and applied to computer experiments, or simulations [Saltelli *et al* 2000].

The major difference between physical and computer experiments is that all aspects of a computer experiment are controllable. Methods developed for physical experiments, where the number of controllable parameters is small, are generally efficient precisely because the number of uncertain parameters is small. When translating these methods to simulations, where every parameter is controllable, the required computational effort is a function of the number of uncertain parameters. The exact

relationship between computational effort and the number of uncertain parameters depends on the analysis method as described below.

Approaching the problem from the opposite direction is the branch of mathematics concerned with range arithmetic and self-validating methods [Stolfi and de Figueiredo 1997]. These theories are characterised by the fact that the uncertainty is embodied in the mathematical representation of the entity and is therefore present throughout the calculation [Neumaier 1990]. The impact of this is that a single simulation can represent all possible outcomes of the uncertainties. These methods arose through the use of finite precision computer arithmetic where inexact results are often encountered, *e.g.* the decimal representation of 1/3. The basic form of range arithmetic is interval arithmetic, which in its generalised form is the well known, and well applied, fuzzy arithmetic [Ross 1995].

This chapter describes and develops the two approaches to uncertainty quantification: external and internal methods.

3.1 External methods

The essence of external methods is that the mathematics of the simulation are not altered, only the describing model, initial conditions, boundary conditions and solution methods. This results in the simulation software being treated as a black box, where different models are analysed and the differences in response examined.

The analogy with physical experiments is relevant as often the interactions within an experiment are not known but a measurable effect occurs when the experiment is started at a different location or temperature. Not knowing what is physically happening in the experiment is not a barrier to understanding the relationship between the controllable aspects of the experiment and the result of the experiment.

With computer simulation and uncertainty analysis the aim of an external method is to alter the input parameters and measure the effect this has on the outputs. The simulation software treats each set of input parameters as a separate model. An external agent has then to manage the subsequent analysis of each result set and

infer the intra- and inter-set relationships.

External methods fall into two broad categories: local and global. Local methods describe how the output of the model varies with respect to changes in individual parameters, whereas global methods quantify the overall uncertainty with respect to variations in all parameters.

All methods are based on statistical techniques. Therefore they have specific areas of application and known weaknesses. It is within this framework that methods have been characterised and selected for their robustness and ability to quantify effects.

Local methods

Differential sensitivity analysis is perhaps the best known of the local methods and is generally robust. The method has been described as the backbone of all sensitivity analysis methods [Hamby 1994] and calculates the effect of uncertainties in each parameter independently. To calculate the effect of uncertainties an initial simulation is undertaken. For each uncertain parameter a simulation is then performed with the uncertain parameter altered to its extreme value, say $+3\sigma$, and an optional simulation with the parameter at its other extreme, -3σ. The effect of the uncertainty is calculated by comparing the results of these simulations against those of the initial simulation. Its main advantages are the ease of application and results interpretation as the differences are entirely due to the single parameter that has been perturbed. Its main weakness is that the effects of uncertainties are assumed to be independent of all other parameters. Therefore, for the effects of uncertainties to be combined superposition has to be assumed to hold. This is not always the case in building physics. For example, assume the infiltration rate and the heat gain from equipment are both uncertain in a room. The effect of a 50% increase in air change rate on peak air temperature is a reduction of $1.85°C$, the effect of a 50% increase in heat gain from the equipment is an increase in peak air temperature of $1.14°C$. If superposition holds then the net effect of simultaneously making these changes would be a reduction of $0.71°C$ in the peak air temperature; in fact, the simulation shows that the effect is a larger reduction, $0.96°C$. Generally superposition will not hold when parameters

are multiplied in an equation, *e.g.* for surface convective flux $q = h_c A(\theta_a - \theta_s)$. If the convection coefficient and the surface area are uncertain then

$$\begin{aligned}
\Delta q_A &= h_c(A + \delta A)(\theta_a - \theta_s) - h_c A(\theta_a - \theta_s) \\
&= h_c \delta A(\theta_a - \theta_s), \\
\Delta q_{hc} &= (h_c + \delta h_c)A(\theta_a - \theta_s) - h_c A(\theta_a - \theta_s) \\
&= \delta h_c A(\theta_a - \theta_s), \\
\Delta q_{A,hc} &= (h_c + \delta h_c)(A + \delta A)(\theta_a - \theta_s) - h_c A(\theta_a - \theta_s) \\
&= [h_c A + \delta h_c A + h_c \delta A + \delta h_c \delta A](\theta_a - \theta_s) - h_c A(\theta_a - \theta_s) \\
&= \Delta q_A + \Delta q_{hc} + \delta h_c \delta A(\theta_a - \theta_s).
\end{aligned}$$

If superposition holds then the combined effect of the uncertainty in area and convection coefficient would have been $\Delta q_A + \Delta q_{hc}$. The additional term $\delta h_c \delta A(\theta_a - \theta_s)$ is a second order effect and will therefore be smaller in magnitude than the first order terms Δq_A and Δq_{hc}. However, the $\delta h_c \delta A(\theta_a - \theta_s)$ term will have a greater effect for larger uncertainties, typically encountered at the early design stage.

To overcome the weaknesses of the differential analysis method the factorial method is sometimes used because it includes the interactions between parameters [Box *et al* 1978]. The method works by altering all the uncertain parameters between simulations so that a simulation is undertaken for all possible combinations of parameter values (*e.g.* $+3\sigma$ and -3σ). The changes are predetermined and as a result the effects of uncertainties can be quantified. This method is efficient for small numbers of uncertain parameters. However, the number of simulations grows factorially with the number of uncertain parameters (N): *e.g.* 2^N when each parameter is simulated at a lower and upper value only; if the simulation is undertaken for mean parameter values as well the number of runs would be 3^N.

There are other local methods which were derived from the above methods, *e.g.* Cotter's method and the method of Morris [Saltelli *et al* 2000]. Cotter's method requires $2N+2$ simulations: an initial simulation is run with all the parameters at their lower value, then each parameter in turn is altered to its upper value while the other

parameters remain at their lower values for the next k simulations. This process is repeated with all the parameters set to their upper values (for a simulation) and then each parameter is altered to its low value (for the remaining k simulations), again one at a time. Morris's method is similar in that only one parameter is changed between simulations: random starting values are chosen within the defined uncertainty distributions and each of the parameters is increased in value by a random amount between simulations, this process is repeated several times from different starting values and with new perturbations each time. These methods, however, are more appropriate to the identification of critical parameters rather than the quantification of the effect on the output. Furthermore, if Cotter's method is incorrectly applied it can fail to find all of the critical parameters [Saltelli *et al* 2000]. This is indicative of a general difficulty encountered with statistically based methods: the correct method has to be selected and appropriately applied. The selection of a method is therefore a delicate step.

The differential and factorial methods are deemed suitable for use in building simulation due to their robustness and ability to accurately quantify the uncertainty in the model output. Both methods require multiple simulations and in the case of factorial analysis the required computational effort can be restrictive. However, as will be shown in sections 3.1.1 and 3.1.2 both methods can be effectively applied in building simulation applications.

Global methods

Monte Carlo analysis is the umbrella under which all global methods sit, the difference between different applications being in the sampling and analysis of the results. The basic premise is that all uncertain parameters are perturbed by random amounts between simulations. Typically 80 simulations are undertaken (the number of simulations required is independent of the number of uncertain parameters) and the mean performance and standard deviation can be calculated by analysing all the results together. Various sampling techniques exist, *e.g.* stratified and Latin hypercube, to ensure that the full range of a parameter's distribution is used. However, the use of

random sampling[1] is advocated as it produces unbiased estimates of the mean and variance, and requires a straightforward analysis to estimate the overall uncertainty in predictions. This is an important consideration as it allows the statistical comparison of two simulations via a significance test. Monte Carlo analysis is described in detail in section 3.1.3.

3.1.1 Differential analysis

The differential method is based on calculating the effect of changing each uncertain parameter in isolation. The method works by altering a model parameter from its initial value to orthogonal points surrounding the initial value *one at a time*, while all other parameters remain at their initial values. This is displayed graphically in figure 3.1. The parameter values, x_{1+}, x_{1-}, x_{2+} and x_{2-} are shown on the x_1 and x_2 axes. The origin of the axes is the datum or normal value for these parameters. The uncertain parameters can take any value along their respective axis. The output is calculated for the datum response R_{Datum} and, in this example, the two parameters are adjusted one at a time to produce a further four outputs: R_{x1+}, R_{x1-}, R_{x2+} and R_{x2-}. In this case both parameters x_1 and x_2 have been varied by one unit above and below their normal values. The response of the system can be calculated by examining the difference between the datum response and each of the four outer responses in turn. In building modelling an example system response could be energy demand while the two uncertain parameters could be building occupancy and the control temperature set point. The resulting performance statistics are thus a direct measurement of the effect of altering the chosen parameter in isolation.

[1] Technically pseudo-random when computer-based.

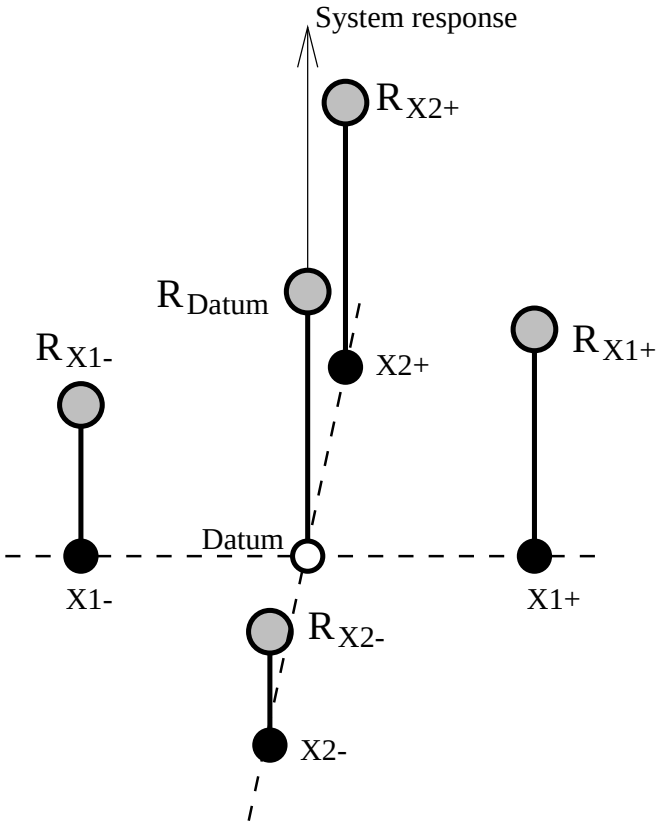

Figure 3.1: Test points and responses of a differential analysis for 2 parameters.

In building applications the system response is generally time based. This can be demonstrated graphically by working in two variables, time and a parameter x_1, although in practical applications many more variables would be included as the method can be extended to any number of variables [Tomovic 1963].

The model is defined as

$$f(t, x_1) = Z(t)$$

and produces a response at the initial value of x_1 as displayed in figure 3.2(a). This response is referred to as the datum response. To measure the effect on the solution of an uncertainty, *e.g.* at $x_1 + \delta x_1$, referred to as the *on* value of parameter x_1, the model is also solved for (see figure 3.2(b))

$$f(t, x_1 + \delta x_1) = Z_{\delta x_1}(t).$$

This gives another set of points in the solution space. To calculate the magnitude of

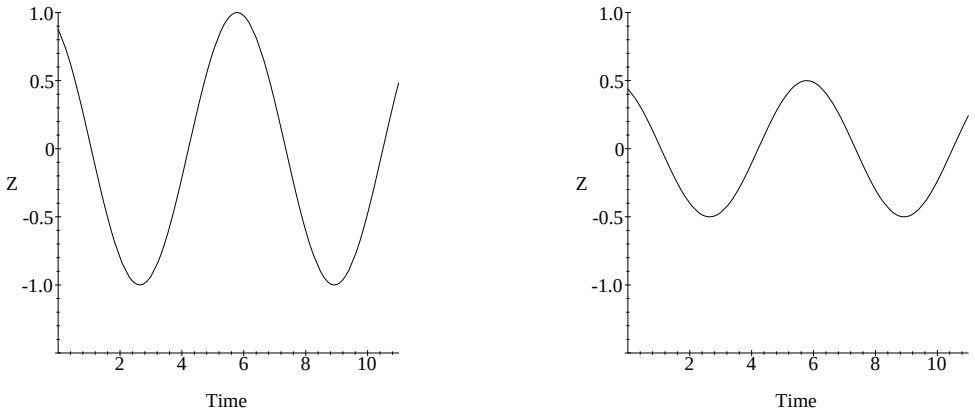

(a) x_1 at mean value

(b) $x_1 + \delta x_1$

Figure 3.2: Response of function $f(t, x_1) = Z(t)$.

the effect that the uncertainty in x_1 has had on the solution, the difference between the *on* solution curve and the *datum* solution curve can be calculated. If more than one parameter is to be analysed and the effects compared then the rate of change between the two solutions is calculated:

$$g(t, x_1) = \frac{f(t, x_1 + \delta x_1) - f(t, x_1)}{\delta x_1}. \tag{3.1}$$

If δx_1 tends to zero then $g(t, x_1) = f'(t, x_1)$, *i.e.* the first differential of our model. This approach assumes that the response to the parameter alteration is linear as displayed in figure 3.3. Note that the effect of varying x_1 varies with time and that the two curves in figure 3.2 are sections through this surface at specific values of x_1.

The curves displayed in figure 3.2 are typical of the temperature in a building when uncertainties in thermal capacity are present. Generally there is more than one variable thus equation 3.1 would represent a partial differential with respect to x_1; the total differential being represented by the sum of the partial derivatives, assuming that the fundamental theorem of superposition holds.

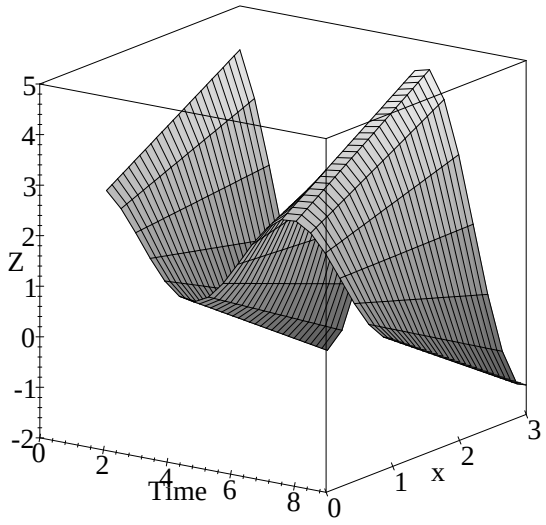

Figure 3.3: Function $f(t, x_1, x_2) = Z(t)$ varying in t and x_1.

Quantifying the first order effect

The classic method for deriving the first derivative of a function as described above requires only $N + 1$ simulations to measure their effects, where N is the number of uncertain parameters. The first simulation would be carried out at the model's initial parameter values to create a datum response and then all further simulations would alter one parameter at a time to their *on* value. By calculating only the mean response and the response at a parameter's *on* value it is not possible to test the linearity assumption; this would require at least three responses.

The method for achieving a linearity test is by taking the differential as a central difference, thus running all the simulations parameters at their *on* and *off* values (*i.e.* $x_i - \delta x_i$). Three system responses have now been generated which can be used for each parameter i: $Z(t)$ (datum), $Z(t)_{i+}$ (response with parameter x_i on) and

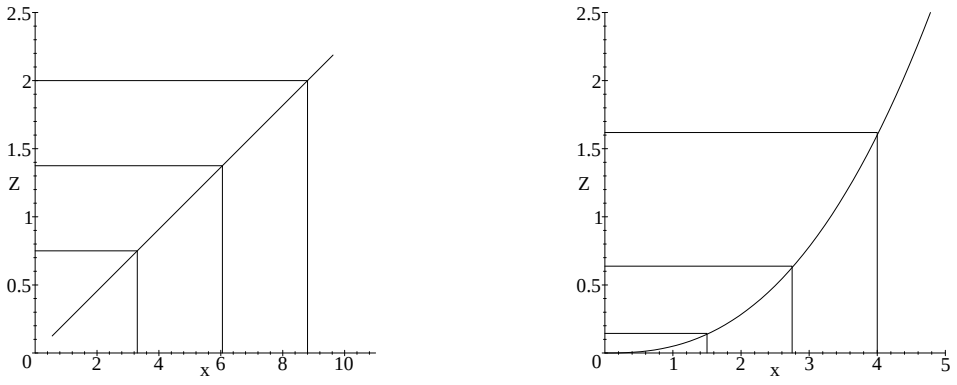

(a) linear (b) non-linear

Figure 3.4: Response types due to a perturbation in x

$Z(t)_{i-}$(response with parameter x_i off). If the response is linear then at all times

$$Z(t) = \frac{Z(t)_{i+} + Z(t)_{i-}}{2}. \tag{3.2}$$

The difference between the two average responses gives a measure of the non-linearity, see figure 3.4. A typical non-linear response can be observed with uncertainties in air change rates. Consider the peak air temperatures in an office with mechanically supplied fresh air. The model has been simulated for five constant volume supply rate scenarios: 1, 2, 3, 4 and 5 air changes per hour. As can be seen in figure 3.5 the effect of increasing the fresh air supply rate has a decreasing benefit. Using equation 3.2 to test for linearity gives:

$$\begin{aligned}
\theta_2 = 36.3 \neq \frac{\theta_1 - \theta_3}{2} = 36.9 \\
\theta_3 = 34.4 \neq \frac{\theta_1 - \theta_3}{2} = 34.7 \\
\theta_4 = 33.1 \neq \frac{\theta_1 - \theta_3}{2} = 33.3.
\end{aligned} \tag{3.3}$$

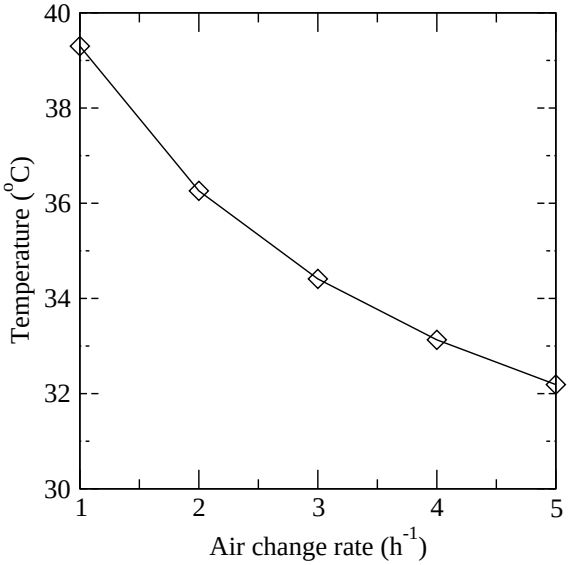

Figure 3.5: Peak air temperatures for varying fresh air change rates.

An estimation of the second order effect ($\beta_{i,i}$) can be found by using a least squares estimation, thus fitting the model:

$$Z(t)_i = \beta(t)_0 + \beta(t)_i x_i + \beta(t)_{i,i} x_i^2 + \epsilon(t). \tag{3.4}$$

The above least squares estimation of the quadratic effect is rarely calculated. This is partially due to any generated equation having validity only in the area modelled for the individual parameters.

However, a dimensionless uncertainty coefficient can be calculated, so that the quantified first order effects can be compared directly. If it is assumed that the effect is linear then the uncertainty coefficient can be defined as [Hamby 1994]

$$\phi_i(t) = \frac{\%_0 \delta Z(t)}{\%_0 \delta x_i} = \frac{\frac{f(t,x_i+\delta x_i)-f(t,x_i)}{f(t,x_i)}}{\frac{\delta x_i}{x_i}}. \tag{3.5}$$

However, in building applications this approach can fail due to responses being zero in some cases. For example, if the measured system response is plant flux and the datum value at a particular time is $0W$ and for parameter x_{2+} is $10W$ then the percentage difference cannot be calculated, rendering the uncertainty coefficient meaningless. A more pragmatic approach is suggested whereby the range in the calculated response

of both parameter states is ranked, *i.e.* the response is not normalised:

$$\Phi_i(t) = \max[Z(t), Z_{i+}(t), Z_{i-}(t)] - \min[Z(t), Z_{i+}(t), Z_{i-}(t)]. \tag{3.6}$$

By this method uncertainties in all aspects of the model can be compared directly, *e.g.* climate parameters and algorithm choice.

To quantify uncertainties which produce a positive and negative response at different times (*e.g.* the response for thermal capacity in figure 3.2), it is necessary to separately examine the average positive and negative responses and the average absolute values of the positive and negative responses:

$$\Phi_{i,ave+} = \frac{\sum_1^{t=T} Z_{i+}(t) - Z(t)}{T} \tag{3.7}$$

$$\Phi_{i,|ave+|} = \frac{\sum_1^{t=T} |Z_{i+}(t) - Z(t)|}{T} \tag{3.8}$$

$$\Phi_{i,ave-} = \frac{\sum_1^{t=T} Z(t) - Z(t)_{i-}}{T} \tag{3.9}$$

$$\Phi_{i,|ave-|} = \frac{\sum_1^{t=T} |Z(t) - Z(t)_{i-}|}{T}. \tag{3.10}$$

If the positive average value is the same as the positive average absolute value, and likewise the negative values, then the system has a constant response to the uncertainty (*i.e.* always the same sign, positive or negative, rather than a constant value). The difference between the positive and negative values is a quantification of the average non-linearity.

Addition of effects

If the effects measured in the analysis are due to independent uncertainties (often not the case in building simulation), *i.e.* superposition holds, then the variances of the effects can be combined [Berry and Lindgren 1990].

The statistical basis for combining the individual effects is that, for the sum of independent variables, the variance of the sum is the sum of the individual variances [Kreyszig 1993]:

$$s^2_{\Sigma Z} = s^2_{Z_1} + ... + s^2_{Z_N}. \tag{3.11}$$

Furthermore, for a linear transformation of the form $Z = a + bX$, the standard deviations in X and Z will be related by the factor b:

$$s_Z = |b| s_X. \tag{3.12}$$

If the uncertain parameter is perturbed by a known multiple of its standard deviation then the measured response will represent the same multiple of the output standard deviation:

$$ks_Z = |b| ks_X. \tag{3.13}$$

The factor b is an effect of the system being modelled and, assuming a linear response, is constant.

It follows that the first step in a differential analysis is to define the magnitude of all the variations as the same multiple, k, of standard deviations from the mean. For example, if $k = 3$ then the value $\delta x_1 = 3s_1$ would represent a bound encompassing 99.9% of all possible values of x_1. Once the various result sets have been generated then the standard deviations can be combined [Lomas and Eppel 1992]:

$$\delta Z_{tot} = \sqrt{\sum_{i=1}^{N} (Z - Z_i)^2}. \tag{3.14}$$

If the relationship between the input uncertainties and the measured response is assumed (or has been shown) to be linear then, if the uncertain parameters are varied by a single standard deviation then the measured response will be equal to a single standard deviation. It follows that

$$\begin{aligned} ks_{\Sigma Z} &= k\sqrt{s_{Z_1}^2 + ... + s_{Z_N}^2} \\ &= \sqrt{(ks_{Z_1})^2 + ... + (ks_{Z_N})^2}. \end{aligned} \tag{3.15}$$

It has been demonstrated (Section 3.1) that the effects of uncertainties in building simulation are not independent (*i.e.* superposition does not hold). Despite this equation 3.15 will produce an adequate estimate of the overall uncertainty in the

output given relatively small uncertainties [Lomas and Eppel 1992].

3.1.2 Factorial analysis

One of the restrictions of differential analysis is that parameter interactions are not accounted for, and this deficiency can lead to an incorrect analysis of a model (*e.g.* by not observing a synergistic effect). One way of removing this restriction is through the use of factorial designs where all possible combinations are investigated [Box *et al* 1978, Gardiner and Gettinby 1998].

Typically all variables to be analysed are tested at two values only: the *on* $(x+\delta x)$ and *off* $(x-\delta x)$ levels. The concept can be visualised for a two parameter case as in figure 3.6 (cf. figure 3.1). The two parameters x_1 and x_2 are tested at all four possible states, producing four system responses. Note that no datum response (as was the case for differential analysis) is produced and that responses are only calculated for parameters at their perturbed values. Two measures of the effect of each individual parameter uncertainty can be found. For parameter x_1, see figure 3.7(a), these are:

$$(Z_{x_1+,x_2+} - Z_{x_1-,x_2+})$$

and

$$(Z_{x_1+,x_2-} - Z_{x_1-,x_2-}).$$

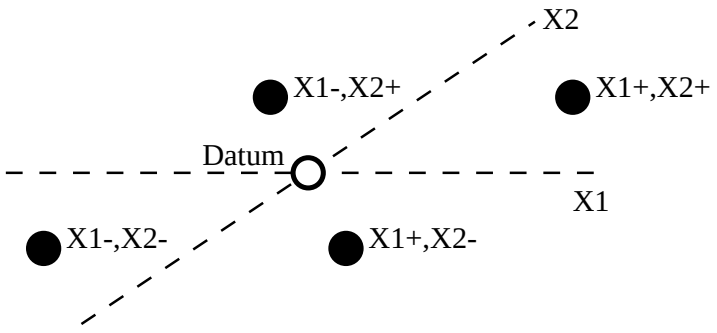

Figure 3.6: Test points for factorial design for 2 parameters.

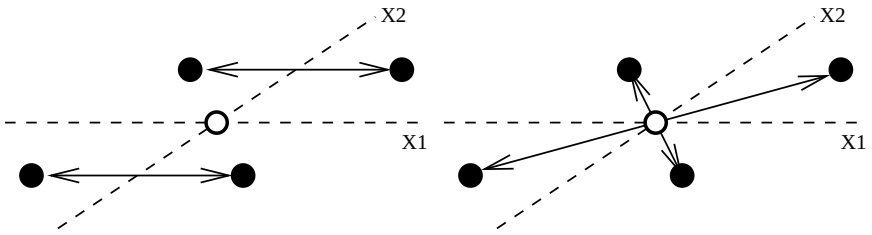

(a) First order effect of x_1. (b) Second order effect of x_1 and x_2.

Figure 3.7: Measures of effect of uncertainties.

The average of these gives the overall measure of the effect,

$$Z_{x_1} = \frac{1}{2}\left[(Z_{x_1+,x_2+} - Z_{x_1-,x_2+}) + (Z_{x_1+,x_2-} - Z_{x_1-,x_2-})\right]. \tag{3.16}$$

Furthermore, as can be seen in figure 3.7(b), there are two measures of the two parameter interaction (the second order effect). Finally, there is a single measure of the mean effect, the average of the four responses. Comparing this with the differential method, which would have required five runs to quantify the first order effects only, the advantage of this method becomes apparent. However, the number of required simulations ($= 2^N$ where N is the number of parameters to be analysed) soon becomes overwhelming.

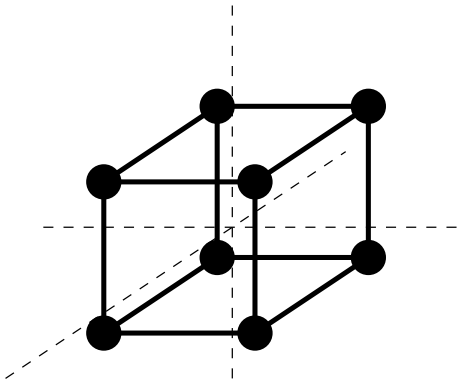

Figure 3.8: Test points for factorial design for 3 parameters.

Efficient methods have been formulated to organise the runs required to achieve a full analysis. Using a three parameter case as an example the design detailed in table 3.1 can be generated ($2^3 = 8$ runs required). The graphical representation

of the modelled cases is depicted in figure 3.8, where the filled in circles represent the simulated models. For each run in table 3.1 the required state of each of the three variables is displayed, *e.g.* for run 1 the experiment is conducted with all parameters at their low or off settings. These parameters could, for example, represent infiltration rate, heater capacity and casual gains, allowing the examination of the effect of individual uncertainties and any possible interactions.

Table 3.1: Factorial design for three variables.

Run	Uncertain Parameter		
	x_1	x_2	x_3
1	-	-	-
2	+	-	-
3	-	+	-
4	+	+	-
5	-	-	+
6	+	-	+
7	-	+	+
8	+	+	+

Thus the responses calculated would represent, for the first run, the response of the building to low infiltration rate, heater capacity and casual gains. In the second run the model's response would be for high infiltration rate and low heater capacity and casual gains.

The analysis procedure for the results of this study is as follows [Box *et al* 1978].

1. Enter the result of each run to the design table, as shown in table 3.2.

2. The average result is $\bar{Z} = \frac{\sum_{i=1}^{R} Z_i}{R}$, where in this example $R = 8$.

3. First order effects are given by associating the sign in the individual parameter column with that run's result, totalling the resulting figures, then dividing by $R/2$. Hence, for parameter x_1, the first order (or main) effect is

$$\Phi_1 = \frac{(Z_2 + Z_4 + Z_6 + Z_8) - (Z_1 + Z_3 + Z_5 + Z_7)}{4}.$$

4. Second order effects, *e.g.* the net effect of varying casual gains and infiltration rate, are given by associating the sign in the interaction parameter column with

Table 3.2: Factorial design for three variables, with interactions and results.

Run	Parameter			Interactions				System
	x_1	x_2	x_3	x_1x_2	x_1x_3	x_2x_3	$x_1x_2x_3$	response
1	-	-	-	+	+	+	-	Z_1
2	+	-	-	-	-	+	+	Z_2
3	-	+	-	-	+	-	+	Z_3
4	+	+	-	+	-	-	-	Z_4
5	-	-	+	+	-	-	+	Z_5
6	+	-	+	-	+	-	-	Z_6
7	-	+	+	-	-	+	-	Z_7
8	+	+	+	+	+	+	+	Z_8

that run's result, totalling the resulting figures, then dividing by $R/2$ as before. The signs in the interaction column are found by multiplying the signs of the individual parameters constituting the interaction.

Clearly factorial designs can become impractical, with R the number of runs required being associated with N parameters via the relationship:

$$R = 2^N. \tag{3.17}$$

For example, if $N = 5$ then the required number of runs would be 32. The results from these runs would give a measure of:

- the average response
- the 5 first order effects,
- the 10 second order effects (the effect of two parameter interactions),
- the 10 third order effects (the effect of three parameter interactions),
- the 5 fourth order effects (the effect of four parameter interactions),
- the fifth order effect.

The number of interactions follows from a combinatorial analysis of the parameters, five in this case: for example, there are ten possible combinations whereby three

parameters can be selected (and hence interact) and only one combination whereby all parameters can be selected.

The interaction effects (second order and above) are generally weaker than the effects of lower orders. Thus, where only first and second order effects are required, only a portion of the factorial design needs to be executed, the resulting designs are known as fractional factorial designs [Box *et al* 1978].

Fractional Factorial Designs

This is a method by which the total number of runs R can be decreased without adversely affecting the results of the analysis. Figure 3.9 shows that for a three parameter design only four simulations, represented by the filled in circles, are required.

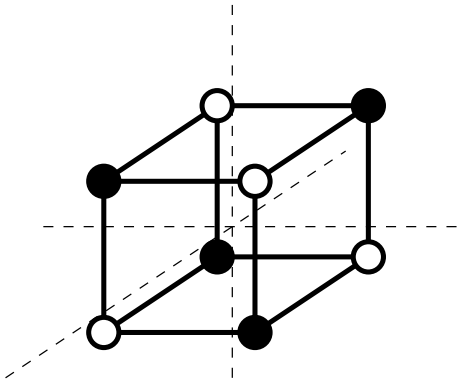

Figure 3.9: Test points for half fraction factorial design for 3 parameters.

To illustrate this, table 3.3 has been generated for four uncertain parameters. The parameter states for variable x_4 have been generated by associating, or *aliasing*, x_4 with the $x_1x_2x_3$ interaction. Aliasing is the mechanism whereby the required states of the parameter x_4 are generated for each of the simulations [Box *et al* 1978]. In this example the full factorial design for three parameters is created, the aliasing mechanism then sets the fourth parameter to the product of the other parameter perturbations for each run. For example, in run 1 the perturbation for x_4 will be $-1 \times -1 \times -1\times = -1$, for run 2 $+1 \times -1 \times -1\times = +1$, and so on. This generates a list of the required states of x_4 for each of the R simulations as displayed in table 3.3.

The effect of this aliasing is displayed in table 3.4 where it can be seen that the

Table 3.3: Fractional factorial design for four variables.

Run	Parameter			
	x_1	x_2	x_3	x_4
1	-	-	-	-
2	+	-	-	+
3	-	+	-	+
4	+	+	-	-
5	-	-	+	+
6	+	-	+	-
7	-	+	+	-
8	+	+	+	+

estimation[2] of the second order effects will be equal for interactions: x_1x_4 and x_2x_3, x_1x_3 and x_2x_4, and x_1x_2 and x_3x_4. For example for x_1x_4 and x_2x_3:

$$\Phi_{1,4} = \frac{Z_1 + Z_2 - Z_3 - Z_4 - Z_5 - Z_6 + Z_7 + Z_8}{4}$$
$$\Phi_{2,3} = \frac{Z_1 + Z_2 - Z_3 - Z_4 - Z_5 - Z_6 + Z_7 + Z_8}{4}$$

so that

$$\Phi_{1,4} = \Phi_{2,3}. \tag{3.18}$$

Furthermore, the first order effects will have the same value as a corresponding third order effect, *e.g.* $\Phi_{1,2,3} = \Phi_4$, $\Phi_{1,2,4} = \Phi_3$. These results are not surprising when the method to design the parameter states is recalled. This effect is termed *confounding* as the estimates generated are the sum of the individual effects, thus if third order effects are assumed to be insignificant then the estimate of the effect of uncertainty in the individual variables will be good. In this case the second order estimates are confounded with each other. Therefore, further runs (*e.g.* those remaining to complete the full factorial design) would be required to gain accurate estimates of their effects.

In general if a fractional factorial design is employed there will be $2^p - 1$ aliases for each effect, where $\frac{1}{2^p}$ is the level of fractionation [Gardiner and Gettinby 1998].

[2] As only a fraction of the full factorial design is being used any results generated will only be estimates of the effects.

Table 3.4: Fractional factorial design for four variables, with interactions and results.

	Parameter				Interaction								
Run	x_1	x_2	x_3	x_4	x_1x_2	x_1x_3	x_1x_4	x_2x_3	x_2x_4	x_3x_4	$x_1x_2x_3$	*etc*	Result
1	-	-	-	-	+	+	+	+	+	+	-	...	Z_1
2	+	-	-	+	-	-	+	+	-	-	+	...	Z_2
3	-	+	-	+	-	+	-	-	+	-	+	...	Z_3
4	+	+	-	-	+	-	-	-	-	+	-	...	Z_4
5	-	-	+	+	+	-	-	-	-	+	+	...	Z_5
6	+	-	+	-	-	+	-	-	+	-	-	...	Z_6
7	-	+	+	-	-	-	+	+	-	-	-	...	Z_7
8	+	+	+	+	+	+	+	+	+	+	+	...	Z_8

The example in table 3.4 is a half fraction, $p = 1$, indicating that only one alias was required to create the design. This alias is also called the *defining contrast* of the design. The value of p is thus the number of defining contrasts used in creating the design, *e.g.* in the example in table 3.4 there was one defining contrast, $x_4 = x_1x_2x_3$. To create a quarter fraction design would therefore require two defining contrasts. As higher degrees of fractionation are used the aliasing between effects will become more complex.

The levels at which aliasing occurs affects the efficacy of this technique. For example, in table 3.4 the second order effects are confounded with each other. The nature of this confounding is the sum of the individual effects; thus if the effect of the x_1x_4 interaction is +2 and the effect of x_2x_3 is -2 then the confounded effect would be zero and, as such, the significance of these interactions is not quantified. For example the uncertain parameters could represent: conductivity, thickness, specific heat capacity and density of a material. In this design, the effect of changing conductivity and density (x_1x_4), and thickness and specific heat capacity (x_2x_3) would be confounded and hence it would not be possible to measure the effect of the second order interaction. The term *design resolution* is used to describe at what levels confounding occurs, *i.e.* to what level of interaction the effects will be quantified; in the present example the resolution is IV.

The confoundings encountered for the most common resolutions[3] are [Box *et al* 1978]:

[3]The design resolution is always given in Roman numerals.

III First order effects are confounded with second order effects, but not with each other.

IV Second order effects are confounded with each other, but first order effects are not confounded with each other *or* with second order effects.

V First and Second order effects are not confounded with each other, but second order effects are confounded with third order effects.

For building simulation, if only the main effects of the uncertainties were to be calculated, then a fractional design of resolution at least III and preferably IV would be required. Two parameter interactions are common in building simulation (see section 6.4). Therefore a design of resolution V would be the most suitable for the majority of building simulation studies. Unfortunately, there does not exist a formula relating the design resolution for the N uncertain variables at a factorisation p [Gardiner and Gettinby 1998, Grove and Davis 1992]. Designs for given resolutions and number of parameters are available in the literature [Box *et al* 1978].

Finally, the above description of the factorial and fractional factorial method can be extended into the time domain in an analogous manner to the differential method 3.1.1. This will allow an examination of how the effects change over time, an aspect of building simulation which was described in section 3.1.1.

3.1.3 Monte Carlo analysis

The previous techniques have relied on a structured approach generating limits on the output by combining and analysing the differences between results sets with known input parameters. The Monte Carlo technique only requires that the model inputs are described by a probability distribution.

The method proceeds by randomly generating perturbed models which lie within the distributions defined for the uncertain parameters, *i.e.* the parameter k is no longer constant. For the previous methods the perturbed models were generated by altering the datum model to specific points on the uncertain parameters' distributions, *e.g.* three standard deviations (see sections 3.1.1 and 3.1.2). For Monte-Carlo analysis

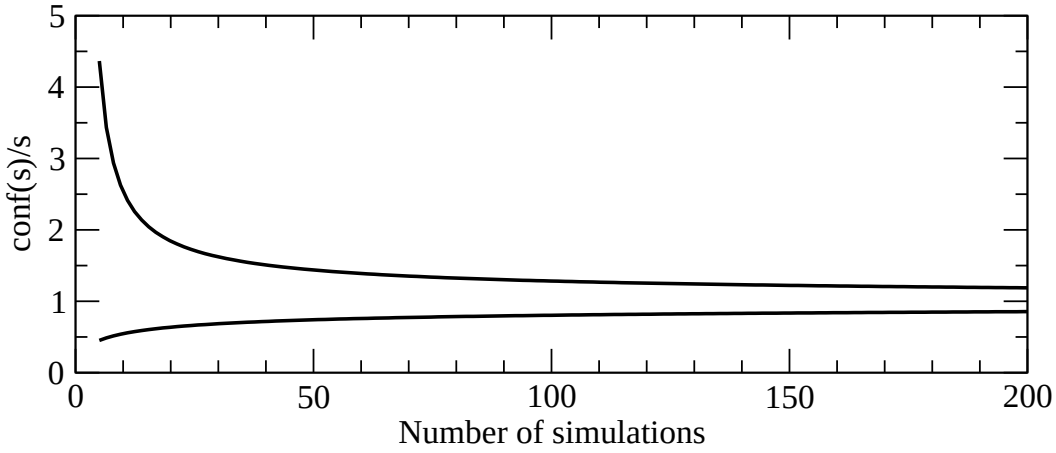

Figure 3.10: Confidence interval on normalised standard deviation

the perturbed models are randomly created by using the probability distributions of the uncertain parameters. This is a subtle difference but more accurately generates a probability distribution for the overall system performance as combinations of extreme responses are by definition unlikely and interactions between parameters are fully accounted for.

The technique relies upon the central limit theorem to estimate the distribution of the predictions. Using the same model as before, many simulations are run at various values of x_1 through x_N (all variables are varied at the same time). Once a sufficient number of simulations have been run, the resulting performance will exhibit a normal distribution, *i.e.* the central limit theorem, equation 3.19 holds. This theorem states that the cumulative total of many variables, regardless of their individual distributions, will be characterised by a normal distribution. This is a generalisation of the DeMoivre-Laplace approximation [Kreyszig 1993] (that the cumulative binomial distribution could be represented by a normal distribution).

$$\lim_{n\to\infty} P\left(\frac{\bar{X}_n - \mu}{\sigma/\sqrt{n}} \leq z\right) = \Phi(z) = \frac{1}{\sqrt{2\pi}} \int_{-\infty}^{z} e^{-u^2/2}\, du \tag{3.19}$$

where $\bar{X}_n$ is the mean of the n measurements X. In other words, the probability that the mean of the measurements standardised by the population mean and variance is less than or equal to z is equal to the integral. Tabulated values of the integral are widely published [Kreyszig 1993].

The method usually requires 60 – 80 simulations regardless of the number of input parameters [Lomas and Eppel 1992]. Thus it is well suited for use in building simulation. Figure 3.10 shows the normalised confidence in the estimation of the standard deviation against the number simulations used to generate the calculation of the standard deviation, it can be seen that after 60 simulations the increase in confidence due to extra simulations is marginal. Also, the restrictions of the differential method do not apply as interactions are fully accounted for. To analyse the results of the simulations, the arithmetic mean and standard deviation can be calculated at each time-step:

$$\bar{Z} = \frac{\sum_{i=1}^{R} Z_i}{R} \tag{3.20}$$

$$s = \sqrt{\frac{1}{R-1}\left(\sum_{i=1}^{R}(Z_i - \bar{Z})^2\right)}. \tag{3.21}$$

A probability curve of an event occurring can now be created (for example, the probability of a building overheating in summer can be quantified). Furthermore, the comparison of different designs can be compared statistically to test the significance of a design alteration. To date this test has been omitted from the design process when simulation has been employed.

Significance testing

Currently users of building simulation use the terms 'significance' and 'insignificance' informally when describing the difference that a design change makes to the building's performance. With the ability to quantify the overall uncertainty in the output (*via* a Monte Carlo analysis), the significance of a design change can be formally quantified using a standard test [Gardiner and Gettinby 1998]. This statistical approach enables the practitioner to differentiate between an apparently significant difference and a truly significant one.

For a statistical test a hypothesis is required, for example $x_1 = x_2$. The statistical test is then performed to discover whether the hypothesis is true or false.

The hypothesis is referred to as the null hypothesis. This gives rise to a counter

assumption or alternate hypothesis which is often easier to test. For example if the hypothesis is $x_1 = x_2$ then alternatives would be:

$$x_1 > x_2 \tag{3.22}$$

$$x_1 < x_2 \tag{3.23}$$

$$x_1 \neq x_2 \tag{3.24}$$

The statistical test requires a significance level. The significance level determines the probability of coming to the wrong conclusion. For example, if the significance level is 5% then one in twenty tests would be rejected even though it was true. Clearly, the lower the significance level the lower the risk of making the wrong decision.

Various statistical tests exist depending upon the information available and what is to be tested [Kreyszig 1993]. In the case of comparing two means of normal distributions (as is the case with results of a Monte Carlo analysis) the following formula is used:

$$t_0 = \sqrt{R}\frac{\mu_x - \mu_y}{\sqrt{s_x^2 + s_y^2}}, \tag{3.25}$$

where t_0 is the test statistic and provided that there were R simulations for each of the two Monte Carlo analyses (x and y). The critical value for this test is read from a table of the t-distribution for R degrees of freedom at the required significance level.

For example, if the annual energy consumption of two designs is to be compared the null hypothesis would be that the energy consumptions are equal. The alternative is the energy consumptions are not equal. Thus, if t_0 is greater than the critical value then the alternative hypothesis is true and the energy consumptions are different.

Non-random sampling

Various alternative sampling procedures have been developed for Monte Carlo analyses [Saltelli *et al* 2000]. Briefly:

Stratified sampling requires the subdivision of the probability distribution of the input factors. Samples are drawn from each stratum of the distribution thus

guaranteeing coverage of the whole distribution. However, the analysis is complicated by requiring weighting of the samples in the calculation of mean and variance.

Latin hypercube sampling is a particular case of stratified sampling where each stratum has equal probability, thus gaining the benefits of stratified sampling without the complications of the analysis. However, the estimated variance has been shown to be biased.

Quasi-random sampling uses a pre-calculated sequence to determine the changes to be made to the input model. Some of these sequences are more effective than others but have the aim of increasing the convergence rate of the Monte Carlo simulations.

However, only random sampling produces unbiased estimates of the mean and standard deviation.

3.1.4 Summary

External methods were originally employed to assess the effects of uncertainties of the few controllable parameters on the outcome of an experiment. These techniques can be applied to computer experiments or simulations and their advantages and disadvantages are summarised in table 3.5. When employing these methods in practice problems of scale and data storage/ retrieval become major issues. The application of these methods is presented in Chapter 5.

Method	Advantages	Disadvantages
Differential	Easy to implement and understand results	Only measures main effects
Factorial	Measures main effects and interactions	Number of simulations required for large number of uncertain parameters
Monte Carlo	Required number of simulations independent of number of uncertain parameters	Only measures overall uncertainty

Table 3.5: Advantages and disadvantages of external methods

3.2 Internal methods

The previous section considered methods of assessing the effects of uncertainty from the outside of the system. However, the treatment of errors in experiments is always taught using a few basic arithmetical relationships whereby an upper bound on the effect of measurement accuracy can be quantified on the result of an experiment. This is the starting point for this section where arithmetical techniques are reviewed.

The motivation for this analysis is that building simulation uses a deterministic approach to provide a solution to the governing conservation equations, as described in chapter 2. If arithmetical methods can be included in the equation-sets themselves then the uncertainty can be fully quantified during a simulation, negating the requirement for multiple simulations (as the effects of uncertainty will be known at all stages of the calculation process, no matter how complex).

3.2.1 Basic treatment

The treatment of errors in simple equations is straightforward and is treated in many texts, *e.g.* [Kreyszig 1993]. Initially two rules must be formulated which enable the bounding of subsequent operations. The value of a number is approximated by a and is represented by the sum of its true value $\tilde{a}$ and error ϵ:

$$a = \tilde{a} + \epsilon. \tag{3.26}$$

The error term has magnitude defined as $|\epsilon| \leq \beta$.

Error propagation

The error bound (β) can be estimated by the following methods. Consider two approximately known numbers:

$$\begin{aligned} x &= \tilde{x} + \epsilon_x; \quad |\epsilon_x| \leq \beta_x \\ y &= \tilde{y} + \epsilon_y; \quad |\epsilon_y| \leq \beta_y \end{aligned} \tag{3.27}$$

Addition and subtraction of x and y behave in a similar manner; subtraction is expanded here:

$$\begin{aligned} |\epsilon_{(x-y)}| &= |x - y - (\tilde{x} - \tilde{y})| \\ &= |x - \tilde{x} - (y - \tilde{y})| \\ &= |\epsilon_x - \epsilon_y| \\ &\leq |\epsilon_x| + |\epsilon_y| \\ &\leq \beta_x + \beta_y. \end{aligned} \tag{3.28}$$

Thus the error in the operation is less than or equal to the sum of the original errors.

Multiplication and division likewise behave in a similar manner. However a new term, the relative error, ϵ_r, is defined as

$$\epsilon_r = \frac{\epsilon}{a} = \frac{a - \tilde{a}}{a}; \quad |\epsilon_r| \leq \beta_r. \tag{3.29}$$

When multiplying two numbers x and y as defined above:

$$\begin{aligned} |\epsilon_{(xy)}| &= |x \cdot y - (\tilde{x} \cdot \tilde{y})| \\ &= |x \cdot y - ((x - \epsilon_x) \cdot (y - \epsilon_y))| \\ &= |y\epsilon_x + x\epsilon_y - \epsilon_x\epsilon_y| \\ &\simeq |y\epsilon_x + x\epsilon_y| \\ \equiv |\epsilon_r| &= |\frac{y\epsilon_x + x\epsilon_y}{xy}| \\ &\leq |\epsilon_{rx}| + |\epsilon_{ry}| \\ &\leq \beta_{rx} + \beta_{ry}. \end{aligned} \tag{3.30}$$

Thus the error in the operation is less than or equal to the sum of the original relative errors.

This is a crude but effective method of analysing the effect of uncertainties in data and can be effectively employed in algorithm design. Applying these rules to a simple

linear system the error in the result becomes

$$|\epsilon| \leq (\beta_{rm} + \beta_{rx}) \cdot (mx) + \beta_c. \tag{3.31}$$

As can be seen any overestimation in the relative error in the calculation of the product is scaled by the product itself before being added to the error in the constant term.

The main limitations with this method are that it only approximates the effect of the uncertainties (by overestimating the maximum uncertainty) and that every calculation has to be analysed individually and that relationships between parameters are ignored thus leading to overestimation. However, alternative methods have been developed and are now discussed.

3.2.2 Range arithmetic overview

Instead of categorising the error as an inequality, this information can be used directly, by range arithmetic methods, within the simulation calculations. All of the methods introduced and subsequently developed in this section are based on interval arithmetic [Neumaier 1990], which in its generalised form is known as fuzzy arithmetic.

The need for a mathematical representation of the inherent uncertainty in information has been addressed for about 40 years. This approach has necessitated the alteration of the basic arithmetical operations. A clearly defined branch of mathematics has resulted, which can deal with the calculation of equations where the parameters are not represented by a single number but rather a range of numbers.

By approaching the problem of solving uncertain systems in such a fashion, the full range of possibilities is being generated at each stage of the solution process and thus none of the information regarding the range of the uncertain information is lost.

By the late 1970's the limitations of interval arithmetic were well documented. The main limitation, identified at this time, was that the assumed probability distribution of the interval is even *i.e.* all possible values in the range are equally possible. The

effect of this is that the resulting predictions were generally over pessimistic about the size of the solution interval. This problem has been addressed, and the generalised form of interval arithmetic, allowing ranges to be described by a membership function, was created: fuzzy arithmetic.

Another limitation of interval arithmetic is that relationships between parameters are ignored. This is of particular importance in building simulation applications as will be demonstrated.

Of course any implementation of such fundamental alterations to the arithmetical operations requires significant changes to the calculation procedures employed in a deterministic simulation tool, as every single operation has to be replaced by an alternative representation that embodies the range arithmetic constructs.

3.2.3 Interval arithmetic

This method relies on the use of *interval numbers* which are defined as a range in the set of real numbers (e.g. π could be represented as $3 \leq \pi \leq 4$ or $[3, 4]$), where each value of the number has equally probability between the limits of the range. The underlying arithmetical operations have to be redefined.

Interval arithmetic applied to systems of equations is ideally suited for uncertainty analysis problems:

> "If x is a vector of approximate data and Δx is a vector containing the bounds for the error in the components of x, one is often interested in the influence of these errors on the result $Z(x)$ of a computational process; *i.e.* one is interested to find a vector ΔZ such that, for given Δx,
>
> $$|Z(\tilde{x}) - Z(x)| \leq \Delta Z \text{ for } |\tilde{\mathrm{x}} - \mathrm{x}| \leq \Delta \mathrm{x}.$$
>
> Sometimes the dependence of ΔZ on Δx is also sought." [Neumaier 1990]

Interval Numbers

An interval number x is defined as a range of values, all equally probable, with a

lower bound defined as $\underline{x}$ and its upper bound defined as $\overline{x}$. A specific element of x is defined as $\tilde{x}$, or mathematically,

$$x \equiv [\underline{x}, \overline{x}] := \{\tilde{x} \in \mathbb{R} | \underline{x} \leq \tilde{x} \leq \overline{x}\}. \tag{3.32}$$

Interval vectors and arrays are defined likewise, with each element consisting of a lower and upper bound. The comparison and inclusion ranges ($\leq, <, \geq, >, \subseteq, \supseteq$) are used componentwise.

Interval Computations

Binary functions

The binary operators, $\circ := \{+, -, *, /\}$ can be applied to intervals where the largest interval resulting from the binary operation is to be found:

$$x \circ y := \{\tilde{x} \circ \tilde{y} | \tilde{x} \in x, \tilde{y} \in y\} \tag{3.33}$$

for all x,y defined in the set of real interval numbers. This restricts the division function to exclude any interval where $0 \in y$. Representing the interval numbers x and y as $x = [\underline{x}, \overline{x}]$ and $y = [\underline{y}, \overline{y}]$, equation 3.33 can be expanded as follows

$$x \circ y := \square\{\underline{x} \circ \underline{y}, \underline{x} \circ \overline{y}, \overline{x} \circ \underline{y}, \overline{x} \circ \overline{y}\} \tag{3.34}$$

where $\square$ is a function describing the set containing the four calculated values. It is possible to calculate the end points of $\square$ directly in most cases. For addition and subtraction see equations 3.35, for multiplication see table 3.6, and for division see table 3.7.

$$\begin{aligned} x + y &= [\underline{x} + \underline{y}, \overline{x} + \overline{y}] \\ x - y &= [\underline{x} - \overline{y}, \overline{x} - \underline{y}] \end{aligned} \tag{3.35}$$

Table 3.6: Interval multiplication (xy)

	$y \geq 0$	$y \ni 0$	$y \leq 0$
$x \geq 0$	$[\underline{x}\underline{y}, \overline{x}\overline{y}]$	$[\overline{x}\underline{y}, \overline{x}\overline{y}]$	$[\overline{x}\underline{y}, \underline{x}\overline{y}]$
$x \ni 0$	$[\underline{x}\overline{y}, \overline{x}\overline{y}]$	$[\min(\underline{x}\overline{y}, \overline{x}\underline{y}), \max(\underline{x}\underline{y}, \overline{x}\overline{y})]$	$[\overline{x}\underline{y}, \underline{x}\underline{y}]$
$x \leq 0$	$[\underline{x}\overline{y}, \overline{x}\underline{y}]$	$[\underline{x}\overline{y}, \underline{x}\underline{y}]$	$[\overline{x}\overline{y}, \underline{x}\underline{y}]$

Table 3.7: Interval division (x/y)

	$y > 0$	$y < 0$
$x \geq 0$	$[\underline{x}/\overline{y}, \overline{x}/\underline{y}]$	$[\overline{x}/\overline{y}, \underline{x}/\underline{y}]$
$x \ni 0$	$[\underline{x}/\underline{y}, \overline{x}/\underline{y}]$	$[\overline{x}/\overline{y}, \underline{x}/\overline{y}]$
$x \leq 0$	$[\underline{x}/\underline{y}, \overline{x}/\overline{y}]$	$[\overline{x}/\underline{y}, \underline{x}/\overline{y}]$

Unary functions

For any unary function, f, the following has to be solved:

$$f(x) = [\min_{\tilde{x} \in x} f(x), \max_{\tilde{x} \in x} f(x)]. \tag{3.36}$$

For monotonic functions[4] an explicit representation of equation 3.36 can be generated:

$$\begin{aligned} \ln x &= [\ln \underline{x}, \ln \overline{x}] \; x \geq 0 \\ \mathrm{e}^{\mathrm{x}} &= [\mathrm{e}^{\underline{\mathrm{x}}}, \mathrm{e}^{\overline{\mathrm{x}}}]. \end{aligned} \tag{3.37}$$

This would be employed in the calculation of local discomfort due to the air temperature difference between ankle and head height according to prENV 1752, where:

$$\mathrm{PPD} = 0.7038 + 0.2974 \delta\theta^{2.7810} - 0.084 \exp^{\delta\theta}. \tag{3.38}$$

The PPD is the percentage of people dissatisfied due to the temperature difference, $\delta\theta$ ($^{\circ}C$). For non-monotonic functions[5] the periodicity of the function can be used to define the range of result of the function.

[4] A monotonic function has a one-to-one relationship between the dependent and independent variable, *e.g.* $y = x$

[5] A non-monotonic function has a many-to-one relationship between the dependent and independent variable, *e.g.* $y = x^2$ or $y = \sin x$

Linear Interval Equations

These arithmetic rules can now be applied to the building conservation equations and their solution. As will be demonstrated, the main problem encountered by a simple implementation is that the solution bounds grow quicker than the solution is found. This effect is known as wrapping [Barbarosie 1995] and can be minimised but not removed.

The wrapping effect

Recalling the zone energy balance equation set of section 2.2.3 the linear system $Ax = b$ is here assumed to be a linear interval system where

$$A = \begin{bmatrix} [\underline{a}_{11}, \overline{a}_{11}] & [\underline{a}_{12}, \overline{a}_{12}] & \cdots \\ [\underline{a}_{21}, \overline{a}_{21}] & \cdots & \cdots \\ \cdots & \cdots & \cdots \\ [\underline{a}_{n1}, \overline{a}_{n1}] & \cdots & [\underline{a}_{nn}, \overline{a}_{nn}] \end{bmatrix}. \tag{3.39}$$

and the vectors x and b are likewise composed of interval numbers. There are two main solution methods to the interval equation $Ax = b$: direct and iterative. The aim of any solution method is not only to find an enclosure bounding the solution but to find the *hull* of the solution set, *i.e.* the tightest possible bound on the solution.

For example, consider transient conduction in an opaque solid material. Assume the material (concrete) is well specified, except for the conductivity which is uncertain, as shown in table 3.8.

Table 3.8: Example thermophysical properties of concrete.

Property	Value	Unit
Density	2000	kg/m^3
Heat capacity	800	J/kgK
Conductivity	[1.4,1.6]	W/mK

The sample of concrete is initially at a constant temperature of 10°C and the two ends of the sample are simultaneously cooled. Recalling equation 2.4, the coefficients

of the arrays can now be generated. The coefficients for the first row are

$$\begin{pmatrix} 2\rho C + \frac{2k\delta t}{(\delta x)^2} & \frac{-2k\delta t}{(\delta x)^2} & 0 \\ \dots & \dots & \dots \\ \dots & \dots & \dots \end{pmatrix} \begin{pmatrix} \theta_{1,t+1} \\ \theta_{2,t+1} \\ \theta_{3,t+1} \end{pmatrix} = \begin{pmatrix} 2\rho C - \frac{2k\delta t}{(\delta x)^2} & \frac{2k\delta t}{(\delta x)^2} & 0 \\ \dots & \dots & \dots \\ \dots & \dots & \dots \end{pmatrix} \begin{pmatrix} \theta_{1,t} \\ \theta_{2,t} \\ \theta_{3,t} \end{pmatrix}.$$

Enumerating the right hand side of the above results in

$$\begin{pmatrix} 3\,200\,000 - [4\,032\,000, 4\,608\,000] & [4\,032\,000, 4\,608\,000] & 0 \\ \dots & \dots & \dots \\ \dots & \dots & \dots \end{pmatrix} \begin{pmatrix} 10 \\ 10 \\ 10 \end{pmatrix}$$

assuming a time step (δt) of $3600s$ and a distance (δx) of $5cm$ between nodes. Following the rules of interval arithmetic the result of this matrix multiplication is

$$[26\,240\,000, 325\,760\,000].$$

In this example, the hull, or smallest solution set is the single value $32\,000\,000$ as the multiplication can be reformulated as

$$\begin{aligned} & 2\rho C\theta_{1,t} + \frac{2k\delta t}{(\delta x)^2}(\theta_{2,t} - \theta_{1,t}) \\ = \;& 3\,200\,000 \times 10 + [4\,032\,000, 4\,608\,000] \times (10 - 10) \\ = \;& 32\,000\,000. \end{aligned}$$

Clearly, the initial solution is a considerable overestimation of the smallest possible solution set. If such overestimations were repeated then the solution of a system of equations could become unbounded, *i.e.* the solution would be the set of real numbers. It should be noted that the initial solution is not incorrect as the correct solution is still bounded by the large range, *i.e.* it has wrapped the smallest possible solution in a larger set.

To minimise this effect requires careful encoding of equations as it is due to interval arithmetic not recognising relationships between numbers. In the above example, the

$\frac{2k\delta t}{(\delta x)^2}$ term was treated as two independent ranges in the initial calculation: this is an unwanted effect of interval arithmetic. This is the main reason for the wrapping effect: at each stage of the calculation the numbers are treated as independent ranges, thus there can be no cancellation [Neumaier 1990] This lack of correlation between uncertainties is a crucial aspect of interval arithmetic and will be referred to later.

Direct solution

Direct solution is generally the preferred solution method for a set of linear equations, as is the case with the building energy conservation equations.

The interval Gaussian elimination method is applied as the normal Gaussian elimination would be, except the arithmetic operations are redefined as described previously. It has been shown that in some cases this method produces the hull of the solution set [Ning and Kearfott 1997]. Despite this, the solution bounds still grow exponentially and with a transient simulation after a few time steps the solution interval is too large to be of practical use.

A more computationally efficient method is the LU decomposition. This approach is particularly suitable to transient energy systems as the decomposition is independent of the right hand side of the equation, and therfore only needs to be calculated once. However, it is not possible to get a tight bound on the decomposed arrays due to the wrapping effect.

Indirect solution

Indirect methods rely on iterative procedures to calculate an approximate solution of the problem. The Gauss-Seidel method for the system of equations $Ax = b$ is

$$x_i^{n+1} = \frac{1}{a_{ii}} \left[b_i - \sum_{j=1}^{i-1} a_{ij} x_j^{n+1} - \sum_{j=i+1}^{N} a_{ij} x_j^n \right]$$

given an initial approximation of the solution x and where n is the iteration number.

The method has been reformulated for interval calculations [Neumaier 1990]:

$$x_i^{n+1} \quad = \quad \Gamma \left(a_{ii} \ , \ b_i - \sum_{j=1}^{i-1} a_{ij} x_j^{n+1} - \sum_{j=i+1}^{N} a_{ij} x_j^n \ , \ x_i^n \right)$$

where the Gauss-Seidel operator Γ is defined as

$$\Gamma(a,b,x) = \begin{cases} b/a \cap x & \text{if } 0 \ni a, \\ \square(x \backslash] \underline{b}/\underline{a}, \underline{b}/\overline{a}[) & \text{if } b > 0 \in a, \\ \square(x \backslash] \overline{b}/\overline{a}, \overline{b}/\underline{a}[) & \text{if } b < 0 \in a, \\ x & \text{if } 0 \in a, b \end{cases}$$

where

$$\begin{aligned} a &= a_{ii} \\ b &= b_i - \sum_{j=1}^{i-1} a_{ij} x_j^{n+1} - \sum_{j=i+1}^{N} a_{ij} x_j^n \\ x &= x_i^n \end{aligned}$$

and the set operation $\square(x \backslash] \underline{b}/\underline{a}, \underline{b}/\overline{a}[)$ means that the updated value x_i^{n+1} is equal to the current x_i^n less the values in the range $(\underline{b}/\underline{a}, \underline{b}/\overline{a})$. This method requires an approximate solution to the problem and calculates successively tighter bounds for each term in the solution array where applicable. It is therefore suited as a step in the solution process after the initial solution by an explicit method, as the overestimation will be reduced by the iterative process. As such, this process can be termed the iterative improvement of the solution.

The advantage of an iterative approach is that the original matrix is used for all stages of the calculation. Thus, the disadvantages of the LU factorisation are removed. However, an iterative approach will require more arithmetical operations than the LU decomposition.

Summary

All of the above methods for sets of interval equations can be termed pessimistic

as they contain all the possible solutions plus some additional non-solutions due to the wrapping of the solution set. There exist methods in geometry theory to define the shape of the boundary of the solution set as a polytope (a multi-faceted body in multi-dimensional space) although the data structures associated with these shapes are cumbersome and not suited to efficient calculations, and hence building energy system simulation. An interesting solution to this problem is proposed by Neumaier where the solution set is not defined as a hypercube but as an ellipsoid, resulting in fewer non-solutions being contained in the solution set [Neumaier 1993]. Again the data structure is more complex for this representation and is not suitable for building energy system simulation. Another approach is to use generalised interval arithmetic, also known as fuzzy arithmetic.

3.2.4 Fuzzy arithmetic

Fuzzy numbers are a direct extension of the principles behind interval numbers. Whereas the probability of the number existing in an interval is equal at all points in interval arithmetic, a fuzzy number's existence is defined as a function: the membership function that defines the vagueness in the value that the number represents.

Fuzzy numbers

An interval number represents a range of possible values that define an entity: a value is either within the interval or outside the interval, there is no ambiguity. In fuzzy arithmetic this representation is termed *crisp* as the limits are clearly defined. However information is rarely clearly defined and the concept of membership emerges. The idea behind membership is to express mathematically the vagueness in a value more clearly than through the use of a lower and upper bound on that value.

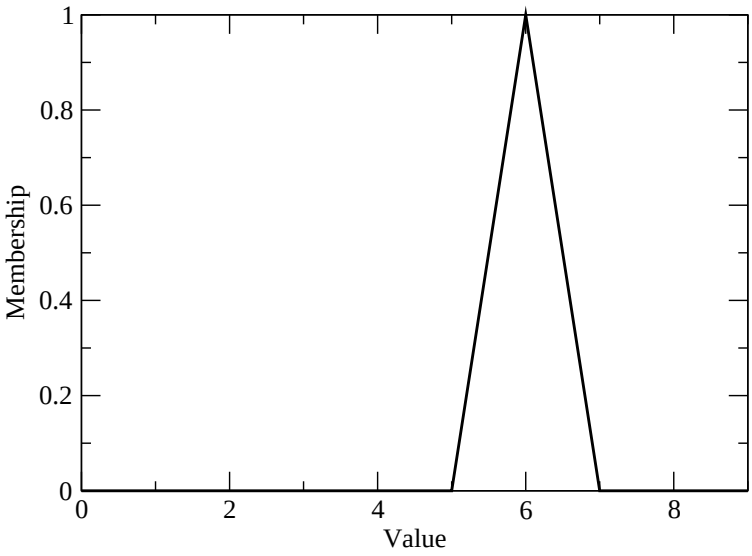

Figure 3.11: Fuzzy representation of 'about 6'.

For example, the air supply rate to a room is $6l/s$. However, due to variations in pressure the rate can vary between $5l/s$ and $7l/s$ but is usually about $6l/s$. In interval arithmetic terms the flow rate would be defined as the interval [5,7], but in fuzzy arithmetic the likelihood of a value can be quantified. This means that the knowledge that the flow rate is usually $6l/s$ can be described. A representation of the air supply rate is shown in figure 3.11. As can be seen the flow rate varies between $5l/s$ and $7l/s$ (as was the case with interval arithmetic) but the most likely rate is $6l/s$.

The y-axis of figure 3.11 represents the degree of membership, which in this case shows that a membership value of zero applies to flow rates of less than $5l/s$ and more than $7l/s$, *i.e.* these states will not occur. The membership value of one for a flow rate of $6l/s$ states that this flow rate level will occur.

Calculations using fuzzy numbers take not only the range of values into account but the membership of the range. The advantage of this style of representation is that the likelihood of extreme values dominating the calculation is reduced while still accounting for these extreme values. The resulting output will evaluate the membership function for all values of the output.

Fuzzy computations

Again the basic arithmetic operations have to be redefined. The definitions are the same as for interval numbers but have to be repeated at different levels of membership to account for the shape of the membership function. The general method is as follows [Ross 1995].

1. Choose membership levels at which the calculation will be performed.
2. Take α cuts at each of these levels, *i.e.* solve the membership function for each of these levels (this results in an interval number).
3. Evaluate each solution of step 2 using interval arithmetic techniques as described in the previous section.
4. Construct the membership function of the resulting solution.

This process can be computationally intensive if many α cuts are taken. The advantage of adopting this method is that at the early design stage models can be created with membership functions spanning a large range of possible values. As the design evolves the membership functions can be refined. As with interval arithmetic, implementation is non-trivial.

There are two criticism of the fuzzy approach. Primarily the history of values (hence the correlations between parameters) is not accounted for. Thus, the problem of wrapping will occur as for interval arithmetic. Secondly, it is not always possible to obtain the solution of a set of simultaneous equations with fuzzy arithmetic [Buckley 1992].

Summary

While the fuzzy approach offers some advantages over the basic interval arithmetic approach, most notably the varying expectation of a value via the membership function, it does not address the major shortcomings of the interval approach. The fuzzy approach is therefore inappropriate for the solution of the building conservation equations.

3.2.5 Affine arithmetic

This method attempts to keep the benefits of the interval arithmetic model as well as tracking the correlations between data. The affine model is a linear transformation of the uncertain quantity where the uncertainty associated with the data is held as a separate token (e.g. π could be represented as $3 \leq \pi \leq 4$ or $3.5 + 0.5\epsilon_1$ where ϵ_1 is the first uncertainty token and $\epsilon_1 = [-1, 1]$); each value of the number is equally likely between the limits of the range as in interval arithmetic [Stolfi and de Figueiredo 1997]. Again the underlying arithmetical operations have to be redefined.

The method was originally developed for ray tracing calculations but is ideally suited for systems of uncertain equations.

Affine Numbers

An affine number, $\hat{x}$, is defined as a range of values, all equally probable, via a first-degree polynomial. A specific element of $\hat{x}$ is defined as $\tilde{x}$, or mathematically

$$\tilde{x} := \hat{x} = x_0 + x_1\epsilon_1 + x_2\epsilon_2 + x_n\epsilon_n. \tag{3.40}$$

The x_i for $i \geq 1$ are uncertainty coefficients (*e.g.* if $\tilde{x}$ represented conductivity then x_0 would be the average conductivity and x_i for $i \geq 1$ would be the uncertainty due to temperature, moisture content *etc*) and the ϵ_i are defined as the interval $[-1, 1]$. Each ϵ_i can thus assume any value between -1 and 1, the overall uncertainty in x being the linear combination of these uncertainties.

Each x_i represents an independent source of uncertainty, either inherently associated with the data or as a result of a calculation, *e.g.* round-off error. Clearly this representation will result in more complicated arithmetic than ordinary interval arithmetic.

The total uncertainty in an affine number is the sum of the uncertainty tokens, $\sum_{i=1}^{N} |x_i|$, and the effect of the individual sources of uncertainty is the magnitude of each uncertainty token, x_i.

Conversions between interval and affine arithmetic

Using the above definition of an affine number, the value of x is guaranteed to be in the range

$$[\hat{x}] = [x_0 - \beta, x_0 + \beta]; \;\; \beta = \sum_{i=1}^{N} |x_i|$$

remembering that the uncertainty tokens are defined as the interval [-1,1].

It is possible to convert an ordinary interval number $[\underline{x}, \overline{x}]$ to its affine representation $\hat{x} = x_0 + x_k\epsilon_k$:

$$x_0 = \frac{\overline{x} + \underline{x}}{2}; \qquad x_k = \frac{\overline{x} - \underline{x}}{2}. \tag{3.41}$$

The uncertainty token, x_k, is a new index and, unless specified, is not related to an existing source of uncertainty, *i.e.* this conversion represents a new independent source of uncertainty and $k = N + 1$. If this uncertainty was related to an existing source of uncertainty then x_k would be assigned the index of that source of uncertainty, *e.g.* $k = 3$.

Affine computations

Arithmetical operations with affine numbers can be either exactly formulated and hence are purely affine operations or require estimation as a non-affine term is approximated, *e.g.* the quadratic term in the product of two affine numbers is linearised.

Affine operations

An affine operation is an operation which can be expanded into an affine combination of the uncertainty tokens

$$\hat{x} \circ \hat{y} = x_0 \circ y_0 + \sum_{i=1}^{N} (x_i \circ y_i)\epsilon_i. \tag{3.42}$$

Three instances of the above are addition, subtraction and multiplication by a constant:

$$x + y \;\; = \;\; x_0 + \sum_{i=1}^{N} x_i\epsilon_i + y_0 + \sum_{j=1}^{N} y_j\epsilon_j$$

$$= x_0 + y_0 + \sum_{k=1}^{N} (x_k\epsilon_k + y_k\epsilon_k), \tag{3.43}$$

$$x - y = x_0 + \sum_{i=1}^{N} x_i\epsilon_i - y_0 + \sum_{j=1}^{N} y_j\epsilon_j$$

$$= x_0 - y_0 + \sum_{k=1}^{N} (x_i\epsilon_k - y_i\epsilon_k), \tag{3.44}$$

$$\alpha x = \alpha(x_0 + \sum_{i=1}^{N} x_i\epsilon_i)$$

$$= \alpha x_0 + \sum_{k=1}^{N} \alpha x_i\epsilon_k. \tag{3.45}$$

For example:

$$\hat{x} = 10 + 4\epsilon_1 - 2\epsilon_3,$$

$$\hat{y} = 3 + 1\epsilon_1 + 4\epsilon_2,$$

$$\hat{x} + \hat{y} = 13 + 5\epsilon_1 + 4\epsilon_2 - 2\epsilon_3.$$

Note that the uncertainty tokens can cancel themselves out, *e.g.* $(\hat{y} - \hat{x}) + \hat{x} = \hat{y}$, which was not the case for interval arithmetic. This is useful for numerical techniques where factorisations are often made, *e.g.* an LU decomposition on a matrix is not a realistic approach with interval arithmetic but is with affine arithmetic.

Non-affine operations

A non-affine operation is a function which cannot be expressed as affine combinations of the uncertainty tokens, *e.g.* multiplication of two affine numbers results in a series of quadratic terms. The process to follow is to map the solution to an affine number; thus the series of quadratic terms becomes a new uncertainty token:

$$\hat{x} \circ \hat{y} = x_0 \circ y_0 + \sum_{i=1}^{N} (x_i \circ y_i)\epsilon_i + \delta\epsilon_{N+1}. \tag{3.46}$$

Note the inclusion of the new uncertainty token (cf. equation 3.42). This new uncertainty token is now defined to be independent of all of the other uncertainty tokens:

this is clearly not the case so the evaluation of the non affine operation should produce the best solution possible in terms of minimizing this new term.

Multiplication of affine numbers

The multiplication of two affine numbers results in a quadratic term:

$$\begin{aligned}\hat{x} \cdot \hat{y} &= \left(x_0 + \sum_{i=1}^{N} x_i \epsilon_i\right) \cdot \left(y_0 + \sum_{j=1}^{N} y_j \epsilon_j\right) \\ &= x_0 \cdot y_0 + \sum_{i=1}^{N} (x_0 y_i + y_0 x_i)\epsilon_i + \left(\sum_{i=1}^{N} x_i \epsilon_i\right) \cdot \left(\sum_{i=1}^{N} y_i \epsilon_i\right). \end{aligned} \tag{3.47}$$

The quadratic term

$$\begin{aligned} Q &= \left(\sum_{i=1}^{N} x_i \epsilon_i\right) \cdot \left(\sum_{i=1}^{N} y_i \epsilon_i\right) \\ &= \sum_{i=1}^{N} \sum_{j=1}^{N} x_i y_j \epsilon_i \epsilon_j \end{aligned} \tag{3.48}$$

is approximated. The best approximation [Stolfi and de Figueiredo 1997] is a constant function of the maximum and minimum values of the quadratic. If

$$\begin{aligned} a &= \max Q \\ b &= \min Q \end{aligned}$$

then the approximation is

$$\begin{aligned} Q &\approx \frac{a+b}{2} + \frac{b-a}{2}\,\epsilon_{N+1} \\ &= \gamma + \delta \epsilon_{N+1} \end{aligned} \tag{3.49}$$

where $\gamma = \frac{a+b}{2}$, $\delta = \frac{b-a}{2}$, and ϵ_{N+1} is a new uncertainty token. The affine approximation of multiplication becomes

$$\hat{x} \cdot \hat{y} = x_0 \cdot y_0 + \gamma + \sum_{i=1}^{N} (x_0 y_i + y_0 x_i)\epsilon_i + \delta \epsilon_{N+1}. \tag{3.50}$$

Due to the difficulty of calculating the bounds of the quadratic term, it is usually estimated as [Stolfi and de Figueiredo 1997]

$$Q \approx \left(\sum_{i=1}^{N} |x_i| \cdot |y_i| \right) \epsilon_{N+1}. \tag{3.51}$$

The resulting affine approximation of multiplication becomes

$$\hat{x} \cdot \hat{y} = x_0 \cdot y_0 + \sum_{i=1}^{N} (x_0 y_i + y_0 x_i)\epsilon_i + Q\epsilon_{N+1}. \tag{3.52}$$

Reciprocal of an affine number

Division is most easily treated as multiplication by the reciprocal. This then shifts the problem to the calculation of the reciprocal of an affine number. As with interval numbers, division by an affine number which includes zero in its range is not possible.

To calculate the reciprocal, an affine approximation must be made. The reciprocal is represented as $f^a(x) = \alpha x + \gamma \pm \delta$ over the interval of $\hat{x}$ or range $[a, b]$. The terms α, γ and δ are calculated using a min-range approximation [Stolfi and de Figueiredo 1997]:

$$\begin{aligned} \alpha &= -\frac{1}{b^2} \\ \gamma &= \frac{(a+b)^2}{2ab^2} \\ \delta &= \frac{(a+b)(a-b)}{2ab^2}. \end{aligned} \tag{3.53}$$

These factors can now be used with the original affine number and the affine approximation of a reciprocal becomes

$$\frac{1}{\hat{x}} = \alpha x_0 + \gamma + \sum_{i=1}^{N} (\alpha x_i)\epsilon_i + \delta\epsilon_{N+1}. \tag{3.54}$$

In a similar approach to calculating the reciprocal of an affine number unary functions can also be approximated. The most appropriate mechanism may not be a min-range, but could be a Chebyshev (min-max) approximation or similar.

Summary

The affine arithmetic representation of uncertain data ensures that any correlations that exist between parameters are maintained. However, all arithmetical operations are not represented exactly by affine relationships resulting in new uncertainty tokens being required to maintain the overall error bound.

3.2.6 Summary

Three arithmetical methods have been presented as possible techniques to integrate uncertainty analysis within building simulation. The methods each require substantive alterations to the calculation procedures underlying building simulation. The implementation of these methods is therefore non-trivial.

Of the three methods only affine arithmetic preserves the relationships between uncertainties. The application of affine arithmetic to building simulation is therefore expanded in chapter 5.

3.3 Discussion

Two approaches to uncertainty quantification have been explored. The first, external methods, involves repeated simulations of perturbed models. Using various statistical techniques, the external methods allow the relationships between the perturbations and the output to be analysed and the overall uncertainty quantified. The second approach, internal methods, involves altering the fundamental arithmetic used in the calculations. As a result only a single simulation is necessary to calculate the total effect of all uncertainties.

Comparing these capabilities with the functionality required of an assessment method, as presented in chapter 2, it is clear that no single external method achieves these objectives. The differential method quantifies individual effects, the factorial method quantifies individual and interacting effects and the Monte Carlo method quantifies the overall uncertainty. Internal methods, specifically affine arithmetic,

can quantify individual and overall effects simultaneously. Therefore, affine arithmetic would appear to be the most applicable method. However, the implementation of internal methods is non-trivial while external methods are relatively straightforward to implement. Thus the choice between methods is not clear. To resolve this issue both approaches have been applied to the detailed simulation program, ESP-r.

Before the methods are applied to a simulation tool adjustments to the data model are required. These adjustments are the subject matter of the next chapter and will permit the use of the analysis methods described in this chapter.

References

Barbarosie C, *Reducing the Wrapping Effect*, Computing, Vol 54, Pt 4, 1995

Berry D A, Lindgren B W, *Statistics theory and methods*, Brooks/Cole Publishing, 1990

Box G E P, Hunter W G, Hunter J S, *Statistics for experimenters*, J Wiley and Sons, 1978

Buckley J J, *Solving Fuzzy Equations*, Fuzzy Sets and Systems, Vol 50, 1992

CEN, *Ventilation for buildings - design criteria for the indoor environment*, prENV 1752, 1996

Gardiner W P, Gettinby G, *Experimental Design Techniques in Statistical Practice*, Horwood Publishing, 1998

Gerald C F, Wheatley P O, *Applied Numerical Analysis*, Addison-Wesley, 1984

Grove D M, Davis T P, *Engineering Quality and Experimental Design*, Longman, 1992

Hamby D M, *A review of techniques for parameter sensitivity analysis of environmental models*, Environmental Monitoring and Assessment, no 32, 1994

Kreyszig E, *Advanced Engineering Mathematics*, J Wiley and Sons, 7th ed, 1993

Lomas K J, Eppel H, *Sensitivity analysis techniques for building thermal simulation programs*, Energy and Buildings, no 19, 1992

Neumaier A, *Interval Methods for Systems of Equations*, Cambridge University Press, 1990

Neumaier A, *The wrapping effect, ellipsoid arithmetic, stability and confidence regions*, Computing supplementum 9, 1993

Ning S, Kearfott R B, *A Comparison of some methods for solving linear interval equations*, SIAM Journal of Numerical Analysis, Vol 34, No 4, 1997

Ross T J, *Fuzzy logic with engineering applications*, McGraw-Hill, 1995

Saltelli A, Chan K, Scott E M, *Sensitivity analysis*, J Wiley and Sons, 2000

Stolfi J, de Figueiredo L H, *Self-validated numerical methods and applications*, 21^{st} Brazilian Mathematics Colloquium, 1997

Tomovic R, *Sensitivity Analysis of Dynamic Systems*, McGraw-Hill, 1963

Chapter 4

Characterising uncertainty in building simulation

Sources of uncertainty are characterised. This is a two stage process. Probability distributions which are applicable for describing parameter variations are sought. The sources of uncertainty are then attributed with suitably quantified probability distributions.

The sources of uncertainty in building simulation were described in chapter 2. With the requirements of the assessment methods as detailed in chapter 3, these sources can now be described in a form suitable for simulation.

Simulation can be considered analogous to an experiment. In experimental work measurements are made which are subject to error and in simulation work data supplied to the model is also likewise subject to error. As such, this chapter begins with a review of measurement theory, deriving an expression of uncertainty in data for building simulation. This expression is then applied, with suitable probability distributions, to data used in simulation. The aim of this process is to produce a mechanism whereby uncertainty limits can be quantified.

4.1 Measurement theory

Measurements are central to any scientific process, the key aspects of a measurement being to quantify a property by a measuring device. It is not possible to measure the true value of a property and thus any measurement is subject to an uncertainty [Rabinovich 2000].

The uncertainty in a measurement is typically divided into two categories: systematic and random. A systematic error is a result of the measurement process and is constant or changes in a regular manner for repeated measurements of the same quantity. A random error cannot be attributed to an aspect of the measuring process and varies in an unknown manner.

This classification of uncertainty in measurements is applicable to data used in building simulation.

4.1.1 Systematic errors

A systematic error when using building simulation is attributable to two causes:

1. using incorrect data for the given parameter, and

2. employing the wrong or incomplete model of the physical process.

Examples of the former include using thermophysical data measured on a dry sample to represent a wetted surface (*e.g.* the brickwork of an exterior facade of a building during inclement weather) or using occupant heat gains corresponding to a particular activity level where this is known to vary. An example of the second cause occurs where thermal bridges are present but the construction heat flow model is restricted to one dimensional flow.

Systematic errors can be reduced through the correct use of data and available modelling facilities. That said, it is not always possible for the practitioner to collect sufficient data or invest the time needed to model all the required processes. An ability to define the uncertainty incurred by using data and models which are not entirely adequate is required. For example, using a specified air change rate for a

natural ventilation study can gain rapid results, but a bulk air flow model may be more appropriate. What is the induced error due to such a modelling simplification?

In these cases the sources of uncertainty relate to a deficiency in the simulation process when compared to the real physical processes being modelled.

Modelling uncertainties can arise through a conscious decision to not model heat flow in three dimensions or to not use an explicit model to calculate air flows. They can also arise as a result of the limitations of the simulation software in relation to the assumptions embedded in the underlying mathematical models.

Uncertainties introduced via a lack of suitable data, or imprecisely defined models, arise in simulation where choice is available, *e.g.* between different algorithms to calculate sky temperature for external longwave exchange, or between insulation products of different conductivity. Again it is possible to know limits to these uncertainties but they cannot be removed without better model definition or data collection. Uncertainties of this type are common in building simulation, especially when using detailed simulation at early design stages where aspects of the building are not well defined.

Systematic uncertainties are not random as they can be removed from the simulation process by increased model resolution or better definition. Unfortunately, it is not possible to determine the value of the uncertainty introduced, and thus remove it from the predictions as it is only possible to quantify what is simulated, not what is not simulated. However, in many cases it is possible to quantify the limits of the uncertainty, thus bounding the true value.

4.1.2 Random errors

Consider a well defined model. The walls of the buildings are modelled in a three dimensional thermal and moisture flow network, connected to CFD domains which represent the internal spaces. Occupants are explicitly modelled with respect to their thermal, moisture and controlling interactions with the building. Such a model would require large quantities of data, but has the potential to predict in detail the performance of the building. Unfortunately, this potentially may not be realised due

to the random errors within data.

Random errors are discovered by measuring the same quantity repeatedly under the same conditions. These measurement errors differ from systematic errors in that they cannot be attributed to a particular cause and every measured quantity contains random errors.

Such uncertainties arise where a suitable model and suitable data exist but there is still a variation in the data. For example, these uncertainties are evident in thermophysical properties: even when the correct product has been selected there is still an uncertainty due to the measurement errors incurred in the derivation of the data. For simulation purposes the random uncertainty in a parameter will be defined as the measurement error in that parameter.

4.1.3 Uncertainty in simulation data

With respect to simulation work, the two error types described above provide a convenient mechanism whereby the sources of uncertainty can be classified. The overall uncertainty in a parameter will be the combination of all systematic and random errors.

Each uncertainty source will have a probability distribution and the overall uncertainty in a parameter used within a simulation will be the sum of these probability distributions. Therefore, to define the errors in data used in simulation, the sources of uncertainty for each parameter must be identified and a probability distribution attributed to each. The following section describes five probability distributions that are relevant to the needs of building simulation.

Section 4.3 then details the systematic and random uncertainties for the most frequently used data, and quantifies limits on this data.

4.2 Probability distributions

The following distributions may be used when modelling uncertainty in building energy systems.

4.2.1 Discrete distribution

The discrete distribution can either be parametric or non-parametric but for both cases is bounded (*i.e.* there are a finite number of options). There are many types of parametric distribution (*e.g.* binomial) but the non-parametric general discrete distribution, as described here, is of most use in building simulation. Consider cases where many models exist to predict a physical phenomenon, for example:

- the distribution of sky radiation can be predicted by several empirical models, or
- convective heat transfer coefficients can be predicted by different relationships, *e.g.* Alamdari and Hammond or Rodgers and Mayhew [ETSU 1987].

In these cases all of the available models are valid to some degree as they are based on experimental data, *e.g.* in the case of sky models their applicability may be related to the building's latitude.

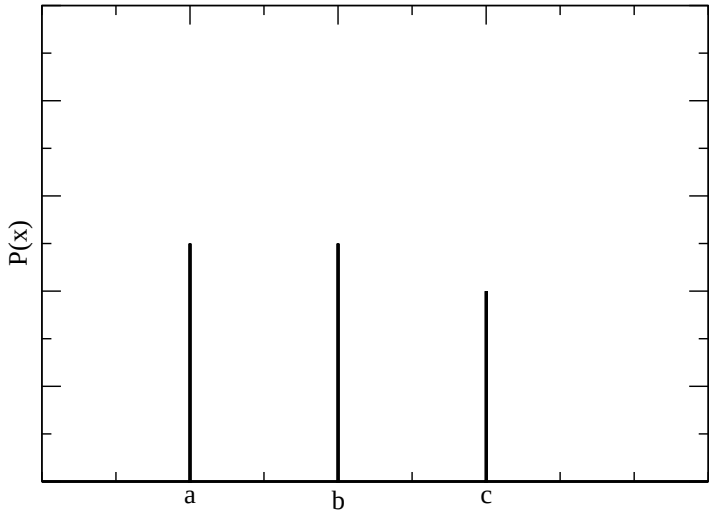

Figure 4.1: Discrete distribution of x.

The discrete distribution requires that each of the possibilities is given a probability of occurrence and that these probabilities sum to one, see figure 4.1. The difficulty of using this distribution is in specifying the probabilities of the different choices, *e.g.* the Klucher and Perez sky models could be assigned the same probability, but what happens if a third model is available which may not be as trusted by the practitioner.

Is the third model half as good, or a third *etc.* Whatever the choice all the probabilities will have to be reset.

4.2.2 Even distribution

The even distribution [Evans *et al* 1993] is a bounded continuous distribution where the probability of the variable taking a value between the bounds is equal, see figure 4.2. This is the implicit assumption in interval arithmetic 3.2.3.

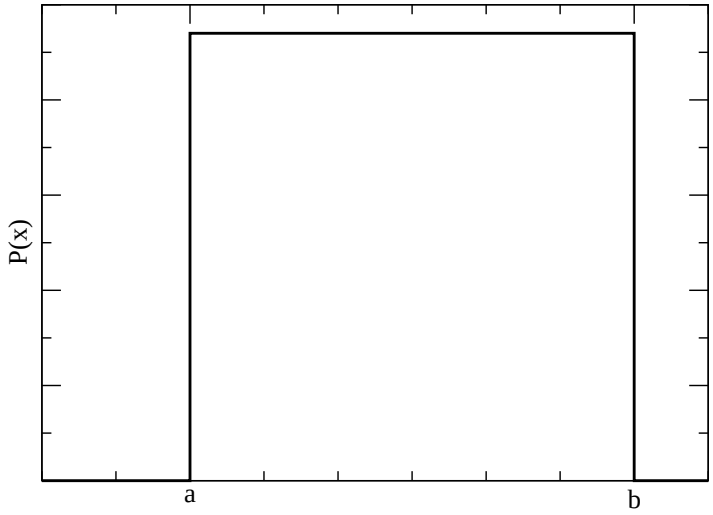

Figure 4.2: Even distribution of x.

The distribution places a larger emphasis on extreme values than do the other continuous distributions and so should be used with care. It is most useful in simulation where attention should be drawn to a poorly defined parameter, say at the early design stage. The distribution is the most suitable for modelling systematic errors as these errors are not random and hence the true value is equally probable throughout the given range. Typical uses of the even distribution could be for casual gains from occupants, or the conductivity of a hygroscopic material.

The mean value of an even distribution is given by

$$\mu = \frac{a+b}{2} \tag{4.1}$$

where a is the minimum possible value and b is the maximum possible value. The

probability distribution function for an uncertain parameter x is constant

$$P(x) = \frac{1}{b-a} \tag{4.2}$$

and the standard deviation is

$$\sigma = \sqrt{\frac{(b-a)^2}{12}}. \tag{4.3}$$

4.2.3 Normal distribution

The normal distribution [Evans *et al* 1993] is the most appropriate distribution for measured physical data. Typical building simulation examples are measured lengths or temperatures. From a given sample the average value is given by

$$\mu = \frac{1}{n}\sum_{i=1}^{n} x_i \tag{4.4}$$

where x_i are the n observed values in the sample. The unbiased sample variance is

$$\sigma^2 = \left(\frac{1}{n-1}\right)\sum_{i=1}^{n}(x_i - \mu)^2. \tag{4.5}$$

The positive square root of the variance is the standard deviation. Throughout this thesis the standard deviation is used in preference to the variance since the value of the standard deviation is expressed in the same units as the mean value and is thus easier to comprehend.

The probability distribution function for a normally distributed variable, see figure 4.3, is unbounded and symmetrical:

$$P(x) = \frac{1}{\sigma(2\pi)^{1/2}} \exp\left[\frac{-(x-\mu)^2}{2\sigma^2}\right]. \tag{4.6}$$

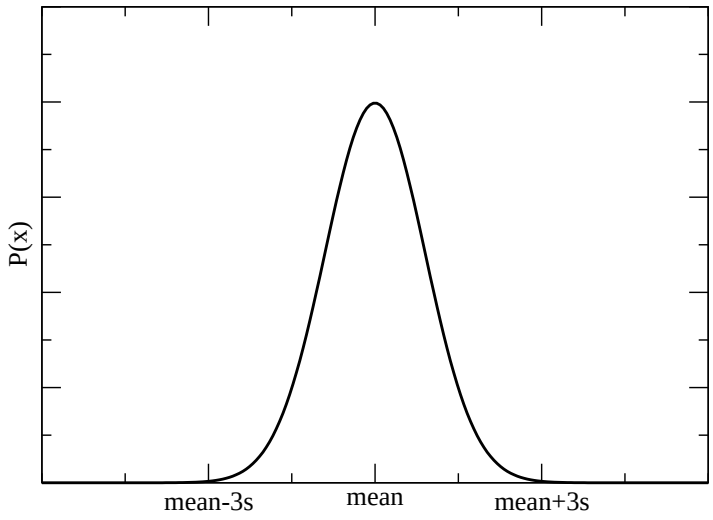

Figure 4.3: Normal distribution of x.

As the distribution is unbounded there is a possibility that a normally distributed parameter could have a non-physical value. For example, a measured length is normally distributed but cannot be negative. This is generally unlikely provided the standard deviation is small compared to the mean, as approximately 68% of the probable values that a variable can take are within one standard deviation of the mean value, 95% are within two standard deviations of the mean and 99.5% within 3 standard deviations of the mean.

It is possible to scale and transform a normally distributed variable:

$$\text{Norm} : \mu, \sigma \simeq [(\text{Norm} : 0, 1) \times \sigma] + \mu \tag{4.7}$$

where Norm : μ, σ is the normal distribution for a variable defined by its mean (μ) and standard deviation (σ). Equation 4.7 implies that (for all practical purposes) if a random number is generated for the standard normal distribution[1] it can then be scaled and transformed by the mean and standard deviation of the uncertain parameter. This relationship is used in uncertainty quantification techniques.

[1]The standard normal distribution has a mean value of zero and a standard deviation of one.

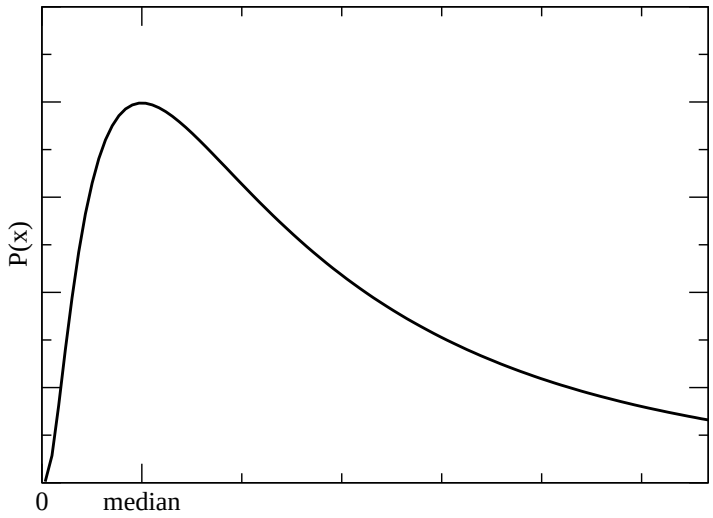

Figure 4.4: Log-normal distribution of x.

4.2.4 Log-normal distribution

The log-normal distribution [Evans *et al* 1993] is produced when two or more variables which are normally distributed are combined as a product. For example, area which is the result of the product of two length measurements will be log-normally distributed. The distribution cannot produce negative quantities and is unbounded towards positive infinity, see figure 4.4.

Typical building simulation examples are the metabolic rate and infiltration rate. Note also that for small standard deviations the log-normal distribution can be approximated by the normal distribution.

The log-normal distribution is related to the normal distribution as follows

$$\begin{aligned} \text{LogN} : m, \sigma &\simeq \exp(\text{Norm} : \mu, \sigma) \simeq \exp[\mu + \sigma(\text{Norm} : 0, 1)] \\ &\simeq m \exp(\sigma \text{Norm} : 0, 1) \end{aligned} \tag{4.8}$$

where $\text{LogN} : m, \sigma$ is the log normal distribution for a variable defined by its median (m) and standard deviation (σ). Thus, if a variable is log-normally distributed then the distribution of the log of the variable will be normal. The average value is therefore

$$\mu' = \frac{1}{n} \sum_{i=1}^{n} \log x_i \tag{4.9}$$

where μ' is the mean of the transformed data. By analogy the variance is [Evans *et al* 1993]

$$\sigma'^2 = \left(\frac{1}{n-1}\right)\sum_{i=1}^{n}(\log x_i - \mu')^2 \tag{4.10}$$

where σ'^2 is the variance of the transformed data. Thus, for random number generation, a normal distribution can be used and then transformed. The following relate the median and variance of the log normal distribution to the distribution of the transformed values

$$m = \exp \mu' \tag{4.11}$$

where m is the median of the distribution and

$$\sigma^2 = m^2 \exp[\sigma'^2(\sigma'^2 - 1)]. \tag{4.12}$$

4.2.5 Triangular distribution

The triangular distribution [Evans *et al* 1993] is a bounded continuous distribution, as shown in figure 4.5. It is often used in fuzzy logic applications and is appropriate here as an intermediate step between the uniform and normal distributions.

In a building simulation context it is a useful distribution because it is described by minimum, maximum and most likely values. For example, the typical occupancy in a space can be augmented by a minimum and maximum occupancy definition to characterise the possible range.

If the distribution is defined in terms of its minimum, maximum and most likely value, a, b and m respectively, then the mean is given by

$$\mu = \frac{a+b+m}{3} \tag{4.13}$$

and the variance by

$$\sigma^2 = \frac{a^2+b^2+m^2-ab-am-bm}{18}. \tag{4.14}$$

To generate random values two unit even distributions are used and the result aver-

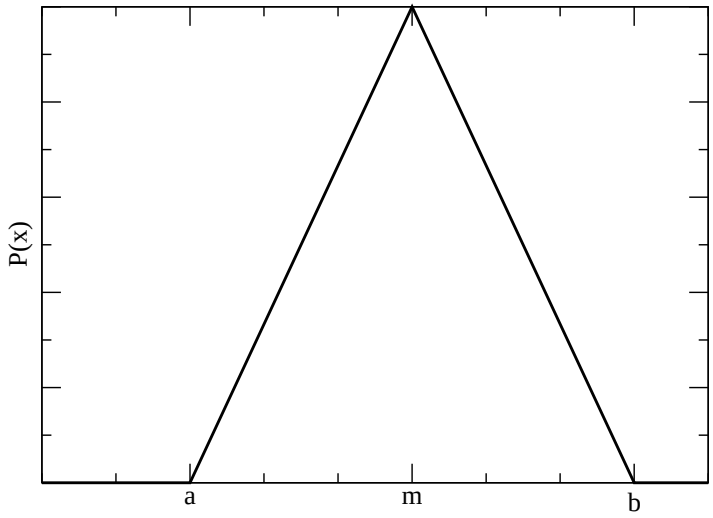

Figure 4.5: Triangular distribution of x.

aged. This averaged value will fit the standard symmetrical triangular distribution[2]; thus, the result should be scaled to fit the general triangular distribution:

$$\text{Tri} : a, b, m = \begin{cases} a + (2(\text{Tri} : 0, 1, 0.5))(m - a) & \text{if Tri} : 0, 1, 0.5 < 0.5, \\ m + (2(\text{Tri} : 0, 1, 0.5) - 1)(b - m) & \text{if Tri} : 0, 1, 0.5 > 0.5, \\ m & \text{if Tri} : 0, 1, 0.5 = 0.5 \end{cases} \quad (4.15)$$

The distribution is useful for modelling design data as the most likely value and the lower and upper limits can be grouped. However, the distribution over-emphasises extreme values and as such draws attention to them (although not as much as the uniform distribution).

4.2.6 Summary

Table 4.1 summarises the applicability, advantages and disadvantages of each of the described distributions.

[2]The standard symmetrical triangular distribution has a median of 0.5, minimum value 0 and maximum value 1.

Table 4.1: Probability distribution functions

Distribution	Advantages	Disadvantages
Discrete	Flexible	Awkward to define
Even	Most simple continuous distribution	Severe overemphasis of extremes
Normal	Well known	Can result in negative values
Log-normal	Positive values only	Can result in extreme positive values
Triangular	Easy to define	Overemphasis of extremes

The sources of uncertainty are now described and probability distributions assigned to each uncertainty type.

4.3 Sources of uncertainty

As described in chapter 2 all data items used to describe the modelled system are subject to a degree of uncertainty. As such, it is outwith the scope of this thesis to describe and quantify the uncertainty sources for all parameters. Rather, the main parameters used to describe a building have been analysed. These parameters comprise the thermophysical properties of constructional materials, casual gains associated with occupancy and appliances, and infiltration rates: without these parameters a model could not be constructed. Furthermore, these parameters are required to be known for effective simulation but at the early design stage they are 'highly unknown' as described in chapter 2. Therefore, if the uncertainty limits can be quantified in these parameters then detailed simulation software can be employed at early design stages. An additional benefit of this process is that the uncertainties quantified in this chapter are used to demonstrate and test the chosen analysis methods in subsequent chapters.

For the three categories existing data is reviewed and analysed. The ranges exhibited in the data will cover all aspects of uncertainty and as such can be used at the outline design stage when uncertainties are greatest. Where necessary a second analysis is undertaken and the sources of uncertainty are decomposed into systematic and random components. The reasons behind this approach are twofold:

1. by identifying all the sources of uncertainty, systematic sources can be removed from the quantification if the model description allows this, and

2. it allows data to be used at the earliest possible stage in the design process when uncertainties are greatest.

The initial approach quantifies the effect of all sources of uncertainty within a parameter, *i.e.* the maximum variation. The outcome of this process is that detailed simulation can be employed during the early design stage.

4.3.1 Thermophysical properties

The following analysis is based on information contained in a report on the harmonisation of thermophysical properties for use in building simulation [Clarke *et al* 1990] except where cited otherwise. This report provides a comprehensive review of available data worldwide and also discusses the inherent variability in the data.

The values for the conductivity, density and specific heat have been analysed and in many cases the values quoted are identical. This is either due to the value being known exactly or the reuse of values for similar materials between experimenters. The latter is most likely to be the case and the report's authors draw attention to this likelihood.

The data presented in the report have been analysed by material class, *e.g.* lightweight concretes, organic insulation materials. For each class an average value for each of the three properties has been calculated as well as the standard deviation. These data will include all sources of error for a given material class.

Theoretical standard deviations are presented in the next section based on measurement accuracy and an error analysis. These values are the minimum variations that can be expected in the data. For some material classes the variation exhibited is smaller than the theoretical minimum; this can be attributed to two reasons:

1. too small a sample size, or

2. data sharing between sources.

Where this occurs, the minimum theoretical variation has been applied to the category.

The result of the combined analysis is a list of generic materials where the properties are described in a form suitable for simulation with uncertainty analysis at an early design stage. When the design is refined, and specific materials known, the uncertainty will be less and the theoretical minimum uncertainties can then be used.

Sources of error

Tables 4.2 and 4.3 detail the systematic and random sources of uncertainty respectively in material thermophysical properties. For each source a suitable probability distribution is identified.

Table 4.2: Systematic uncertainty sources in thermophysical properties.

Uncertainty source	Conductivity	Density	Specific heat	Distribution
Data choice	✓	✓	✓	Discrete
Temperature	✓	×	✓	Even
Moisture content	✓	✓	✓	Even
Age	✓	✓	✓	Even

Table 4.3: Random uncertainty sources in thermophysical properties.

Uncertainty source	Conductivity	Density	Specific heat	Distribution
Measurement	✓	✓	✓	Normal

Systematic errors are typically described by an even distribution, as the error is not random and can be removed by more detailed modelling. This is the case with temperature, moisture and age effects. The choice of element will, however, be a discrete choice as only specific entries can be selected. The measurement error is purely random as it cannot be removed by more detailed modelling, therefore the normal distribution is suitable. The overall uncertainty in a property is the combination of systematic and random errors and their associated probability distributions.

Error quantification

The most straightforward of the three properties to measure is density, although

moisture content may have a significant effect and there is no measurement standard. Conductivity can be measured with an error of less than 5% for a given moisture content using recognised test methods, *e.g.* the guarded hot box method [BS 1987]. Finally, there is no standard for measuring specific heat capacity. This property is difficult to measure as the conductivity of the material affects the rate at which heat can be added.

Thermal conductivity

The measurement of thermal conductivity with the guarded hot box or similar equipment provides reasonably accurate measurements, as detailed previously, for a specific conditioned sample. The condition of a building material can vary considerably with respect to moisture content and to a lesser extent age and temperature. It has been estimated that the variation in conductivity due to location and orientation can be as much as 30-40% [Hyde 1996]. Lesser magnitudes of uncertainty, 30%, have been noted within samples of the same material, despite a constant density for all the samples. Therefore, there exists considerable uncertainty in the conductivity of a material when applied in buildings and subjected to moisture and other effects.

The effect of moisture is to increase the uncertainty in all thermophysical properties in material categories: non-hygroscopic, inorganic-porous and organic-hygroscopic. Moisture content of materials in use are quoted [Clarke *et al* 1990] from two sources: 1% — 5% [CIBSE 2001], and 5% and 10% [Jakob 1949] for inner and external surfaces respectively. From this information, typical moisture contents for non-hygroscopic, inorganic-porous and organic-hygroscopic materials have been set at 1%, 4% and 7% respectively.

The effect of these assumptions on conductivity can be assessed using moisture conversion coefficients [BS 1998]. The function of these coefficients is to convert a material's conductivity for a specific moisture content to the conductivity at another moisture content:

$$k' = kF_m \tag{4.16}$$

where the moisture conversion factor, F_m, is given by

$$F_m = \exp^{f_u(u_1 - u_2)} \tag{4.17}$$

or

$$F_m = \exp^{f_\psi(\psi_1 - \psi_2)} \tag{4.18}$$

where f_u and f_ψ are the moisture conversion coefficients for mass-by-mass and volume-by-volume moisture contents respectively. The effect of the above moisture contents would be an additional uncertainty of 5%, 15% and 25% for non-hygroscopic, inorganic-porous and organic-hygroscopic materials respectively.

The effect of temperature can likewise be described by temperature conversion coefficients [BS 1998]. A temperature change of $10°C$ will result in a 5% change in conductivity in most materials. For concrete and other inorganic-porous materials the change can be as low as 1% for the same temperature change. The relationship is non-linear:

$$F_\theta = \exp^{f_\theta(\delta\theta)} \tag{4.19}$$

where F_θ is the conversion factor for a given temperature change $\delta\theta$ and the material dependent conversion coefficient f_θ. For smaller temperature fluctuations the effect will be considerably less. The average effect for a temperature change of $10°C$ is an uncertainty of 4% [BS 1998].

Density

Density is normally measured for a dry sample of a material. To achieve this for hygroscopic materials the sample is heated to $105°C$ and its mass measured until there is less than a 1% difference in successive measurement [IEA 1991].

The effect of moisture on density will be more marked for lightweight materials, for a given moisture content. Non-hygroscopic materials are water permeable and are typically used in dry conditions. They generally have low densities so the effect of moisture in a sample of the material will be significant. Inorganic-porous materials

are generally heavier weight materials and absorb larger amounts of moisture due to the locations where they are used in buildings, *e.g.* external walls. Finally, organic-hygroscopic materials have a strong affinity for moisture and generally have lower densities. The effect of moisture content on density [IEA 1991] may be calculated from

$$\rho' = \rho + w \tag{4.20}$$

where ρ' is the density of the moist sample, ρ the dry sample and w the mass of moisture per unit volume of the dry material. Converting this expression to use the more common dimensionless measure of moisture content gives

$$\rho' = \rho + \frac{u\rho}{100} \tag{4.21}$$

and

$$\rho' = \rho + 10\psi \tag{4.22}$$

where u is the mass-by-mass and ψ the volume-by-volume moisture content; both values are expressed as percentages. Using the moisture contents assumed above introduces uncertainties of 13%, 4% and 11% for non-hygroscopic, inorganic-porous and organic-hygroscopic materials respectively.

Specific heat capacity

The standard method of measuring specific heat capacity is to supply a known quantity of heat to a material sample and then measure the temperature rise. A simple calculation then yields the specific heat capacity:

$$C = \frac{Q}{m\Delta\theta} \tag{4.23}$$

where Q is the net heat supplied to the sample, m is the sample mass and ΔT is the measured temperature difference.

There exists a number of error sources relating to the quantity of heat supplied, the temperature measurement, the temperature distribution within the sample, the mass

of the sample and heat loss from the sample. Generally, the higher the thermal the conductivity of a sample the smaller the error in the measurement of the specific heat capacity. The high thermal conductivity results in the sample exhibiting an even temperature distribution and allows the sample to be easily insulated. Therefore, there is a relationship between thermal conductivity and the accuracy to which specific heat capacity can be measured.

The rate of heat gain to a sample will be determined by the material's conductivity as will the heat loss. Therefore, the error will possibly be twice the error in the conductivity measurement, *i.e.* 10%. This error estimate may be arrived at by alternative reasoning based on the fact that the required measurements are effectively the same as for the guarded hot box [BS 1987]: heat supplied, heat lost (through guard), temperature in several locations and sample size. The guarded hot box standard defines steady state as the point when the measured temperatures in the plane normal to the heat flow are within $0.5°C$. Therefore, assuming the sample was raised in temperature by $10°C$, the error in ΔT would be 10%. The accuracy with which these measurements can be taken are [BS 1987]: heat supplied 0.25%, heat lost 1% and sample size 1%. Combining these errors, as described in section 3.2.1, gives an overall error of 12.25%.

The effect of moisture on the specific heat capacity of a sample may be determined from [IEA 1991]

$$C' = C + 4187\frac{w}{\rho} \tag{4.24}$$

where C' is the specific heat capacity of the moist sample, C the dry sample, w the mass of moisture per unit volume of the dry material, ρ the density of the dry sample and $4187 J/kgK$ the specific heat capacity of water. Converting this expression to use a dimensionless measures of moisture content gives

$$C' = C + 41.87u \tag{4.25}$$

and

$$C' = C + 4187\frac{10\psi}{\rho} \tag{4.26}$$

where u is the mass-by-mass and ψ the volume-by-volume moisture content; both values are expressed as percentages. Using the moisture contents assumed above introduces uncertainties of 4%, 19% and 8% for non-hygroscopic, inorganic-porous and organic-hygroscopic materials respectively.

Typical element uncertainties are summarised in table 4.4. These uncertainties represent the minimum theoretical values for a material in use. It should be noted that there is a strong correlation between the properties of a material due to sources of uncertainty. For example, moisture content would impact upon the conductivity, density and specific heat capacity simultaneously. This relationship is easily defined with the affine representation of an uncertainty as each property would share an uncertainty token for each common uncertainty source.

Table 4.4: Uncertainty quantification by material type.

Category	Conductivity	Density	Specific heat
Impermeables	$5\% + (\exp^{f_\theta(\delta\theta)} - 1)100\%$	1%	12.25%
Non-hygroscopic	$5\% + (\exp^{f_\psi(\delta\psi)} + \exp^{f_\theta(\delta\theta)} - 2)100\%$	$1\% + \frac{10\delta\psi}{\rho}100\%$	$12.25\% + \frac{41870\delta\psi}{\rho C}100\%$
Inorganic-porous	$5\% + (\exp^{f_u(\delta u)} + \exp^{f_\theta(\delta\theta)} - 2)100\%$	$1\% + \frac{u\rho}{100\rho}100\%$	$12.25\% + \frac{41.87\delta u}{C}100\%$
Organic-hygroscopic	$5\% + (\exp^{f_\psi(\delta\psi)} + \exp^{f_\theta(\delta\theta)} - 2)100\%$	$1\% + \frac{10\delta\psi}{\rho}100\%$	$12.25\% + \frac{41870\delta\psi}{\rho C}100\%$

Table 4.5: Summary of thermophysical data availability.

Material class	Number of measurements	Material class	Number of measurements
Asbestos board	5	Float glass	7
Asbestos cement	2	Cellular glass	7
Bitumen	4	Inorganic insulation	84
Asphalt	5	Organic insulation	124
Heavyweight blockwork	6	Non-ferrous metal	11
Mediumweight blockwork	15	Ferrous metal	7
Lightweight blockwork	17	Mortars and sealant	5
Clay brick	21	Plasterboard	18
Silicate brick	2	Plasters	19
Heavyweight aggregate	14	Plastics (PVC's)	3
Mediumweight aggregate	24	Rubber	5
Lightweight aggregate	28	Render and screed	8
Aerated concrete	30	Soil	12
Lightweight concrete	29	Natural stone	39
Reinforced concrete	5	Ceramic tile	5
Carpet	3	Clay tile	12
Underfelt	9	Timber	27
Glass block	2	Timber board	56

Thermophysical data

The quantity of data available for each material class varies considerably as summarised in table 4.5. In many cases the confidence in the estimation of the mean and standard deviation will be low. In these cases the standard deviations calculated from the expressions in table 4.4, using the moisture contents identified previously, will be more applicable. Table 4.6 shows a typical result of this analysis. Data for all material classes is presented in appendix A.

As can be seen in table 4.6, the category uncertainty is significantly larger than the entity standard deviation. This is to be expected, especially when there is a statistically significant quantity of data available. In this case, the theoretical standard deviation for specific heat capacity was greater than that calculated from the data. Therefore, the theoretical standard deviation was used for the category.

The CEN values [CEN 1998], where available, are displayed in Appendix A. No sources are identified for the data in this standard and it is suspected that these values are derived from the same data sources as identified by Clarke *et al.* Typically the average CEN values are less than two standard deviations of the average material

Table 4.7: Surface properties of unpainted materials

	Absorptivity	Std dev	Emissivity	Std dev
Metals polished	0.32	0.07	0.05	0.01
Metals	0.56	0.12	0.24	0.06
Brick (light)	0.49	0.04	0.90	0.02
Brick (dark)	0.76	0.04	0.90	0.02
Stone (natural)	0.63	0.10	0.91	0.02
Plaster	0.40	0.03	0.90	0.02
Concrete	0.68	0.04	0.90	0.02

values for a given category. This would suggest that the CEN values are based on the same data sources.

Table 4.6: Thermophysical properties of mediumweight aggregates

	Conductivity (W/mK)	Density (kg/m^3)	Specific Heat Capacity (J/kgK)
Average	0.718	1428	842
Std dev	0.324	376	90
Entity std dev	0.070	24	90
CEN value	1.15-1.35	1800-2000	1000

Surface properties

These can generally be measured with good accuracy. However, there is a lack of standards relating to measurements in use. It is important for surface measurements to be made with the material in use as the effects of ageing can be significant [CIBSE 1986].

A review of the data from Clarke *et al* gives rise to the data in table 4.7. As can be seen the variation in the values is low. As a result of these low variations no theoretical minimum values were calculated.

4.3.2 Casual gains

The generic term *casual gains* refers to the heat produced by the occupants and equipment within a building. This can be a major source of heat in a modern office. The following sections identify and quantify the uncertainties in this data.

Metabolic rate

On reviewing published data [ASHRAE 1989, BS 1995, CIBSE 2001, Fanger 1970, Galbraith *et al* 1989, NASA 1973, Parsons and Hamley 1989, Passmore and Durnin 1967], it is evident that no new and publicly available data has been measured since the early 1970's, and that most of the sources refer to previous studies. For these reasons it was concluded that the data presented by Fanger [Fanger 1970] provides the most applicable basis for this analysis.

Sources of error

There are three principal sources of error in metabolic rate data:

1. Measurement errors related to the accuracy of the equipment and how intrusive it is on the subject.

2. Task performance related to how the person carries out the task.

3. Activity description related to how accurately the activity is described and how it is understood by the user of the data.

The measurement error is composed of random and systematic components, whereas the final two sources are systematic. The metabolic rate can be measured by either monitoring the heart rate or measuring the oxygen consumption and carbon dioxide production of a person. The latter method is more accurate [ASHRAE 1989]: 3% error given a 10% error in calculating the oxygen consumption and carbon dioxide production. Measuring the respiratory air flows will impede the subject and introduce a systematic error. When applying the data there is usually more than one person in a building and the combined casual gain's distribution will tend towards a normal distribution (section 3.1.3). At low occupancies, say less than ten people, the triangular distribution will be more appropriate.

The mechanisms by which heat and moisture are transferred to a building from occupants (convection, radiation and evaporation) also require modelling. Typically, the heat gains from these mechanisms are specified as fixed percentages of the total

gain. However, this approach ignores prevailing environmental conditions, which will dictate the magnitudes of the transfer over time. Therefore, by using a time invariant percentage for the transfer mechanisms, a systematic uncertainty is introduced. Again this uncertainty will be evenly distributed for a single person. For small groups the appropriate distribution will be triangular and for large groups normal.

ASHRAE [1989] estimates that for engineering purposes the combined error is unimportant for activities with metabolic rates below $165W$[3] but rises to 'as much as 50%' for activities with metabolic rates greater than $320W$. Parsons and Hamley [1989] suggest that the error is 'not greater than 100%'. They conclude that the likely error is in the region of 50% and that general descriptions of activities should be used.

Error quantification

The initial analysis, as suggested by Parsons and Hamley [1989], identifies general activity descriptions. To achieve this, the available data [Fanger 1970] was plotted as shown in figure 4.6. As can be seen, there are four identifiable groups as follows.

1. Sedentary: $70W$ – $130W$ corresponding to *Sleeping* through *Standing, relaxed.*
2. Light work: $130W$ – $250W$ corresponding to *Laboratory work* through *Locksmith.*
3. Medium work: $200W$ – $425W$ corresponding to *Walking, on flat at* $4.0km/h$ through *Jogging, on flat at* $6.4km/h$.
4. Exercising: $425W$ – $950W$ corresponding to *Moving* $50kg$ *bags* through *Wrestling.*

If a task can be well described then the uncertainty in the total gain will be 50% as indicated above. The sensible gain will be convected and radiated into the space: the convective portion of this gain will be on average 55% with an uncertainty of $\pm$20% [ASHRAE 1989].

Several models of humans have been proposed [ASHRAE 1989] and recently a model of a human, predicting the magnitude of the heat gains dynamically has been

[3] All metabolic rates given here assume a DuBois surface area of $1.83m^2$.

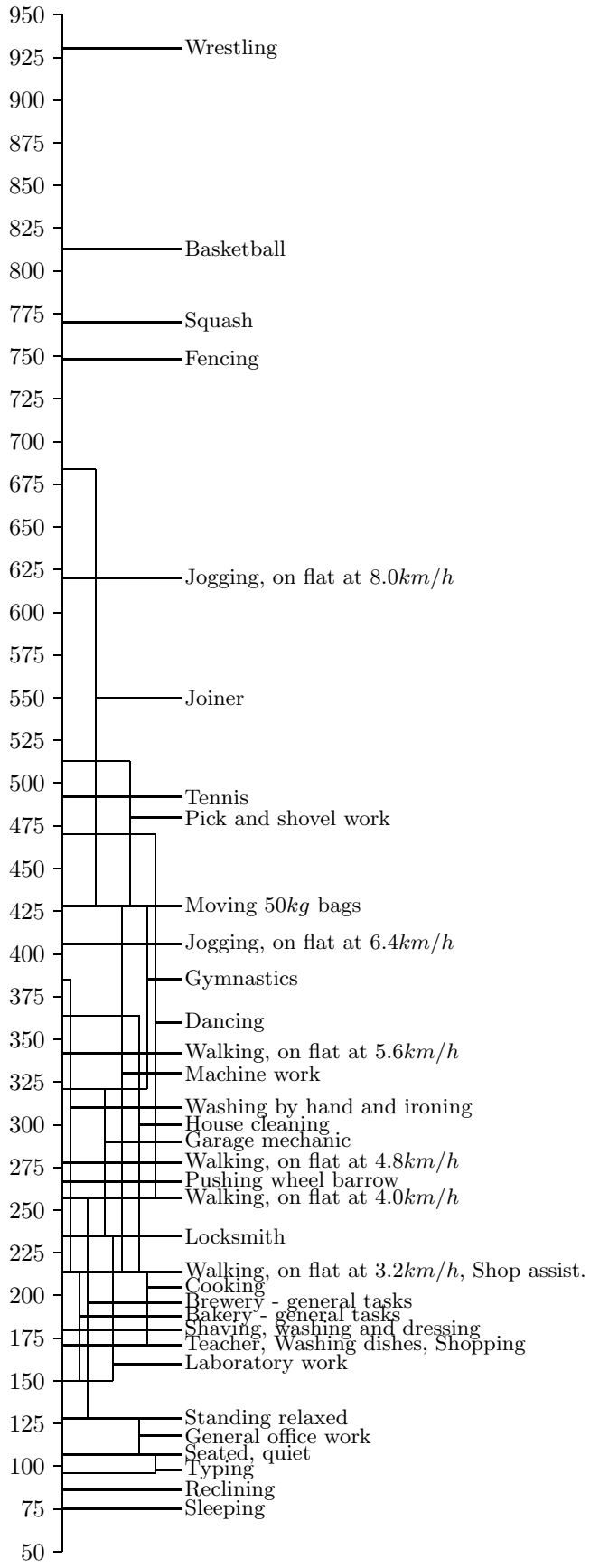

Figure 4.6: Metabolic rate data (W).

developed [Fiala *et al* 2000]. By implementing a model of this type in a detailed simulation program, the uncertainty, both in total gain and in heat transfer mechanism, can be further reduced.

Electrical equipment

The heat gain from electrical equipment can dominate the thermal environment in many buildings, *e.g.* IT classrooms, call centres and large offices. Therefore, accurate knowledge of the heat gains from equipment is required. All electrical equipment used in buildings converts the power used to heat, therefore by knowing the power consumption the total heat gain to the space will be known.

Sources of error

The majority of uncertainties will be systematic (the random uncertainty due to the measuring power consumption will be small). The systematic sources of uncertainty relate to equipment specification and usage and are typically larger. Therefore, an even probability distribution should be used when describing the heat gains from individual items of equipment. As with heat gains from occupants, when more items of equipment are used then the appropriate distribution will be triangular, and normal for many items.

Error quantification

The error in heat gain from a measured item of equipment could be less than 1% [Parsloe and Hejab 1992]. However, at early design stages the make of equipment is unlikely to have been specified, and in speculative developments will never be known to the design team. Therefore alternative specifications are required.

A review of data for general heat gains in offices [EEO 1995] shows that the heat gain to a typical office varies only slightly over the course of a day. However, over all measured offices the maximum and minimum demands were $32W/m^2$ and $7W/m^2$ respectively, between 10am and 5pm. This represents a significant range.

If the office equipment can be quantified but not identified (*e.g.* ten computers of

an unknown type) then the data in table 4.8 can be used. This table reproduces the minimum, mean and maximum small power loads as reported in the best practice programme guides [EEO 1995, DETR 1996]. As can be seen there is a large variation in the heat gain from office equipment.

Table 4.8: Heat gains from office equipment.

Equipment	Power demand (W)		
	Minimum	Mean	Maximum
Computer (PC+VDU)	50	100	185
Photocopier	120	600	1080
Printer — laser	35	110	145
Printer — ink-jet	20	60	100
Printer — dot matrix	10	35	70
Fax machine	15	25	35
Vending machine	300	525	750

Finally, if the equipment power rating is known but the power consumption has not been measured then the error could be as large as 61% [Parsloe and Hejab 1992]. On reviewing equipment heat gain data produced by ASHRAE [1989], the average recommended gain was found to be 75% of the maximum gain, with a standard deviation of 15%. This would suggest that an uncertainty of 61% is extreme.

To summarise: the quantification of heat gain to a space depends on the information available. In order of decreasing uncertainty the available options are as follows.

1. Apply $20^{+}_{-}12W/m^2$ for a general office.

2. Use the data in table 4.8.

3. Refer to the BSRIA report [Parsloe and Hejab 1992] to determine if the specific equipment has been measured. This is increasing unlikely as time progresses and new equipment is manufactured; therefore, use 75% of the maximum power rating with a standard deviation of 15%.

The heat gain to the space from small power loads will be primarily convected into the space. The percentage convected will vary between 60% and 80% [CIBSE 2001].

4.3.3 Infiltration

Infiltration modelling can be achieved through specified air change rates or by detailed flow simulation as described in chapter 2. At the early design stage the appropriate modelling choice is the specification of air change rates and the variability in this parameter is required.

Sources of error

Infiltration is highly correlated to building construction quality and building use. The construction quality will affect the unintended leakage of air through the buildings structure and as such will be a systematic error. The usage of the building will likewise be a systematic error; where an advanced modelling approach is employed it is necessary to describe the opening and closing of windows *etc.* The weather and local micro climate will also effect the infiltration rate. When modelling infiltration as an air change rate the errors will also be systematic as the error cannot be specified exactly without more detailed modelling.

Error quantification

The International Energy Agency standards show that in countries such as Sweden and Norway, where building air tightness is generally higher than in the UK, the average infiltration rate is $0.15h^{-1}$. This may be compared to the UK the average of $0.35h^{-1}$ [Johnstone *et al* 1999] with a variation from $0.15h^{-1}$ to $1.25h^{-1}$.

The variation in infiltration between buildings in specific categories has been examined in Sweden [Pettersen 1997]. The results show that the standard deviation varies from 1/3 to 4/5 of the mean measured infiltration rate and on average is 1/2 of the mean infiltration rate.

Table 4.9: Calculation air change rates.

Construction	Air change rate (h^{-1})		
	Mean	Maximum	Std deviation
Standard	0.33	0.81	0.102
Tight	0.21	0.50	0.061

Table 4.10: Simulated air change rates.

Building	Air change rate (h^{-1})		
	Mean	Maximum	Std deviation
House A	0.13	0.43	0.068
House B	0.10	0.36	0.056
Typical UK	0.35	1.25	0.183

ASHRAE suggest two formulae for estimating infiltration rates in domestic properties [ASHRAE 1989]. These formulae relate the air change rate to building construction, temperature difference and wind speed. Assuming a constant indoor air temperature of $21°C$, the data in table 4.9 was generated based on an annual calculation using the UK climate reference year. In this case the standard deviations observed are about 1/3 of the mean air change rate and the maximum values are about 2.5 times greater than the mean.

Another approach to quantification is to model the air movement throughout the building in more detail via a flow network. This involves identifying and describing all the air flow paths in the building.

Using this approach and measured data from a study by Johnstone *et al*[1999], a simple flow network was created. The study presented air change rates as a function of pressure difference between the inside and outside of the building. All purpose-built ventilation openings (*e.g.* window vents and extract fans) were sealed during the tests. The resulting data was reduced and an average infiltration rate calculated. Using the presented functions for the two measured houses and a typical UK house three simple air flow networks were created. These were simulated for a year using the UK reference climate and the results scaled to match the calculated average air change rate. Finally, the variation in air change rate calculated as a function of the average. The results are displayed in table 4.10, where the typical UK air change rates are as presented above and assuming the range from minimum to maximum represents six standard deviations.

As can be seen in table 4.10 the maximum air change rate is about 3.5 times larger than the average and the standard deviation is about half of the average value.

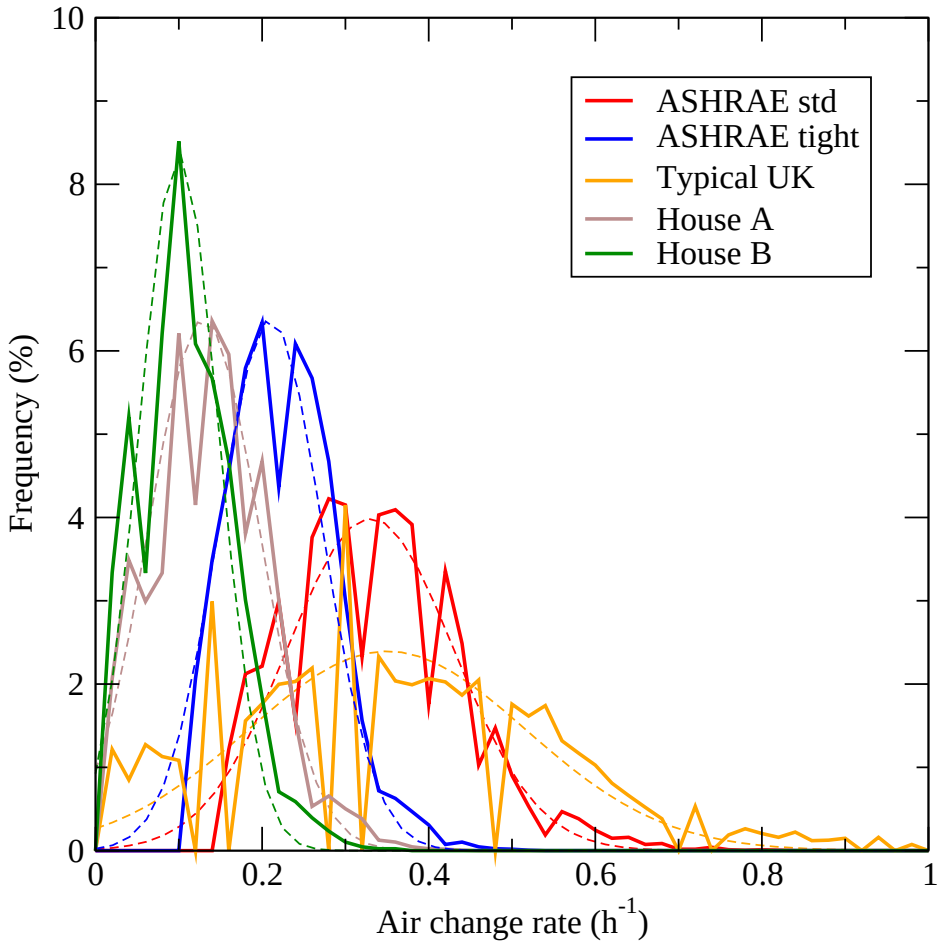

Figure 4.7: Distribution of air change rate from annual simulations.

Figure 4.7 shows the frequency of air change rates for all five of the above examples (tables 4.9 and 4.10). Each curve has a normal distribution curve overlayed (in the same colour, broken line). As can be seen the distributions are approximately normal, despite the log-normal distribution being the ideal distribution to describe these data. This would suggest that for standard deviations up to 1/2 of the mean it is possible to approximate the variation in infiltration rates with the normal distribution.

The current design process focuses on the maximum infiltration rate for heat loss calculations and as a result guides produce tables of this data [*e.g.* CIBSE 2001]. Data such as these contains a systematic error because it does not model the process it represents. The above simulations have shown that by including temperature and wind speed in the calculation there is a normal distribution of air change rates throughout the year with the mean value approximately 1/3 of the maximum and

the standard deviation equal to 1/3 of the mean.

4.4 Summary

This chapter has described the process by which uncertainty can be characterised. The process has been demonstrated on three types of thermal simulation data: thermophysical properties, casual gains and infiltration rates. These three data types are the minimum data required to describe a building for thermal simulation.

Two analysis procedures were employed: analysis of existing data and the use of detailed modeling. Analysing existing data provides a suitable mechanism for quantifying the uncertainty in parameters provided that the data is of good quality. This is not necessarily the case, for example:

- Most data used in building simulation is old – some of the data predates 1970. While some processes should not change in principle, better measurement techniques now exist for gathering data, including the inherent variability.

- Many of the measurements are from small sample sizes or unrepresentative samples. This is particularly true for metabolic heat gains where some sample sizes reported in the literature are for one or two people, or in the case of NASA for physically fit young males.

To overcome a lack of data detailed modelling can be usefully employed. This was demonstrated by using an air flow network to calculate the variation in air change rates. This approach could be used to bound the uncertainties of other systematic errors *e.g.* the effect of thermal bridges when using a one dimensional heat transfer model.

The next stage in the process is to identify a suitable mechanism whereby the quantification techniques of chapter 3 can be implemented within a simulation tool.

References

American Society of Heating, Refrigerating and Air-Conditioning Engineers, *ASHRAE Fundamentals*, Atlanta GA, USA, 1989

British Standard, *Methods for determining thermal insulating properties - Section 3.1 Guarded hot box method*, BS 874-3.1:1987, 1987

British Standard, *Moderate thermal environments - Determination of PMV and PPD indices and specification of the conditions for thermal comfort*, BS EN ISO 7730:1994, 1994

British Standard, *Building materials - Procedures for determining declared and design thermal values*, BS EN ISO 10456:final draft, 1998

CEN, *Building materials and products - Hygrothermal properties - Tabulated design values*, prEN 12524 (draft), 1998

Chartered Institute of Building Service Engineers, *CIBSE Guide Volume A*, London, 2001

Chartered Institute of Building Service Engineers, *CIBSE Indoor lighting manual*, London, 1986

Clarke J A, *Energy Simulation in Building Design*, Butterworth Heinemann, 2nd ed, 2001

Clarke J A, Yaneske P P, Pinney A A, *The Harmonisation of Thermal Properties of Building Materials*, BRE, 1990

DETR, *Managing Energy Use*, Good Practice Guide 119, 1996

Energy Efficiency Office, *Energy Efficiency in Offices - Small Power Loads*, Energy Consumption Guide 35, 1995

ETSU *Report on Heat Transfer at Internal Building Surfaces*, Energy Technology Support Unit, UK Department of Energy, June 1987

Evans M, Hastings N, Peacock B, *Statistical Distributions*, J Wiley and Sons, 1993

Fanger P O, *Thermal Comfort*, McGraw-Hill 1970

Fiala D, Lomas K J, Stohrer M, *Dynamic simulation of human heat transfer and thermal comfort, results and application*, Proc. Indoor Air Quality Conference, Edinburgh, 2000

Galbraith G H, Mclean R C, Stewart D *Occupational hot exposures: a review of heat and mass transfer theory*, Journal of Engineering in Medicine 1989

Hyde D, *Email communication of draft CEN standard (prEN ISO 10456) inc. comments*, 1996

International Energy Agency, *Annex XIV: Condensation and energy*, volume 1, 1991

Jakob M, *Heat transfer, part 1*, Chapman and Hall, 1949

Johnstone C, Clarke J, McElroy L, *Mainholm Road, Air: Pressurisation Testing to Determine Air Leakage Characteristics*, ESRU Technical Report, Strathclyde University, 1999

NASA, *Bioastronautics Data Book*, 1973

Parsloe C, Hejab M, *Small Power Loads*, BSRIA technical note 8.92, 1992

Parsons K C, Hamley E J, *Practical methods for the simulation of human metabolic heat production*, Thermal physiology, 1989

Passmore R, Durnin J V G A, *Energy, Work and Leisure*, Heinemann 1967

Pettersen T D, *Uncertainty analysis of energy consumption in dwellings*, PhD Thesis, The Norwegian University of Science and Technology, Trondheim, Norway, 1997

Rabinovich S G, *Measurement Errors and Uncertainties, Theory and Practice*, Springer, 2nd edition, 2000

Chapter 5

Implementation

Internal and external methods are applied to the ESP-r system. Interaction points with the existing computational system are identified and the necessary alterations detailed.

This chapter describes the integration of the uncertainty analysis methods selected in Chapter 3 into the ESP-r system [ESRU 2001]. As described in chapter 2, the system uses control volume conservation equations to establish the building model. Each technical domain (thermal, air flow *etc*) has its own set of conservation equations and specialised solution engine. This allows each domain to be solved efficiently, and at an appropriate solution time step. Information is shared between domains at each time step and, where necessary, an iterative approach is taken to ensure consistency between the domains. This process is summarised in figure 5.1.

The data model required to describe any building system is large. Before simulations can be undertaken, the data model has to be transformed into a form suitable for simulation. This process requires the calculation of conservation equation coefficients: some of these are non-simulation specific and some are simulation specific. Examples of non-simulation specific coefficients include surface areas and orientations, while an example of a simulation specific coefficient is the Fourier number, which depends on the user defined time step. There are also time varying coefficients required in the conservation equations, for example, heat transfer coefficients. All of these coefficients

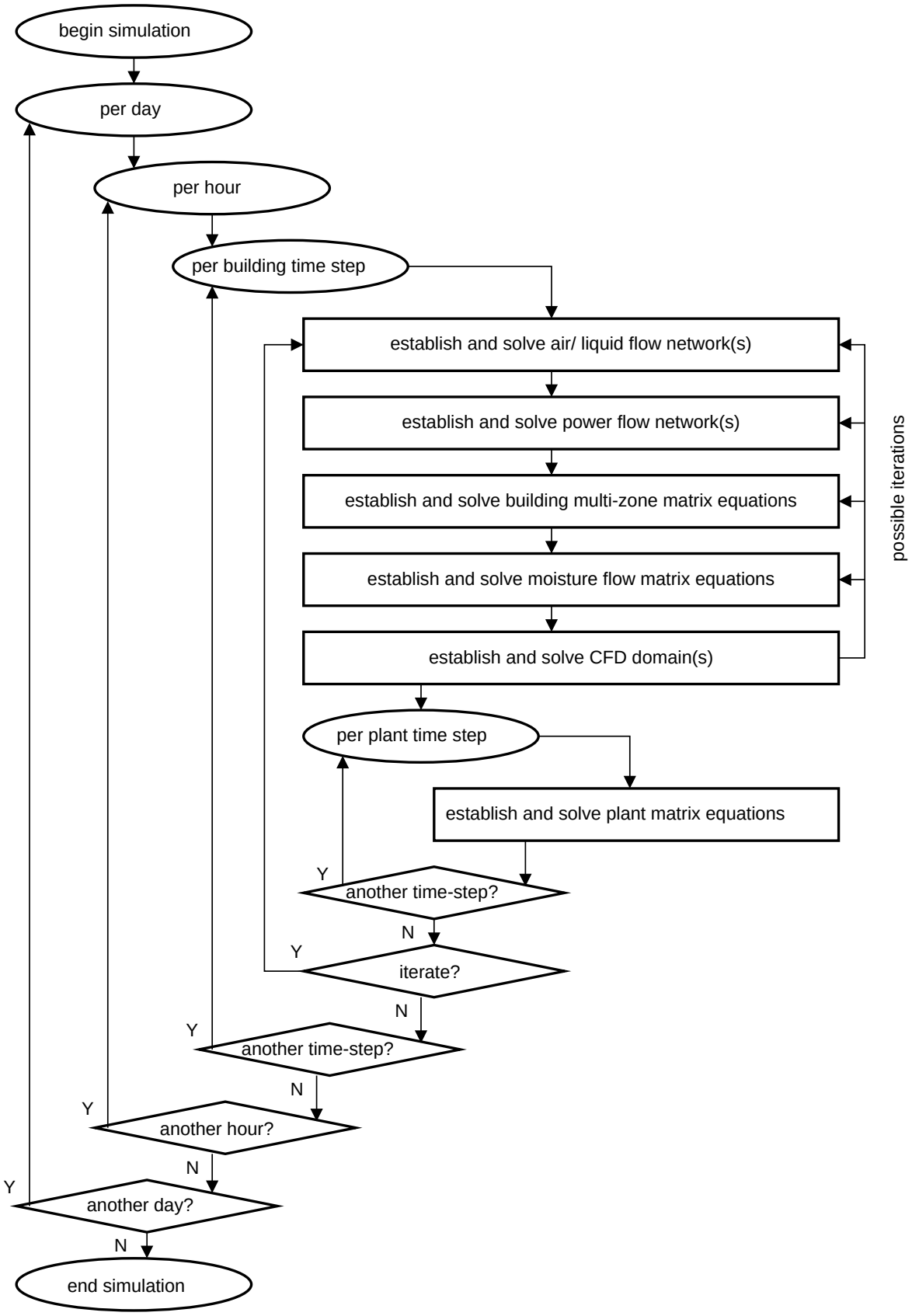

Figure 5.1: Time step solution of modelled domains (from Clarke 2001).

will be affected by uncertainties and the implementation of uncertainty analysis techniques will be required to interact with the calculation routines at suitable points in the computational process.

The process followed by ESP-r is depicted in figure 5.2. The system configuration file is read by the system and then, on a zone-by-zone basis, the zone descriptive files are read. These files contain geometry data, construction data and operations data. These data are subject to a degree of pre-calculation, to quantify the time invariant coefficients, as the files are read by the system. Once all the zones have been read, the simulation requires further information to proceed, *e.g.* time step. This allows the specific coefficients to be calculated and the final decomposition of input data into a form suitable for simulation. The model is now ready for solution and the simulation can proceed.

The two approaches to uncertainty quantification described in chapter 3 require interaction with the system at different levels. The external methods envelope the simulation engine and all perturbations to the data model are made externally. In addition to updating the data model, internal methods require the simulation engine to be enhanced. Therefore, the implementation of the external methods is more straightforward than for internal methods.

5.1 External methods

Implementation of the external methods is a three stage process:

1. definition of uncertain data;
2. execution of multiple simulations as required by the analysis method;
3. extraction of analysis results to quantify the effects of uncertain data.

The general requirements regarding implementation are now described and the key processes at each stage of the simulation process elucidated.

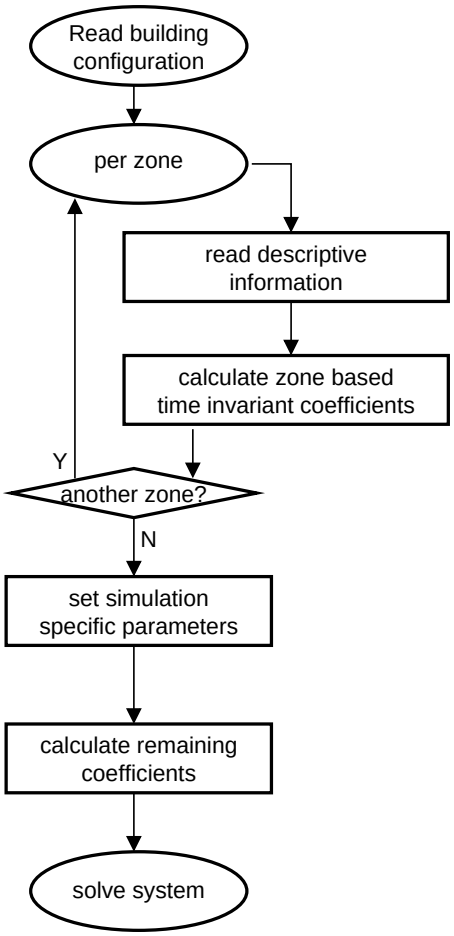

Figure 5.2: Building equation parameter set-up.

5.1.1 General considerations

The definition of a building system for simulation consists of a large set of data, typically comprising hundreds of parameters. The majority of these parameters are specific to the modelled building. An uncertainty analysis requires that items of data within this structure be clearly identified as uncertain and information assigned to describe the magnitude of this uncertainty.

A probability distribution can be ascribed to each uncertain parameter to determine how the value of the parameter varies. To enable this definition, a distribution type is selected and the data associated with the chosen distribution defined, *e.g.* for a normal distribution the associated data would be the standard deviation.

Of the chosen methods, only the Monte Carlo technique requires the distribution to be identified. The differential and factorial analyses require only two test values to

Table 5.1: Common data requirements for uncertainty analysis methods.

Method	Parameter identification	Probability distribution	Uncertainty magnitude
Differential	✓	×	✓
Factorial	✓	×	✓
Monte Carlo	✓	✓	✓

proceed. However, if the results of the differential method are to be compared then it is convenient to analyse the model at a known point on the probability distribution defining the uncertainty, *e.g.* at three standard deviations from the mean value. These requirements are summarised in table 5.1.

As noted, the differential and factorial methods do not require a distribution to be identified. However, if the distribution is identified then in the case of the differential method (and assuming that the standard assumptions hold as described in section 3.1.1) the same distribution type can be assigned to the output of the analysis.

Thus, the three identified data items are necessary for the majority of the methods and should be held for all definitions as this allows the defined uncertainty to be used for all analysis methods.

All three methods require repeated simulations to be performed on perturbed models. The methods treat the simulation engine of the software as a 'black box' and therefore the perturbations have to be activated in the data model before each simulation is initiated.

Each of the methods require specific alterations to the data model between simulations. Specifically:

The differential method requires only one variable at a time to be perturbed; thus the base case model is recreated before each simulation and one parameter adjusted to its extreme value, three standard deviations.

The factorial method requires all variables to be adjusted to either their maximum or minimum extreme values (three standard deviations) for each simulation.

The Monte Carlo method requires all parameters to be adjusted for each simulation to a random point in their probability distribution.

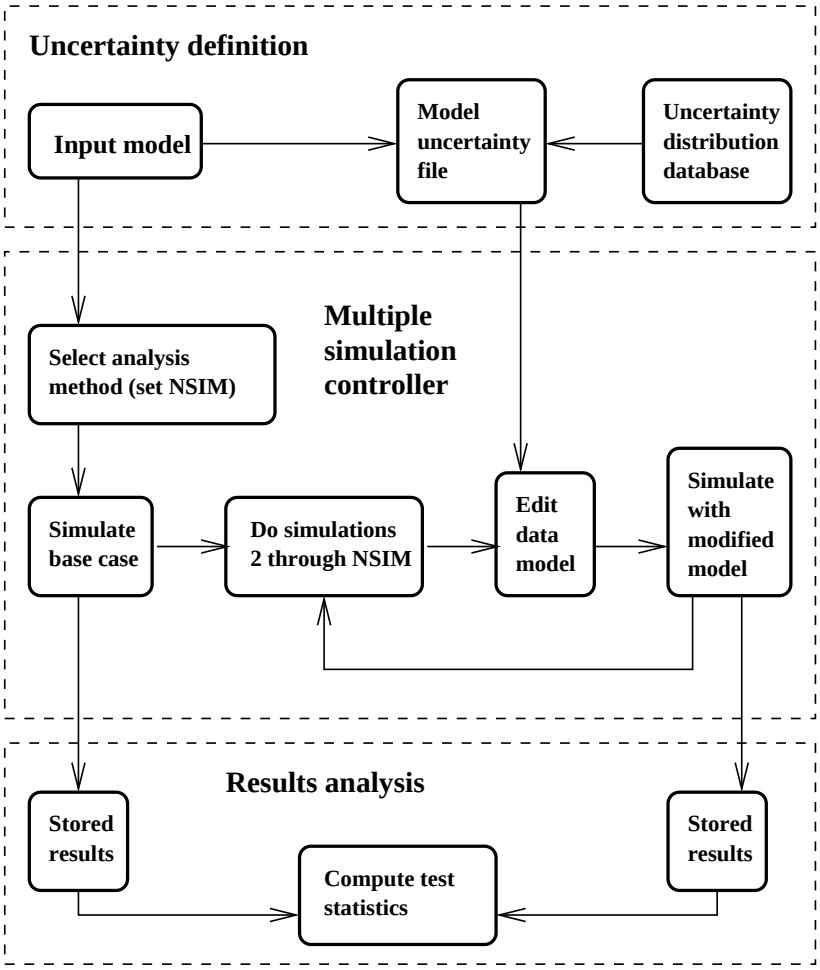

Figure 5.3: Integration of uncertainty analysis in ESP-r.

A *multiple simulation controller* is required to manage this process. The purpose of this controller is to ensure that the correct perturbations are effected in the data model and that the correct number of simulations are invoked.

The analysis of the ensuing results sets is clearly method specific. However, the process will require that multiple results sets can be analysed simultaneously and the differences between the sets examined.

5.1.2 Integration into ESP-r

The characteristics of an uncertainty analysis tool have been identified in the previous section. The implementation of these characteristics in the ESP-r system is summarised in figure 5.3.

Uncertainty definition

The definition of an uncertainty requires three information aspects:

1. the magnitude of the uncertainty in a parameter;

2. its probability distribution; and

3. the locations (spatial and temporal) where uncertainties are applicable.

These aspects are combined to complete the definition by associating the uncertain model parameters with particular locations in the building. This definition procedure allows flexibility for the model user, *e.g.* the magnitude of an uncertainty can vary with location or many uncertainties may apply to a single location.

The management of uncertainty definitions is controlled *via* a single uncertainty manager. The purpose of the manager is to interrogate the existing model and prompt the user for uncertainty definitions pertinent to their model and to allow maintenance of existing uncertainties. For example, uncertainties in the model will generally reduce as the design progresses and therefore the defined uncertainties have to be revised. The implementation maintains the definition of uncertainties separately from the main data model. This enables the portability of uncertainty definitions between projects, where applicable. In future a rule-based definition procedure could be added to the uncertainty manager allowing automatic attribution of uncertainties.

The definition process interface is shown in figure 5.4. Initially the user selects the uncertain parameter and then assigns a distribution. In the example shown here the conductivity of plate glass has been defined as the uncertain parameter. Note that the model has been interrogated by the uncertainty manager and only those construction materials used in the model are presented to the user. A normal distribution has been assigned to this parameter with the standard deviation expressed as a percentage of the mean value.

Once the uncertainties throughout the model have been defined, the user can initiate simulations that include uncertainty.

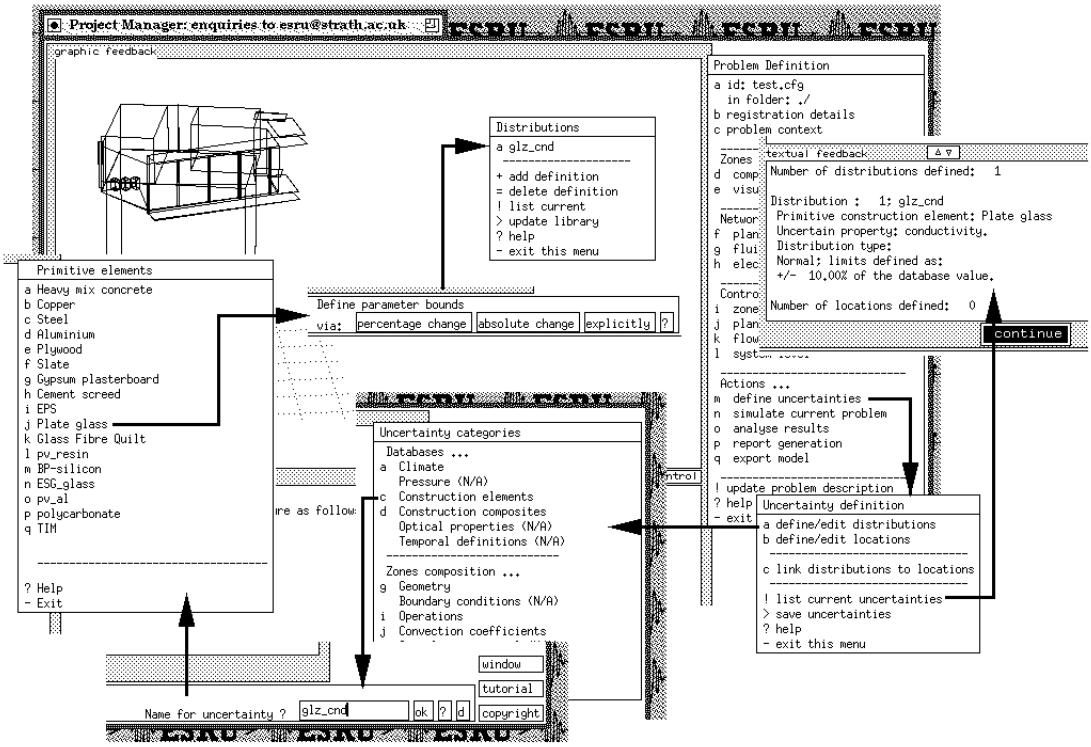

Figure 5.4: Attribution of uncertainties in ESP-r.

Multiple simulation controller

Simulating with the defined uncertainties requires the existence of a simulation controller, which implements the necessary parameter changes to the data model and initiates the simulations. The controller reads the input data model into memory and all subsequent changes to the model are made to this memory image to avoid corruption of the original model.

The simulation controller has three principal interactions with the simulation engine:

1. set-up of perturbation array;

2. perturbation of time invariant aspects of the data model;

3. perturbation of time varying aspects of the data model.

The set-up of the perturbation is summarised in figure 5.5. The controller's task is to define the perturbation array and commission simulations. The time step solution

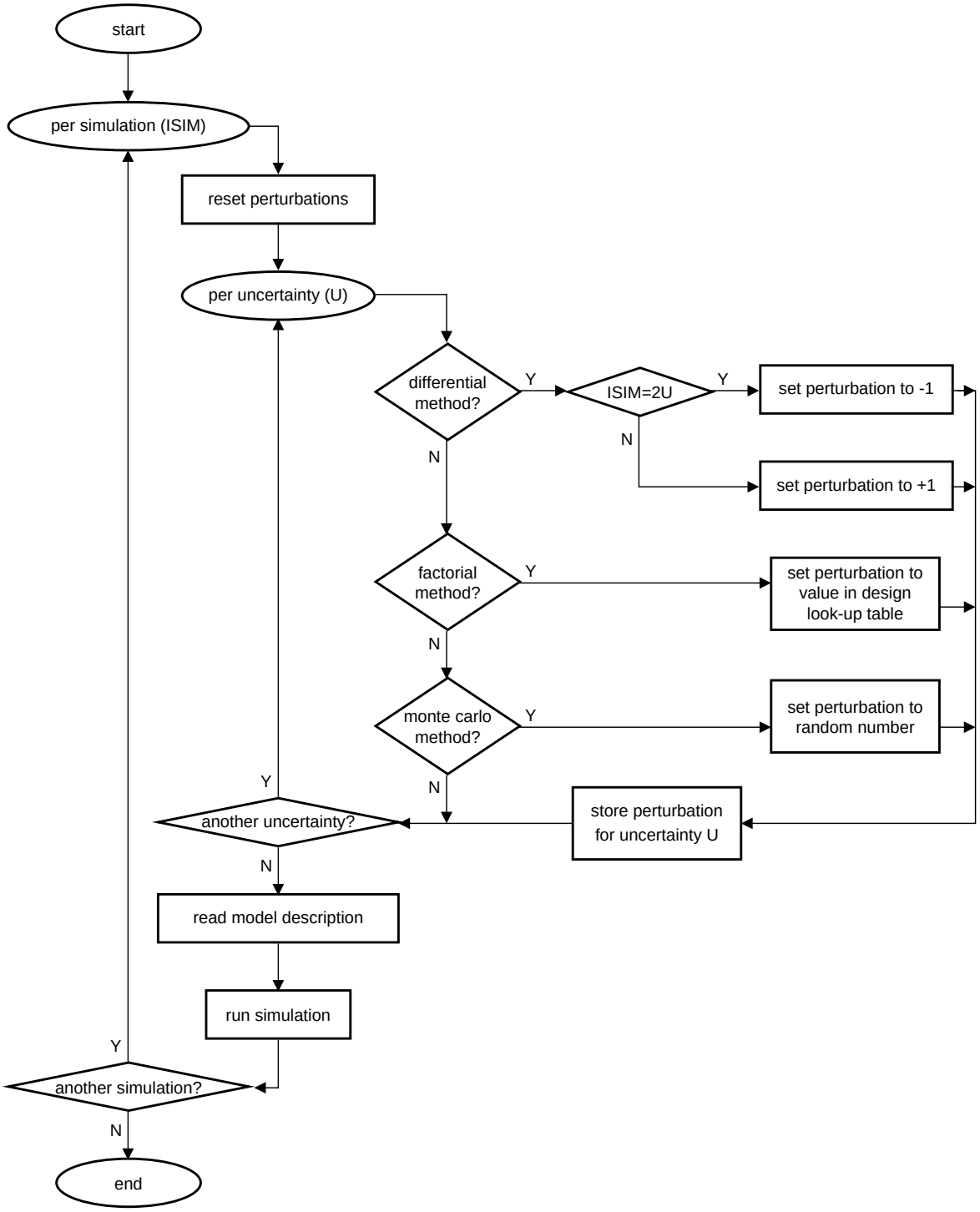

Figure 5.5: Multiple simulation controller: perturbation array set-up.

of modelled domains of figure 5.1 is represented by the 'run simulation' action and the 'read model description' action is displayed in figure 5.2.

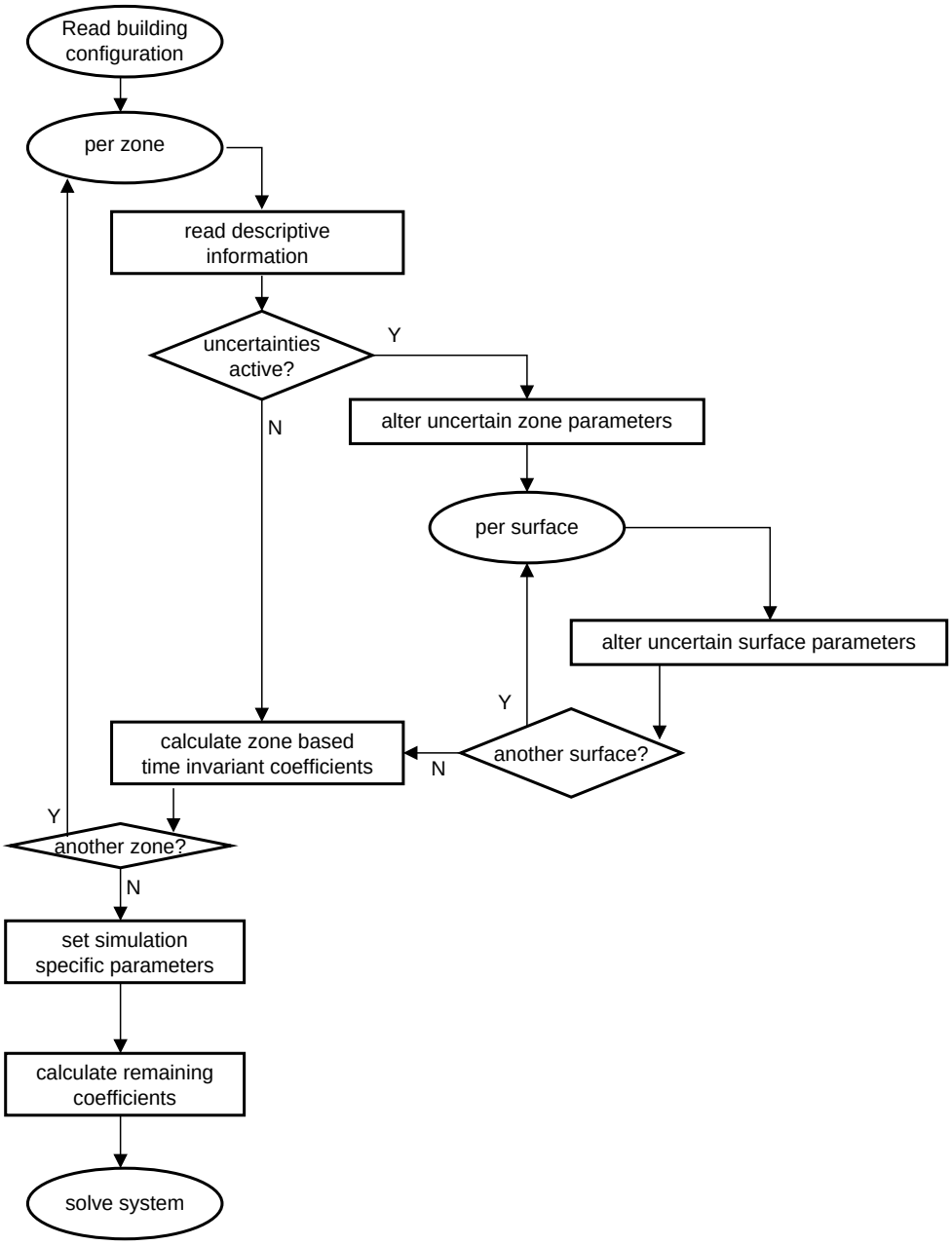

Figure 5.6: Building equation parameter set-up, for time invariant uncertainties.

The values in the perturbation array are set according to the analysis method chosen. For example, only one uncertainty will be perturbed at a time when the differential method is active. The design look-up table used for the factorial method is pre-calculated (*e.g.* see figure 3.1). The perturbation values are independent of the distribution, they are merely factors to be applied to the specific uncertainties during

the final two actions of the simulation controller. The perturbations are applied at two interaction locations with the existing ESP-r code. Time invariant uncertainties can be set during the loading of the model description into memory and time varying uncertainties are applied during the simulation.

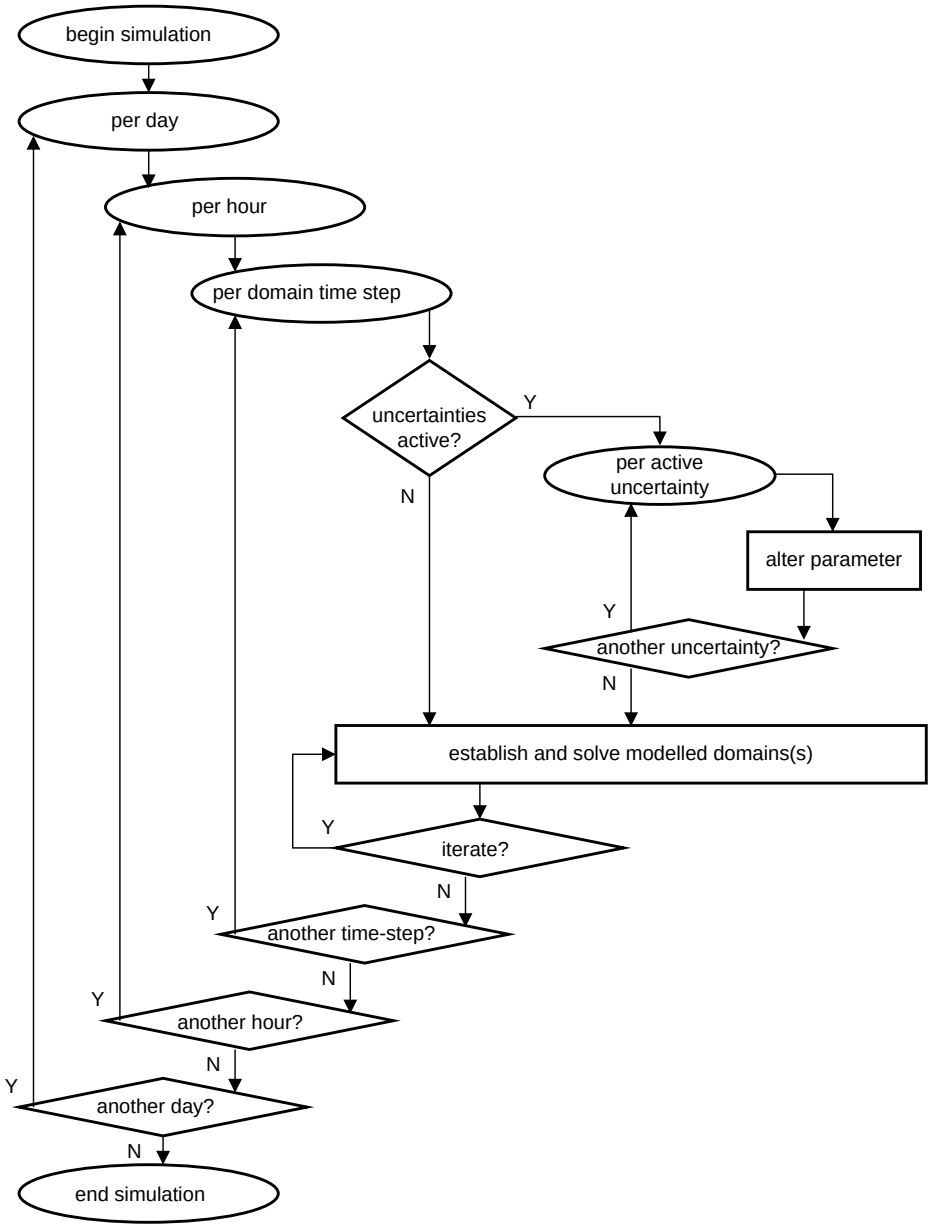

Figure 5.7: Building equation parameter set-up, for time varying uncertainties.

The simulation controller implements changes to the data model as the problem description files are reloaded into the system (figure 5.6). This approach guarantees that all coefficients are initially reset to their base case values before application

of the perturbation data. Since the data is perturbed before the calculation of the equation coefficients, the existing equation set-up routines of ESP-r can be used. This procedure ensures that the perturbed model is imposed upon all the necessary coefficients in the conservation equations.

Figure 5.7 elaborates the interaction of the simulation controller when temporal uncertainties are active. The separate domains of figure 5.1 have been combined in the 'establish and solve modelled domain(s)' action. The interaction point for temporal uncertainties is at the beginning of the time step loop ensuring that the perturbed data is present in the future time row equations.

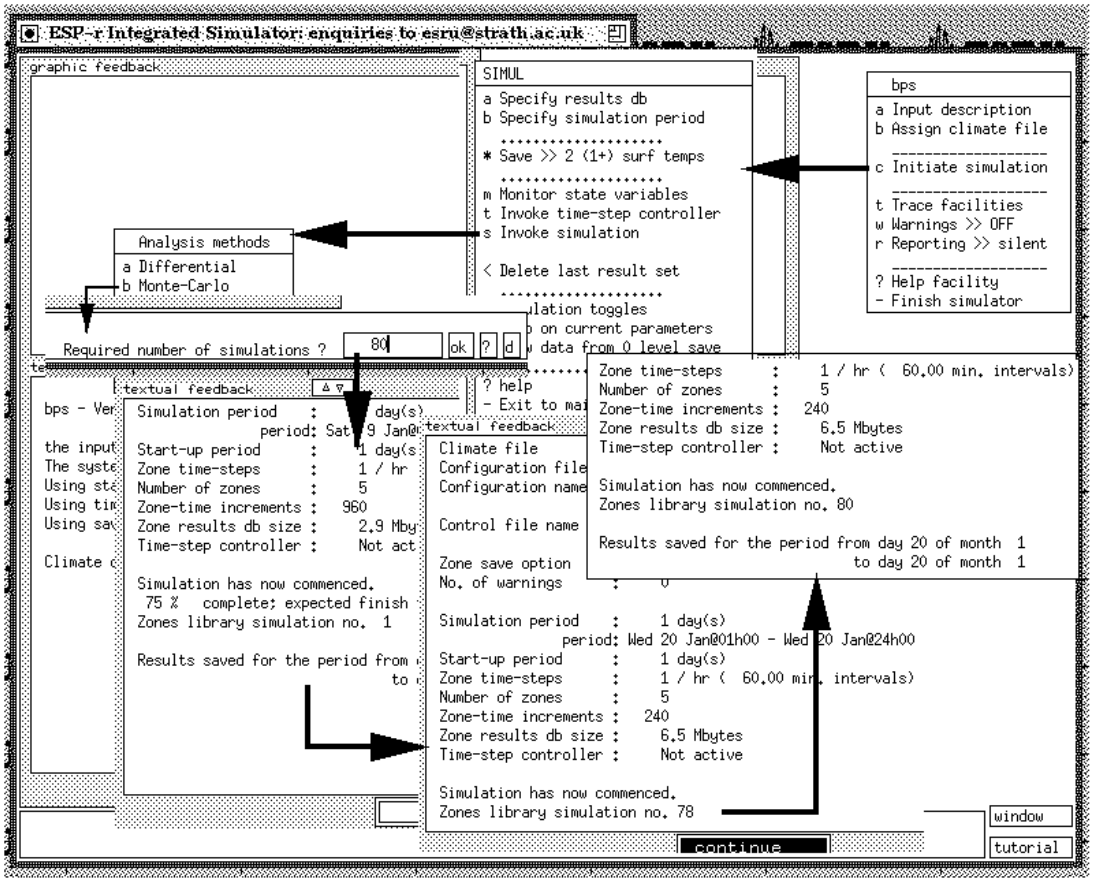

Figure 5.8: Multiple simulations for uncertainty assessment in ESP-r.

This complexity is hidden from the user and only minimal interaction is required. As can be seen in figure 5.8, the interface requires only an analysis method to be chosen (upper left of figure) and the multiple simulations are automatically commis-

sioned, with progress feedback provided (lower half of the figure).

Results analysis

There are three possible approaches to the storing of the results generated by the simulations:

1. the performance assessment metric is the only information stored from the simulations;
2. the full results files for each simulation are stored in separate files; and
3. performance information for each simulation is stored as different 'sets' in a single results file.

The advantages and disadvantages of each approach are listed in table 5.2.

Table 5.2: Comparison of result storage methods.

	Method 1	Method 2	Method 3
Disc space required for data storage and breadth of stored performance information	Small as only one selected performance assessment metric time series data would be stored for each simulation.	Large as a broad range of performance assessment metrics would be stored for each simulation.	Large as a broad range of performance assessment metrics would be stored for each simulation.
Results analysis	Could cause some problems due to minimal amount of information stored.	Separate files, therefore the same problems as currently exist.	Careful data recovery needed due to all results being kept in one file.
Results with different set lengths	Overcome in all cases through use of multiple simulation controller ensuring identical simulation period.		
Results handling procedure	ESP-r's results analysis facility would be used after each simulation, but further results analysis facilities would be needed to analyse the individual performance assessment metrics generated by this method.	ESP-r's results analysis facility would need to be able to read in multiple results files for this method or produce output for a separate analysis tool.	ESP-r's results analysis facility would need to be able to read in multiple result sets from the same file for this method.

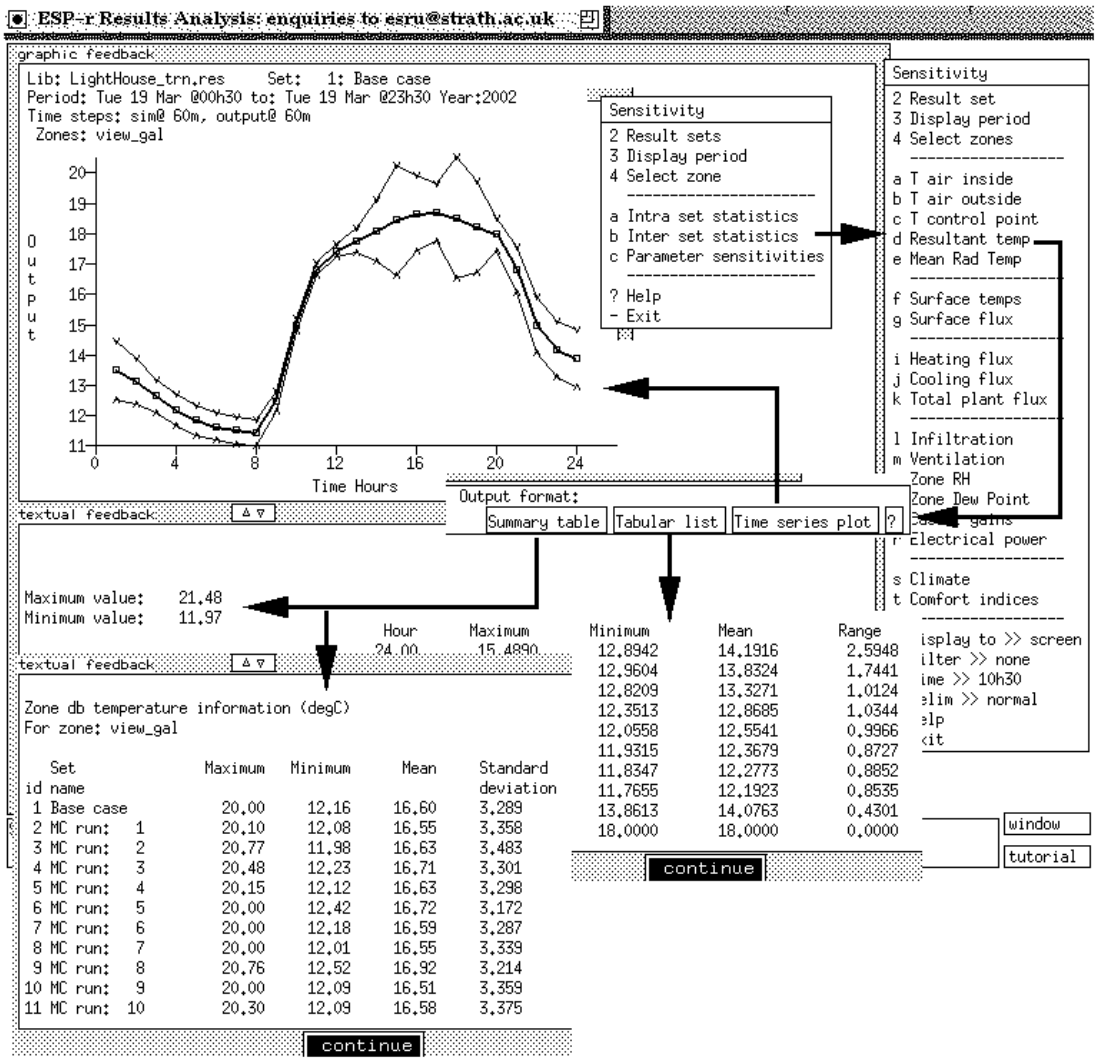

Figure 5.9: Analysis of uncertainty assessment in ESP-r.

Method 3 was chosen because this allows several metrics to be stored during the simulation allowing the effects of uncertainty to be quantified against several measures, *e.g.* peak temperature, plant load and thermal comfort. This requires ESP-r's result analysis facility to examine more than one results set at a time, and perform comparisons between sets. The analysis of multiple result sets is dependent on the uncertainty quantification method chosen at simulation time. With full results being stored for each simulation, the possibility of the full range of analysis currently available within the ESP-r system is available for each set. This allows the examination of the causes of extreme results and helps to identify possible parameter values that

would be detrimental to building performance. As can be seen in figure 5.9, the user is offered a full range of assessment metrics and output formats. Note the time varying effects of the uncertainties in the time series plot.

Summary

The external methods have been imbedded within the ESP-r simulator to ensure that they will stay compatible with future versions of the software. The interactions between the uncertainty analysis routines and the existing software have been elaborated. The adopted philosophy is to minimise the interactions with ESP-r's calculation procedures. This simplifies validation requirements as explained in chapter 6.

To verify the robustness of the implementation mechanism classes of uncertainties can currently be defined. This ensures that as further sources of uncertainty are quantified (in addition to those in chapter 4) their effects can be quantified.

Thermophysical properties: conductivity, density, specific heat capacity, absorptivity, emissivity and vapour diffusivity.

Constructions: layer thickness and composite reference.

Casual gains: total gain, sensible/latent ratio and convective/radiative ratio of sensible portion.

Air flow: Infiltration and ventilation air change rates and ventilation source temperature.

Geometry: zone volume and surface areas.

Climate: ambient temperature, direct and diffuse solar radiation, wind speed and direction and relative humidity.

Control: Set point and heater/chiller capacity for basic control.

Algorithm: convection coefficients.

The addition of new parameters to which uncertainty can be applied is a straightforward process.

The next section elaborates the application of internal methods to the core equation sets of the simulation engine.

5.2 Internal methods

The previous section considered simulation as a black box and as such did not use information on the parameter distributions during the calculations. This section develops the internal methods introduced in chapter 3. The techniques developed in this section characterise parameters as values *and* distributions and impose this information on the calculation procedure. This enables the overall uncertainty to be quantified, and the parameters causing this uncertainty to be identified, in a single simulation. Internal methods have been applied to the core equations of the thermal domain of ESP-r[1].

5.2.1 Range arithmetic considerations

There are some basic considerations which will affect the successful embedding of range arithmetic methods into the control volume conservation equations. The primary concern of any implementation must be in preserving the relationships between parameters, otherwise a parameter occurring in the expression of separate matrix coefficients may take on a high value for one coefficient and simultaneously take on a low value in the other. Referring back to the definition of subtraction in interval arithmetic (section 3.2.3), this non-sensible instance can be exemplified:

$$x - x = [1, 2] - [1, 2] = [-1, 1]. \tag{5.1}$$

[1]In integrated modelling there are other technical domains, *e.g.* CFD, moisture *etc.* These domains also require that sets of conservation equations be defined and solved. In this respect they are analogous to the thermal domain and so the technique described here is equally applicable to these domains.

Clearly if the range $[1, 2]$ represented the same data item then the result of the subtraction would be zero. Relationships of this kind are not easy to identify in a general application of interval arithmetic. The conductivity, density, specific heat and thickness of a material appear in multiple locations within the coefficient matrices, thus the above problem would occur in an interval arithmetic application. The same equation in affine arithmetic would be:

$$x - x = (1.5 + 0.5\epsilon_1) - (1.5 + 0.5\epsilon_1) = 0 \tag{5.2}$$

where $\epsilon_1 = [-1, 1]$.

When considering the solution of the matrix formulation, the choice is between a direct and indirect method. The solver of choice for a linear equation set (as is the case in the thermal domain) is a direct method requiring a LU decomposition of the future time-row coefficient matrix. This approach is computationally efficient since, given time invariant coefficients, the decomposition is calculated once at the beginning of a simulation and can be used for all time steps thereafter. However, when introducing uncertainties into the data, the efficiency of the LU decomposition results in variables being reused: if correlations between data items are not preserved then non sensible results will be calculated. This was clearly shown in the example in section 3.2.3 where the LU decomposition of a matrix using interval arithmetic was elaborated.

In an attempt to overcome this problem an indirect method can be used to solve the equations at each time step, for example the Gauss-Seidel method. This method has the advantage that the original future time-row matrix is used directly at each time step. However, as noted above, correlations between entries in the original matrix should still be preserved. For example, the conductivity of a node will appear three times in the same sum when the product of $\mathbf{A}.\theta_{\mathbf{t+1}}$ and $\mathbf{B}.\theta_{\mathbf{t}}$ is calculated.

Of the internal methods presented in chapter 3 only affine arithmetic preserves the relationship between data items and the source of any uncertainty. The following sections detail the application of affine arithmetic to the control volume conservation

equations comprising ESP-r's thermal energy balance model.

Energy balance for solid nodes

Recall the general equation for transient conduction in a solid node as presented in section 2.2.1. This equation is now extended to include uncertainties through the use of affine arithmetic.

The fundamental energy balance for the node is unchanged since no new energy flow paths are created. Thus, equation 2.4 is the valid starting point. However, the physical properties affecting the energy transfer mechanisms are now functions of their inherent uncertainties. Recalling the definition of an affine number, the representation of, for example, an uncertain conductivity at node i is given by

$$k_i = k_{i,0} + \sum_{j=1}^{\nu} k_{i,j}\epsilon_j \tag{5.3}$$

where $k_{i,0}$ is the average value of conductivity and the $k_{i,j}\epsilon_j$ represent the variation in conductivity due to each of the ν sources of uncertainty. Likewise all of the other terms in equation 2.4 can be represented in their affine forms. The length of time step, δt, is imposed on the solution process by the user and as such has no associated uncertainty. All of the remaining parameters are functions of the building being modelled:

ρ, C and k are properties of the materials and are susceptible to measurement errors and uncertainties due to moisture content *etc*,

δx is the thickness of the element and is subject to measurement errors and construction uncertainties; likewise the volume of the node V,

the various fluxes are also uncertain, *e.g.* plant losses might be less than or greater than expected, solar gain will reduce over time due to the accumulation of a dirt film on the glazing. The magnitude of these uncertainties will be calculated elsewhere, *e.g.* during the calculation of solar absorbed/transmitted through the glazing.

As a result of these uncertainties the temperature of the node will itself be uncertain. The result of all these uncertainties is that equation 2.4 becomes equation 5.4.

$$\begin{aligned}
&\left(2(\rho_{i,0}+\sum_{j=1}^{\nu}\rho_{i,j}\epsilon_j)(C_{i,0}+\sum_{j=1}^{\nu}C_{i,j}\epsilon_j)+\frac{2(k_{i,0}+\sum_{j=1}^{\nu}k_{i,j}\epsilon_j)\delta t}{(\delta x_{i,0}+\sum_{j=1}^{\nu}\delta x_{i,j}\epsilon_j)^2}\right)(\theta_{i,t+1,0}+\sum_{j=1}^{\nu}\theta_{i,t+1,j}\epsilon_j)\\
&-\frac{(k_{i,0}+\sum_{j=1}^{\nu}k_{i,j}\epsilon_j)\delta t}{(\delta x_{i,0}+\sum_{j=1}^{\nu}\delta x_{i,j}\epsilon_j)^2}\left((\theta_{i+1,t+1,0}+\sum_{j=1}^{\nu}\theta_{i+1,t+1,j}\epsilon_j)+(\theta_{i-1,t+1,0}+\sum_{j=1}^{\nu}\theta_{i-1,t+1,j}\epsilon_j)\right)\\
&-\frac{(q_{\mathrm{plant,i,t+1,0}}+\sum_{j=1}^{\nu}q_{\mathrm{plant,i,t+1,j}}\epsilon_j)\delta t}{(V_{i,0}+\sum_{j=1}^{\nu}V_{i,j}\epsilon_j)}-\frac{(q_{\mathrm{solar,i,t+1,0}}+\sum_{j=1}^{\nu}q_{\mathrm{solar,i,t+1,j}}\epsilon_j)\delta t}{(V_{i,0}+\sum_{j=1}^{\nu}V_{i,j}\epsilon_j)}\quad=\\
&\left(2(\rho_{i,0}+\sum_{j=1}^{\nu}\rho_{i,j}\epsilon_j)(C_{i,0}+\sum_{j=1}^{\nu}C_{i,j}\epsilon_j)-\frac{2(k_{i,0}+\sum_{j=1}^{\nu}k_{i,j}\epsilon_j)\delta t}{(\delta x_{i,0}+\sum_{j=1}^{\nu}\delta x_{i,j}\epsilon_j)^2}\right)(\theta_{i,t,0}+\sum_{j=1}^{\nu}\theta_{i,t,j}\epsilon_j)\\
&+\frac{(k_{i,0}+\sum_{j=1}^{\nu}k_{i,j}\epsilon_j)\delta t}{(\delta x_{i,0}+\sum_{j=1}^{\nu}\delta x_{i,j}\epsilon_j)^2}\left((\theta_{i+1,t,0}+\sum_{j=1}^{\nu}\theta_{i+1,t,j}\epsilon_j)+(\theta_{i-1,t,0}+\sum_{j=1}^{\nu}\theta_{i-1,t,j}\epsilon_j)\right)\\
&+\frac{(q_{\mathrm{plant,i,t,0}}+\sum_{j=1}^{\nu}q_{\mathrm{plant,i,t,j}}\epsilon_j)\delta t}{(V_{i,0}+\sum_{j=1}^{\nu}V_{i,j}\epsilon_j)}+\frac{(q_{\mathrm{solar,i,t,0}}+\sum_{j=1}^{\nu}q_{\mathrm{solar,i,t,j}}\epsilon_j)\delta t}{(V_{i,0}+\sum_{j=1}^{\nu}V_{i,j}\epsilon_j)}
\end{aligned}\tag{5.4}$$

As can be seen in equation 5.4 the uncertain parameters are now represented by affine numbers. The state variable, θ, is likewise represented in an affine form. In this manner the uncertainty in the parameters will be accounted for during the calculation and will be quantified in the state variables.

This is the general conservation equation for a solid node with uncertainties included. It should be noted that for any given set of values for the uncertainty tokens (ϵ_j), equation 5.4 reduces to equation 2.4. Recall that the numbering of uncertainty tokens is consistent throughout the model; therefore, uncertainty tokens for all properties can be related. For example, if density and specific heat capacity have a magnitude associated with uncertainty token j then both properties are implicitly defined as being correlated and if an uncertainty is not applicable to a parameter then its magnitude is zero.

Energy balance for surface nodes

Equation 2.8 is now extended to include uncertainties.

$$
\begin{aligned}
&\left[2(\rho_{i,0} + \sum_{j=1}^{\nu} \rho_{i,j}\epsilon_j)(C_{i,0} + \sum_{j=1}^{\nu} C_{i,j}\epsilon_j) \right. \\
&\qquad + \frac{2(k_{i,0} + \sum_{j=1}^{\nu} k_{i,j}\epsilon_j)\delta t}{(\delta x_{i,0} + \sum_{j=1}^{\nu} \delta x_{i,j}\epsilon_j)^2} \\
&\quad + \sum_{s=1}^{m} \frac{(h_{r,s,0} + \sum_{j=1}^{\nu} h_{r,s,j}\epsilon_j)(A_{i,0} + \sum_{j=1}^{\nu} A_{i,j}\epsilon_j)\delta t}{(V_{i,0} + \sum_{j=1}^{\nu} V_{i,j}\epsilon_j)} \\
&\quad \left. + \frac{(h_{c,s,0} + \sum_{j=1}^{\nu} h_{c,s,j}\epsilon_j)(A_{i,0} + \sum_{j=1}^{\nu} A_{i,j}\epsilon_j)\delta t}{(V_{i,0} + \sum_{j=1}^{\nu} V_{i,j}\epsilon_j)} \right] \quad \cdot \quad (\theta_{i,t+1,0} + \sum_{j=1}^{\nu} \theta_{i,t+1,j}\epsilon_j) \\
&\qquad - \left[\frac{2(k_{i,0} + \sum_{j=1}^{\nu} k_{i,j}\epsilon_j)\delta t}{(\delta x_{i,0} + \sum_{j=1}^{\nu} \delta x_{i,j}\epsilon_j)^2} \right] \quad \cdot \quad (\theta_{i+1,t+1,0} + \sum_{j=1}^{\nu} \theta_{i+1,t+1,j}\epsilon_j) \\
&\qquad - \frac{(q_{\text{plant,i,t+1,0}} + \sum_{j=1}^{\nu} q_{\text{plant,i,t+1,j}}\epsilon_j)\delta t}{(V_{i,0} + \sum_{j=1}^{\nu} V_{i,j}\epsilon_j)} \\
&\qquad - \frac{(q_{\text{solar,i,t+1,0}} + \sum_{j=1}^{\nu} q_{\text{solar,i,t+1,j}}\epsilon_j)\delta t}{(V_{i,0} + \sum_{j=1}^{\nu} V_{i,j}\epsilon_j)} \\
&- \left[\sum_{s=1}^{m} \frac{(h_{r,s,0} + \sum_{j=1}^{\nu} h_{r,s,j}\epsilon_j)(A_{i,0} + \sum_{j=1}^{\nu} A_{i,j}\epsilon_j)\delta t}{(V_{i,0} + \sum_{j=1}^{\nu} V_{i,j}\epsilon_j)} \right] \quad \cdot \quad (\theta_{s,t+1,0} + \sum_{j=1}^{\nu} \theta_{s,t+1,j}\epsilon_j) \\
&\quad - \left[\frac{(h_{c,0} + \sum_{j=1}^{\nu} h_{c,j}\epsilon_j)(A_{i,0} + \sum_{j=1}^{\nu} A_{i,j}\epsilon_j)\delta t}{(V_{i,0} + \sum_{j=1}^{\nu} V_{i,j}\epsilon_j)} \right] \quad \cdot \quad (\theta_{\text{fluid},t+1,0} + \sum_{j=1}^{\nu} \theta_{\text{fluid},t+1,j}\epsilon_j) = \\
&\qquad \left[2(\rho_{i,0} + \sum_{j=1}^{\nu} \rho_{i,j}\epsilon_j)(C_{i,0} + \sum_{j=1}^{\nu} C_{i,j}\epsilon_j) \right. \\
&\qquad - \frac{2(k_{i,0} + \sum_{j=1}^{\nu} k_{i,j}\epsilon_j)\delta t}{(\delta x_{i,0} + \sum_{j=1}^{\nu} \delta x_{i,j}\epsilon_j)^2} \\
&\quad - \sum_{s=1}^{m} \frac{(h_{r,s,0} + \sum_{j=1}^{\nu} h_{r,s,j}\epsilon_j)(A_{i,0} + \sum_{j=1}^{\nu} A_{i,j}\epsilon_j)\delta t}{(V_{i,0} + \sum_{j=1}^{\nu} V_{i,j}\epsilon_j)} \\
&\quad \left. - \frac{(h_{c,s,0} + \sum_{j=1}^{\nu} h_{c,s,j}\epsilon_j)(A_{i,0} + \sum_{j=1}^{\nu} A_{i,j}\epsilon_j)\delta t}{(V_{i,0} + \sum_{j=1}^{\nu} V_{i,j}\epsilon_j)} \right] \quad \cdot \quad (\theta_{i,t,0} + \sum_{j=1}^{\nu} \theta_{i,t,j}\epsilon_j) \\
&\qquad + \left[\frac{2(k_{i,0} + \sum_{j=1}^{\nu} k_{i,j}\epsilon_j)\delta t}{(\delta x_{i,0} + \sum_{j=1}^{\nu} \delta x_{i,j}\epsilon_j)^2} \right] \quad \cdot \quad (\theta_{i+1,t,0} + \sum_{j=1}^{\nu} \theta_{i+1,t,j}\epsilon_j) \\
&\qquad + \frac{(q_{\text{plant,i,t,0}} + \sum_{j=1}^{\nu} q_{\text{plant,i,t,j}}\epsilon_j)\delta t}{(V_{i,0} + \sum_{j=1}^{\nu} V_{i,j}\epsilon_j)} \\
&\qquad + \frac{(q_{\text{solar,i,t,0}} + \sum_{j=1}^{\nu} q_{\text{solar,i,t,j}}\epsilon_j)\delta t}{(V_{i,0} + \sum_{j=1}^{\nu} V_{i,j}\epsilon_j)} \\
&+ \left[\sum_{s=1}^{m} \frac{(h_{r,s,0} + \sum_{j=1}^{\nu} h_{r,s,j}\epsilon_j)(A_{i,0} + \sum_{j=1}^{\nu} A_{i,j}\epsilon_j)\delta t}{(V_{i,0} + \sum_{j=1}^{\nu} V_{i,j}\epsilon_j)} \right] \quad \cdot \quad (\theta_{s,t,0} + \sum_{j=1}^{\nu} \theta_{s,t,j}\epsilon_j) \\
&\quad + \left[\frac{(h_{c,0} + \sum_{j=1}^{\nu} h_{c,j}\epsilon_j)(A_{i,0} + \sum_{j=1}^{\nu} A_{i,j}\epsilon_j)\delta t}{(V_{i,0} + \sum_{j=1}^{\nu} V_{i,j}\epsilon_j)} \right] \quad \cdot \quad (\theta_{\text{fluid},t,0} + \sum_{j=1}^{\nu} \theta_{\text{fluid},t,j}\epsilon_j) \qquad (5.5)
\end{aligned}
$$

In this case there are additional uncertainties associated with the longwave radiation and convection terms:

h_r is a property of the zone's surface materials and areas and so is susceptible to measurement errors and uncertainties due to dirt *etc*,

h_c is an empirical coefficient and is therefore susceptible to measurement errors.

The resulting expansion of the general equation for a surface node gives rise to equation 5.5, where the uncertain parameters and state variables are again represented as affine numbers. This is the general equation for a surface node where uncertainties exist. Again it should be noted that for any given set of values for the uncertainty tokens (ϵ_j) equation 5.5 reduces to equation 2.8.

Various expressions for the convective heat transfer coefficient exist [Beausoleil-Morrison 2001]. One such expression used in ESP-r is the Alamdari and Hammond correlation

$$h_c = \left(\left[a \left(\frac{\Delta\theta}{d} \right)^{1/4} \right]^6 + \left[b(\Delta\theta)^{1/3} \right]^6 \right)^{1/6} \tag{5.6}$$

where a and b are empirical coefficients and $\Delta\theta$ is the temperature difference between the solid and fluid and d is a characteristic dimension. This equation would be used at each time step to calculate the time varying heat transfer coefficient. The four parameters described above can be replaced by affine terms. In the case of temperature difference the solid and fluid terms will have uncertainty tokens associated with all sources of uncertainty. The characteristic dimension will only have an uncertainty associated with its size. The empirical coefficients can be assigned uncertainty tokens relating to the spread of experimental data. Therefore, the resulting affine expression of h_c will include all possible values for a specific temperature difference and characteristic dimension (due to the inclusion of uncertainty in a and b), the uncertainty due to the size of the characteristic dimension and the uncertainty due to the prevailing temperature difference. Note it is only possible to know the uncertainty in the prevailing temperature difference by integrating the effects of uncertainty into the conservation equations.

Energy balance for fluid nodes

Equation 2.11 is now extended to include uncertainties. In this case there are additional uncertainties associated with the advection term:

$\dot{m}$ is a function of uncertain parameters including wind direction, speed, pressure coefficients, temperature; and

C is a property of air and is subject to measurement errors.

The expansion of the general equation for a fluid node gives rise to the equation 5.7.

$$
\begin{aligned}
&\left[2(\rho_{i,0}+\sum_{j=1}^{\nu}\rho_{i,j}\epsilon_j)(C_{i,0}+\sum_{j=1}^{\nu}C_{i,j}\epsilon_j)\right.\\
&+\sum_{s=1}^{m}\frac{(h_{c,s,0}+\sum_{j=1}^{\nu}h_{c,s,j}\epsilon_j)(A_{s,0}+\sum_{j=1}^{\nu}A_{s,j}\epsilon_j)\delta t}{(V_{i,0}+\sum_{j=1}^{\nu}V_{i,j}\epsilon_j)}\\
&\left.+\sum_{r=1}^{p}\frac{(\dot{m}_{r,0}+\sum_{j=1}^{\nu}\dot{m}_{r,j}\epsilon_j)(C_{r,0}+\sum_{j=1}^{\nu}C_{r,j}\epsilon_j)\delta t}{(V_{i,0}+\sum_{j=1}^{\nu}V_{i,j}\epsilon_j)}\right] \cdot (\theta_{i,t+1,0}+\sum_{j=1}^{\nu}\theta_{i,t+1,j}\epsilon_j)\\
&-\frac{(q_{\text{plant},t+1,0}+\sum_{j=1}^{\nu}q_{\text{plant},t+1,j}\epsilon_j)\delta t}{(V_{i,0}+\sum_{j=1}^{\nu}V_{i,j}\epsilon_j)}\\
&-\left[\sum_{s=1}^{m}\frac{(h_{c,s,0}+\sum_{j=1}^{\nu}h_{c,s,j}\epsilon_j)(A_{s,0}+\sum_{j=1}^{\nu}A_{s,j}\epsilon_j)\delta t}{(V_{i,0}+\sum_{j=1}^{\nu}V_{i,j}\epsilon_j)}\right] \cdot (\theta_{s,t+1,0}+\sum_{j=1}^{\nu}\theta_{s,t+1,j}\epsilon_j)\\
&-\left[\sum_{r=1}^{p}\frac{(\dot{m}_{r,0}+\sum_{j=1}^{\nu}\dot{m}_{r,j}\epsilon_j)(C_{i,0}+\sum_{j=1}^{\nu}C_{i,j}\epsilon_j)\delta t}{(V_{i,0}+\sum_{j=1}^{\nu}V_{i,j}\epsilon_j)}\right] \cdot (\theta_{\text{srcfluid},t+1,0}+\sum_{j=1}^{\nu}\theta_{\text{srcfluid},t+1,j}\epsilon_j) =\\
&\left[2(\rho_{i,0}+\sum_{j=1}^{\nu}\rho_{i,j}\epsilon_j)(C_{i,0}+\sum_{j=1}^{\nu}C_{i,j}\epsilon_j)\right.\\
&-\sum_{s=1}^{m}\frac{(h_{c,s,0}+\sum_{j=1}^{\nu}h_{c,s,j}\epsilon_j)(A_{s,0}+\sum_{j=1}^{\nu}A_{s,j}\epsilon_j)\delta t}{(V_{i,0}+\sum_{j=1}^{\nu}V_{i,j}\epsilon_j)}\\
&\left.-\sum_{r=1}^{p}\frac{(\dot{m}_{r,0}+\sum_{j=1}^{\nu}\dot{m}_{r,j}\epsilon_j)(C_{r,0}+\sum_{j=1}^{\nu}C_{r,j}\epsilon_j)\delta t}{(V_{i,0}+\sum_{j=1}^{\nu}V_{i,j}\epsilon_j)}\right] \cdot (\theta_{i,t,0}+\sum_{j=1}^{\nu}\theta_{i,t,j}\epsilon_j)\\
&+\frac{(q_{\text{plant},t+1,0}+\sum_{j=1}^{\nu}q_{\text{plant},t+1,j}\epsilon_j)\delta t}{(V_{i,0}+\sum_{j=1}^{\nu}V_{i,j}\epsilon_j)}\\
&+\left[\sum_{s=1}^{m}\frac{(h_{c,s,0}+\sum_{j=1}^{\nu}h_{c,s,j}\epsilon_j)(A_{s,0}+\sum_{j=1}^{\nu}A_{s,j}\epsilon_j)\delta t}{(V_{i,0}+\sum_{j=1}^{\nu}V_{i,j}\epsilon_j)}\right] \cdot (\theta_{s,t,0}+\sum_{j=1}^{\nu}\theta_{s,t,j}\epsilon_j)\\
&+\left[\sum_{r=1}^{p}\frac{(\dot{m}_{r,0}+\sum_{j=1}^{\nu}\dot{m}_{r,j}\epsilon_j)(C_{i,0}+\sum_{j=1}^{\nu}C_{i,j}\epsilon_j)\delta t}{(V_{i,0}+\sum_{j=1}^{\nu}V_{i,j}\epsilon_j)}\right] \cdot (\theta_{\text{srcfluid},t,0}+\sum_{j=1}^{\nu}\theta_{\text{srcfluid},t,j}\epsilon_j) \qquad (5.7)
\end{aligned}
$$

This is the general equation for a fluid node where uncertainties exist. Again it should be noted that for any given set of values for the uncertainty tokens (ϵ_j) equation 5.7 reduces to equation 2.11.

5.2.2 Solution methods including uncertainties

For a given building an equation set can be established using equations 5.4, 5.5 and 5.7. These equations must then be solved for each required time step. The solution procedure will require non-affine operations (*e.g.* multiplication and division), resulting in temperature terms for future time steps being expressed in terms of uncertainties in the input data and calculation uncertainties. These calculation uncertainties can now propagate through the simulation and potentially dominate. Thus, any implementation of affine arithmetic must preserve the initial descriptions and minimise the use of non-affine calculations. This has two immediate consequences:

1. The LU decomposition of the future time row coefficients matrix is not appropriate due to the repeated multiplications and divisions necessary to gain the decomposed matrix. Thus an iterative approach is necessary.

2. The fundamental solution algorithms should be re-appraised. Initially these algorithms were optimised in order to minimise the number of operations undertaken to obtain a solution. Now the algorithms should be optimised in order to minimise the number of *non-affine* operations required.

For these reasons a Gauss-Seidel iterative solver has been employed. Within the Gauss-Seidel method each row of coefficients is divided by the diagonal element of the future time step coefficients matrix for that row. In normal arithmetic this results in the diagonal elements having a value of one. The result of these divisions in an affine arithmetic implementation is the creation of multiple new uncertainty tokens (one for each division). These aspects of the affine arithmetic implementation are elaborated in chapter 6 *via* numerical examples.

5.2.3 Other domains

Affine arithmetic can also be applied to the other aspects of the building relating to HVAC, control systems, renewable energy components and lighting. To achieve this the affine approach should be applied to the mathematical models for the air flow, moisture and electrical domains.

In the case of air flow, for example, as described in section 2.2.2 two approaches are possible: network air flow and CFD. In the case of network air flow the mass flow rate between two volumes was given by the general relationship $\dot{m} = f(\Delta P)$. In the case of a crack this function can be represented by a expression involving two empirical coefficients (see equation 2.13). Both of these coefficients will be uncertain due to measurement errors. The density of air will also be uncertain as it is a function of the fluid's temperature and is empirically measured. The source of uncertainty in pressure difference will depend on wind velocity and pressure coefficient for boundary control volumes and, for non-boundary control volumes, the uncertainty will be a function of the uncertain mass flow rates into the control volume. The resulting affine expression for flow through a crack, based on the power law representation of equation 2.13, is

$$\begin{aligned}\dot{m}_{i,0} + \sum_{j=1}^{\nu} \dot{m}_{i,j}\epsilon_j = \\ (\rho_{b,0} + \sum_{j=1}^{\nu} \rho_{b,j}\epsilon_j) \cdot (\kappa_{i,0} + \sum_{j=1}^{\nu} \kappa_{i,j}\epsilon_j) \cdot \\ \left((P_{a,0} + \sum_{j=1}^{\nu} P_{a,j}\epsilon_j) - (P_{b,0} + \sum_{j=1}^{\nu} P_{b,j}\epsilon_j) \right)^{(n_{i,0} + \sum_{j=1}^{\nu} n_{i,j}\epsilon_j)}\end{aligned} \tag{5.8}$$

for connection i between fluid volumes a and b. This expression for flow through a crack is non-linear. Therefore, an iterative solution procedure is required and the method presented in the previous section could be usefully employed.

Likewise, the affine representation could be applied to continuity and the conservation of momentum, energy and concentration equations which comprise the CFD approach. This would entail the replacement of the parameters of these equations by

affine representations. For example, consider the momentum equation. The governing parameter for the diffusion term is

$$\mu_{\text{ef}} = \mu_{\text{t}} + \mu$$

where μ_{t} is the eddy viscosity and μ the molecular viscosity (both $kgm^{-1}s^{-1}$). The eddy viscosity is a function of both the fluid properties and the flow conditions. One expression for the eddy viscosity is [Munson *et al* 1998]

$$\mu_{\text{t}} = \rho l_m^2 \left| \frac{d\bar{u}}{dy} \right| .$$

The fluid density, ρ, will be subject to uncertainty as a result of any uncertainties in temperature For example, from a boundary condition where the surface temperature is represented as described in section 5.2.1. The mean velocity, $\bar{u}$, will be subject to uncertainty derived from the flow field, including boundary conditions. The mixing length, l_m, will likewise be uncertain. All of these terms should be replaced by affine representations. The same modifications should be made to the source term of the momentum equation set which includes pressure, density, temperature and thermal expansion terms which are all subject to uncertainty. It would also be necessary to introduce affine terms into the continuity, energy and concentration equations so as the effects of uncertainty are calculated throughout the CFD domain.

In both of these approaches to flow modelling there would be a significant increase in the number of non-affine operations, due to the use of non-linear expressions. Careful consideration must be given to avoid the new affine terms created by these operations dominating the solution.

5.3 Summary

The integration of uncertainty quantification methods into an existing simulation environment has been described. The integration of external methods requires only the data model to be altered, whereas the internal methods require the conservation equations to be updated as well. External methods, however, require multiple simulations and as a result careful data management for the perturbed model creation and results analysis.

References

Beausoleil-Morrison I, *The Adaptive Coupling of Heat and Air Flow Modelling Dynamic Whole-Building Simulation*, PhD thesis, University of Strathclyde, Glasgow, UK, 2001

Clarke J A, *Energy Simulation in Building Design*, 2^{nd} edition, Butterworth-Heinmann 2001

Energy Systems Research Unit, *http://www.esru.strath.ac.uk*

Munsong B R, Young D F, Okiishi T H, *Fundamentals of Fluid Mechanics*, 3^{rd} edition, John Wiley and Sons, 1998

Chapter 6

Verification and applicability

The implementations of the selected methods are verified. This requires a suitable testing method. The appropriateness of the uncertainty method to accommodate specific design issues is identified.

The uncertainty analysis methods as implemented in ESP-r require to be verified and their applicability confirmed. The verification process, however, does not need to validate the methods themselves. The external methods have been verified previously and are in general use [Saltelli *et al* 2000]. The applied internal method is self-validating in that the correct answer will always be bounded by the solution, given the initial bounds. However, the implementation of each method has to be verified. The verification method is applied to the external and internal methods via example thermal models.

6.1 Verification method

The process employed is based on validation techniques used previously in building simulation.

There are three traditional validation procedures used in building simulation: comparison with analytical solutions, comparison with other models and comparison with

measured data. These methods are, in the order given, increasingly expensive to apply although increasingly comprehensive. To collect measured data of the required quality for comparisons with simulations is difficult and hence expensive, but will test models under realistic conditions. Analytical comparisons are easily made but are generally not representative of realistic conditions, *e.g.* adiabatic boundary conditions are easily defined in a numerical model but are not realised in practice. Inter-model comparisons offer the developer the benefits of realistic test conditions with the ease of application of analytical tests. However, such comparisons could show good agreement between the models even when all models are invalid.

ESP-r has been tested using all three validation methods [*e.g.* CEN 1997, Judkoff and Neymark 1995, Lomas 1996]; a comprehensive list of studies has also been produced [Strachan 2000]. Therefore, ESP-r can be used as a valid model against which to test the internal method due to the necessary changes to the conservation equations.

External methods are implemented within ESP-r as a wrapper around the simulation engine. Therefore, the process has to verify:

1. the correct variables are being modified for each simulation; and
2. the solution of the perturbed model is identical to that of an identically perturbed independent model.

The first item above can be checked by examining code and through proper reporting during simulations. The second item can be checked by running an independent simulation of a perturbed model to compare against the automatically perturbed model. A successful result of the second test will imply that the first test is also satisfied. An inter-model comparison is therefore the most appropriate test mechanism for assessing the implementation of external methods. To check that the correct results are obtained for the external methods requires the checking of only a few lines of code, as test two will have confirmed that the correct data is being recovered from each of the multiple simulations, all that remains is the determination of differences, averages *etc.*

For the internal method the procedure has to test:

1. that the solution with no uncertainties applied is the same as that from the existing version of ESP-r;

2. the quantified uncertainties are similar to those generated by the external methods.

Again, an inter-model comparison is the most appropriate test mechanism.

Therefore, the verification process adopted takes the form of an inter-model comparison. Each perturbed model simulated by an external method is equivalent to a reference model which can be created and simulated independently. The results from both models should then be identical. The internal method should produce answers comparable to the external methods but in a single simulation. Therefore, the internal method can be verified against the solution of the external methods.

Three models are referred to throughout this chapter:

base case model is the unperturbed model;

perturbed model is the model automatically perturbed by the multiple simulation controller; and

reference model is an independently created model (equivalent to a perturbed model) for the inter-model comparison.

To focus on the pertinent aspects of the tests, basic models have been selected that encapsulate the principal thermal processes occurring in a building. The verification procedure also has to ensure that the differences in the models are clearly reported and that the results recovery is suitably comprehensive. These three aspects of the test are elaborated in the following sections with the comparisons made at each stage reported in sections 6.2 and 6.3.

6.1.1 Test models

The criteria for a test model is that it should be representative of the physical process for which uncertainties are to be tested and that the model should be simple so as

not to confuse the test results. To achieve these criteria two models were employed in the current work. For the external methods the model must have the relevant parameters defined for the uncertainty implementation to be tested. For the internal method the model has to focus on transient conduction as the equations developed for this method focus on this aspect of the building conservation equation set.

The first model used (figure 6.1) is representative of an office building. The model allows uncertainty quantification in the following parameters to be verified:

1. conductivity,
2. density,
3. specific heat capacity,
4. layer thickness,
5. casual gains,
6. infiltration and ventilation rates,
7. climate conditions,
8. control parameters.

For the second model the CEN transient conduction test has been selected [CEN 1997]. The model is of a cube, where heat is conducted through the walls. The model details are given in appendix B. The model allows the implementation of uncertainties in the following parameters to be verified:

1. conductivity,
2. heat capacity,
3. thickness.

The details of these two models is of less importance than an ability to examine the difference between the required models and the results from simulations over the same period.

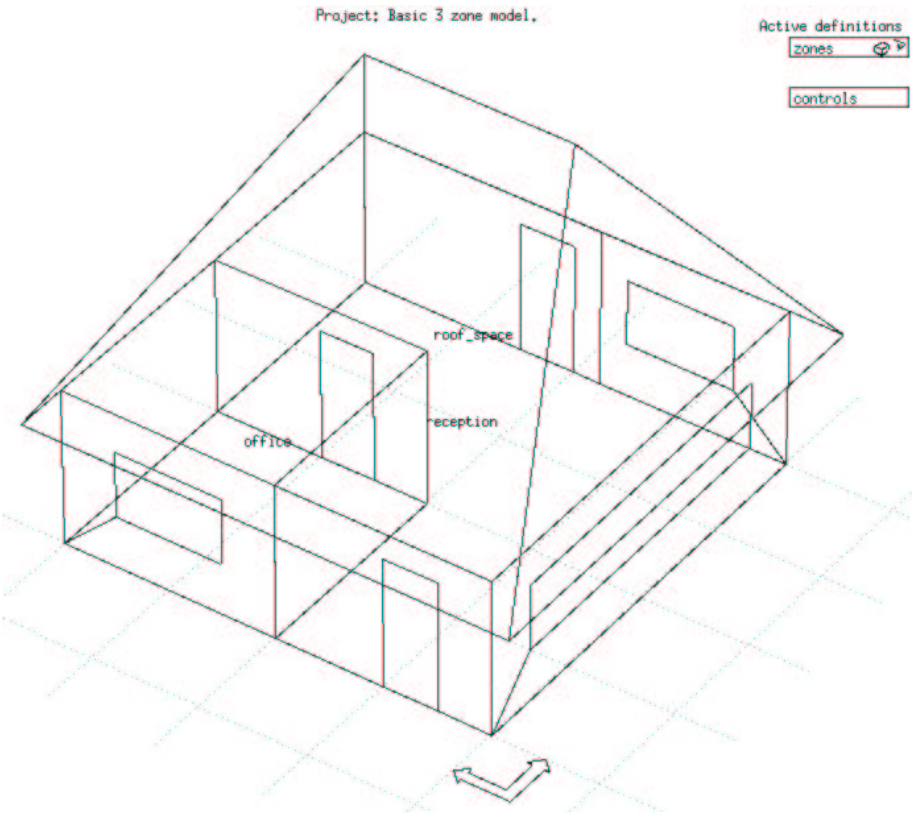

Figure 6.1: Three zone example model.

6.1.2 Model reporting

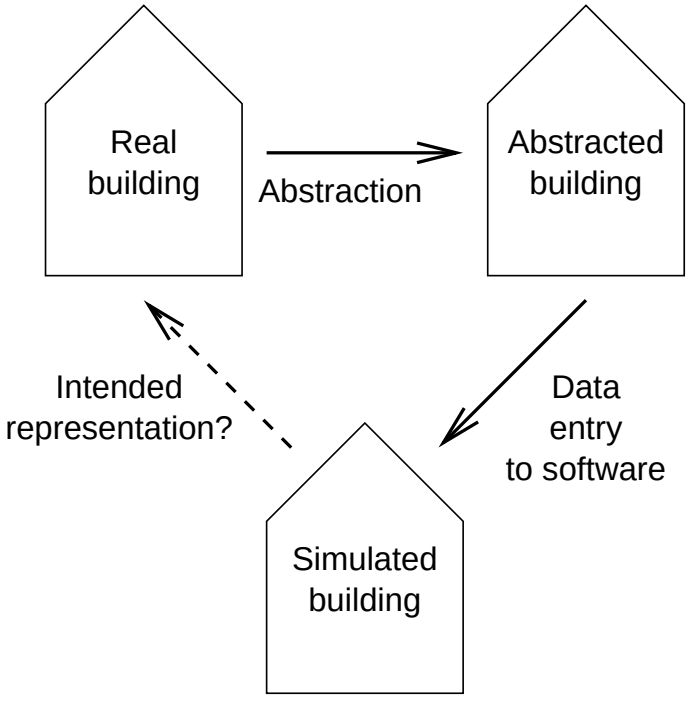

Figure 6.2: Simulation models.

To ensure that the base case model and the perturbed model have only the intended differences, a comprehensive reporting facility was added to ESP-r. Three versions of a building exist, one real and two virtual: the real building, the abstracted building (*i.e.* the building the practitioner intends to simulate) and the simulated building (*i.e.* the building represented by the data entered into the software). The translation process between the real building and the two models is shown in figure 6.2. As can be seen the only differences between models 2 and 3 are due to user input errors. Therefore, if the simulation software can report back to the practitioner details of their model, the practitioner can identify where errors exist and the intended representation of the real building can be checked.

By using this facility two models can be compared and the differences between them identified as shown in figure 6.3. A reference model is created with intentional differences from the base case model. This stage is a manual process and is represented by a broken line (automatic processes are represented by a solid line). Reports are generated for both models and the differences in these reports identified. The final check is to ensure that the differences between the reports are identical to the intended perturbations, *i.e.* the correct reference model has been created. Individual reference models are required for every set of perturbations that are to be tested.

The advantage of using this system is that the software is generating the reports, hence minimizing the likelihood of human error.

6.1.3 Results reporting

Ensuring that the data model has been correctly altered (see section 5.1.2) requires simulations to be compared as the multiple simulation controller automatically resets and updates the data model during the simulation process. This check is made by comparing the results of two simulations.

The simulation run of the model using an external method will contain result sets from each of the perturbed models. The simulation of the reference model will represent one of the models created during the multiple simulations. The output of the corresponding models (perturbed and reference) is then compared. This process

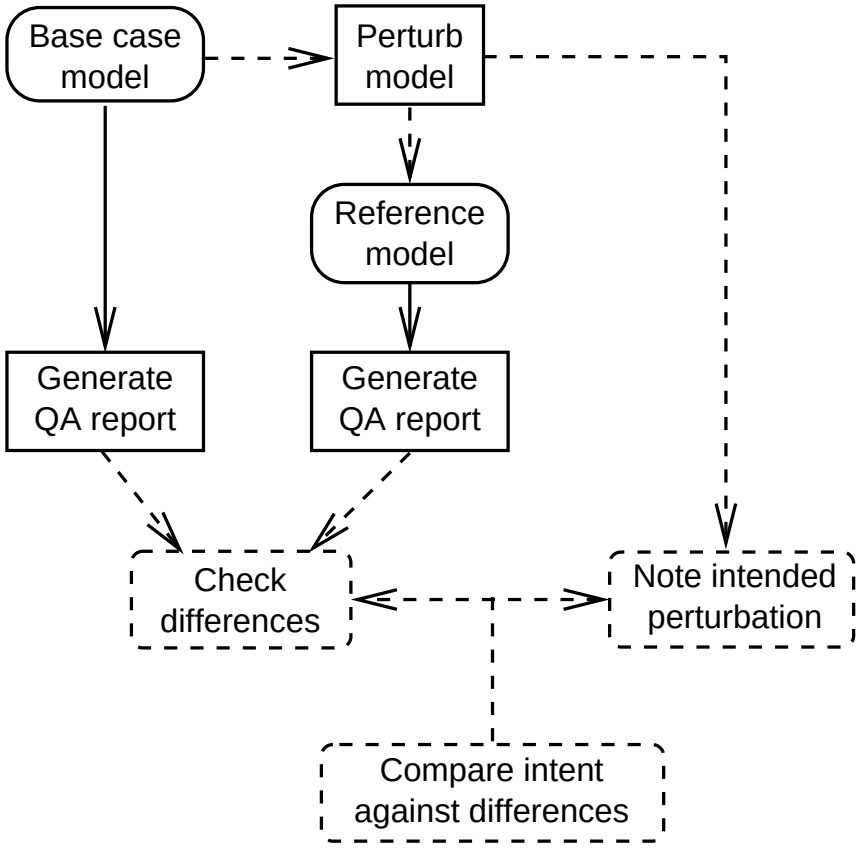

Figure 6.3: Checking correct application of perturbations.

is repeated for each uncertainty type.

The comparison process is depicted in figure 6.4. As can be seen, the model is simulated with uncertainties active and the results for each individual simulation are extracted (perturbed model results). This is an automatic process (represented by solid lines). For each perturbed model a reference model is created. This is a manual process (represented by broken lines) and the model is therefore checked by the method described in the previous section. Each reference model is simulated separately and reference result sets created (an automatic process). If the multiple simulation controller is resetting and updating the data model correctly there should be no differences between the corresponding result sets.

To reduce the likelihood of human error the simulation and results extraction processes were automated.

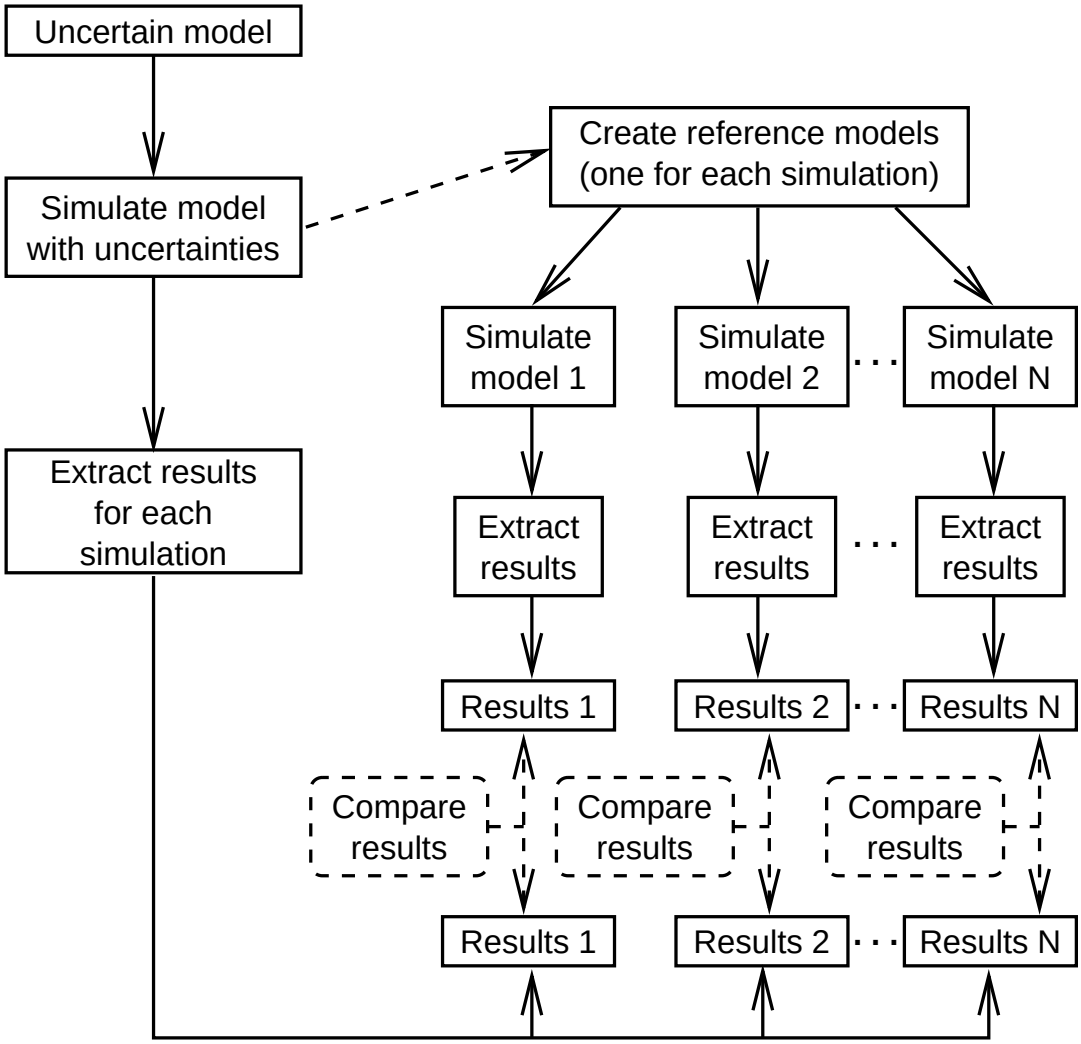

Figure 6.4: Checking correct simulation of perturbations.

6.2 External methods

The office model introduced above was used to verify that the correct data was manipulated for each of the three external methods and for each type of uncertainty.

6.2.1 Differential analysis

Uncertainties of the eight previously listed types were analysed. The uncertainties are listed in table 6.1. Note that these uncertainties have been arbitrarily selected for the purpose of verification.

The differential analysis of this model requires 57 simulations and therefore 56 reference models have to be created (as the first simulation is of the base case model).

Table 6.1: Uncertainties defined for verification model

Parameter	Uncertainty
Climate parameter: Dry bulb temperature	$2.00°C$
Climate parameter: Direct normal solar	10.00%
Climate parameter: Diffuse horiz solar	10.00%
Climate parameter: Wind speed	10.00%
Climate parameter: Wind direction	10.00°
Climate parameter: Relative humidity	10.00%
Material: Heavy mix concrete conductivity	10.00%
Material: Heavy mix concrete density	10.00%
Material: Heavy mix concrete specific	10.00%
Material: Breeze block emissivity	10.00%
Material: Breeze block absorptivity	10.00%
Comp constr: 'extern wall' insulation layer thickness	10.00%
Total casual gain, type: occupants	10.00%
Sensible casual gain, type: occupants	10.00%
Latent casual gain, type: occupants	10.00%
Radiant fraction casual gain, type: occupants	0.20
Total casual gain, type: lighting	10.00%
Sensible casual gain, type: lighting	10.00%
Latent casual gain, type: lighting	10.00%
Radiant fraction casual gain, type: lighting	0.20
Total casual gain, type: equipment	10.00%
Sensible casual gain, type: equipment	10.00%
Latent casual gain, type: equipment	10.00%
Radiant fraction casual gain, type: equipment	0.20
Scheduled infiltration	10.00%
Scheduled ventilation	10.00%
Control: Max heating flux	10.00%
Control: Heating set point	$2.00°C$

Each of the 56 reference models represents a perturbed model created during the differential analysis.

These models have been created and added to the ESP-r suite of benchmark models. The analysis process within this suite is automated, allowing a user to verify the implementation. In all cases exactly the same output is generated from the perturbed model and the corresponding reference model. Therefore, the implementation of the listed parameters has been successfully verified.

To demonstrate the efficacy of this procedure, the direct solar irradiance was deliberately set high in the reference model by $1W/m^2$ for a single time step. The results of the verification test are displayed in figure 6.5. The highlighted lines in the figure

show where the difference between the two models occurs. The differences are small: $0.01°C$ in average air temperature, $0.01W$ in average and maximum infiltration load, and smaller differences in ventilation loads and relative humidity.

Although these differences are insignificant in terms of building performance, they should not exist if the two models are identical. If the direct solar radiation is reset to its correct value the models produce identical output. Clearly, the testing procedure is sensitive to errors in the model and therefore, if the multiple simulation controller did not manipulate the data model correctly the test would have failed.

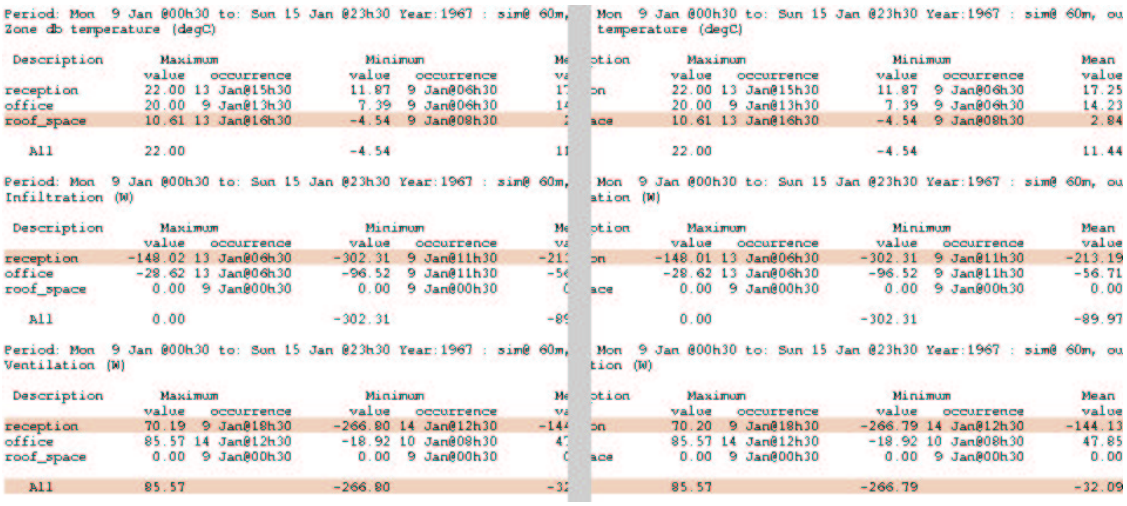

Period: Mon 9 Jan @00h30 to: Sun 15 Jan @23h30 Year:1967 : sim@ 60m,
Zone db temperature (degC)

Description	Maximum value	Maximum occurrence	Minimum value	Minimum occurrence	Me va
reception	22.00	13 Jan@15h30	11.87	9 Jan@06h30	17
office	20.00	9 Jan@13h30	7.39	9 Jan@06h30	14
roof_space	10.61	13 Jan@16h30	-4.54	9 Jan@08h30	2
All	22.00		-4.54		11

Mon 9 Jan @00h30 to: Sun 15 Jan @23h30 Year:1967 : sim@ 60m, ou
temperature (degC)

otion	Maximum value	Maximum occurrence	Minimum value	Minimum occurrence	Mean value
on	22.00	13 Jan@15h30	11.87	9 Jan@06h30	17.25
	20.00	9 Jan@13h30	7.39	9 Jan@06h30	14.23
ace	10.61	13 Jan@16h30	-4.54	9 Jan@08h30	2.84
	22.00		-4.54		11.44

Period: Mon 9 Jan @00h30 to: Sun 15 Jan @23h30 Year:1967 : sim@ 60m,
Infiltration (W)

Description	Maximum value	Maximum occurrence	Minimum value	Minimum occurrence	Me va
reception	-148.02	13 Jan@06h30	-302.31	9 Jan@11h30	-213
office	-28.62	13 Jan@06h30	-96.52	9 Jan@11h30	-56
roof_space	0.00	9 Jan@00h30	0.00	9 Jan@00h30	0
All	0.00		-302.31		-89

Mon 9 Jan @00h30 to: Sun 15 Jan @23h30 Year:1967 : sim@ 60m, ou
ation (W)

otion	Maximum value	Maximum occurrence	Minimum value	Minimum occurrence	Mean value
on	-148.01	13 Jan@06h30	-302.31	9 Jan@11h30	-213.19
	-28.62	13 Jan@06h30	-96.52	9 Jan@11h30	-56.71
ace	0.00	9 Jan@00h30	0.00	9 Jan@00h30	0.00
	0.00		-302.31		-89.97

Period: Mon 9 Jan @00h30 to: Sun 15 Jan @23h30 Year:1967 : sim@ 60m,
Ventilation (W)

Description	Maximum value	Maximum occurrence	Minimum value	Minimum occurrence	Me va
reception	70.19	9 Jan@18h30	-266.80	14 Jan@12h30	-144
office	85.57	14 Jan@12h30	-18.92	10 Jan@08h30	47
roof_space	0.00	9 Jan@00h30	0.00	9 Jan@00h30	0
All	85.57		-266.80		-32

Mon 9 Jan @00h30 to: Sun 15 Jan @23h30 Year:1967 : sim@ 60m, ou
tion (W)

otion	Maximum value	Maximum occurrence	Minimum value	Minimum occurrence	Mean value
on	70.20	9 Jan@18h30	-266.79	14 Jan@12h30	-144.13
	85.57	14 Jan@12h30	-18.92	10 Jan@08h30	47.85
ace	0.00	9 Jan@00h30	0.00	9 Jan@00h30	0.00
	85.57		-266.79		-32.09

Figure 6.5: Verification comparison - failure (differences highlighted).

All 56 reference models produced identical results to the perturbed models created automatically by the multiple simulation controller.

6.2.2 Factorial analysis

The process for verifying the implementation of the factorial method is essentially the same as for the differential method. The main difference is that multiple parameters are perturbed simultaneously by the multiple simulation controller.

In the implementation employed, the data perturbation routines are independent of the analysis method (see section 5.1.2). The implication of this is that if the data model is correctly updated for a specific uncertainty then this will be true for all methods. Therefore, it is only necessary to verify that the correct perturbations are

made to verify the factorial method. Nevertheless, the same verification process was undertaken, as this will confirm that the correct perturbations and simulations have been enabled by the multiple simulation controller. As can be seen in table 6.2, a subset of the uncertainties in table 6.1 was used in the process due to the limitations of the factorial method: the required number of simulations being a function of the uncertainties defined. In this case the full factorial analysis was undertaken resulting in 16 simulations.

Table 6.2: Uncertainties defined for verification model

Parameter	Uncertainty
Climate parameter: Dry bulb temperature	$2.00°C$
Material: Heavy mix concrete conductivity	10.00%
Total casual gain, type: occupancy	10.00%
Scheduled infiltration	10.00%

The models for the factorial analysis have also been added to the ESP-r suite of benchmark models. The multiple simulation controller steps through the required model changes for the factorial method and the output was compared to that of the reference models as before. Again there are no differences between the results sets indicating that the correct perturbations are made to the data model.

6.2.3 Monte Carlo analysis

Given the successful verification of the differential and factorial methods it is unnecessary to embark on a full verification of the Monte Carlo implementation. However, the distributions for the perturbation of each uncertain parameter should be checked. The same uncertainties as for the differential method were used in the verification test (table 6.1) with a normal distribution applied to each parameter.

Table 6.3 shows a comparison of the uncertainty definition and the perturbed values used during the simulations. As expected, the mean and standard deviation of the values used in the 80 simulation runs do not match the defined value and uncertainty magnitude exactly. Figure 6.6 shows a histogram of the thickness values with the ideal distribution overlaid. The mean values are not statistically different at a 95% confidence level and therefore verify this aspect of the implementation.

Table 6.3: Uncertainty definitions and perturbed parameters

Parameter	Defined value	Uncertainty magnitude	Sample mean	Standard deviation
Insulation thickness (m)	0.075	10%	0.0738	0.0064
Sensible heat gain 1 (W)	800	10%	801.9	75.7
Sensible heat gain 2 (W)	540	10%	539.4	48.8

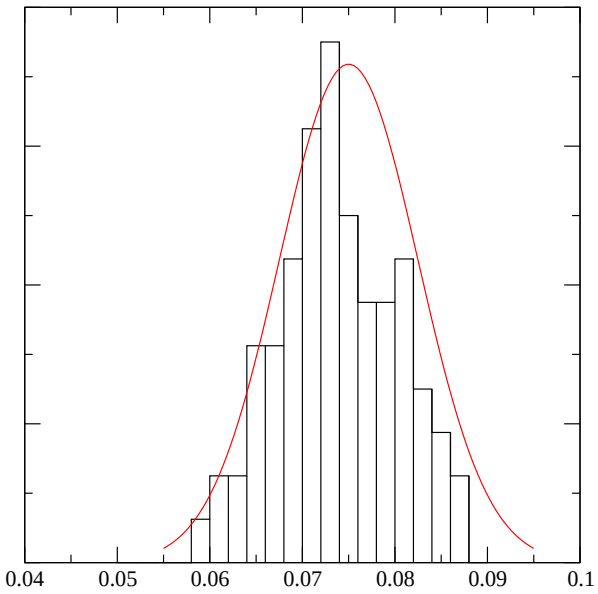

Figure 6.6: Perturbed thickness values including ideal distribution

6.2.4 Summary

For each of the tests the results were as expected, *i.e.* the correct data was identified and altered by the multiple simulation controller and the results from a perturbed model are identical to a reference model. From this it can be concluded that the three external methods have been correctly implemented.

6.3 Internal methods

The theory developed for the internal method focused on transient conduction and therefore the CEN standard for transient conduction was selected as a suitable test model.

6.3.1 Matrix formulation and solution

The CEN test model [CEN 1997] (see also Appendix B) comprises a cube ($1m \times 1m \times 1m$) which is subjected to a step change in external air temperature. The response of the internal air temperature is measured for three different construction types in the following simulations.

To enable solution the cube is discretised into control volumes. Control volumes are identified as representing the following:

1. external boundary air,
2. external surface,
3. mid-construction,
4. internal surface, and
5. internal air.

Item one in the above list is known at all times and the four unknown temperatures are calculated over time. As the boundary conditions are identical for all surfaces and the construction of each surface is also identical, the problem can be reduced to that of heat conduction through a slab of cross section area $6m^2$ exposed to an enclosed air volume of $1m^3$. This is shown in figure 6.7, where the nodes are numbered one through five from the external boundary node.

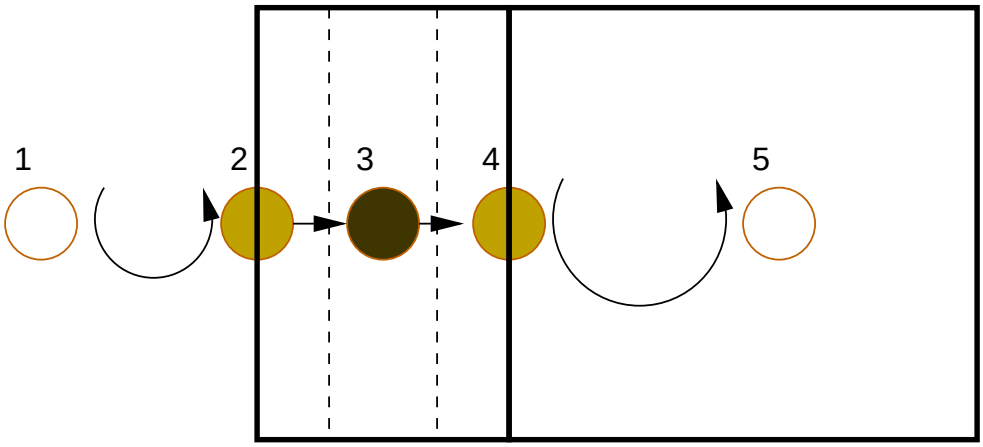

Figure 6.7: Discretisation of CEN conduction model

As can be seen in figure 6.7 there are three control volume types in this model:

- two fluid control volumes (numbers 1 and 5);
- two surface control volumes (numbers 2 and 4); and
- one solid control volumes (number 3).

Energy balance matrix equation

The equation set requires the establishment of the coefficients for the general equation:

$$\mathbf{A} \cdot \theta_{\mathbf{t+1}} = \mathbf{B} \cdot \theta_{\mathbf{t}} \tag{6.1}$$

The expanded matrices showing the individual elements are (note that all of these terms are affine numbers):

$$\begin{pmatrix} a_{1,1} & a_{1,2} & & & \\ a_{2,1} & a_{2,2} & a_{2,3} & & \\ & a_{3,2} & a_{3,3} & a_{3,4} & \\ & & a_{4,3} & a_{4,4} & a_{4,5} \\ & & & a_{5,4} & a_{5,5} \end{pmatrix} \begin{pmatrix} \theta_{1,t+1} \\ \theta_{2,t+1} \\ \theta_{3,t+1} \\ \theta_{4,t+1} \\ \theta_{5,t+1} \end{pmatrix} = \begin{pmatrix} b_{1,1} & b_{1,2} & & & \\ b_{2,1} & b_{2,2} & b_{2,3} & & \\ & b_{3,2} & b_{3,3} & b_{3,4} & \\ & & b_{4,3} & b_{4,4} & b_{4,5} \\ & & & b_{5,4} & b_{5,5} \end{pmatrix} \begin{pmatrix} \theta_{1,t} \\ \theta_{2,t} \\ \theta_{3,t} \\ \theta_{4,t} \\ \theta_{5,t} \end{pmatrix}$$

External boundary node

As the temperature for this node is known at all times the coefficients for the first row of the matrices are:

$$\begin{aligned} a_{1,1} &= 1.0 \\ a_{1,2} &= 0.0 \end{aligned} \tag{6.2}$$

$$\begin{aligned} b_{1,1} &= 1.0 \\ b_{1,2} &= 0.0 \end{aligned} \tag{6.3}$$

The convection exchange between this node and the surface node is added to the terms for the surface node. This ensures that the temperature at the boundary node is treated as a known parameter.

External surface node

The external surface node is an expression of equation 5.5. The coefficients are as follows:

$$\begin{aligned}
a_{2,1} &= -\frac{(h_{c,0}+\sum_{j=1}^{\nu} h_{c,j}\epsilon_j)(A_{2,0}+\sum_{j=1}^{\nu} A_{2,j}\epsilon_j)\delta t}{(V_{2,0}+\sum_{j=1}^{\nu} V_{2,j}\epsilon_j)} \\
a_{2,2} &= 2(\rho_{2,0}+\sum_{j=1}^{\nu}\rho_{2,j}\epsilon_j)(C_{2,0}+\sum_{j=1}^{\nu} C_{2,j}\epsilon_j)+\frac{(k_{2,0}+\sum_{j=1}^{\nu} k_{2,j}\epsilon_j)\delta t}{(\delta x_{2,0}+\sum_{j=1}^{\nu}\delta x_{2,j}\epsilon_j)^2} \\
&\quad +\frac{(h_{c,0}+\sum_{j=1}^{\nu} h_{c,j}\epsilon_j)(A_{2,0}+\sum_{j=1}^{\nu} A_{2,j}\epsilon_j)\delta t}{(V_{2,0}+\sum_{j=1}^{\nu} V_{2,j}\epsilon_j)} \\
a_{2,3} &= -\frac{(k_{2,0}+\sum_{j=1}^{\nu} k_{2,j}\epsilon_j)\delta t}{(\delta x_{2,0}+\sum_{j=1}^{\nu}\delta x_{2,j}\epsilon_j)^2}
\end{aligned} \tag{6.4}$$

$$\begin{aligned}
b_{2,1} &= \frac{(h_{c,0}+\sum_{j=1}^{\nu} h_{c,j}\epsilon_j)(A_{2,0}+\sum_{j=1}^{\nu} A_{2,j}\epsilon_j)\delta t}{(V_{2,0}+\sum_{j=1}^{\nu} V_{2,j}\epsilon_j)} \\
b_{2,2} &= 2(\rho_{2,0}+\sum_{j=1}^{\nu}\rho_{2,j}\epsilon_j)(C_{2,0}+\sum_{j=1}^{\nu} C_{2,j}\epsilon_j)-\frac{(k_{2,0}+\sum_{j=1}^{\nu} k_{2,j}\epsilon_j)\delta t}{(\delta x_{2,0}+\sum_{j=1}^{\nu}\delta x_{2,j}\epsilon_j)^2} \\
&\quad -\frac{(h_{c,0}+\sum_{j=1}^{\nu} h_{c,j}\epsilon_j)(A_{2,0}+\sum_{j=1}^{\nu} A_{2,j}\epsilon_j)\delta t}{(V_{2,0}+\sum_{j=1}^{\nu} V_{2,j}\epsilon_j)} \\
b_{2,3} &= \frac{(k_{2,0}+\sum_{j=1}^{\nu} k_{2,j}\epsilon_j)\delta t}{(\delta x_{2,0}+\sum_{j=1}^{\nu}\delta x_{2,j}\epsilon_j)^2}
\end{aligned} \tag{6.5}$$

Note that in this example there are no radiative exchange, solar or plant flux terms.

Solid opaque node

The solid opaque node is an expression of equation 5.4. The coefficients are as follows:

$$
\begin{aligned}
a_{3,2} &= -\frac{(k_{3,0}+\sum_{j=1}^{\nu} k_{3,j}\epsilon_j)\delta t}{(\delta x_{3,0}+\sum_{j=1}^{\nu} \delta x_{3,j}\epsilon_j)^2} \\
a_{3,3} &= 2(\rho_{3,0}+\sum_{j=1}^{\nu} \rho_{3,j}\epsilon_j)(C_{3,0}+\sum_{j=1}^{\nu} C_{3,j}\epsilon_j)+\frac{2(k_{3,0}+\sum_{j=1}^{\nu} k_{3,j}\epsilon_j)\delta t}{(\delta x_{3,0}+\sum_{j=1}^{\nu} \delta x_{3,j}\epsilon_j)^2} \\
a_{3,4} &= -\frac{(k_{3,0}+\sum_{j=1}^{\nu} k_{3,j}\epsilon_j)\delta t}{(\delta x_{3,0}+\sum_{j=1}^{\nu} \delta x_{3,j}\epsilon_j)^2}
\end{aligned} \tag{6.6}
$$

$$
\begin{aligned}
b_{3,2} &= \frac{(k_{3,0}+\sum_{j=1}^{\nu} k_{3,j}\epsilon_j)\delta t}{(\delta x_{3,0}+\sum_{j=1}^{\nu} \delta x_{3,j}\epsilon_j)^2} \\
b_{3,3} &= 2(\rho_{3,0}+\sum_{j=1}^{\nu} \rho_{3,j}\epsilon_j)(C_{3,0}+\sum_{j=1}^{\nu} C_{3,j}\epsilon_j)-\frac{2(k_{3,0}+\sum_{j=1}^{\nu} k_{3,j}\epsilon_j)\delta t}{(\delta x_{3,0}+\sum_{j=1}^{\nu} \delta x_{3,j}\epsilon_j)^2} \\
b_{3,4} &= \frac{(k_{3,0}+\sum_{j=1}^{\nu} k_{3,j}\epsilon_j)\delta t}{(\delta x_{3,0}+\sum_{j=1}^{\nu} \delta x_{3,j}\epsilon_j)^2}
\end{aligned} \tag{6.7}
$$

Note that in this example there are no solar or plant flux terms.

Internal surface node

The internal surface node is an expression of equation 5.5. The coefficients are as follows:

$$
\begin{aligned}
a_{4,3} &= -\frac{(k_{4,0}+\sum_{j=1}^{\nu} k_{4,j}\epsilon_j)\delta t}{(\delta x_{4,0}+\sum_{j=1}^{\nu} \delta x_{4,j}\epsilon_j)^2} \\
a_{4,4} &= 2(\rho_{4,0}+\sum_{j=1}^{\nu} \rho_{4,j}\epsilon_j)(C_{4,0}+\sum_{j=1}^{\nu} C_{4,j}\epsilon_j)+\frac{(k_{4,0}+\sum_{j=1}^{\nu} k_{4,j}\epsilon_j)\delta t}{(\delta x_{4,0}+\sum_{j=1}^{\nu} \delta x_{4,j}\epsilon_j)^2} \\
&\quad +\frac{(h_{c,0}+\sum_{j=1}^{\nu} h_{c,j}\epsilon_j)(A_{4,0}+\sum_{j=1}^{\nu} A_{4,j}\epsilon_j)\delta t}{(V_{4,0}+\sum_{j=1}^{\nu} V_{4,j}\epsilon_j)} \\
a_{4,5} &= -\frac{(h_{c,0}+\sum_{j=1}^{\nu} h_{c,j}\epsilon_j)(A_{4,0}+\sum_{j=1}^{\nu} A_{4,j}\epsilon_j)\delta t}{(V_{4,0}+\sum_{j=1}^{\nu} V_{4,j}\epsilon_j)}
\end{aligned} \tag{6.8}
$$

$$
\begin{aligned}
b_{4,3} &= \frac{(k_{4,0}+\sum_{j=1}^{\nu} k_{4,j}\epsilon_j)\delta t}{(\delta x_{4,0}+\sum_{j=1}^{\nu} \delta x_{4,j}\epsilon_j)^2} \\
b_{4,4} &= 2(\rho_{4,0}+\sum_{j=1}^{\nu} \rho_{4,j}\epsilon_j)(C_{4,0}+\sum_{j=1}^{\nu} C_{4,j}\epsilon_j) - \frac{(k_{4,0}+\sum_{j=1}^{\nu} k_{4,j}\epsilon_j)\delta t}{(\delta x_{4,0}+\sum_{j=1}^{\nu} \delta x_{4,j}\epsilon_j)^2} \\
&\quad -\frac{(h_{c,0}+\sum_{j=1}^{\nu} h_{c,j}\epsilon_j)(A_{4,0}+\sum_{j=1}^{\nu} A_{4,j}\epsilon_j)\delta t}{(V_{4,0}+\sum_{j=1}^{\nu} V_{4,j}\epsilon_j)} \\
b_{4,5} &= \frac{(h_{c,0}+\sum_{j=1}^{\nu} h_{c,j}\epsilon_j)(A_{4,0}+\sum_{j=1}^{\nu} A_{4,j}\epsilon_j)\delta t}{(V_{4,0}+\sum_{j=1}^{\nu} V_{4,j}\epsilon_j)}
\end{aligned} \tag{6.9}
$$

Note that in this example there are no radiative exchange, solar or plant flux terms.

Internal air node

The internal air node is an expression of equation 5.7. The coefficients are as follows:

$$
\begin{aligned}
a_{5,4} &= -\frac{(h_{c,5,0}+\sum_{j=1}^{\nu} h_{c,5,j}\epsilon_j)(A_{5,0}+\sum_{j=1}^{\nu} A_{5,j}\epsilon_j)\delta t}{(V_{5,0}+\sum_{j=1}^{\nu} V_{5,j}\epsilon_j)} \\
a_{5,5} &= 2(\rho_{5,0}+\sum_{j=1}^{\nu} \rho_{5,j}\epsilon_j)(C_{5,0}+\sum_{j=1}^{\nu} C_{5,j}\epsilon_j) \\
&\quad +\frac{(h_{c,5,0}+\sum_{j=1}^{\nu} h_{c,5,j}\epsilon_j)(A_{5,0}+\sum_{j=1}^{\nu} A_{5,j}\epsilon_j)\delta t}{(V_{5,0}+\sum_{j=1}^{\nu} V_{5,j}\epsilon_j)}
\end{aligned} \tag{6.10}
$$

$$
\begin{aligned}
b_{5,4} &= \frac{(h_{c,5,0}+\sum_{j=1}^{\nu} h_{c,5,j}\epsilon_j)(A_{5,0}+\sum_{j=1}^{\nu} A_{5,j}\epsilon_j)\delta t}{(V_{5,0}+\sum_{j=1}^{\nu} V_{5,j}\epsilon_j)} \\
b_{5,5} &= 2(\rho_{5,0}+\sum_{j=1}^{\nu} \rho_{5,j}\epsilon_j)(C_{5,0}+\sum_{j=1}^{\nu} C_{5,j}\epsilon_j) \\
&\quad -\frac{(h_{c,5,0}+\sum_{j=1}^{\nu} h_{c,5,j}\epsilon_j)(A_{5,0}+\sum_{j=1}^{\nu} A_{5,j}\epsilon_j)\delta t}{(V_{5,0}+\sum_{j=1}^{\nu} V_{5,j}\epsilon_j)}
\end{aligned} \tag{6.11}
$$

Note that in this example there are no advection or plant flux terms.

This equation set can now be solved over time. The node temperatures and uncertainty will be calculated directly.

6.3.2 Verification of affine model

Two simulation process have been used at this stage:

1. The original ESP-r program, and

2. The affine version of the program.

For both simulation options the model used has been simulated with and without uncertainties applied. Recall that the affine approach only requires a single simulation for a given set of uncertainties compared with the multiple simulations and analyses (*i.e.* differential and Monte Carlo) required by external methods for the same set of uncertainties.

Comparison of solutions without uncertainties

Tables 6.4 and 6.5, and figure 6.8 show the results of the simulations without uncertainty. The affine model was run for an extended period of time and the final results, typically after $250hrs$ are given as the time ∞ (this was primarily to verify that the affine solution remained stable). The results of the affine model in table 6.4 compare well with the ESP-r data in table 6.5. As can be seen in figure 6.8 the difference between the ESP-r and affine simulations is less than $0.2°C$ at all times. There are several sources of the differences between models, including: rounding differences (probable cause of bias shown), slight differences in model configuration (*e.g.* ESP-r cannot have an air heat capacity of zero), and in averaging of results to get data at hourly intervals. In the solution of the building conservation equation set the state variable (temperature) will be solved for each time row. Therefore, for a simulation with a one hour time step the temperature will be known at half past the hour. Thus to calculate temperatures at hourly intervals requires the data from two time rows to be averaged, regardless of how small the time step is made. Therefore, larger differences will occur when the time step is longer and the second derivative of temperature with respect to time is greater. As the CEN standard [CEN 1997] allows a maximum variation of $0.5°C$. these results were taken as verification of the affine model of transient thermal conduction without uncertainty.

Table 6.4: Affine solution without uncertainty.

Time (hours)	Case		
	1	2	3
1	20.017	21.432	27.647
2	20.101	25.105	29.972
6	21.287	29.599	30.000
12	23.444	29.991	30.000
24	26.364	30.000	30.000
120	29.968	30.000	30.000
∞	29.973	30.000	30.000

Table 6.5: Original ESP-r predictions without uncertainty.

Time (hours)	Case		
	1	2	3
1	19.99	21.35	27.80
2	20.04	25.14	29.96
6	21.31	29.61	29.99
12	23.48	29.98	29.99
24	26.37	29.99	29.99
120	29.99	29.99	29.99

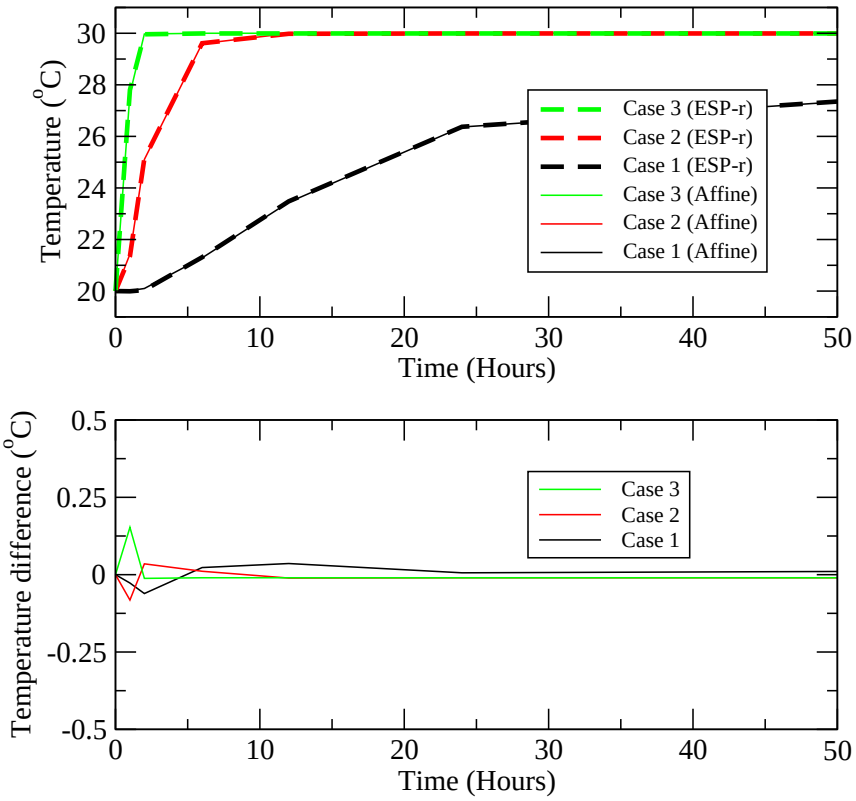

Figure 6.8: Air temperature for standard tests.

Comparison of solutions with uncertainties

A systematic test of the effects of including uncertainties was undertaken. A factorial design provides the best test methodology as all possible combinations of the test states are analysed. Such a process involves many tests for all possible parameters and their combinations. The following test sequence was devised.

1. Test each parameter individually at uncertainties of 1%, 5% and 10%.
2. Test combinations of two parameters at the same uncertainty levels.
3. Continue with more parameters being included.

There are only three parameters that are available for assigning uncertainties in the base case model: conductivity, heat capacity (either the density or specific heat capacity) and thickness. In total 64 simulations were executed and analysed. This includes the simulation with zero uncertainty in all parameters. The results of all 63 simulations (which include uncertainties) are reported in Appendix C.

The results can be categorised as follows:

1. Fully converged: the individual uncertainty tokens and the sum of the uncertainty tokens tend to zero as the simulation time tends to infinity for all three cases, for example table C.49 in Appendix C. Two simulations fall into this category.
2. Partially converged: the individual uncertainty tokens converge but the sum of the tokens does not, for example table C.2. Fifty of the simulations fall into this category.
3. Divergent solutions: neither the individual uncertainty tokens nor the sum of the tokens converge, for example table C.44. Eleven simulations fall into this category.

Typical examples from each of these categories are now discussed and compared with results from appropriate external methods.

Fully converged solutions

The results from a fully converged solution are presented in table 6.6. As can be seen for each case the uncertainty token θ_{con} and the sum of the uncertainty tokens (these include the results of non affine operations) tends to zero as time tends to infinity. These results are commensurate with expectations of the behaviour of the physical system.

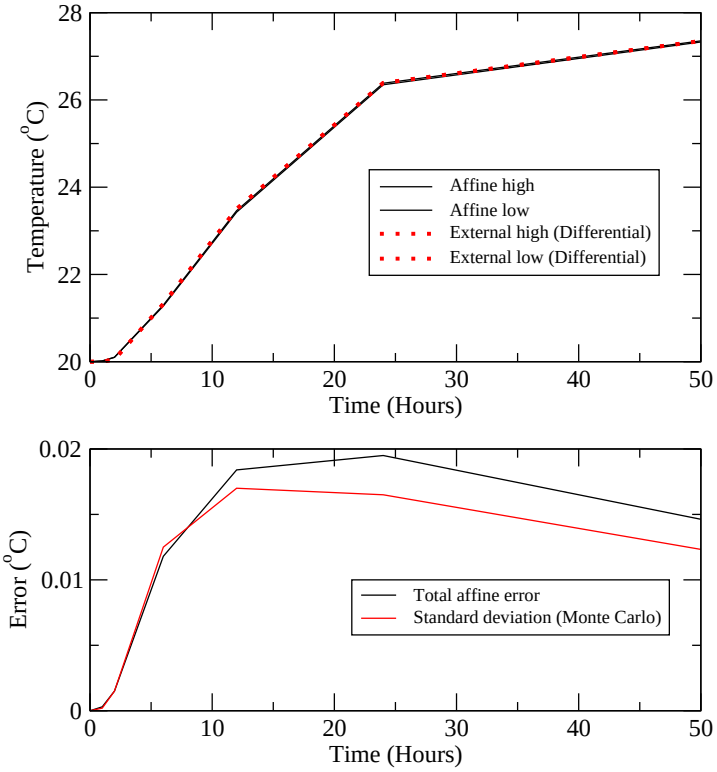

Figure 6.9: Air temperature for case 1.

If the conductivity were to increase by 1% then $\epsilon_{con} = 1$ and the resulting air temperatures would then be $\theta_0 + \theta_{con}$ at all times. This is a sensible result. The value of θ_{con} represents the uncertainty in temperature due to the first order effects of the uncertainty in conductivity. The total uncertainty includes the effects due to non affine operations. As expected, the total uncertainty is greater than the first order effects. It should also be observed that the integrity of the physical system is maintained *i.e.* no temperatures greater than $30°C$ are possible for all values of ϵ_i and the uncertainty in temperature reduces to zero as the system reaches steady

Table 6.6: Affine solution for conductivity uncertainty of 1%.

Time	Case 1			
(hours)	θ_0	θ_{con}	$\sum \theta_i$	$\sum \lvert\theta_i\rvert$
1	20.0172	0.0003	0.0003	0.0003
2	20.1009	0.0014	0.0014	0.0015
6	21.2866	0.0114	0.0117	0.0118
12	23.4442	0.0172	0.0180	0.0184
24	26.3645	0.0170	0.0187	0.0195
120	29.9676	0.0007	0.0013	0.0015
∞	29.9734	0.0006	0.0011	0.0013
Time	Case 2			
(hours)	θ_0	θ_{con}	$\sum \theta_i$	$\sum \lvert\theta_i\rvert$
1	21.4323	0.0166	0.0169	0.0171
2	25.1049	0.0401	0.0415	0.0421
6	29.5986	0.0126	0.0144	0.0150
12	29.9906	0.0006	0.0008	0.0009
24	30.0000	0.0000	0.0000	0.0000
∞	30.0000	0.0000	0.0000	0.0000
Time	Case 3			
(hours)	θ_0	θ_{con}	$\sum \theta_i$	$\sum \lvert\theta_i\rvert$
1	27.6470	0.0028	0.0060	0.0077
2	29.9723	0.0001	0.0046	0.0068
6	30.0000	0.0000	0.0023	0.0034
12	30.0000	0.0000	0.0006	0.0010
∞	30.0000	0.0000	0.0004	0.0007

state. Finally, if the uncertainty in conductivity was zero (*i.e.* $\epsilon_{con} = 0$) then the same results as the normal calculation (table 6.4) are achieved.

Differential and Monte Carlo analysis were undertaken to enable a comparison with these results. Table 6.7 shows the results of these simulations: the $\delta\theta^+$ and $\delta\theta^-$ values relate to the differential analysis and the σ values relate to the Monte Carlo analysis; as expected the two analysis methods produce effectively the same results. As can be seen in figure 6.9 the total affine error ($\sum |\theta_i|$) is of the same magnitude as the standard deviation predicted by an 80 run Monte Carlo analysis. The individual effect of the uncertainty in conductivity (θ_{con} in table 6.6) is also similar to the variation predicted by the differential analysis ($\delta\theta^+$ and $\delta\theta^-$ in table 6.7).

From this data it can be concluded that the affine solution for a single uncertain parameter shows good agreement with the traditional external methods.

Table 6.7: External method solutions for conductivity uncertainty of 1%.

Time	Case 1			
(hours)	θ_0	$\delta\theta^+$	$\delta\theta^-$	σ
1	20.0003	0.0003	-0.0003	0.0002
2	20.0510	0.0017	-0.0010	0.0015
6	21.3119	0.0130	-0.0121	0.0125
12	23.4826	0.0177	-0.0164	0.0170
24	26.3728	0.0176	-0.0155	0.0165
120	29.9364	0.0026	-0.0011	0.0011
Time	Case 2			
(hours)	θ_0	$\delta\theta^+$	$\delta\theta^-$	σ
1	21.3572	0.0194	-0.0195	0.0200
2	25.1434	0.0408	-0.0414	0.0421
6	29.6194	0.0117	-0.0122	0.0122
12	29.9889	0.0005	-0.0006	0.0006
24	29.9972	0.0001	-0.0001	0.0001
120	29.9973	0.0000	0.0000	0.0000
Time	Case 3			
(hours)	θ_0	$\delta\theta^+$	$\delta\theta^-$	σ
1	27.8043	0.0027	-0.0028	0.0028
2	29.9699	0.0002	-0.0001	0.0002
6	29.9969	0.0000	0.0000	0.0000
12	29.9970	0.0000	0.0000	0.0000
24	29.9972	0.0000	0.0000	0.0000
120	29.9973	0.0000	-0.0001	0.0000

Partially converged solutions

Table 6.8 shows data from a typical partially converged affine simulation. The individual uncertainty tokens have tended to zero as the simulation progresses (as expected) but the overall uncertainty, represented by the sum of the uncertainty tokens has continued to expand for cases 1 and 3. Figure 6.10 shows the overall uncertainty diverging for the affine solution of case 1.

Comparing these individual uncertainty tokens with the affine simulations for single uncertainties: for conductivity see table 6.6 and for density see table C.13. From these comparisons it can be seen that the affine simulations produce the same response for the individual uncertainty tokens regardless of the number of uncertainties defined. Further comparisons of the data in appendix C will confirm that this is not an isolated result.

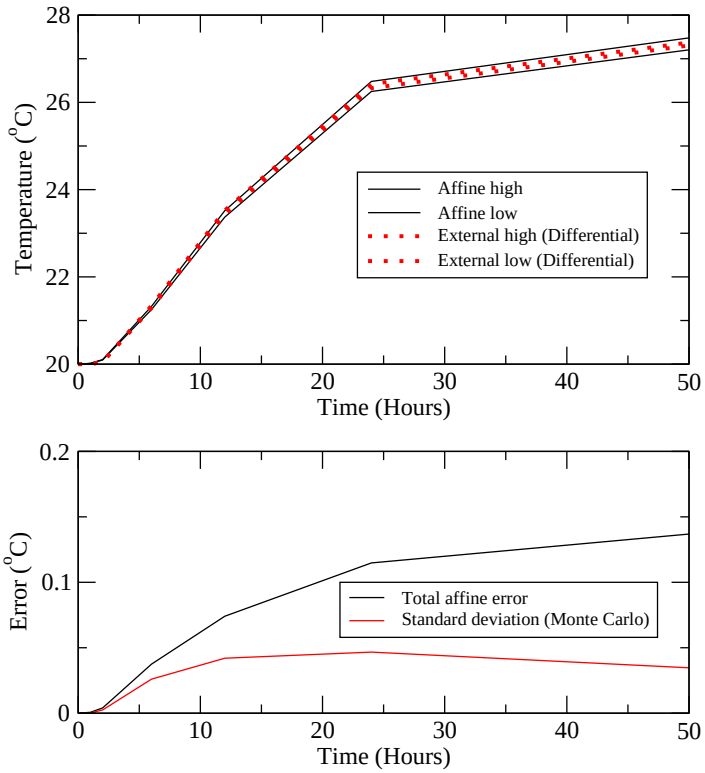

Figure 6.10: Air temperature for case 1.

Table 6.8: Affine solution for density and conductivity uncertainty of 1%.

Time	Case 1				
(hours)	θ_0	θ_{den}	θ_{con}	$\sum\theta$	$\sum\lvert\theta\rvert$
1	20.0172	-0.0004	0.0003	-0.0001	0.0007
2	20.1009	-0.0023	0.0014	-0.0006	0.0040
6	21.2866	-0.0207	0.0114	-0.0044	0.0375
12	23.4442	-0.0369	0.0172	-0.0013	0.0741
24	26.3645	-0.0421	0.0170	0.0262	0.1148
120	29.9676	-0.0019	0.0007	0.1769	0.1962
∞	29.9734	-0.0016	0.0006	0.1791	0.1981
Time	Case 2				
(hours)	θ_0	θ_{den}	θ_{con}	$\sum\theta$	$\sum\lvert\theta\rvert$
1	21.4323	-0.0189	0.0166	-0.0002	0.0380
2	25.1049	-0.0442	0.0401	0.0046	0.0944
6	29.5986	-0.0138	0.0127	0.0103	0.0396
12	29.9906	-0.0007	0.0006	0.0016	0.0032
24	30.0000	-0.0000	0.0000	0.0000	0.0000
∞	30.0000	0.0000	0.0000	0.0000	0.0000
Time	Case 3				
(hours)	θ_0	θ_{den}	θ_{con}	$\sum\theta$	$\sum\lvert\theta\rvert$
1	27.6470	-0.0223	0.0028	0.0316	0.0999
2	29.9723	-0.0015	0.0001	0.1042	0.1539
6	30.0000	0.0000	0.0000	0.2119	0.3046
12	30.0000	0.0000	0.0000	0.3258	0.4684
∞	30.0000	0.0000	0.0000	0.3715	0.5342

Table 6.9: External method solutions for conductivity and density uncertainty of 1%.

Time (hours)	Case 1	
	θ_0	σ
1	20.0003	0.0002
2	20.0510	0.0025
6	21.3119	0.0260
12	23.4826	0.0420
24	26.3728	0.0467
120	29.9364	0.0023
Time (hours)	Case 2	
	θ_0	σ
1	21.3572	0.0278
2	25.1434	0.0587
6	29.6194	0.0171
12	29.9889	0.0008
24	29.9972	0.0001
120	29.9973	0.0000
Time (hours)	Case 3	
	θ_0	σ
1	27.8043	0.0218
2	29.9699	0.0015
6	29.9969	0.0000
12	29.9970	0.0000
24	29.9972	0.0000
120	29.9973	0.0000

Furthermore, if the converged solutions (cases 1 and 2) are compared with the output from the Monte Carlo simulations (tables 6.8 and 6.9) it can be seen that the solution for case 2 bounds the Monte Carlo results. The reason for the overestimation of the overall bound is due to the estimation of non-affine operations and is discussed in the next section.

From this data it can be concluded that the affine solution for multiple uncertain parameters shows good agreement with the differential method in all cases and for some cases with the Monte Carlo method.

Divergent solutions

The simulation of uncertainties using affine arithmetic does not always produce bounded results. As can be seen in table 6.10, the uncertainty tokens sometimes diverge and an unbounded solution occurs. The reasons for this are now examined.

Examining all of the tables in appendix C it is clear that there are two consistent threads to the cases where the solution becomes unbounded.

Table 6.10: Uncertainties: density 10%, thickness 10%, conductivity 10%.

Time	Case 1					
(hours)	θ_0	θ_{den}	θ_{thk}	θ_{con}	$\sum\theta$	$\sum\lvert\theta\rvert$
1	20.0172	-0.0056	-0.0213	0.0041	0.4900	1.5551
2	20.1009	-0.0311	-0.1169	0.0224	9.3625	22.1748
6	21.2866	-0.3277	-1.1375	0.1960	$> 1000.$	$> 1000.$
12	23.4442	-0.8508	-2.6781	0.3903	$> 1000.$	$> 1000.$
24	26.3645	-2.3562	-6.9613	0.8847	$> 1000.$	$> 1000.$
120	29.9676	$< -1000.$	$< -1000.$	423.7654	∞	∞
∞	29.9734	$< -1000.$	$< -1000.$	547.7548	∞	∞
Time	Case 2					
(hours)	θ_0	θ_{den}	θ_{thk}	θ_{con}	$\sum\theta$	$\sum\lvert\theta\rvert$
1	21.4323	-0.5724	-2.5921	0.6033	$> 1000.$	$> 1000.$
2	25.1049	-2.3644	-10.8479	2.5526	∞	∞
6	29.5986	-47.2850	-217.3026	51.2034	∞	∞
12	29.9906	$< -1000.$	$< -1000.$	$> 1000.$	∞	∞
24	30.0000	$< -1000.$	$< -1000.$	$< -1000.$	∞	∞
∞	30.0000	$< -1000.$	$< -1000.$	$< -1000.$	∞	∞
Time	Case 3					
(hours)	θ_0	θ_{den}	θ_{thk}	θ_{con}	$\sum\theta$	$\sum\lvert\theta\rvert$
1	27.6470	∞	∞	∞	∞	∞
2	29.9723	∞	∞	∞	∞	∞
6	30.0000	∞	∞	∞	∞	∞
12	30.0000	∞	∞	∞	∞	∞
∞	30.0000	∞	∞	∞	∞	∞

1. The magnitudes of the uncertainties are large.

2. Uncertainties in thickness cause failure more often than for the same magnitude of uncertainty in density or conductivity.

These characteristics are resolved by referring to the solution procedure. In the first case the coefficients of the **A** matrix (see equation 6.1) become dominated by the magnitude of the uncertainty tokens with respect to the magnitude of the constant value, *i.e.*

$$\frac{\sum_{i=1}^{\nu} a_i}{a_0} > x \tag{6.12}$$

where a is an element of the coefficient matrix **A**.

On analysing the divergent cases, failure will occur when x is greater than ~ 0.45. This figure is quite large considering that in all the cases analysed the largest uncertainties defined are 10% in any one parameter. The second observation identifies the cause of the problem.

When calculating some of the coefficients of the **A** array new uncertainty tokens are generated due to non affine operations. For example, the node thickness is $\frac{1}{\delta x^2}$ in the coefficient (recall equation 2.4). This two stage process increases the magnitude of the sum of the uncertainty tokens considerably, especially the division stage. The initial increase in error token is due to the estimation of the new error token as part of the multiplication process (recall equation 3.52 where the non-linear term is approximated). The new term is independent of the existing terms; thus the correlations between it and the existing uncertainty tokens are lost. In the case of division the new error token is calculated based on the range of the maximum interval of the affine number. Recall equation 3.54, where the magnitude of the new error token is

$$\frac{(a+b)(a-b)}{2ab^2}$$

given a the minimum value of the affine number; b the maximum. Again this new term is independent of the existing error tokens. To reduce these effects the number of non-affine operations were minimised and the order of operations was examined to achieve the current implementation. Further improvements could be made in this respect.

6.3.3 Summary

The power of a carefully implemented range arithmetic implementation for assessing uncertainty has been demonstrated: in one simulation individual contributions and overall uncertainty can be quantified. For single uncertainties the results showed good agreement with the differential and Monte Carlo methods. For more than one uncertainty the results again showed good agreement with the differential method. However, in some cases (generally larger uncertainties and uncertainty in thickness) the overall error estimation became unbounded. This was due to the creation of new affine terms as a result of non-affine operations. Perhaps the greatest benefit of the affine approach is that, as uncertainties are known at all times, action can be taken during the simulation based on the current effects of uncertainty, for example, in building control laws or in adaptive solution processing between algorithms to reduce

the overall uncertainty.

6.4 Applicability

All of the methods studied have their weaknesses and areas where they are not applicable. Individual external methods are only applicable for specific problems, and are summarised again:

- Differential analysis is only suitable for calculating individual parameter uncertainties.
- Factorial analysis is suitable for calculating parameter sensitivities and interactions.
- Monte Carlo analysis is only useful for generating overall error bands in the predictions.
- Affine approach quantifies first order effects (comparable to differential) and overall uncertainty (comparable to Monte Carlo).

No one method provides an answer to the questions of what is the total error/ uncertainty in the predictions and which parameters have the greatest influence upon this error. To answer these questions requires not only multiple simulations but multiple analyses.

6.4.1 General approach

The three external methods can be applied in buildings based on the assumptions described in chapter 3. As the internal method is deterministic, not statistical, there are no similar assumptions as to its application.

As described, the three external methods answer separate questions related to the behaviour of the modelled building. Once uncertainties have been defined the differential method can be used for an initial analysis. This would identify the parameters whose uncertainties significantly affect the simulation output. These critical parameters can then be used in a factorial analysis to identify any synergistic effects. The

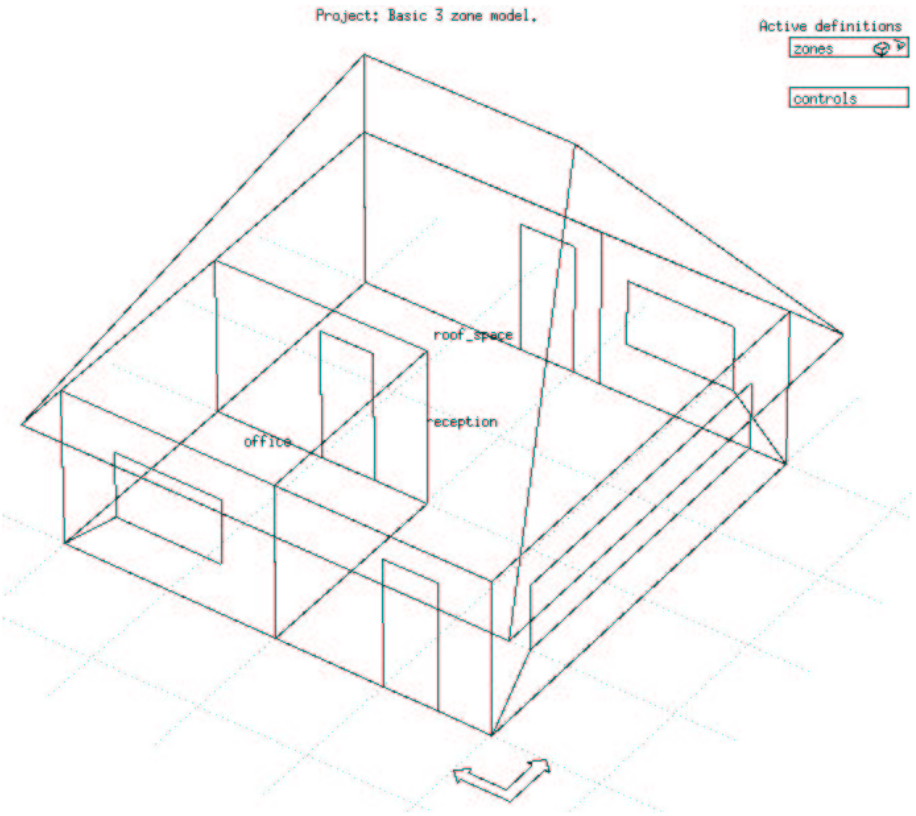

Figure 6.11: Three zone example model.

Monte Carlo method would be used to quantify the overall uncertainty in the simulation predictions with all the uncertain input parameters active. However, a second Monte Carlo simulation can be run with only the critical parameters identified in the differential method active. The results of this second Monte Carlo simulation should be effectively the same as for the first simulation if all the critical parameters have been identified.

6.4.2 Test model

To elaborate the above discussion of the implementation of uncertainty analysis in ESP-r the use of the methods is now demonstrated on a simple model as shown in figure 6.11.

The model corresponds to a small office. The construction of the external walls is of a traditional insulated brick type and the internal partitions are dry lined blockwork. The space is occupied and heated between 9am and 5pm. In addition to the casual

Table 6.11: Uncertainties defined for model

Parameter	Uncertainty
Conductivity of external wall insulation	20%
Conductivity of external wall brick facing	20%
Capacity of external wall internal block	20%
Solar absorptivity of internal walls	20%
Longwave emissivity of internal walls	20%
Ambient temperature	$3°C$
Direct solar radiation	20%
Equipment casual gains	20%
Infiltration	20%

gains from people and equipment, there is a 24hr base load from equipment left on overnight.

Uncertainties

Uncertainties have been defined for a cross-section of the parameters used to define this model and are listed in table 6.11. These uncertainties have been assigned large values for the purpose of demonstrating the methods (typical magnitudes of uncertainties were elaborated in chapter 4).

Simulations

The model was simulated for a seven day period in winter and the effect of the above uncertainties on the required heating energy quantified. Three sets of simulations were undertaken: differential analysis, factorial analysis and a Monte Carlo analysis as described in the general approach.

6.4.3 Results and discussion

The results from the three analyses are presented separately.

Differential analysis

The base case energy consumption for the reception space is $14.03kWh$ for the simulated week. Table 6.12 shows the results from the differential analysis. There is no

Table 6.12: Differential analysis results

Parameter	Status	Energy consumption (kWh)
Base case		14.03
Conductivity of external wall insulation	high	15.65
	low	12.45
Conductivity of external wall brick facing	high	14.08
	low	13.97
Capacity of external wall internal block	high	14.26
	low	13.73
Solar absorptivity of internal walls	high	14.03
	low	14.03
Longwave emissivity of internal walls	high	14.07
	low	13.93
Ambient temperature	high	9.61
	low	21.16
Direct solar radiation	high	13.84
	low	14.27
Equipment casual gains	high	10.48
	low	19.80
Infiltration	high	15.77
	low	12.46

measurable effect due to the change in solar absorptivity although large effects occur due to changes in the conductivity of the external wall insulation and infiltration rate.

As previously suggested the calculation of dimensionless sensitivity coefficients can result in non-sensible outcomes. In this example the ambient temperature is close or equal to $0°C$ for a large period during the simulation; thus, the percentage change in temperature would be large or undefinable. Therefore relative differences have been calculated as given in table 6.13.

It is clear from table 6.13 that the parameters to which the required heating energy is most sensitive are: conductivity of the external wall insulation; ambient temperature; equipment casual gains and infiltration rate.

It can also be seen that the uncertainties have a non-linear effect. For example, the effect of increasing ambient temperatures by $3°C$ is a reduction of the required heating energy by $4.42kWh$ and the effect of reducing ambient temperatures by $3°C$ is an increase of the required heating energy by $7.13kWh$. This observation is typical

Table 6.13: Differential analysis results - relative change

Parameter	Status	Energy consumption (kWh)
Conductivity of external wall insulation	high	1.62
	low	-1.58
Conductivity of external wall brick facing	high	0.05
	low	-0.06
Capacity of external wall internal block	high	0.23
	low	-0.30
Solar absorptivity of internal walls	high	0.00
	low	0.00
Longwave emissivity of internal walls	high	0.04
	low	-0.10
Ambient temperature	high	-4.42
	low	7.13
Direct solar radiation	high	-0.19
	low	0.24
Equipment casual gains	high	-3.55
	low	5.77
Infiltration	high	1.74
	low	-1.57

of building systems.

Averaging the effects and calculating the standard deviation (assuming that all the effects are independent) results in an energy consumption of $14.03^{+}_{-}7.78kWh$. The independence of each parameter's effects is now analysed.

Factorial analysis

The four most sensitive parameters from the differential analysis were tested using a factorial analysis. The parameters have been labelled as follows:

A conductivity of external wall insulation;

B ambient temperature;

C equipment casual gains; and

D infiltration rate.

The results of this analysis are presented in table 6.14.

Table 6.14: Factorial analysis results

Effect	Estimate (kWh)
Average	15.73
Main effect A	2.95
Main effect B	-11.48
Main effect C	-9.17
Main effect D	2.97
Interaction AB	-1.03
Interaction AC	-0.38
Interaction AD	0.12
Interaction BC	2.96
Interaction BD	-0.99
Interaction CD	-0.37
Interaction ABC	0.01
Interaction ABD	0.02
Interaction ACD	0.03
Interaction BCD	-0.06
Interaction ABCD	-0.02

Comparing the relative importance of the main effects with the differential analysis shows the same order of importance of the four parameters analysed.

The interactions between the uncertainties show that the combined effect of uncertainties in ambient temperature and the other uncertain parameters is significant but the interactions between other parameters (excluding ambient temperature) are not significant. The interactions between three and four parameters is also not significant. This is typical of building simulation in that only the main effects and two factor interactions are important.

A fractional factorial simulation where all the uncertainties were active was undertaken. To identify main effects and two factor interactions without confounding a design resolution of IV is required. This required 128 simulations for the 9 uncertain parameters.

The results displayed in table 6.15 confirm that the initially selected four parameters were the only important parameters and that no other synergistic effects occur in this model.

Table 6.15: Fractional factorial analysis, significant results

Effect	Estimate (kWh)
Average	15.74
Main effect A	2.94
Main effect B	-11.48
Main effect C	-9.17
Main effect D	2.97
Interaction AB	-1.03
Interaction BC	2.95
Interaction BD	-0.99

Monte Carlo analysis

Finally the model was analysed using the Monte Carlo method. The results show that the average energy consumption is $16.05^{+}_{-}7.77kWh$. The average energy consumption predicted by this method is higher than both the differential method's base case and the factorial method. This would indicate that there is a non-linear relationship between the uncertainties and the heating energy required.

6.4.4 Summary

The example of the use of the three external methods showed that the differential analysis identified the four parameters which most influenced the energy consumption. The factorial method was then used to check for interactions between the parameters - three interactions were identified as having an effect. Finally a Monte Carlo analysis was undertaken to quantify the overall uncertainty in the energy consumption. This showed that the effect of the interactions was minimal as the standard deviation calculated was only slightly different from that calculated via the differential method ($7.77kWh$ for the Monte Carlo method compared with $7.78kWh$ for the differential method).

In a design context the engineer could then focus on: the estimation of the heat gains in the space, the infiltration rate, the conductivity of the insulation and the choice of an appropriate climate file with respect to temperature, to improve the accuracy of the simulation

Affine arithmetic techniques have been shown to produce a bounded solution for an uncertain system in a single simulation. The solution compares well with those of the multiple simulations of the external methods for some cases only. The successful solutions are generally for cases with small uncertainties. Reasons for the failed solutions were given and suggested modifications are given in chapter 8.

It can be concluded that the affine approach works well for small uncertainties, however the external methods are more robust. Despite this the affine approach provides information on individual and overall effect of uncertainties in a single simulation. To achieve this using external methods would require two analyses, each involving multiple simulations. In addition to this efficiency the affine approach quantifies the effects of uncertainties during the simulation; therefore, allowing control actions to be taken or information on prevailing uncertainties to be passed between domains.

References

CEN, *Transient conduction in building simulation software*, prEN ISO 13791, 1997

Judkoff R D and Neymark J S, *A procedure for testing the ability of whole building energy simulation programs to thermally model the building fabric*, Journal of Solar Engineering, Vol 117, February 1995

Jensen S O (Editor) *Validation of Building Energy Simulation Programs*, final report, PASSYS project EUR 15115 EN (European Commission), 1994

Lomas K J, *The UK applicability study: an evaluation of thermal simulation programs for passive solar house design*, Building and Environment, Vol 31, No 3, 1996

Saltelli A, Chan K, Scott E M, *Sensitivity Analysis*, J Wiley and Sons, 2000

Strachan P, *ESP-r: Summary of Validation Studies*, ESRU Technical Report, University of Strathclyde, Glasgow, 2000

Chapter 7

Case studies

The insights gained from uncertainty analysis are now explored in the context of real buildings.

To demonstrate the external uncertainty quantification methods (see also Macdonald and Strachan [2001]) and the effect of assessing uncertainty on the design process the following case studies are presented.

1. Early design stage use of detailed simulation.
2. Critical plant sizing at the detailed design stage.
3. Comparison of designs.

The first case examines the impact of uncertainty on the performance of a building at the early design stage, where the impact of decision making is greatest and the information necessary is highly uncertain. By including uncertainty more useful information can be delivered.

The second case is crucial in design as the plant size in a building has a direct impact on capital and running costs. For example, the author was involved in a project where the required cooling load for the building was such that large diameter ductwork and hence large steel structure would be required. A slight reduction (in the region of $1W/m^2$) in cooling load would enable the use of smaller ductwork and structure. The cost implication of the smaller structure was a saving of £1.2M.

Clearly, if the plant could be critically designed and the risk of overheating quantified the design team could make an informed decision on whether to risk the smaller structure.

In the final case the significance of a design alteration is tested. Discussions with engineers have shown that a reduction in peak summer temperatures of $1°C$ is seen as significant by some and insignificant by others. By using a significance test the effect of a design change can be quantified and this could resolve such arguments based on practitioners viewpoints.

All three cases are based on consultancy or research projects undertaken by the author.

7.1 Early design stage

Glasgow City Council initiated a programme of upgrading their secondary schools in 1998. The purpose of the modelling work was to quantify the peak summer temperatures and to assess if cooling plant was required. The maximum allowable resultant temperature was $26°C$.

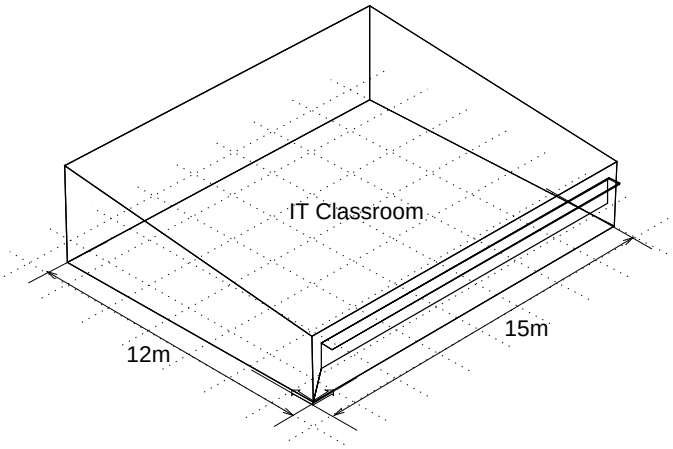

Figure 7.1: Model of typical IT classroom.

A model of a typical classroom was created. For the purposes of this comparison only the IT rooms are considered. Figure 7.1 shows a representation of the model created. The following information was available.

- Geometry: the floor area was known and a planned glazed area (35%) based on architectural considerations. The orientation of the building was specified and a $0.5m$ wide shading device was to be installed above the south facing window.
- Construction: the overall construction was lightweight with double glazing. The external construction U-value was to be $< 0.4W/m^2K$.
- Occupancy: the maximum number of occupants was specified as 35.
- Equipment: one computer per person and $8W/m^2$ lighting.
- Fresh air: the rooms were to be naturally ventilated or if cooling was necessary supplied with minimum fresh air for the occupants.

The largest uncertainties were associated with the construction properties, as no specific materials were specified, and the internal gains as maximum, not typical, usage was known.

As the model is for the early design stage specific data should not be used; rather the highly unknown data of chapter 4 should be used. By using this data with uncertainties the range of data will extend over all possible materials and usage levels. The details of these elements are presented in tables 7.1, 7.2, 7.3 and 7.4.

Table 7.1: Scheduled operations in school model.

Infiltration information			
Day type	Period	Infiltration (ac/h)	Ventilation (ac/h)
Weekday	0 – 8	0.50	0.00
Weekday	8 – 16	3.00	0.00
Weekday	16 – 24	0.50	0.00
Saturday	0 – 24	0.50	0.00
Sunday	0 – 24	0.50	0.00
Casual gains information			
Gain type	Period	Sensible gain (W)	Convective fraction ($-$)
Computers	9 – 12	3500.0	0.70
Computers	13 – 16	3500.0	0.70
Lights	8 – 16	1440.0	0.50
Occupants	8 – 16	3500.0	0.50

Table 7.2: Construction materials used in school model with uncertainties.

Details of opaque composite: external wall						
Description	Thick (m)	Conduct (W/mK)	Density (kg/m^3)	Spec heat (J/kgK)	Absorb $(-)$	Emiss $(-)$
BRICK clay average	0.1000	0.789	1720.	837.	0.90	0.76
INSULATION average	0.0880	0.039	38.	1072.	—	—
air	0.0500	—	—	—	—	—
PLASTERBOARD average	0.0120	0.191	704.	1359.	0.91	0.22
Details of opaque composite: internal partition						
Description	Thick (m)	Conduct (W/mK)	Density (kg/m^3)	Spec heat (J/kgK)	Absorb $(-)$	Emiss $(-)$
PLASTERBOARD average	0.0120	0.191	704.	1359.	0.91	0.22
air 0.17 0.17 0.17	0.0500	—	—	—	—	—
PLASTERBOARD average	0.0120	0.191	704.	1359.	0.91	0.22
Details of opaque composite: double glazing						
Description	Thick (m)	Conduct (W/mK)	Density (kg/m^3)	Spec heat (J/kgK)	Absorb $(-)$	Emiss $(-)$
GLASS float average	0.0060	1.294	2509.	820.	0.83	0.06
air	0.0120	—	—	—	—	—
GLASS float average	0.0060	1.294	2509.	820.	0.83	0.06
Details of opaque composite: roof						
Description	Thick (m)	Conduct (W/mK)	Density (kg/m^3)	Spec heat (J/kgK)	Absorb $(-)$	Emiss $(-)$
METAL non ferrous average	0.0030	224.000	6278.	544.	0.24	0.56
air	0.0250	—	—	—	—	—
INSULATION average	0.0930	0.039	38.	1072.	—	—
PLASTERBOARD average	0.0120	0.191	704.	1359.	0.91	0.22
Details of opaque composite: floor						
Description	Thick (m)	Conduct (W/mK)	Density (kg/m^3)	Spec heat (J/kgK)	Absorb $(-)$	Emiss $(-)$
CONCRETE heavy average	0.1400	1.491	2179.	864.	0.90	0.40
air	0.0500	—	—	. —	—	—
TIMBER boards average	0.0190	0.201	648.	1845.	—	—
CARPET average	0.0060	0.060	183.	1740.	0.90	0.78

Table 7.3: Uncertainty (3σ) in casual gains and infiltration.

Parameter	Variation
Computer gain	1000—6475 W
Occupancy sensible gain	1400—4550 W
Infiltration rate	$\pm$50%

Table 7.4: Uncertainty (1σ) in thermophysical properties.

Parameter	Property	Average value	Standard deviation
BRICK clay average	$k(W/mK)$	0.789	0.261
	$\rho(kg/m^3)$	1720.	301.
	$C(J/kgK)$	837.	90.
INSULATION average	$k(W/mK)$	0.039	0.014
	$\rho(kg/m^3)$	38.	27.
	$C(J/kgK)$	1072.	298.
PLASTERBOARD average	$k(W/mK)$	0.191	0.150
	$\rho(kg/m^3)$	704.	379.
	$C(J/kgK)$	1359.	615.
GLASS float average	$k(W/mK)$	1.294	0.690
	$\rho(kg/m^3)$	2509.	105.
	$C(J/kgK)$	820.	50.
METAL non ferrous average	$k(W/mK)$	1.294	107.
	$\rho(kg/m^3)$	2509.	2876.
	$C(J/kgK)$	820.	223.
CONCRETE heavy average	$k(W/mK)$	1.491	0.300
	$\rho(kg/m^3)$	2179.	149.
	$C(J/kgK)$	864.	92.
TIMBER boards average	$k(W/mK)$	0.201	0.274
	$\rho(kg/m^3)$	648.	254.
	$C(J/kgK)$	1845.	870.
CARPET average	$k(W/mK)$	0.060	0.006
	$\rho(kg/m^3)$	183.	21.
	$C(J/kgK)$	1740.	658.

The resultant temperature profile with error bars for the classroom can be seen in figure 7.2. These results are from a Monte Carlo simulation.

Table 7.5: Risk of overheating.

Probability level	Hours $> 26°C$
16%	9
50%	36
84%	54

An analysis of the risk of overheating can be seen in table 7.5. The probability levels reported correspond to the average prediction ($P = 50\%$), one standard deviation below the average ($P = 16\%$) and one standard deviation above the average ($P = 84\%$). From this it can be concluded that there is a 50% probability that there will be 36 hours when overheating occurs. Figure 7.3 shows how the number of overheating hours varies against deviations from the average performance. The overheating hours were calculated in steps of 1/2 a standard deviation. It can be

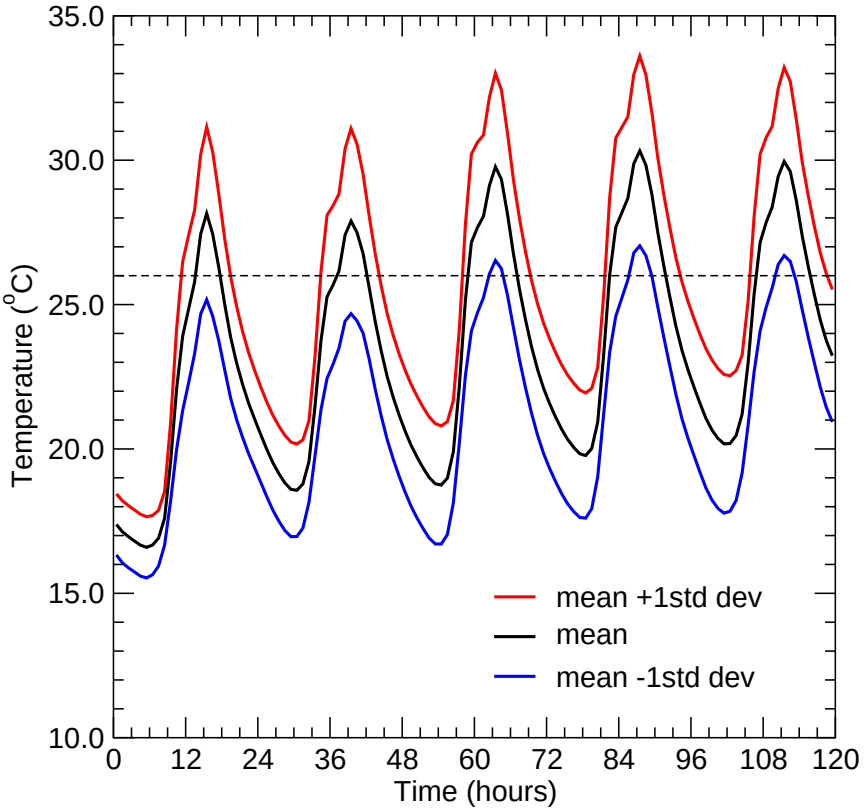

Figure 7.2: Resultant temperature profile with uncertainties.

seen that overheating would be eliminated by reducing the average performance by between 1 and 1.5 standard deviations.

To discover the critical parameters affecting the resultant temperature a differential analysis was conducted. The purpose of this analysis is to identify which elements of the model should be critically specified to achieve the necessary performance change to eliminate overheating.

The results of the differential analysis can be seen in table 7.6, the parameters contributing most to the uncertainty in the predictions are the infiltration, occupancy gain, equipment gain and the choice of some construction materials. Parameters which resulted in a change of less than $0.2°C$ have been removed from the table. The average effects are calculated from equation 3.7. As can be seen in the case of plasterboard the average change in temperature is quite small (typically $< 0.05°C$) but the average absolute change is much larger (typically $\approx 0.5°C$). This is a standard result for an uncertainty in thermal capacity: by decreasing or increasing the thermal

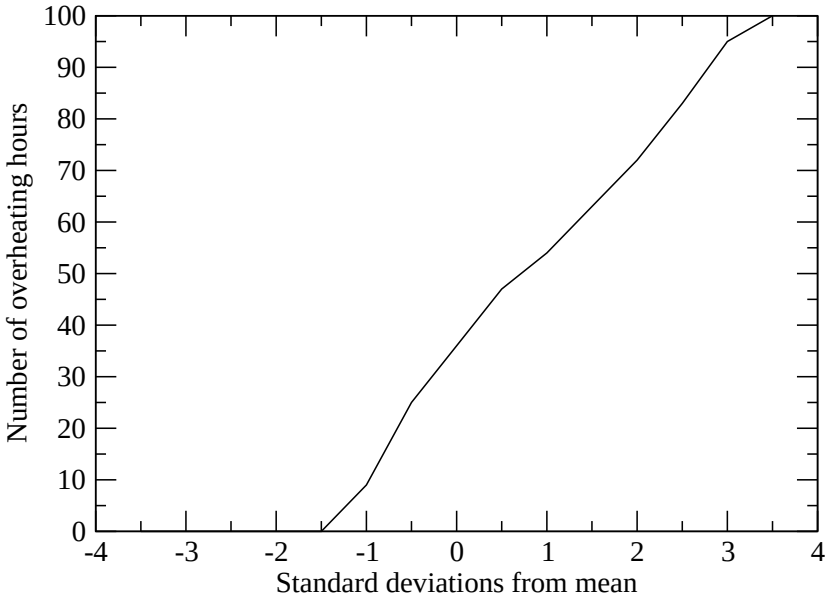

Figure 7.3: Overheating hours for given deviations from mean performance.

capacity (either density or specific heat) the magnitude of the daily temperature variation is greater or smaller respectively but the average remains essentially the same. This shows the need for both measurements of the average effect when quantifying uncertainty in building simulation.

Table 7.6: Results from differential analysis (Resultant temperature, $°C$).

Parameter	Low change effect		High change effect	
	mean	mean(abs diff)	mean	mean(abs diff)
Insulation conductivity	0.389	0.391	-0.302	0.305
Plaster density	-0.059	0.568	0.010	0.419
Plaster specific heat	-0.040	0.467	0.011	0.361
Timber conductivity	0.339	1.347	-0.014	0.145
Infiltration	0.881	0.881	-0.690	0.690
Occupancy gain	-1.522	1.522	0.764	0.764
Computer gain	-1.318	1.318	1.597	1.597

It is clear that the majority of the construction materials have little effect on the risk of overheating. However, the plasterboard does have an effect which is slightly less than that of the ventilation. The architect could now be given freedom over materials' choice except for the plasterboard, insulation and timber . The preferred properties would be higher then average conductivity for the insulation, and a plaster with higher density and specific heat capacity is probably preferable to reduce the

magnitude of daily temperature variations; the conductivity of timber should likewise be higher.

The main sources of uncertainty in the predictions will be from the heat gains in computers and from the occupants. The effect of lower occupancy and heat gains from computers is as expected *i.e.* the room becomes cooler by $1.5°C$ and $1.3°C$ respectively for a change in heat gain of one standard deviation. This information can, in the case of computers, be used for specifying low heat gain equipment and is maybe an indication that automatic energy saving capabilities should be enabled to minimise the heat gain.

A model without uncertainty was also created. The purpose of this model is to compare the performance using current simulation capabilities against the performance of the model with uncertainties. The attribution of this model was achieved by selecting specific materials from the construction materials database and assuming full occupancy and computer use. The model data are presented in tables 7.1 and 7.7

Comparing figure 7.2 with figure 7.4, it can be seen that the average temperature from the uncertain model is greater. This would indicate that the model chosen without uncertainties performed better than could be expected, *i.e.* it underpredicted the overheating. Quantifying the difference there are 26 hours of overheating in the model without uncertainty compared to 36 hours in the uncertain model, an underestimation of 28% or 1/2 a standard deviation.

On examining the energy balance for the classroom the three largest gains were found to be:

- opaque internal surfaces convective gain (29%).
- computer heat gain (28%),
- occupancy heat gain (27%), and

The classroom is clearly dominated by casual gains. However, the large gain from the internal surfaces would suggest that there is a significant solar gain (which is absorbed in the surface and then convected to the air).

Table 7.7: Construction materials used in school model.

Details of opaque composite: external wall						
Description	Thick (m)	Conduct (W/mK)	Density (kg/m^3)	Spec heat (J/kgK)	Absorb $(-)$	Emiss $(-)$
Lt brown brick	0.1000	0.960	2000.	650.	0.90	0.70
Glasswool	0.0880	0.040	250.	840.	—	—
air	0.0500	—	—	—	—	—
White painted plaster	0.0120	0.190	950.	840.	0.91	0.22
Details of opaque composite: internal partition						
Description	Thick (m)	Conduct (W/mK)	Density (kg/m^3)	Spec heat (J/kgK)	Absorb $(-)$	Emiss $(-)$
White painted plaster	0.0120	0.190	950.	840.	0.91	0.22
air	0.0500	—	—	—	—	—
White painted plaster	0.0120	0.190	950.	840.	0.91	0.22
Details of opaque composite: double glazing						
Description	Thick (m)	Conduct (W/mK)	Density (kg/m^3)	Spec heat (J/kgK)	Absorb $(-)$	Emiss $(-)$
Plate glass	0.0060	0.760	2710.	837.	0.83	0.05
air	0.0120	—	—	—	—	—
Plate glass	0.0060	0.760	2710.	837.	0.83	0.05
Details of opaque composite: roof						
Description	Thick (m)	Conduct (W/mK)	Density (kg/m^3)	Spec heat (J/kgK)	Absorb $(-)$	Emiss $(-)$
aluminium	0.0030	210.000	2700.	880.	0.22	0.20
air	0.0250	—	—	—	—	—
Glass fibre quilt	0.0950	0.040	12.	840.	—	—
White painted plaster	0.0120	0.190	950.	840.	0.91	0.22
Details of opaque composite: floor						
Description	Thick (m)	Conduct (W/mK)	Density (kg/m^3)	Spec heat (J/kgK)	Absorb $(-)$	Emiss $(-)$
Heavy mix concrete	0.1400	1.400	2100.	653.	0.90	0.65
air	0.0500	—	—	—	—	—
Chipboard	0.0190	0.150	800.	2093.	—	—
Carpet	0.0060	0.060	186.	1360.	0.90	0.60

A comparison of the analyses shows that there is a degree of consistency. In both cases the high internal gains were identified as major contributers to the overheating. However, by including uncertainties extra information has been generated as follows.

1. The risk of overheating was quantified and showed that there was a high probability that the room would overheat and that the simulation without uncertainty was optimistic in its estimate of 26 hours greater than $26°C$.

2. Three materials (plasterboard, timber and insulation) were identified as having a noticeable effect on the overheating. The outcome of this is twofold: for these

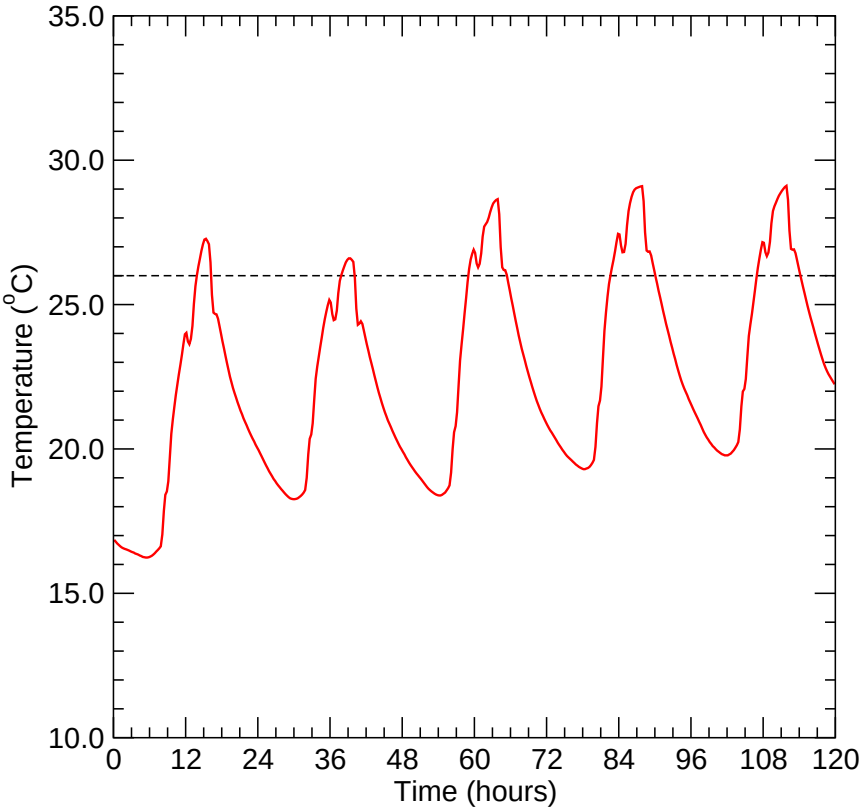

Figure 7.4: Resultant temperature profile without uncertainties.

materials the final selection should be considered carefully with respect to the thermal properties; and for other materials the architect now has the freedom to choose these based on other constraints (*e.g.* cost, environmental impact), provided the thermal properties are within the simulated ranges.

3. Areas of specific concern have been identified from the uncertain model: the heat gain from computers and occupants, the minimum air supply rate to the room. These areas should be the focus of increased attention during the next stage of the design process.

The inclusion of uncertainty in the early design stage has increased the quality of the simulation process with respect to the information generated about the design. The additional benefits were the quantification of large uncertainties present at this design stage and the identification of critical parameters in the design. The next example shows how uncertainty analysis can be employed at a later design stage, where uncertainties are less.

7.2 Critical plant sizing

As the centrepiece of Glasgow's celebrations as UK City of Architecture and Design in 1999, a city centre building of architectural significance was refurbished: the Lighthouse Building by Charles Rennie Mackintosh, constructed in 1896 (figure 7.5). The refurbishment concentrated on maintaining the good design practice shown by the original architect while introducing modern services to the building, including many new sources of heat: computer terminals, halogen lighting, escalators and lifts *etc.*

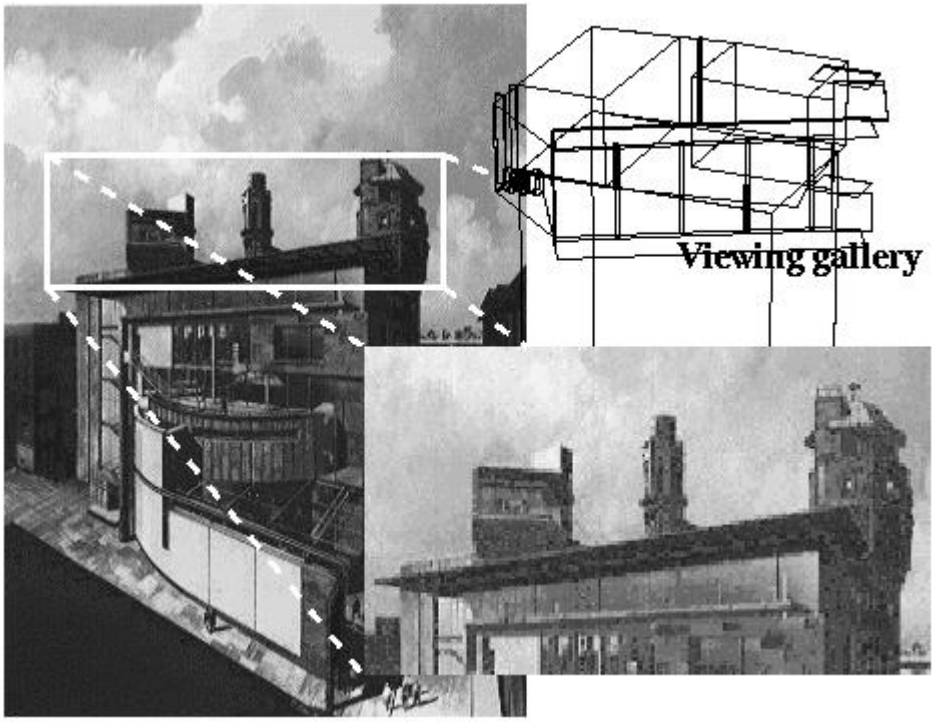

Figure 7.5: Lighthouse viewing gallery.

The purpose of this study was to quantify the annual heating energy consumption and maximum load in the viewing gallery. The maximum load was calculated including uncertainties in thermophysical properties, occupancy and infiltration. A second simulation was undertaken with a deliberately undersized plant to quantify the risk of underheating and the potential savings due to smaller capital and running costs. A model of the viewing gallery was created as shown in figure 7.5

Table 7.8: Thermophysical property distributions.

Parameter	Property	Average value	Standard deviation
Heavy mix concrete	$k(W/mK)$	1.68	0.144
	$\rho(kg/m^3)$	2304	36
	$C(J/kgK)$	869	91
Copper	$k(W/mK)$	333	3.7
	$\rho(kg/m^3)$	8858	21
	$C(J/kgK)$	398	22
Steel	$k(W/mK)$	46	0.7
	$\rho(kg/m^3)$	7800	26
	$C(J/kgK)$	497	20
Aluminium	$k(W/mK)$	211	3.7
	$\rho(kg/m^3)$	2733	21
	$C(J/kgK)$	880	22
Plywood	$k(W/mK)$	0.16	0.028
	$\rho(kg/m^3)$	622	26
	$C(J/kgK)$	1718	128
Slate	$k(W/mK)$	1.72	0.245
	$\rho(kg/m^3)$	2150	42
	$C(J/kgK)$	1110	90
Gypsum plasterboard	$k(W/mK)$	0.28	0.019
	$\rho(kg/m^3)$	950	12
	$C(J/kgK)$	882	111
Cement screed	$k(W/mK)$	0.9	0.077
	$\rho(kg/m^3)$	1452	25
	$C(J/kgK)$	910	93
EPS	$k(W/mK)$	0.035	0.003
	$\rho(kg/m^3)$	28	3
	$C(J/kgK)$	1328	57
Plate glass	$k(W/mK)$	0.95	0.067
	$\rho(kg/m^3)$	2515	8
	$C(J/kgK)$	828	33
Glass Fibre quilt	$k(W/mK)$	0.035	0.003
	$\rho(kg/m^3)$	32	3
	$C(J/kgK)$	851	57

Table 7.9: Operations profile distributions.

Parameter	Standard deviation
Occupancy sensible gain	16 %
Infiltration rate	33 %

For this case study, uncertainties were defined for constructions (table 7.8), and scheduled operations (table 7.9) based on the information presented in chapter 4. The construction uncertainties (table 7.8) were restricted to those affecting only the viewing gallery, and the time-varying uncertainties (table 7.9) were valid throughout

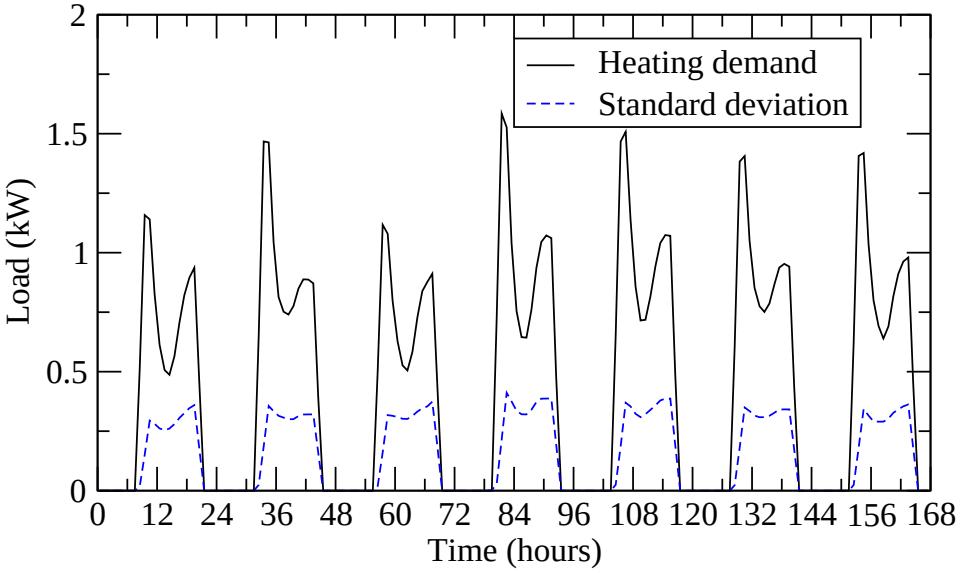

Figure 7.6: Viewing gallery heater load with error bands.

the simulation period.

The heating demand and associated uncertainty was calculated as shown in figure 7.6. As can be seen the standard deviation varies with time (in this example the standard deviation tends to be larger in the afternoon). The peak heating demand was $1.58kW$ for the average performance.

Assuming that only $1kW$ heaters were available one design option would be to install two units. However, to examine the probability of underheating a further analysis was undertaken with the maximum heater load restricted to $1kW$: approximately 2/3 of the maximum load from the initial analysis. This figure represents insufficient heater power to achieve the setpoint temperature for 25 hours in figure 7.6.

Table 7.10: Annual energy consumption for heating (kWh).

	Mean -1σ	Mean	Mean $+1\sigma$
Unlimited heater power	2396	2865	3335
Limited heater power	2208	2477	2747

The annual heating energy consumption was calculated again and is displayed in table 7.10 together with the data for the unlimited heater power case. The average energy saving is 13% by adopting the limited heater power (not including any gain in running at higher part load efficiencies).

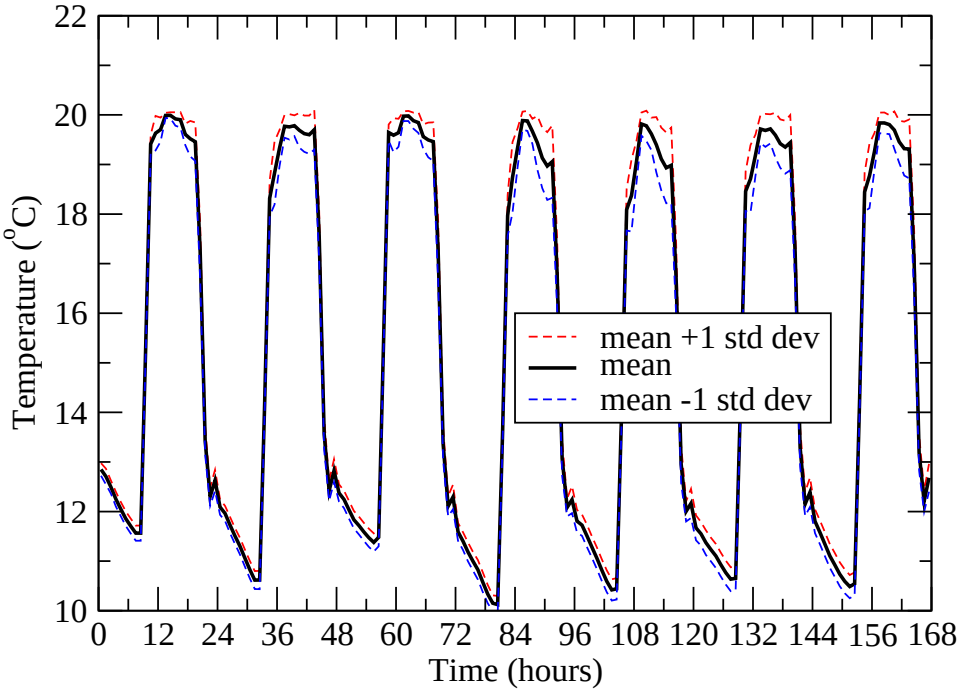

Figure 7.7: Viewing gallery temperature with error bands.

By limiting heater power there will be periods when underheating occurs. The temperature profile of the viewing gallery is shown in figure 7.7. As can be seen, the average temperature seldomly reaches the control set point of $20°C$, *i.e.* underheating occurs.

Table 7.11: Risk of underheating during occupied hours.

Probability level	Percent hours $< 19°C$
16%	45
50%	26
84%	16

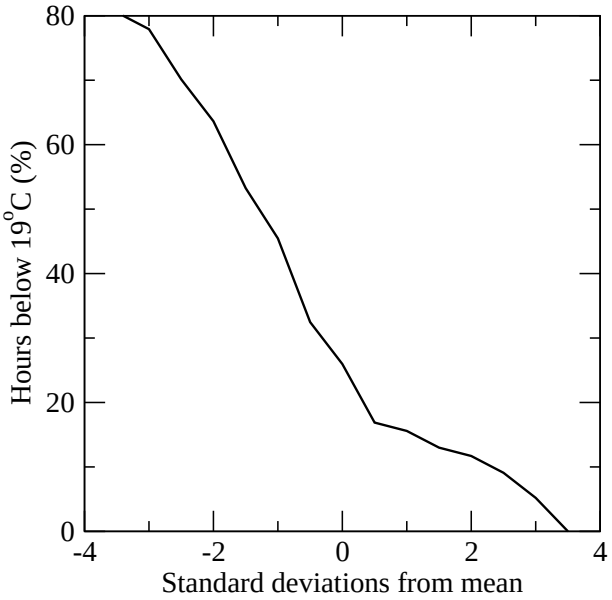

Figure 7.8: Underheating for given deviations from mean performance.

The degree of underheating is quantified as the percentage of occupied hours when the temperature is below $19°C$, table 7.11. The probability levels reported correspond to the average prediction ($P = 50\%$), one standard deviation below the average ($P = 16\%$) and one standard deviation above the average ($P = 84\%$). Figure 7.8 shows how the percentage of underheating hours varies against deviations from the average performance. From this it can be concluded that there is a 50% probability that there will be at least 26% of occupied hours when underheating occurs. Alternatively, the probability of temperatures less than $19°C$ occurring for 50% of occupied hours is 10%.

The client is now capable of making an informed decision on plant size taking the possible energy savings (one unit instead of two and 13% annual energy savings) and the risk of potential underheating into consideration.

7.3 Comparison of designs

For the final case study a speculative office development was selected. The purpose of the model was to quantify the peak summer temperatures for two alternative designs. The design change modelled replaced the clear float double glazing in the building

with antisun double glazing. The visible transmission of the glazing units was 76% and 63% respectively. The significance of the difference in the air temperature predictions was calculated. A model of the whole building was created as shown in figure 7.9.

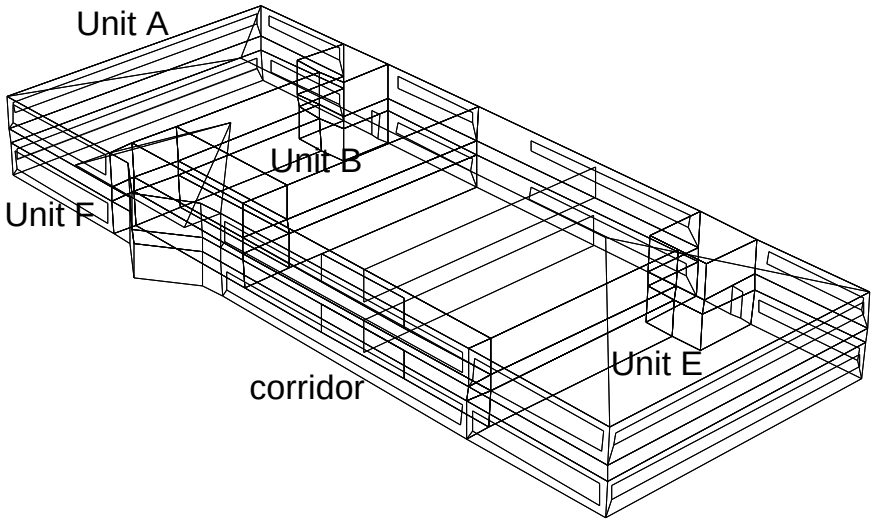

Figure 7.9: Model of office development.

Table 7.12: Uncertainty in material properties.

Material	Conductivity (W/mk)	Density (kg/m^3)	Specific Heat (J/kgK)
Aluminium	3.7	21	22
Block white painted inner	0.025	12	96
Chipboard	0.021	25	134
Common earth	0.107	31	92
Glass Fibre quilt	0.003	3	57
Gravel based	0.107	31	92
Gypsum plaster	0.052	21	92
Heavy mix concrete	0.144	36	91
Oak (radial)	0.021	25	134
Plate glass	0.067	8	33
Steel	0.7	26	20
White marble	0.245	42	90
White painted Gypboard	0.019	12	111
Wilton carpet	0.008	4	79

The uncertainties in the construction materials are given in table 7.12. As the specific materials were known the uncertainty was based on the material's category as described in chapter 4, see table 4.4 for details. The uncertainties in infiltration, occupancy and heat gains from equipment were defined as 33%, 16% and 15%

Table 7.13: Peak air temperatures and standard deviations ($^{\circ}C$).

Space	Double glazing		Solar control glazing		$\Delta\theta$
	θ	σ	θ	σ	
Unit A	26.05	1.66	25.41	1.64	0.64
Unit B	25.08	1.128	24.53	0.89	0.55
Unit E	26.77	1.45	25.87	1.17	0.90
Unit F	24.17	0.75	23.48	0.56	0.69
Corridor	28.14	1.65	26.19	1.47	1.95

respectively. Importantly, the uncertainties were the same for both designs.

The difference in peak summer air temperature due to the design change for five spaces in the building were calculated, as displayed in table 7.13. As can be seen the temperature reduction is between $0.55^{\circ}C$ and $1.95^{\circ}C$.

The significance statistic (t_0) of the temperature difference was calculated and is presented in table 7.14. See section 3.1.3 for details on significance testing.

Table 7.14: Significance of reduction in peak air temperatures.

Space	$\Delta\theta$ ($^{\circ}C$)	t_0 (–)
Unit A	0.64	2.71
Unit B	0.55	3.09
Unit E	0.90	4.31
Unit F	0.69	6.65
Corridor	1.95	7.89

If the value of the significance statistic, t_0, is greater than a critical value then the modification is said to be significantly different. The critical value depends on the number of degrees of freedom and the significance level chosen. The number of degrees of freedom is equal to the number of runs used in the Monte Carlo analysis and typical significance levels are 95%, 99% and 99.9%. The greater the significance level the greater the confidence that the result is correct.

If a significance level of 99.9% is chosen then the critical value of the significance statistic for this case is 3.17. This would indicate that only the corridor, Units E and F were significantly affected by the change in glazing type. Examining the temperature differences in the spaces, table 7.14, it can be seen that Units A and F have similar temperature reductions. Despite this the design change is significant in Unit A but not

in Unit F. This exemplifies the importance of significance testing: apparently similar changes can be significant or insignificant due to the impact of equal uncertainties in different spaces.

Another choice of significance level, 95%, gives $t_0 = 1.66$ in which case all of the spaces are significantly affected by the change in glazing type.

The importance of significance testing has been demonstrated. It is impossible to ascertain the significance of a design change on the basis of a single value: the standard deviation in that value must be calculated as well.

7.4 Summary

The benefits of uncertainty analysis have been demonstrated via the three case studies. The first case study illustrated how simulation can be used at the early design stages with increased efficacy (as more information pertaining to the building performance was generated). The additional benefits were that highly uncertain information was used to create the model and that the main parameters contributing to the overall uncertainty were identified. This allowed modelling effort to be concentrated on the critical areas. An extension of this focusing would be during construction where quality control could likewise be concentrated on these aspects of the building. Also of note was that by not accounting for uncertainties the risk of overheating was underestimated. The second study showed how plant size could be dramatically reduced at a risk of underperformance. This underperformance was quantified and could be acceptable to the design team. The final case study demonstrated the importance of significance testing between designs. Despite the effect of the design change being approximately equal in two of the examined spaces the significance of the change varied considerably. Only by assessing uncertainty can this increased knowledge of the building's performance be gained.

References

Macdonald I, Strachan P, *Practical application of uncertainty analysis*, Energy and Buildings, Vol 33, pp 219-227, 2001

Chapter 8

Conclusions and future work

The aims of this thesis were as follows.

1. Review uncertainty assessment methods.
2. Identify the sources of uncertainty as they impact upon building simulation.
3. Identify suitable probability distributions to describe the uncertain parameters.
4. Implement quantitative methods for analysing the effect on simulation outputs.

These aims have been addressed by identifying and integrating three external methods within the ESP-r system, namely: differential analysis; factorial analysis and Monte Carlo analysis. An alternative, internal, approach has been developed and is advocated as superior to the external methods as only a single simulation is required and the uncertainty information is available throughout the simulation. Common data used in building simulation programs has been reviewed to quantify the uncertainty within the data.

These advances enable simulation users to:

1. quantify overall uncertainty in model predictions. This enables risk based decision making, and significance testing between design options; and
2. quantify the uncertainty due to individual parameters for the specific building being analysed. This will enable guided quality assurance (QA) procedures to

be adopted, *i.e.* QA can focus upon the parameters in the model with the largest contribution to the output uncertainty.

These aspects of the efficacy of uncertainty based simulations were demonstrated in a number of case studies.

Overall, this thesis represents a contribution towards the inclusive and routine treatment of uncertainty in building simulation.

External methods

Quantification methods from experimental techniques and sensitivity analysis were selected to quantify the effect of uncertainties in simulation. These methods comprise the differential, factorial and Monte Carlo techniques. The advantages and disadvantages of the three methods are summarised in table 8.1. Each method requires multiple simulations of deliberately perturbed models: given N uncertain parameters the differential method requires $2N + 1$ simulations, the factorial N^2 simulations and the Monte Carlo 80 simulations regardless of the number of uncertain parameters.

Method	Advantages	Disadvantages
Differential	Easy to implement and understand results	Only measures main effects
Factorial	Measures main effects and interactions	Number of simulations required for large number of uncertain parameters
Monte Carlo	Required number of simulations independent of number of uncertain parameters	Only measures overall uncertainty

Table 8.1: Advantages and disadvantages of external methods

To apply these methods to a mature simulation environment (ESP-r) required updating the data model and identifying where the methods interact with the simulation process. This required the creation of a simulation controller which enables the required perturbations to the data model between simulations, depending on the chosen analysis method. The results created when simulating with uncertainties require to be examined in a manner consistent with the analysis method chosen. This required modifications to the results analysis module of ESP-r to enable differences

between simulation run results to be analysed.

The implementation of the external methods was verified via an inter-model comparison with separate reference models. The reference models were created to represent the perturbed models created by the simulation controller. To verify that the intended perturbation had been made to the reference model required updating ESP-r to produce a status report of the current model. Differences in these reports could then be analysed. These reports have proven useful in general simulation work as an aid to model quality assurance.

Internal methods

Several techniques exist within mathematics to embody imprecise information within a deterministic calculation procedure, including interval and fuzzy arithmetic. It was discovered that these techniques are unsuitable for use in building simulation as the relationships between uncertainties in matrix coefficients are not preserved, leading to overestimation of the effects of uncertainty. A correlation sensitive modification to interval arithmetic was investigated, namely affine arithmetic.

Affine arithmetic was applied to the building thermal energy conservation equation set and demonstrated to produce quantification of individual and overall uncertainty. To achieve these quantifications with the external methods requires a differential and a Monte Carlo analysis, *i.e.* multiple simulations and analyses are replaced by a single simulation.

The implementation required the careful analysis of the calculation procedure in order to minimise the number of non-affine operations. These operations produce a new uncertainty token which is not correlated to any of the existing tokens. In the cases where the method failed these new tokens dominated the solution. In general all addition and subtraction operations were computed before multiplication, division and other non-affine operations. It was discovered that using an iterative approach to matrix solution was better than using a direct method. This was attributed to the original coefficients remaining unaltered in the iterative scheme (hence no new uncertainty tokens) and fewer non-affine operations (although the total number of

operations may increase).

The results of the affine simulations were verified by an inter-model comparison with the external methods. For small uncertainties the predictions made by the affine method agreed with those of a differential and Monte Carlo analysis. However, for larger uncertainties the method failed to produce useful bounds on the predictions. Reasons for this were identified and include issues such as matrix multiplication where new (unnecessary) uncertainty tokens are currently produced. Future work aims to remove these and improve the performance of the method. For current applications a combination of internal and external methods will be required until these limitations are overcome for the affine approach.

In addition to only requiring a single analysis to quantify the first order and overall effects of uncertainty the effects of uncertainty are known throughout the calculation procedure. This allows information exchange between technical domains with respect to the effects of uncertainty and uncertainty based control actions to be enabled. In principle the method should be applied to building simulation programs although there are several technical issues to overcome, principally the convergence of overall error bounds and alternative probability distributions for uncertainty tokens.

The internal method has been demonstrated on the ESP-r system and will be applicable to any other set of conservation equations using the control volume method.

Simulation data

Current design methods employ data for worst conditions: maximum occupancy, peak solar gain and ambient temperature *etc* for a summer design condition and the opposite for a winter design condition. This approach does not allow consideration of the variability of the data used in simulation.

When simulating with uncertainties the variability in the simulation data is required. To this end the thermophysical properties of building materials, casual gains from people and equipment, and infiltration rates were examined.

The quantification process showed that data available for simulation is typically quite old. However, expressions to quantify the uncertainty were generated and ap-

plied to the current data.

Analysis approach

The use of uncertainty analysis in building simulation allows effective simulation use at earlier design stages. The resulting simulations will produce results encompassing all possible outcomes based on the defined uncertainties. The analysis will also inform the design team on which aspects of their design are critical to the occupant's comfort and building's energy consumption; for example, building form, construction or assumptions on occupancy levels. Therefore, the design constraints are clearly defined at the early design stage. The converse of this is also true in that the elements of the design which are not critical to the building's environmental performance can be chosen on the basis of other considerations, for example architectural merit or cost.

Future work

Three main areas have been identified for future research as follows.

- External methods. The methods chosen were selected for their robustness and ease of understanding (for the user). With their application future researchers will be able to test other, more efficient, methods (for example, with respect to simulation runs).

- Internal methods. The affine arithmetic approach has been shown to produce bounded results. However, refinements to the method could increase its robustness, as described below.

- Data. The review of the common data for simulation highlighted the lack of good data for building simulation and the lack of documentation as to the variability inherent in this data.

It is the author's view that the quantitative information delivered from the routine use of uncertainty quantification can be used to guide future research into building simulation: why devote resources to measuring an unimportant parameter in relation to building performance? For example, if it is shown that convection coefficients are

critical to the performance of all buildings then research resource should be directed at providing suitable new correlations.

Potential extensions to affine arithmetic

It has been shown that the affine approach is a feasible solution to the treatment of uncertainties within building simulation. However, the approach adopted can be improved in a number of ways.

Affine array operations

Affine array addition is an affine process. Therefore, it can be calculated on a term by term basis as is the case with normal array addition. Affine array multiplication, however, is a non-affine process.

Consider two affine arrays $\mathbf{A}$ and θ, and their product. Calculating on a term by term basis, the non-affine terms of each multiplication are approximated, and then totalled. There will be a new error term created for each multiplication. For an array of dimension $n \times n$ this would create n^2 new independent error terms.

However, if the non-affine terms are not approximated before the addition step, then additional correlations will be preserved. If and only if any non-affine terms remain (as they could cancel) then an approximation would be made and only a single new error term would result from the operation, resulting in only n new error terms. This is a non-trivial calculation and adjustment to the implementation of affine arithmetic because matrix multiplication would have to be separately encoded from normal multiplication.

Non-linear polynomial calculations

A further extension would be to extend the description of the affine number to higher degrees. The resulting polynomial would no longer be an affine number, due to the ϵ^n terms. This would allow increased accuracy in the calculation of the uncertainties.

The definition of the basic operations would have to be revisited and new approximating equations for the higher order terms developed. This approach could

overcome the problems identified in the cases of unbounded solutions.

A useful analysis would be to measure the effect that each higher order uncertainty token has on the solution. Perhaps a quadratic representation would be sufficient as typically factorial analyses show that two parameter interactions are important but higher order interactions are less so.

Fuzzy affine terms

Another alteration to the affine representation would be to redefine the uncertainty token ϵ as a fuzzy number instead of an interval number. This would introduce the advantages of the fuzzy representations but would entail a large increase in computational effort. Again the basic operations would have to be revisited, especially the new uncertainty tokens introduced in non-affine operations: how will the membership function be defined?

Introducing uncertainty considerations to design practices

During this research the author made several informal enquiries of practitioners as to their perception of the variability in data used in simulation. The responses were not surprising in that the design had to achieve a certain target and current worst case design data would be used, with no variation from this stance.

This belief poses two barriers to the use of uncertain data in design work:

1. Current practitioners are trained to use single values for parameters and thus the idea of variability is alien and difficult for them to accept.

2. As they are unable to accept variability in modelling data they are unable to consider quantifying the data.

These barriers must be overcome. This could be achieved through training and suitable demonstrations of the process.

An initial step would be a formal survey of practitioners' views and treatment of uncertainty. This should be followed by seminars or articles in industry publications, *e.g.* the Scottish Energy Systems Group's newsletter or the CIBSE Journal.

The interpretation of the results of an uncertainty analysis should also be explored in a design context. It is suspected that different professions within the design process could use uncertainty assessments differently: perhaps services engineers would be mainly interested in the risk of the building failing to provide comfortable conditions, whereas architects may be more interested in creating a robust design.

Extensions to uncertainty analysis approach

Finally, the overall approach could be refined in several aspects, generally related to uncertainty definition. Typical uncertainties could be defined in a system database and as a data item is defined an uncertainty could be automatically applied to the data item. This would ease the definition procedure but would incur data model management problems as items are added and deleted from the model, *e.g.* surfaces. An alternative approach would be to use the current definition procedure (post model creation) and to automatically assign uncertainties based on a set of attribution rules. A prototype of this method has been applied for construction materials based on the material type: impermeable, non-hygroscopic, inorganic-porous and organic-hygroscopic. The rules could be expanded to cover issues such as surface orientation, location (external wall, internal wall, *etc*), and zone usage.

Appendix A

Thermophysical properties

For the entity standard deviations given here the following assumptions were used.

Moisture contents: 1%, 4% and 7% for non-hygroscopic, inorganic-porous and organic-hygroscopic materials respectively;

Temperature: $10°C$ variation for all materials.

Asbestos

Table A.1: Thermophysical properties of boards

	Conductivity (W/mK)	Density (kg/m^3)	Specific Heat Capacity (J/kgK)
Average	0.430	1488	958
Std dev	0.153	501	109
Entity std dev	0.042	18	95

Table A.2: Thermophysical properties of cements

	Conductivity (W/mK)	Density (kg/m^3)	Specific Heat Capacity (J/kgK)
Average	0.775	1750	840
Std dev	0.346	29	90
Entity std dev	0.075	29	90

Bitumen and Asphalt

Table A.3: Thermophysical properties of bitumen

	Conductivity (W/mK)	Density (kg/m^3)	Specific Heat Capacity (J/kgK)
Average	0.237	1188	1135
Std dev	0.186	346	384
Entity std dev	0.012	4	46
CEN value	0.17-0.23	1050-1100	1000

Table A.4: Thermophysical properties of asphalt

	Conductivity (W/mK)	Density (kg/m^3)	Specific Heat Capacity (J/kgK)
Average	1.050	2146	1232
Std dev	0.308	266	431
Entity std dev	0.055	7	50
CEN value	0.700	2100	1000

Blockwork

Table A.5: Thermophysical properties of heavyweight blockwork

	Conductivity (W/mK)	Density (kg/m^3)	Specific Heat Capacity (J/kgK)
Average	0.922	1925	840
Std dev	0.243	189	90
Entity std dev	0.089	32	90

Table A.6: Thermophysical properties of mediumweight blockwork

	Conductivity (W/mK)	Density (kg/m^3)	Specific Heat Capacity (J/kgK)
Average	0.513	1299	827
Std dev	0.259	258	89
Entity std dev	0.049	22	89

Table A.7: Thermophysical properties of lightweight blockwork

	Conductivity (W/mK)	Density (kg/m^3)	Specific Heat Capacity (J/kgK)
Average	0.258	695	981
Std dev	0.040	147	399
Entity std dev	0.025	12	96

Bricks

Table A.8: Thermophysical properties of clay bricks

	Conductivity (W/mK)	Density (kg/m^3)	Specific Heat Capacity (J/kgK)
Average	0.789	1720	837
Std dev	0.261	301	90
Entity std dev	0.077	25	90

Table A.9: Thermophysical properties of silicate bricks

	Conductivity (W/mK)	Density (kg/m^3)	Specific Heat Capacity (J/kgK)
Average	1.250	2000	840
Std dev	0.354	33	90
Entity std dev	0.121	33	90

Table A.11: Thermophysical properties of heavyweight aggregates

	Conductivity (W/mK)	Density (kg/m^3)	Specific Heat Capacity (J/kgK)
Average	1.491	2179	864
Std dev	0.300	149	92
Entity std dev	0.144	36	91
CEN value	1.65-2.00	2200-2400	1000

Table A.10: Thermophysical properties of mediumweight aggregates

	Conductivity (W/mK)	Density (kg/m^3)	Specific Heat Capacity (J/kgK)
Average	0.718	1428	842
Std dev	0.324	376	90
Entity std dev	0.070	24	90
CEN value	1.15-1.35	1800-2000	1000

Table A.12: Thermophysical properties of lightweight aggregates

	Conductivity (W/mK)	Density (kg/m^3)	Specific Heat Capacity (J/kgK)
Average	0.480	1177	851
Std dev	0.185	301	90
Entity std dev	0.046	20	90

Table A.13: Thermophysical properties of aerated concrete

	Conductivity (W/mK)	Density (kg/m^3)	Specific Heat Capacity (J/kgK)
Average	0.267	676	915
Std dev	0.229	304	241
Entity std dev	0.026	11	93

Table A.14: Thermophysical properties of lightweight concrete

	Conductivity (W/mK)	Density (kg/m^3)	Specific Heat Capacity (J/kgK)
Average	0.313	891	839
Std dev	0.144	309	90
Entity std dev	0.030	15	90

Table A.15: Thermophysical properties of reinforced concrete

	Conductivity (W/mK)	Density (kg/m^3)	Specific Heat Capacity (J/kgK)
Average	1.680	2310	840
Std dev	0.540	225	90
Entity std dev	0.162	38	90
CEN value	2.3-2.5	2300-2400	1000

Floor coverings

Table A.16: Thermophysical properties of carpets

	Conductivity (W/mK)	Density (kg/m^3)	Specific Heat Capacity (J/kgK)
Average	0.060	183	1740
Std dev	0.008	21	658
Entity std dev	0.008	4	79
CEN value	0.06	200	1300

Table A.17: Thermophysical properties of underfelts

	Conductivity (W/mK)	Density (kg/m^3)	Specific Heat Capacity (J/kgK)
Average	0.052	132	843
Std dev	0.015	107	233
Entity std dev	0.007	4	51
CEN value	0.05-0.01	120-270	1300-1500

Glass

Table A.19: Thermophysical properties of glass blocks

	Conductivity (W/mK)	Density (kg/m^3)	Specific Heat Capacity (J/kgK)
Average	1.050	3000	840
Std dev	0.495	707	34
Entity std dev	0.055	10	34
CEN value	1.2	2000	750

Table A.18: Thermophysical properties of float glass

	Conductivity (W/mK)	Density (kg/m^3)	Specific Heat Capacity (J/kgK)
Average	1.294	2509	820
Std dev	0.690	105	50
Entity std dev	0.067	8	33
CEN value	1.0	2500	750

Table A.20: Thermophysical properties of cellular glass

	Conductivity (W/mK)	Density (kg/m^3)	Specific Heat Capacity (J/kgK)
Average	0.054	149	814
Std dev	0.008	19	44
Entity std dev	0.003	1	33

Insulation

Table A.21: Thermophysical properties of inorganic insulation

	Conductivity (W/mK)	Density (kg/m^3)	Specific Heat Capacity (J/kgK)
Average	0.039	38	1072
Std dev	0.014	27	298
Entity std dev	0.003	3	57

Table A.22: Thermophysical properties of organic insulation

	Conductivity (W/mK)	Density (kg/m^3)	Specific Heat Capacity (J/kgK)
Average	0.054	84	796
Std dev	0.022	59	153
Entity std dev	0.004	4	50

Metals

Table A.23: Thermophysical properties of non-ferrous metals

	Conductivity (W/mK)	Density (kg/m^3)	Specific Heat Capacity (J/kgK)
Average	224	6278	544
Std dev	107	2876	223
Entity std dev	3.7	21	22
CEN value	65-380	2800-8900	380-880

Table A.24: Thermophysical properties of ferrous metals

	Conductivity (W/mK)	Density (kg/m^3)	Specific Heat Capacity (J/kgK)
Average	44	7807	501
Std dev	18	154	27
Entity std dev	0.7	26	20
CEN value	17-50	7500-7900	450-460

Mortars and sealants

Table A.25: Thermophysical properties of mortars and sealants

	Conductivity (W/mK)	Density (kg/m^3)	Specific Heat Capacity (J/kgK)
Average	0.914	1782	856
Std dev	0.341	145	91
Entity std dev	0.088	30	91
CEN value	0.12-0.50	720-1450	1000

Plaster and boards

Table A.26: Thermophysical properties of boards and sheets

	Conductivity (W/mK)	Density (kg/m^3)	Specific Heat Capacity (J/kgK)
Average	0.191	704	1359
Std dev	0.150	379	615
Entity std dev	0.019	12	111
CEN value	0.25	900	1000

Table A.27: Thermophysical properties of plasters

	Conductivity (W/mK)	Density (kg/m^3)	Specific Heat Capacity (J/kgK)
Average	0.534	1264	889
Std dev	0.252	425	122
Entity std dev	0.052	21	92
CEN value	0.18-0.70	600-1600	1000

Plastics and rubbers

Table A.28: Thermophysical properties of PVC's

	Conductivity (W/mK)	Density (kg/m^3)	Specific Heat Capacity (J/kgK)
Average	0.283	1210	1103
Std dev	0.188	165	327
Entity std dev	0.015	4	45
CEN value	0.16-0.50	910-1400	900-2200

Table A.29: Thermophysical properties of rubbers

	Conductivity (W/mK)	Density (kg/m^3)	Specific Heat Capacity (J/kgK)
Average	0.137	894	1524
Std dev	0.111	753	364
Entity std dev	0.007	3	62
CEN value	0.06-0.25	60-1700	1000-2140

Renders and screeds

Table A.30: Thermophysical properties of renders and screeds

	Conductivity (W/mK)	Density (kg/m^3)	Specific Heat Capacity (J/kgK)
Average	0.787	1481	904
Std dev	0.341	390	125
Entity std dev	0.077	25	93

Soils

Table A.31: Thermophysical properties of soils

	Conductivity (W/mK)	Density (kg/m^3)	Specific Heat Capacity (J/kgK)
Average	1.106	1878	885
Std dev	0.469	402	324
Entity std dev	0.107	31	92
CEN value	1.5-2.0	1200-2200	910-2500

Stone

Table A.32: Thermophysical properties of stone

	Conductivity (W/mK)	Density (kg/m^3)	Specific Heat Capacity (J/kgK)
Average	2.536	2545	829
Std dev	0.862	323	162
Entity std dev	0.245	42	90
CEN value	1.1-3.5	1600-2800	1000

Tiles

Table A.33: Thermophysical properties of ceramic tiles

	Conductivity (W/mK)	Density (kg/m^3)	Specific Heat Capacity (J/kgK)
Average	1.060	1920	844
Std dev	0.261	349	34
Entity std dev	0.055	6	34
CEN value	1.3	2300	840

Table A.34: Thermophysical properties of clay tiles

	Conductivity (W/mK)	Density (kg/m^3)	Specific Heat Capacity (J/kgK)
Average	0.932	1610	818
Std dev	0.406	436	89
Entity std dev	0.090	27	89
CEN value	1.0	2000	800

Timber

Table A.35: Thermophysical properties of timber

	Conductivity (W/mK)	Density (kg/m^3)	Specific Heat Capacity (J/kgK)
Average	0.151	578	2162
Std dev	0.042	148	646
Entity std dev	0.021	25	134
CEN value	0.13-0.18	500-700	1600

Table A.36: Thermophysical properties of timber boards

	Conductivity (W/mK)	Density (kg/m^3)	Specific Heat Capacity (J/kgK)
Average	0.201	684	1845
Std dev	0.274	254	870
Entity std dev	0.028	26	128
CEN value	0.09-0.24	300-1000	1600

Appendix B

Standard transient conduction test

The following is based on a report [Macdonald] on the documentation for the CEN standard and the compliance of the ESP-r system.

Conduction through opaque surfaces

This test requires the prediction of internal air temperatures at several time intervals after a step change has been made to the ambient air temperature.

Test assumptions

The following assumptions were made:

1. The test is for unidirectional heat flow only.
2. There are no short-wave exchanges in the model.
3. There are no exchanges due to infiltration or ventilation.
4. Surface emissivities $(\epsilon_i, \epsilon_e) \leq 0.001$ and absorptivities $(\alpha_i, \alpha_e) \leq 0.001$.
5. The thermal capacity of the internal air is zero.

Geometry

The test zone shall have internal dimensions: $1.0 \times 1.0 \times 1.0(m)$

Constructions

Three different constructions were tested. In each test all surfaces in the zone were given the same construction. The material properties are as follows:

Table B.1: Constructions used in tests

Material	Conductivity $\lambda(W/mK)$	Density $\rho(kg/m^3)$	Specific heat capacity $C(kJ/kgK)$	Layer thickness $s(m)$
Render	1.20	2000	1.0	0.20
Insulation	0.04	50	1.0	0.10
Paper	0.14	800	1.5	0.005

Convection coefficients

Time invarient convection coefficients were used as detailed in table B.2.

Table B.2: Convective heat transfer coefficients

Property	Value
Internal, $h_{c,i}$	2.5 W/m^2K
External, $h_{c,e}$	8.0 W/m^2K

Boundary conditions

Each boundary in the zone has identical conditions as described below.

The zone will be subjected to a step change of $10°C$ in ambient air temperature as depicted in Figure B.1.

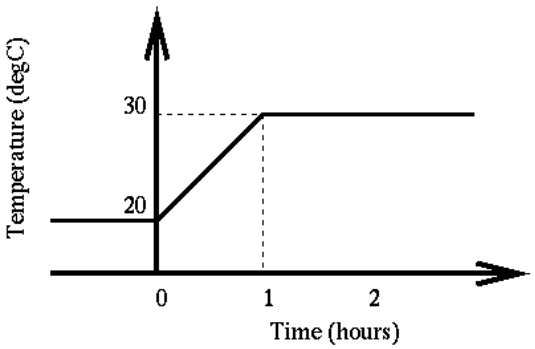

Figure B.1: Variation of ambient air temperature.

ESP-r predictions

The results of the ESP-r simulations are in table B.3. These results were used in the following sections as the correct solution to each of the problems. The requirement for compliance with the CEN standard was that the simulation results should be within $0.5°C$ of the correct (analytical) solution.

Table B.3: ESP-r predictions

Test no.	Time (hrs)					
	1	2	6	12	24	120
1	19.99	20.04	21.31	23.48	26.37	29.99
2	21.35	25.14	29.61	29.98	29.99	29.99
3	27.80	29.96	29.99	29.99	29.99	29.99

References

Macdonald I A, *Review of European Standard prEN ISO 13791 (draft) and its Application to the ESP-r system*, ESRU project report, 1997

Appendix C

Affine arithmetic simulations results tables

The tables presented here are for the complete set of simulations using the affine arithmetic approach to uncertainty quantification. The tests were all centered on appraising transient conduction through three single layer constructions: heavyweight, mediumweight and lightweight, test 1, 2 and 3 respectively. The conductivity, density and thickness of the layer were simulated, for all combinations, at four levels of uncertainty: 0%, 1%, 5% and 10%.

Table C.1: Uncertainties: density 1%, conductivity 1%.

Time	Case 1				
(hours)	θ_0	θ_{den}	θ_{con}	$\sum \theta_i$	$\sum \lvert\theta_i\rvert$
1	20.0172	-0.0004	0.0003	-0.0001	0.0007
2	20.1009	-0.0023	0.0014	-0.0006	0.0040
6	21.2866	-0.0207	0.0114	-0.0044	0.0375
12	23.4442	-0.0369	0.0172	-0.0013	0.0741
24	26.3645	-0.0421	0.0170	0.0262	0.1148
120	29.9676	-0.0019	0.0007	0.1769	0.1962
∞	29.9734	-0.0016	0.0006	0.1791	0.1981
Time	Case 2				
(hours)	θ_0	θ_{den}	θ_{con}	$\sum \theta_i$	$\sum \lvert\theta_i\rvert$
1	21.4323	-0.0189	0.0166	-0.0002	0.0380
2	25.1049	-0.0442	0.0401	0.0046	0.0944
6	29.5986	-0.0138	0.0127	0.0103	0.0396
12	29.9906	-0.0007	0.0006	0.0016	0.0032
24	30.0000	-0.0000	0.0000	0.0000	0.0000
∞	30.0000	0.0000	0.0000	0.0000	0.0000
Time	Case 3				
(hours)	θ_0	θ_{den}	θ_{con}	$\sum \theta_i$	$\sum \lvert\theta_i\rvert$
1	27.6470	-0.0223	0.0028	0.0316	0.0999
2	29.9723	-0.0015	0.0001	0.1042	0.1539
6	30.0000	0.0000	0.0000	0.2119	0.3046
12	30.0000	0.0000	0.0000	0.3258	0.4684
∞	30.0000	0.0000	0.0000	0.3715	0.5342

Table C.2: Uncertainties: density 1%, thickness 1%, conductivity 1%.

Time	Case 1					
(hours)	θ_0	θ_{den}	θ_{thk}	θ_{con}	$\sum \theta_i$	$\sum \lvert\theta_i\rvert$
1	20.0172	-0.0004	-0.0014	0.0003	-0.0011	0.0028
2	20.1009	-0.0023	-0.0075	0.0014	-0.0057	0.0156
6	21.2866	-0.0207	-0.0645	0.0115	-0.0270	0.1586
12	23.4442	-0.0370	-0.1085	0.0173	0.0533	0.3956
24	26.3645	-0.0422	-0.1187	0.0171	0.6250	1.1549
120	29.9676	-0.0020	-0.0053	0.0007	$> 1000.$	$> 1000.$
∞	29.9734	-0.0017	-0.0045	0.0006	$> 1000.$	$> 1000.$
Time	Case 2					
(hours)	θ_0	θ_{den}	θ_{thk}	θ_{con}	$\sum \theta_i$	$\sum \lvert\theta_i\rvert$
1	21.4323	-0.0189	-0.0713	0.0167	-0.0082	0.2157
2	25.1049	-0.0443	-0.1694	0.0403	0.1769	0.7862
6	29.5986	-0.0140	-0.0536	0.0128	3.9405	5.9930
12	29.9906	-0.0007	-0.0027	0.0006	81.6700	120.9659
24	30.0000	-0.0000	-0.0000	0.0000	$> 1000.$	$> 1000.$
∞	30.0000	0.0000	0.0000	0.0000	$> 1000.$	$> 1000.$
Time	Case 3					
(hours)	θ_0	θ_{den}	θ_{thk}	θ_{con}	$\sum \theta_i$	$\sum \lvert\theta_i\rvert$
1	27.6470	-0.0232	-0.0522	0.0029	$> 1000.$	$> 1000.$
2	29.9723	-0.0017	-0.0037	0.0002	$> 1000.$	$> 1000.$
6	30.0000	0.0000	0.0000	0.0000	∞	∞
12	30.0000	0.0000	0.0000	0.0000	∞	∞
∞	30.0000	0.0000	0.0000	0.0000	∞	∞

Table C.3: Uncertainties: density 1%, thickness 5%, conductivity 1%.

Time	Case 1					
(hours)	θ_0	θ_{den}	θ_{thk}	θ_{con}	$\sum\theta_i$	$\sum\lvert\theta_i\rvert$
1	20.0172	-0.0004	-0.0073	0.0003	0.0027	0.0339
2	20.1009	-0.0024	-0.0398	0.0015	0.0428	0.2101
6	21.2866	-0.0214	-0.3426	0.0123	3.3100	5.6871
12	23.4442	-0.0387	-0.5838	0.0186	113.9151	153.2107
24	26.3645	-0.0458	-0.6596	0.0190	$> 1000.$	$> 1000.$
120	29.9676	-0.0029	-0.0398	0.0010	$> 1000.$	$> 1000.$
∞	29.9734	-0.0025	-0.0343	0.0009	$> 1000.$	$> 1000.$
Time	Case 2					
(hours)	θ_0	θ_{den}	θ_{thk}	θ_{con}	$\sum\theta_i$	$\sum\lvert\theta_i\rvert$
1	21.4323	-0.0207	-0.4062	0.0191	$> 1000.$	$> 1000.$
2	25.1049	-0.0499	-0.9929	0.0473	$> 1000.$	$> 1000.$
6	29.5986	-0.0193	-0.3846	0.0184	∞	∞
12	29.9906	-0.0013	-0.0268	0.0013	∞	∞
24	30.0000	-0.0000	-0.0001	0.0000	∞	∞
∞	30.0000	0.0000	0.0000	0.0000	∞	∞
Time	Case 3					
(hours)	θ_0	θ_{den}	θ_{thk}	θ_{con}	$\sum\theta_i$	$\sum\lvert\theta_i\rvert$
1	27.6470	-0.6232	-6.8547	0.0541	∞	∞
2	29.9723	-16.1516	-177.3959	1.3774	∞	∞
6	30.0000	$< -1000.$	$< -1000.$	$> 1000.$	∞	∞
12	30.0000	$< -1000.$	$< -1000.$	$< -1000.$	∞	∞
∞	30.0000	$< -1000.$	$< -1000.$	$< -1000.$	∞	∞

Table C.4: Uncertainties: density 1%, thickness 10%, conductivity 1%.

Time	Case 1					
(hours)	θ_0	θ_{den}	θ_{thk}	θ_{con}	$\sum\theta_i$	$\sum\lvert\theta_i\rvert$
1	20.0172	-0.0005	-0.0193	0.0004	0.1363	0.5041
2	20.1009	-0.0027	-0.1045	0.0020	2.0215	4.8552
6	21.2866	-0.0257	-0.9207	0.0166	$> 1000.$	$> 1000.$
12	23.4442	-0.0524	-1.7308	0.0276	$> 1000.$	$> 1000.$
24	26.3645	-0.0812	-2.5218	0.0358	$> 1000.$	$> 1000.$
120	29.9676	-0.0862	-2.5730	0.0333	∞	∞
∞	29.9734	-0.0847	-2.5235	0.0326	∞	∞
Time	Case 2					
(hours)	θ_0	θ_{den}	θ_{thk}	θ_{con}	$\sum\theta_i$	$\sum\lvert\theta_i\rvert$
1	21.4323	-0.0400	-1.8240	0.0427	$> 1000.$	$> 1000.$
2	25.1049	-0.1282	-5.9375	0.1408	∞	∞
6	29.5986	-0.4394	-20.4100	0.4852	∞	∞
12	29.9906	-1.7030	-79.1114	1.8807	∞	∞
24	30.0000	-18.1336	-842.3913	20.0261	∞	∞
∞	30.0000	$< -1000.$	$< -1000.$	$> 1000.$	∞	∞
Time	Case 3					
(hours)	θ_0	θ_{den}	θ_{thk}	θ_{con}	$\sum\theta_i$	$\sum\lvert\theta_i\rvert$
1	27.6470	∞	∞	∞	∞	∞
2	29.9723	∞	∞	∞	∞	∞
6	30.0000	∞	∞	∞	∞	∞
12	30.0000	∞	∞	∞	∞	∞
∞	30.0000	∞	∞	∞	∞	∞

Table C.5: Uncertainties: density 1%, conductivity 5%.

Time	Case 1				
(hours)	θ_0	θ_{den}	θ_{con}	$\sum \theta_i$	$\sum \lvert\theta_i\rvert$
1	20.0172	-0.0004	0.0013	0.0010	0.0020
2	20.1009	-0.0023	0.0072	0.0057	0.0109
6	21.2866	-0.0207	0.0572	0.0567	0.1045
12	23.4442	-0.0369	0.0861	0.1347	0.2315
24	26.3645	-0.0422	0.0851	0.3524	0.5176
120	29.9676	-0.0019	0.0034	62.9072	79.4939
∞	29.9734	-0.0017	0.0029	77.4327	97.8478
Time	Case 2				
(hours)	θ_0	θ_{den}	θ_{con}	$\sum \theta_i$	$\sum \lvert\theta_i\rvert$
1	21.4323	-0.0189	0.0833	0.0780	0.1232
2	25.1049	-0.0442	0.2007	0.2244	0.3362
6	29.5986	-0.0139	0.0635	0.1919	0.2612
12	29.9906	-0.0007	0.0032	0.0524	0.0682
24	30.0000	-0.0000	0.0000	0.0035	0.0046
∞	30.0000	0.0000	0.0000	0.0000	0.0000
Time	Case 3				
(hours)	θ_0	θ_{den}	θ_{con}	$\sum \theta_i$	$\sum \lvert\theta_i\rvert$
1	27.6470	-0.0229	0.0144	$> 1000.$	$> 1000.$
2	29.9723	-0.0017	0.0008	$> 1000.$	$> 1000.$
6	30.0000	0.0000	0.0000	∞	∞
12	30.0000	0.0000	0.0000	∞	∞
∞	30.0000	0.0000	0.0000	∞	∞

Table C.6: Uncertainties: density 1%, thickness 1%, conductivity 5%.

Time	Case 1					
(hours)	θ_0	θ_{den}	θ_{thk}	θ_{con}	$\sum \theta_i$	$\sum \lvert\theta_i\rvert$
1	20.0172	-0.0004	-0.0014	0.0013	0.0002	0.0046
2	20.1009	-0.0023	-0.0075	0.0072	0.0023	0.0257
6	21.2866	-0.0208	-0.0646	0.0574	0.0701	0.2788
12	23.4442	-0.0371	-0.1087	0.0864	0.3912	0.8421
24	26.3645	-0.0424	-0.1192	0.0856	2.7672	4.0818
120	29.9676	-0.0020	-0.0054	0.0035	$> 1000.$	$> 1000.$
∞	29.9734	-0.0017	-0.0046	0.0030	$> 1000.$	$> 1000.$
Time	Case 2					
(hours)	θ_0	θ_{den}	θ_{thk}	θ_{con}	$\sum \theta_i$	$\sum \lvert\theta_i\rvert$
1	21.4323	-0.0190	-0.0715	0.0837	0.1364	0.4148
2	25.1049	-0.0445	-0.1699	0.2021	0.8600	1.7537
6	29.5986	-0.0141	-0.0540	0.0645	22.5949	34.0566
12	29.9906	-0.0007	-0.0027	0.0033	$> 1000.$	$> 1000.$
24	30.0000	-0.0000	-0.0000	0.0000	$> 1000.$	$> 1000.$
∞	30.0000	0.0000	0.0000	0.0000	$> 1000.$	$> 1000.$
Time	Case 3					
(hours)	θ_0	θ_{den}	θ_{thk}	θ_{con}	$\sum \theta_i$	$\sum \lvert\theta_i\rvert$
1	27.6470	-0.0253	-0.0568	0.0155	∞	∞
2	29.9723	-0.0022	-0.0047	0.0010	∞	∞
6	30.0000	0.0000	0.0000	0.0000	∞	∞
12	30.0000	0.0000	0.0000	0.0000	∞	∞
∞	30.0000	0.0000	0.0000	0.0000	∞	∞

Table C.7: Uncertainties: density 1%, thickness 5%, conductivity 5%.

Time	Case 1					
(hours)	θ_0	θ_{den}	θ_{thk}	θ_{con}	$\sum \theta_i$	$\sum \lvert\theta_i\rvert$
1	20.0172	-0.0004	-0.0073	0.0014	0.0062	0.0426
2	20.1009	-0.0024	-0.0399	0.0077	0.0720	0.2689
6	21.2866	-0.0215	-0.3446	0.0615	5.1443	8.5511
12	23.4442	-0.0392	-0.5905	0.0940	223.8296	311.2855
24	26.3645	-0.0470	-0.6753	0.0969	$> 1000.$	$> 1000.$
120	29.9676	-0.0033	-0.0456	0.0059	$> 1000.$	$> 1000.$
∞	29.9734	-0.0029	-0.0395	0.0051	$> 1000.$	$> 1000.$
Time	Case 2					
(hours)	θ_0	θ_{den}	θ_{thk}	θ_{con}	$\sum \theta_i$	$\sum \lvert\theta_i\rvert$
1	21.4323	-0.0210	-0.4113	0.0964	$> 1000.$	$> 1000.$
2	25.1049	-0.0508	-1.0112	0.2406	$> 1000.$	$> 1000.$
6	29.5986	-0.0204	-0.4077	0.0974	∞	∞
12	29.9906	-0.0015	-0.0304	0.0073	∞	∞
24	30.0000	-0.0000	-0.0001	0.0000	∞	∞
∞	30.0000	0.0000	0.0000	0.0000	∞	∞
Time	Case 3					
(hours)	θ_0	θ_{den}	θ_{thk}	θ_{con}	$\sum \theta_i$	$\sum \lvert\theta_i\rvert$
1	27.6470	-30.3422	-330.8660	11.7855	∞	∞
2	29.9723	$< -1000.$	$< -1000.$	$> 1000.$	∞	∞
6	30.0000	$< -1000.$	$< -1000.$	$< -1000.$	∞	∞
12	30.0000	$< -1000.$	$< -1000.$	$< -1000.$	∞	∞
∞	30.0000	$< -1000.$	$< -1000.$	$< -1000.$	∞	∞

Table C.8: Uncertainties: density 1%, thickness 10%, conductivity 5%.

Time	Case 1					
(hours)	θ_0	θ_{den}	θ_{thk}	θ_{con}	$\sum \theta_i$	$\sum \lvert\theta_i\rvert$
1	20.0172	-0.0005	-0.0195	0.0019	0.1771	0.6375
2	20.1009	-0.0028	-0.1058	0.0104	2.7197	6.5504
6	21.2866	-0.0264	-0.9424	0.0847	$> 1000.$	$> 1000.$
12	23.4442	-0.0552	-1.8134	0.1430	$> 1000.$	$> 1000.$
24	26.3645	-0.0908	-2.7997	0.1958	$> 1000.$	$> 1000.$
120	29.9676	-0.1865	-5.5477	0.3580	∞	∞
∞	29.9734	-0.1892	-5.6260	0.3624	∞	∞
Time	Case 2					
(hours)	θ_0	θ_{den}	θ_{thk}	θ_{con}	$\sum \theta_i$	$\sum \lvert\theta_i\rvert$
1	21.4323	-0.0430	-1.9612	0.2294	$> 1000.$	$> 1000.$
2	25.1049	-0.1449	-6.6999	0.7932	∞	∞
6	29.5986	-0.7066	-32.7478	3.8852	∞	∞
12	29.9906	-4.9903	-231.2975	27.4422	∞	∞
24	30.0000	-150.8759	$< -1000.$	829.6814	∞	∞
∞	30.0000	$< -1000.$	$< -1000.$	$> 1000.$	∞	∞
Time	Case 3					
(hours)	θ_0	θ_{den}	θ_{thk}	θ_{con}	$\sum \theta_i$	$\sum \lvert\theta_i\rvert$
1	27.6470	∞	∞	∞	∞	∞
2	29.9723	∞	∞	∞	∞	∞
6	30.0000	∞	∞	∞	∞	∞
12	30.0000	∞	∞	∞	∞	∞
∞	30.0000	∞	∞	∞	∞	∞

Table C.9: Uncertainties: density 1%, conductivity 10%.

Time	Case 1				
(hours)	θ_0	θ_{den}	θ_{con}	$\sum \theta_i$	$\sum \lvert\theta_i\rvert$
1	20.0172	-0.0004	0.0026	0.0024	0.0037
2	20.1009	-0.0023	0.0144	0.0140	0.0208
6	21.2866	-0.0208	0.1146	0.1517	0.2181
12	23.4442	-0.0370	0.1725	0.4279	0.6099
24	26.3645	-0.0424	0.1709	1.8235	2.5222
120	29.9676	-0.0020	0.0070	$> 1000.$	$> 1000.$
∞	29.9734	-0.0017	0.0060	$> 1000.$	$> 1000.$
Time	Case 2				
(hours)	θ_0	θ_{den}	θ_{con}	$\sum \theta_i$	$\sum \lvert\theta_i\rvert$
1	21.4323	-0.0189	0.1668	0.1933	0.2613
2	25.1049	-0.0443	0.4023	0.6107	0.8062
6	29.5986	-0.0140	0.1278	1.1608	1.5718
12	29.9906	-0.0007	0.0064	1.6951	2.3113
24	30.0000	-0.0000	0.0000	3.3299	4.5371
∞	30.0000	0.0000	0.0000	12.5433	17.0770
Time	Case 3				
(hours)	θ_0	θ_{den}	θ_{con}	$\sum \theta_i$	$\sum \lvert\theta_i\rvert$
1	27.6470	-0.0252	0.0308	∞	∞
2	29.9723	-0.0021	0.0020	∞	∞
6	30.0000	0.0000	-0.0000	∞	∞
12	30.0000	0.0000	-0.0000	∞	∞
∞	30.0000	0.0000	0.0000	∞	∞

Table C.10: Uncertainties: density 1%, thickness 1%, conductivity 10%.

Time	Case 1					
(hours)	θ_0	θ_{den}	θ_{thk}	θ_{con}	$\sum \theta_i$	$\sum \lvert\theta_i\rvert$
1	20.0172	-0.0004	-0.0014	0.0027	0.0020	0.0071
2	20.1009	-0.0023	-0.0075	0.0144	0.0130	0.0404
6	21.2866	-0.0208	-0.0647	0.1150	0.2278	0.4893
12	23.4442	-0.0372	-0.1092	0.1734	1.1945	1.9793
24	26.3645	-0.0428	-0.1202	0.1725	13.8112	19.9421
120	29.9676	-0.0021	-0.0057	0.0074	$> 1000.$	$> 1000.$
∞	29.9734	-0.0018	-0.0048	0.0063	$> 1000.$	$> 1000.$
Time	Case 2					
(hours)	θ_0	θ_{den}	θ_{thk}	θ_{con}	$\sum \theta_i$	$\sum \lvert\theta_i\rvert$
1	21.4323	-0.0190	-0.0717	0.1680	0.3730	0.7660
2	25.1049	-0.0447	-0.1707	0.4061	2.3478	3.9945
6	29.5986	-0.0143	-0.0548	0.1310	186.0227	286.1891
12	29.9906	-0.0007	-0.0028	0.0067	$> 1000.$	$> 1000.$
24	30.0000	-0.0000	-0.0000	0.0000	$> 1000.$	$> 1000.$
∞	30.0000	0.0000	0.0000	0.0000	$> 1000.$	$> 1000.$
Time	Case 3					
(hours)	θ_0	θ_{den}	θ_{thk}	θ_{con}	$\sum \theta_i$	$\sum \lvert\theta_i\rvert$
1	27.6470	-0.0309	-0.0690	0.0358	∞	∞
2	29.9723	-0.0039	-0.0085	0.0035	∞	∞
6	30.0000	0.0000	0.0000	0.0000	∞	∞
12	30.0000	0.0000	0.0000	0.0000	∞	∞
∞	30.0000	0.0000	0.0000	0.0000	∞	∞

Table C.11: Uncertainties: density 1%, thickness 5%, conductivity 10%.

Time	Case 1					
(hours)	θ_0	θ_{den}	θ_{thk}	θ_{con}	$\sum \theta_i$	$\sum \lvert\theta_i\rvert$
1	20.0172	-0.0004	-0.0073	0.0029	0.0109	0.0552
2	20.1009	-0.0024	-0.0401	0.0155	0.1146	0.3589
6	21.2866	-0.0217	-0.3476	0.1239	8.6445	14.2236
12	23.4442	-0.0399	-0.6004	0.1905	544.9329	793.8455
24	26.3645	-0.0488	-0.6991	0.1996	$> 1000.$	$> 1000.$
120	29.9676	-0.0041	-0.0560	0.0145	$> 1000.$	$> 1000.$
∞	29.9734	-0.0035	-0.0489	0.0126	$> 1000.$	$> 1000.$
Time	Case 2					
(hours)	θ_0	θ_{den}	θ_{thk}	θ_{con}	$\sum \theta_i$	$\sum \lvert\theta_i\rvert$
1	21.4323	-0.0214	-0.4186	0.1962	$> 1000.$	$> 1000.$
2	25.1049	-0.0522	-1.0379	0.4936	$> 1000.$	$> 1000.$
6	29.5986	-0.0222	-0.4438	0.2119	∞	∞
12	29.9906	-0.0018	-0.0368	0.0176	∞	∞
24	30.0000	-0.0000	-0.0002	0.0001	∞	∞
∞	30.0000	0.0000	0.0000	0.0000	∞	∞
Time	Case 3					
(hours)	θ_0	θ_{den}	θ_{thk}	θ_{con}	$\sum \theta_i$	$\sum \lvert\theta_i\rvert$
1	27.6470	$< -1000.$	$< -1000.$	$< -1000.$	∞	∞
2	29.9723	$< -1000.$	$< -1000.$	$< -1000.$	∞	∞
6	30.0000	$< -1000.$	∞	$< -1000.$	∞	∞
12	30.0000	∞	∞	∞	∞	∞
∞	30.0000	∞	∞	∞	∞	∞

Table C.12: Uncertainties: density 1%, thickness 10%, conductivity 10%.

Time	Case 1					
(hours)	θ_0	θ_{den}	θ_{thk}	θ_{con}	$\sum \theta_i$	$\sum \lvert\theta_i\rvert$
1	20.0172	-0.0005	-0.0198	0.0039	0.2441	0.8597
2	20.1009	-0.0028	-0.1076	0.0210	3.9796	9.7003
6	21.2866	-0.0274	-0.9732	0.1737	$> 1000.$	$> 1000.$
12	23.4442	-0.0594	-1.9354	0.3011	$> 1000.$	$> 1000.$
24	26.3645	-0.1061	-3.2462	0.4460	$> 1000.$	$> 1000.$
120	29.9676	-0.5521	-16.3577	2.0915	∞	∞
∞	29.9734	-0.5850	-17.3284	2.2145	∞	∞
Time	Case 2					
(hours)	θ_0	θ_{den}	θ_{thk}	θ_{con}	$\sum \theta_i$	$\sum \lvert\theta_i\rvert$
1	21.4323	-0.0478	-2.1745	0.5077	$> 1000.$	$> 1000.$
2	25.1049	-0.1732	-7.9834	1.8860	∞	∞
6	29.5986	-1.4119	-65.2303	15.4377	∞	∞
12	29.9906	-23.4128	$< -1000.$	256.0038	∞	∞
24	30.0000	$< -1000.$	$< -1000.$	$> 1000.$	∞	∞
∞	30.0000	$< -1000.$	$< -1000.$	$< -1000.$	∞	∞
Time	Case 3					
(hours)	θ_0	θ_{den}	θ_{thk}	θ_{con}	$\sum \theta_i$	$\sum \lvert\theta_i\rvert$
1	27.6470	∞	∞	∞	∞	∞
2	29.9723	∞	∞	∞	∞	∞
6	30.0000	∞	∞	∞	∞	∞
12	30.0000	∞	∞	∞	∞	∞
∞	30.0000	∞	∞	∞	∞	∞

Table C.13: Uncertainties: density 1%.

Time	Case 1			
(hours)	θ_0	θ_{den}	$\sum \theta_i$	$\sum \lvert\theta_i\rvert$
1	20.0172	-0.0004	-0.0004	0.0004
2	20.1009	-0.0023	-0.0022	0.0024
6	21.2866	-0.0207	-0.0181	0.0234
12	23.4442	-0.0369	-0.0268	0.0469
24	26.3645	-0.0420	-0.0147	0.0694
120	29.9676	-0.0019	0.0393	0.0431
∞	29.9734	-0.0016	0.0382	0.0414

Time	Case 2			
(hours)	θ_0	θ_{den}	$\sum \theta_i$	$\sum \lvert\theta_i\rvert$
1	21.4323	-0.0189	-0.0181	0.0196
2	25.1049	-0.0442	-0.0412	0.0471
6	29.5986	-0.0138	-0.0105	0.0172
12	29.9906	-0.0007	-0.0003	0.0011
24	30.0000	-0.0000	0.0000	0.0000
∞	30.0000	0.0000	0.0000	0.0000

Time	Case 3			
(hours)	θ_0	θ_{den}	$\sum \theta_i$	$\sum \lvert\theta_i\rvert$
1	27.6470	-0.0223	-0.0199	0.0246
2	29.9723	-0.0015	-0.0010	0.0021
6	30.0000	0.0000	0.0000	0.0000
12	30.0000	0.0000	0.0000	0.0000
∞	30.0000	0.0000	0.0000	0.0000

Table C.14: Uncertainties: density 1%, thickness 1%.

Time	Case 1				
(hours)	θ_0	θ_{den}	θ_{thk}	$\sum \theta_i$	$\sum \lvert\theta_i\rvert$
1	20.0172	-0.0004	-0.0014	-0.0015	0.0024
2	20.1009	-0.0023	-0.0075	-0.0076	0.0133
6	21.2866	-0.0207	-0.0645	-0.0481	0.1337
12	23.4442	-0.0369	-0.1084	-0.0062	0.3210
24	26.3645	-0.0422	-0.1185	0.3844	0.8401
120	29.9676	-0.0019	-0.0053	$> 1000.$	$> 1000.$
∞	29.9734	-0.0017	-0.0045	$> 1000.$	$> 1000.$

Time	Case 2				
(hours)	θ_0	θ_{den}	θ_{thk}	$\sum \theta_i$	$\sum \lvert\theta_i\rvert$
1	21.4323	-0.0189	-0.0713	-0.0396	0.1745
2	25.1049	-0.0443	-0.1693	0.0499	0.6139
6	29.5986	-0.0140	-0.0535	2.4411	3.7712
12	29.9906	-0.0007	-0.0027	38.9170	57.5456
24	30.0000	-0.0000	-0.0000	$> 1000.$	$> 1000.$
∞	30.0000	0.0000	0.0000	$> 1000.$	$> 1000.$

Time	Case 3				
(hours)	θ_0	θ_{den}	θ_{thk}	$\sum \theta_i$	$\sum \lvert\theta_i\rvert$
1	27.6470	-0.0228	-0.0515	$> 1000.$	$> 1000.$
2	29.9723	-0.0016	-0.0036	$> 1000.$	$> 1000.$
6	30.0000	0.0000	0.0000	∞	∞
12	30.0000	0.0000	0.0000	∞	∞
∞	30.0000	0.0000	0.0000	∞	∞

Table C.15: Uncertainties: density 1%, thickness 5%.

Time	Case 1				
(hours)	θ_0	θ_{den}	θ_{thk}	$\sum \theta_i$	$\sum \lvert\theta_i\rvert$
1	20.0172	-0.0004	-0.0073	0.0019	0.0320
2	20.1009	-0.0024	-0.0398	0.0361	0.1970
6	21.2866	-0.0213	-0.3421	2.9470	5.1326
12	23.4442	-0.0386	-0.5823	96.6809	129.0629
24	26.3645	-0.0456	-0.6561	$> 1000.$	$> 1000.$
120	29.9676	-0.0028	-0.0386	$> 1000.$	$> 1000.$
∞	29.9734	-0.0024	-0.0332	$> 1000.$	$> 1000.$
Time	Case 2				
(hours)	θ_0	θ_{den}	θ_{thk}	$\sum \theta_i$	$\sum \lvert\theta_i\rvert$
1	21.4323	-0.0206	-0.4051	$> 1000.$	$> 1000.$
2	25.1049	-0.0497	-0.9887	$> 1000.$	$> 1000.$
6	29.5986	-0.0190	-0.3795	∞	∞
12	29.9906	-0.0013	-0.0260	∞	∞
24	30.0000	-0.0000	-0.0001	∞	∞
∞	30.0000	0.0000	0.0000	∞	∞
Time	Case 3				
(hours)	θ_0	θ_{den}	θ_{thk}	$\sum \theta_i$	$\sum \lvert\theta_i\rvert$
1	27.6470	-0.3509	-3.8670	∞	∞
2	29.9723	-3.8205	-41.9919	∞	∞
6	30.0000	$< -1000.$	$< -1000.$	∞	∞
12	30.0000	$< -1000.$	$< -1000.$	∞	∞
∞	30.0000	$< -1000.$	$< -1000.$	∞	∞

Table C.16: Uncertainties: density 1%, thickness 10%.

Time	Case 1				
(hours)	θ_0	θ_{den}	θ_{thk}	$\sum \theta_i$	$\sum \lvert\theta_i\rvert$
1	20.0172	-0.0005	-0.0192	0.1275	0.4755
2	20.1009	-0.0027	-0.1041	1.8777	4.5117
6	21.2866	-0.0255	-0.9156	$> 1000.$	$> 1000.$
12	23.4442	-0.0517	-1.7119	$> 1000.$	$> 1000.$
24	26.3645	-0.0791	-2.4611	$> 1000.$	$> 1000.$
120	29.9676	-0.0721	-2.1488	∞	∞
∞	29.9734	-0.0702	-2.0888	∞	∞
Time	Case 2				
(hours)	θ_0	θ_{den}	θ_{thk}	$\sum \theta_i$	$\sum \lvert\theta_i\rvert$
1	21.4323	-0.0393	-1.7935	$> 1000.$	$> 1000.$
2	25.1049	-0.1246	-5.7743	∞	∞
6	29.5986	-0.3940	-18.3106	∞	∞
12	29.9906	-1.3281	-61.7282	∞	∞
24	30.0000	-11.0681	-514.4369	∞	∞
∞	30.0000	-482.8711	$< -1000.$	∞	∞
Time	Case 3				
(hours)	θ_0	θ_{den}	θ_{thk}	$\sum \theta_i$	$\sum \lvert\theta_i\rvert$
1	27.6470	∞	∞	∞	∞
2	29.9723	∞	∞	∞	∞
6	30.0000	∞	∞	∞	∞
12	30.0000	∞	∞	∞	∞
∞	30.0000	∞	∞	∞	∞

Table C.17: Uncertainties: density 5%, conductivity 1%.

Time	Case 1				
(hours)	θ_0	θ_{den}	θ_{con}	$\sum \theta_i$	$\sum \lvert\theta_i\rvert$
1	20.0172	-0.0021	0.0003	-0.0013	0.0030
2	20.1009	-0.0116	0.0014	-0.0061	0.0173
6	21.2866	-0.1043	0.0115	0.0078	0.2193
12	23.4442	-0.1867	0.0174	0.4153	0.8023
24	26.3645	-0.2156	0.0173	4.6671	5.2091
120	29.9676	-0.0109	0.0008	$> 1000.$	$> 1000.$
∞	29.9734	-0.0093	0.0006	$> 1000.$	$> 1000.$
Time	Case 2				
(hours)	θ_0	θ_{den}	θ_{con}	$\sum \theta_i$	$\sum \lvert\theta_i\rvert$
1	21.4323	-0.0945	0.0167	-0.0519	0.1388
2	25.1049	-0.2213	0.0402	-0.0664	0.3817
6	29.5986	-0.0696	0.0127	0.1908	0.3404
12	29.9906	-0.0035	0.0006	0.1038	0.1152
24	30.0000	-0.0000	0.0000	0.0125	0.0130
∞	30.0000	0.0000	0.0000	0.0002	0.0002
Time	Case 3				
(hours)	θ_0	θ_{den}	θ_{con}	$\sum \theta_i$	$\sum \lvert\theta_i\rvert$
1	27.6470	-0.1117	0.0028	0.8079	1.3077
2	29.9723	-0.0077	0.0001	9.9101	12.8592
6	30.0000	0.0000	0.0000	$> 1000.$	$> 1000.$
12	30.0000	0.0000	0.0000	$> 1000.$	$> 1000.$
∞	30.0000	0.0000	0.0000	$> 1000.$	$> 1000.$

Table C.18: Uncertainties: density 5%, thickness 1%, conductivity 1%.

Time	Case 1					
(hours)	θ_0	θ_{den}	θ_{thk}	θ_{con}	$\sum \theta_i$	$\sum \lvert\theta_i\rvert$
1	20.0172	-0.0021	-0.0014	0.0003	-0.0018	0.0059
2	20.1009	-0.0116	-0.0075	0.0014	-0.0079	0.0341
6	21.2866	-0.1047	-0.0650	0.0115	0.0874	0.4690
12	23.4442	-0.1879	-0.1102	0.0175	1.3950	2.2300
24	26.3645	-0.2183	-0.1224	0.0175	24.8164	28.9674
120	29.9676	-0.0115	-0.0062	0.0008	$> 1000.$	$> 1000.$
∞	29.9734	-0.0099	-0.0053	0.0007	$> 1000.$	$> 1000.$
Time	Case 2					
(hours)	θ_0	θ_{den}	θ_{thk}	θ_{con}	$\sum \theta_i$	$\sum \lvert\theta_i\rvert$
1	21.4323	-0.0949	-0.0716	0.0168	0.0117	0.4293
2	25.1049	-0.2227	-0.1702	0.0405	0.6433	1.8376
6	29.5986	-0.0709	-0.0544	0.0130	28.1880	39.2674
12	29.9906	-0.0036	-0.0028	0.0007	$> 1000.$	$> 1000.$
24	30.0000	-0.0000	-0.0000	0.0000	$> 1000.$	$> 1000.$
∞	30.0000	0.0000	0.0000	0.0000	$> 1000.$	$> 1000.$
Time	Case 3					
(hours)	θ_0	θ_{den}	θ_{thk}	θ_{con}	$\sum \theta_i$	$\sum \lvert\theta_i\rvert$
1	27.6470	-0.1170	-0.0527	0.0029	$> 1000.$	$> 1000.$
2	29.9723	-0.0087	-0.0038	0.0002	$> 1000.$	$> 1000.$
6	30.0000	0.0000	0.0000	0.0000	∞	∞
12	30.0000	0.0000	0.0000	0.0000	∞	∞
∞	30.0000	0.0000	0.0000	0.0000	∞	∞

Table C.19: Uncertainties: density 5%, thickness 5%, conductivity 1%.

Time	Case 1					
(hours)	θ_0	θ_{den}	θ_{thk}	θ_{con}	$\sum \theta_i$	$\sum \lvert\theta_i\rvert$
1	20.0172	-0.0022	-0.0074	0.0003	0.0060	0.0462
2	20.1009	-0.0120	-0.0403	0.0015	0.0793	0.3002
6	21.2866	-0.1093	-0.3497	0.0124	7.1532	11.2897
12	23.4442	-0.2021	-0.6070	0.0192	396.9647	536.9802
24	26.3645	-0.2499	-0.7153	0.0203	$> 1000.$	$> 1000.$
120	29.9676	-0.0234	-0.0645	0.0017	$> 1000.$	$> 1000.$
∞	29.9734	-0.0205	-0.0565	0.0015	$> 1000.$	$> 1000.$
Time	Case 2					
(hours)	θ_0	θ_{den}	θ_{thk}	θ_{con}	$\sum \theta_i$	$\sum \lvert\theta_i\rvert$
1	21.4323	-0.1050	-0.4119	0.0193	$> 1000.$	$> 1000.$
2	25.1049	-0.2548	-1.0135	0.0482	$> 1000.$	$> 1000.$
6	29.5986	-0.1029	-0.4108	0.0196	∞	∞
12	29.9906	-0.0077	-0.0309	0.0015	∞	∞
24	30.0000	-0.0000	-0.0001	0.0000	∞	∞
∞	30.0000	0.0000	0.0000	0.0000	∞	∞
Time	Case 3					
(hours)	θ_0	θ_{den}	θ_{thk}	θ_{con}	$\sum \theta_i$	$\sum \lvert\theta_i\rvert$
1	27.6470	-4.2298	-9.2977	0.0728	∞	∞
2	29.9723	-170.2542	-373.8277	2.8887	∞	∞
6	30.0000	$< -1000.$	$< -1000.$	$> 1000.$	∞	∞
12	30.0000	$< -1000.$	$< -1000.$	$< -1000.$	∞	∞
∞	30.0000	$< -1000.$	$< -1000.$	$< -1000.$	∞	∞

Table C.20: Uncertainties: density 5%, thickness 10%, conductivity 1%.

Time	Case 1					
(hours)	θ_0	θ_{den}	θ_{thk}	θ_{con}	$\sum \theta_i$	$\sum \lvert\theta_i\rvert$
1	20.0172	-0.0026	-0.0198	0.0004	0.1866	0.6452
2	20.1009	-0.0141	-0.1074	0.0021	2.8737	6.7171
6	21.2866	-0.1362	-0.9692	0.0173	$> 1000.$	$> 1000.$
12	23.4442	-0.2940	-1.9190	0.0299	$> 1000.$	$> 1000.$
24	26.3645	-0.5199	-3.1836	0.0438	$> 1000.$	$> 1000.$
120	29.9676	-2.3948	-14.1917	0.1817	∞	∞
∞	29.9734	-2.5233	-14.9485	0.1913	∞	∞
Time	Case 2					
(hours)	θ_0	θ_{den}	θ_{thk}	θ_{con}	$\sum \theta_i$	$\sum \lvert\theta_i\rvert$
1	21.4323	-0.2117	-1.9296	0.0452	$> 1000.$	$> 1000.$
2	25.1049	-0.7049	-6.5199	0.1544	∞	∞
6	29.5986	-3.1732	-29.4288	0.6986	∞	∞
12	29.9906	-19.5905	-181.6927	4.3132	∞	∞
24	30.0000	-469.3584	$< -1000.$	103.3371	∞	∞
∞	30.0000	$< -1000.$	$< -1000.$	$> 1000.$	∞	∞
Time	Case 3					
(hours)	θ_0	θ_{den}	θ_{thk}	θ_{con}	$\sum \theta_i$	$\sum \lvert\theta_i\rvert$
1	27.6470	∞	∞	∞	∞	∞
2	29.9723	∞	∞	∞	∞	∞
6	30.0000	∞	∞	∞	∞	∞
12	30.0000	∞	∞	∞	∞	∞
∞	30.0000	∞	∞	∞	∞	∞

Table C.21: Uncertainties: density 5%, conductivity 5%.

Time	Case 1				
(hours)	θ_0	θ_{den}	θ_{con}	$\sum \theta_i$	$\sum \lvert\theta_i\rvert$
1	20.0172	-0.0021	0.0013	0.0000	0.0046
2	20.1009	-0.0116	0.0072	0.0018	0.0267
6	21.2866	-0.1046	0.0576	0.1260	0.3560
12	23.4442	-0.1876	0.0871	1.0678	1.5631
24	26.3645	-0.2177	0.0872	14.9810	16.9449
120	29.9676	-0.0114	0.0040	$> 1000.$	$> 1000.$
∞	29.9734	-0.0097	0.0034	$> 1000.$	$> 1000.$
Time	Case 2				
(hours)	θ_0	θ_{den}	θ_{con}	$\sum \theta_i$	$\sum \lvert\theta_i\rvert$
1	21.4323	-0.0946	0.0835	0.0471	0.2515
2	25.1049	-0.2218	0.2014	0.2724	0.7679
6	29.5986	-0.0702	0.0642	1.1119	1.4277
12	29.9906	-0.0035	0.0032	1.6441	1.9080
24	30.0000	-0.0000	0.0000	2.6977	3.1182
∞	30.0000	0.0000	0.0000	7.0657	8.1648
Time	Case 3				
(hours)	θ_0	θ_{den}	θ_{con}	$\sum \theta_i$	$\sum \lvert\theta_i\rvert$
1	27.6470	-0.1158	0.0145	$> 1000.$	$> 1000.$
2	29.9723	-0.0085	0.0008	$> 1000.$	$> 1000.$
6	30.0000	0.0000	0.0000	∞	∞
12	30.0000	0.0000	0.0000	∞	∞
∞	30.0000	0.0000	0.0000	∞	∞

Table C.22: Uncertainties: density 5%, thickness 1%, conductivity 5%.

Time	Case 1					
(hours)	θ_0	θ_{den}	θ_{thk}	θ_{con}	$\sum \theta_i$	$\sum \lvert\theta_i\rvert$
1	20.0172	-0.0021	-0.0014	0.0013	-0.0003	0.0081
2	20.1009	-0.0116	-0.0076	0.0072	0.0021	0.0477
6	21.2866	-0.1050	-0.0652	0.0579	0.2801	0.7134
12	23.4442	-0.1891	-0.1108	0.0877	3.0391	4.3052
24	26.3645	-0.2211	-0.1239	0.0884	83.8296	101.4945
120	29.9676	-0.0123	-0.0067	0.0043	$> 1000.$	$> 1000.$
∞	29.9734	-0.0106	-0.0057	0.0037	$> 1000.$	$> 1000.$
Time	Case 2					
(hours)	θ_0	θ_{den}	θ_{thk}	θ_{con}	$\sum \theta_i$	$\sum \lvert\theta_i\rvert$
1	21.4323	-0.0952	-0.0718	0.0841	0.2090	0.7068
2	25.1049	-0.2237	-0.1709	0.2033	1.8734	3.5768
6	29.5986	-0.0718	-0.0551	0.0658	150.3908	213.7605
12	29.9906	-0.0037	-0.0028	0.0034	$> 1000.$	$> 1000.$
24	30.0000	-0.0000	-0.0000	0.0000	$> 1000.$	$> 1000.$
∞	30.0000	0.0000	0.0000	0.0000	$> 1000.$	$> 1000.$
Time	Case 3					
(hours)	θ_0	θ_{den}	θ_{thk}	θ_{con}	$\sum \theta_i$	$\sum \lvert\theta_i\rvert$
1	27.6470	-0.1289	-0.0579	0.0157	∞	∞
2	29.9723	-0.0115	-0.0050	0.0011	∞	∞
6	30.0000	0.0000	0.0000	0.0000	∞	∞
12	30.0000	0.0000	0.0000	0.0000	∞	∞
∞	30.0000	0.0000	0.0000	0.0000	∞	∞

Table C.23: Uncertainties: density 5%, thickness 5%, conductivity 5%.

Time	Case 1					
(hours)	θ_0	θ_{den}	θ_{thk}	θ_{con}	$\sum\theta_i$	$\sum\lvert\theta_i\rvert$
1	20.0172	-0.0022	-0.0074	0.0014	0.0102	0.0570
2	20.1009	-0.0121	-0.0404	0.0078	0.1181	0.3786
6	21.2866	-0.1104	-0.3527	0.0626	10.8218	16.9711
12	23.4442	-0.2059	-0.6172	0.0973	818.0381	$> 1000.$
24	26.3645	-0.2593	-0.7406	0.1048	$> 1000.$	$> 1000.$
120	29.9676	-0.0292	-0.0801	0.0103	$> 1000.$	$> 1000.$
∞	29.9734	-0.0258	-0.0709	0.0091	∞	∞
Time	Case 2					
(hours)	θ_0	θ_{den}	θ_{thk}	θ_{con}	$\sum\theta_i$	$\sum\lvert\theta_i\rvert$
1	21.4323	-0.1065	-0.4178	0.0979	$> 1000.$	$> 1000.$
2	25.1049	-0.2602	-1.0349	0.2461	$> 1000.$	$> 1000.$
6	29.5986	-0.1101	-0.4396	0.1049	∞	∞
12	29.9906	-0.0090	-0.0360	0.0086	∞	∞
24	30.0000	-0.0000	-0.0002	0.0000	∞	∞
∞	30.0000	0.0000	0.0000	0.0000	∞	∞
Time	Case 3					
(hours)	θ_0	θ_{den}	θ_{thk}	θ_{con}	$\sum\theta_i$	$\sum\lvert\theta_i\rvert$
1	27.6470	-299.6561	-652.3724	22.7209	∞	∞
2	29.9723	$< -1000.$	$< -1000.$	$> 1000.$	∞	∞
6	30.0000	$< -1000.$	$< -1000.$	$< -1000.$	∞	∞
12	30.0000	$< -1000.$	$< -1000.$	$< -1000.$	∞	∞
∞	30.0000	$< -1000.$	$< -1000.$	$< -1000.$	∞	∞

Table C.24: Uncertainties: density 5%, thickness 10%, conductivity 5%.

Time	Case 1					
(hours)	θ_0	θ_{den}	θ_{thk}	θ_{con}	$\sum\theta_i$	$\sum\lvert\theta_i\rvert$
1	20.0172	-0.0026	-0.0200	0.0020	0.2413	0.8196
2	20.1009	-0.0144	-0.1090	0.0106	3.8923	9.1743
6	21.2866	-0.1407	-0.9967	0.0885	$> 1000.$	$> 1000.$
12	23.4442	-0.3134	-2.0318	0.1565	$> 1000.$	$> 1000.$
24	26.3645	-0.5970	-3.6299	0.2462	$> 1000.$	$> 1000.$
120	29.9676	-6.2197	-36.7309	2.3306	∞	∞
∞	29.9734	-6.7980	-40.1433	2.5465	∞	∞
Time	Case 2					
(hours)	θ_0	θ_{den}	θ_{thk}	θ_{con}	$\sum\theta_i$	$\sum\lvert\theta_i\rvert$
1	21.4323	-0.2296	-2.0889	0.2440	$> 1000.$	$> 1000.$
2	25.1049	-0.8076	-7.4541	0.8813	∞	∞
6	29.5986	-5.3829	-49.7998	5.8989	∞	∞
12	29.9906	-64.0725	-592.7786	70.2173	∞	∞
24	30.0000	$< -1000.$	$< -1000.$	$> 1000.$	∞	∞
∞	30.0000	$< -1000.$	$< -1000.$	$< -1000.$	∞	∞
Time	Case 3					
(hours)	θ_0	θ_{den}	θ_{thk}	θ_{con}	$\sum\theta_i$	$\sum\lvert\theta_i\rvert$
1	27.6470	∞	∞	∞	∞	∞
2	29.9723	∞	∞	∞	∞	∞
6	30.0000	∞	∞	∞	∞	∞
12	30.0000	∞	∞	∞	∞	∞
∞	30.0000	∞	∞	∞	∞	∞

Table C.25: Uncertainties: density 5%, conductivity 10%.

Time	Case 1				
(hours)	θ_0	θ_{den}	θ_{con}	$\sum \theta_i$	$\sum \lvert\theta_i\rvert$
1	20.0172	-0.0021	0.0027	0.0017	0.0068
2	20.1009	-0.0116	0.0144	0.0122	0.0401
6	21.2866	-0.1050	0.1155	0.3140	0.5880
12	23.4442	-0.1890	0.1750	2.5355	3.3778
24	26.3645	-0.2207	0.1764	60.6709	72.0456
120	29.9676	-0.0122	0.0086	$> 1000.$	$> 1000.$
∞	29.9734	-0.0105	0.0073	$> 1000.$	$> 1000.$
Time	Case 2				
(hours)	θ_0	θ_{den}	θ_{con}	$\sum \theta_i$	$\sum \lvert\theta_i\rvert$
1	21.4323	-0.0949	0.1674	0.1947	0.4341
2	25.1049	-0.2227	0.4043	0.8851	1.5252
6	29.5986	-0.0711	0.1299	6.2125	7.8894
12	29.9906	-0.0036	0.0066	50.2984	62.8281
24	30.0000	-0.0000	0.0000	$> 1000.$	$> 1000.$
∞	30.0000	0.0000	0.0000	$> 1000.$	$> 1000.$
Time	Case 3				
(hours)	θ_0	θ_{den}	θ_{con}	$\sum \theta_i$	$\sum \lvert\theta_i\rvert$
1	27.6470	-0.1282	0.0312	∞	∞
2	29.9723	-0.0113	0.0021	∞	∞
6	30.0000	0.0000	-0.0000	∞	∞
12	30.0000	0.0000	-0.0000	∞	∞
∞	30.0000	0.0000	0.0000	∞	∞

Table C.26: Uncertainties: density 5%, thickness 1%, conductivity 10%.

Time	Case 1					
(hours)	θ_0	θ_{den}	θ_{thk}	θ_{con}	$\sum \theta_i$	$\sum \lvert\theta_i\rvert$
1	20.0172	-0.0021	-0.0014	0.0027	0.0018	0.0114
2	20.1009	-0.0117	-0.0076	0.0145	0.0157	0.0675
6	21.2866	-0.1056	-0.0655	0.1161	0.5994	1.1421
12	23.4442	-0.1909	-0.1118	0.1766	7.0101	9.5606
24	26.3645	-0.2252	-0.1261	0.1795	381.2774	485.2646
120	29.9676	-0.0136	-0.0073	0.0095	$> 1000.$	$> 1000.$
∞	29.9734	-0.0117	-0.0063	0.0081	$> 1000.$	$> 1000.$
Time	Case 2					
(hours)	θ_0	θ_{den}	θ_{thk}	θ_{con}	$\sum \theta_i$	$\sum \lvert\theta_i\rvert$
1	21.4323	-0.0956	-0.0721	0.1689	0.5403	1.2025
2	25.1049	-0.2252	-0.1721	0.4093	4.6611	7.7165
6	29.5986	-0.0734	-0.0562	0.1343	$> 1000.$	$> 1000.$
12	29.9906	-0.0039	-0.0030	0.0071	$> 1000.$	$> 1000.$
24	30.0000	-0.0000	-0.0000	0.0000	$> 1000.$	$> 1000.$
∞	30.0000	0.0000	0.0000	0.0000	$> 1000.$	$> 1000.$
Time	Case 3					
(hours)	θ_0	θ_{den}	θ_{thk}	θ_{con}	$\sum \theta_i$	$\sum \lvert\theta_i\rvert$
1	27.6470	-0.1599	-0.0714	0.0367	∞	∞
2	29.9723	-0.0216	-0.0094	0.0039	∞	∞
6	30.0000	-0.0000	0.0000	0.0000	∞	∞
12	30.0000	0.0000	0.0000	0.0000	∞	∞
∞	30.0000	0.0000	0.0000	0.0000	∞	∞

Table C.27: Uncertainties: density 5%, thickness 5%, conductivity 10%.

Time	Case 1					
(hours)	θ_0	θ_{den}	θ_{thk}	θ_{con}	$\sum \theta_i$	$\sum \lvert\theta_i\rvert$
1	20.0172	-0.0022	-0.0074	0.0029	0.0161	0.0729
2	20.1009	-0.0122	-0.0407	0.0156	0.1750	0.4989
6	21.2866	-0.1119	-0.3570	0.1265	17.9095	28.3466
12	23.4442	-0.2112	-0.6318	0.1982	$> 1000.$	$> 1000.$
24	26.3645	-0.2732	-0.7780	0.2185	$> 1000.$	$> 1000.$
120	29.9676	-0.0402	-0.1101	0.0280	∞	∞
∞	29.9734	-0.0360	-0.0987	0.0251	∞	∞
Time	Case 2					
(hours)	θ_0	θ_{den}	θ_{thk}	θ_{con}	$\sum \theta_i$	$\sum \lvert\theta_i\rvert$
1	21.4323	-0.1087	-0.4261	0.1996	$> 1000.$	$> 1000.$
2	25.1049	-0.2681	-1.0658	0.5067	$> 1000.$	$> 1000.$
6	29.5986	-0.1215	-0.4846	0.2312	∞	∞
12	29.9906	-0.0113	-0.0450	0.0215	∞	∞
24	30.0000	-0.0001	-0.0003	0.0002	∞	∞
∞	30.0000	0.0000	0.0000	0.0000	∞	∞
Time	Case 3					
(hours)	θ_0	θ_{den}	θ_{thk}	θ_{con}	$\sum \theta_i$	$\sum \lvert\theta_i\rvert$
1	27.6470	$< -1000.$	$< -1000.$	$< -1000.$	∞	∞
2	29.9723	$< -1000.$	$< -1000.$	$< -1000.$	∞	∞
6	30.0000	∞	∞	∞	∞	∞
12	30.0000	∞	∞	∞	∞	∞
∞	30.0000	∞	∞	∞	∞	∞

Table C.28: Uncertainties: density 5%, thickness 10%, conductivity 10%.

Time	Case 1					
(hours)	θ_0	θ_{den}	θ_{thk}	θ_{con}	$\sum \theta_i$	$\sum \lvert\theta_i\rvert$
1	20.0172	-0.0027	-0.0204	0.0040	0.3331	1.1153
2	20.1009	-0.0147	-0.1113	0.0216	5.7833	13.8758
6	21.2866	-0.1471	-1.0357	0.1823	$> 1000.$	$> 1000.$
12	23.4442	-0.3422	-2.1992	0.3333	$> 1000.$	$> 1000.$
24	26.3645	-0.7243	-4.3637	0.5801	$> 1000.$	$> 1000.$
120	29.9676	-23.3132	-136.9727	17.1700	∞	∞
∞	29.9734	-26.7727	-157.2959	19.7166	∞	∞
Time	Case 2					
(hours)	θ_0	θ_{den}	θ_{thk}	θ_{con}	$\sum \theta_i$	$\sum \lvert\theta_i\rvert$
1	21.4323	-0.2578	-2.3398	0.5456	$> 1000.$	$> 1000.$
2	25.1049	-0.9848	-9.0611	2.1371	∞	∞
6	29.5986	-11.6417	-107.3292	25.3544	∞	∞
12	29.9906	-352.8982	$< -1000.$	768.5956	∞	∞
24	30.0000	$< -1000.$	$< -1000.$	$> 1000.$	∞	∞
∞	30.0000	$< -1000.$	$< -1000.$	$< -1000.$	∞	∞
Time	Case 3					
(hours)	θ_0	θ_{den}	θ_{thk}	θ_{con}	$\sum \theta_i$	$\sum \lvert\theta_i\rvert$
1	27.6470	∞	∞	∞	∞	∞
2	29.9723	∞	∞	∞	∞	∞
6	30.0000	∞	∞	∞	∞	∞
12	30.0000	∞	∞	∞	∞	∞
∞	30.0000	∞	∞	∞	∞	∞

Table C.29: Uncertainties: density 5%.

Time	Case 1			
(hours)	θ_0	θ_{den}	$\sum \theta_i$	$\sum \lvert\theta_i\rvert$
1	20.0172	-0.0021	-0.0016	0.0026
2	20.1009	-0.0116	-0.0080	0.0152
6	21.2866	-0.1043	-0.0180	0.1905
12	23.4442	-0.1865	0.2979	0.6709
24	26.3645	-0.2151	3.4302	3.8605
120	29.9676	-0.0107	$> 1000.$	$> 1000.$
∞	29.9734	-0.0092	$> 1000.$	$> 1000.$
Time	Case 2			
(hours)	θ_0	θ_{den}	$\sum \theta_i$	$\sum \lvert\theta_i\rvert$
1	21.4323	-0.0944	-0.0744	0.1145
2	25.1049	-0.2212	-0.1360	0.3064
6	29.5986	-0.0695	0.0917	0.2308
12	29.9906	-0.0035	0.0495	0.0564
24	30.0000	-0.0000	0.0033	0.0033
∞	30.0000	0.0000	0.0000	0.0000
Time	Case 3			
(hours)	θ_0	θ_{den}	$\sum \theta_i$	$\sum \lvert\theta_i\rvert$
1	27.6470	-0.1114	-0.0202	0.2026
2	29.9723	-0.0076	0.0389	0.0541
6	30.0000	0.0000	0.0003	0.0003
12	30.0000	0.0000	0.0000	0.0000
∞	30.0000	0.0000	0.0000	0.0000

Table C.30: Uncertainties: density 5%, thickness 1%.

Time	Case 1				
(hours)	θ_0	θ_{den}	θ_{thk}	$\sum \theta_i$	$\sum \lvert\theta_i\rvert$
1	20.0172	-0.0021	-0.0014	-0.0022	0.0053
2	20.1009	-0.0116	-0.0075	-0.0103	0.0309
6	21.2866	-0.1046	-0.0650	0.0462	0.4185
12	23.4442	-0.1877	-0.1100	1.1115	1.8834
24	26.3645	-0.2176	-0.1221	18.2545	21.1716
120	29.9676	-0.0114	-0.0061	$> 1000.$	$> 1000.$
∞	29.9734	-0.0097	-0.0052	$> 1000.$	$> 1000.$
Time	Case 2				
(hours)	θ_0	θ_{den}	θ_{thk}	$\sum \theta_i$	$\sum \lvert\theta_i\rvert$
1	21.4323	-0.0948	-0.0715	-0.0306	0.3721
2	25.1049	-0.2225	-0.1701	0.4194	1.5314
6	29.5986	-0.0707	-0.0542	18.4662	25.6670
12	29.9906	-0.0036	-0.0027	$> 1000.$	$> 1000.$
24	30.0000	-0.0000	-0.0000	$> 1000.$	$> 1000.$
∞	30.0000	0.0000	0.0000	$> 1000.$	$> 1000.$
Time	Case 3				
(hours)	θ_0	θ_{den}	θ_{thk}	$\sum \theta_i$	$\sum \lvert\theta_i\rvert$
1	27.6470	-0.1152	-0.0519	$> 1000.$	$> 1000.$
2	29.9723	-0.0084	-0.0037	$> 1000.$	$> 1000.$
6	30.0000	0.0000	0.0000	∞	∞
12	30.0000	0.0000	0.0000	∞	∞
∞	30.0000	0.0000	0.0000	∞	∞

Table C.31: Uncertainties: density 5%, thickness 5%.

Time	Case 1				
(hours)	θ_0	θ_{den}	θ_{thk}	$\sum \theta_i$	$\sum \lvert\theta_i\rvert$
1	20.0172	-0.0022	-0.0073	0.0049	0.0438
2	20.1009	-0.0120	-0.0402	0.0705	0.2827
6	21.2866	-0.1091	-0.3489	6.4321	10.1959
12	23.4442	-0.2012	-0.6047	332.7754	446.4390
24	26.3645	-0.2477	-0.7096	$> 1000.$	$> 1000.$
120	29.9676	-0.0223	-0.0613	$> 1000.$	$> 1000.$
∞	29.9734	-0.0195	-0.0537	$> 1000.$	$> 1000.$
Time	Case 2				
(hours)	θ_0	θ_{den}	θ_{thk}	$\sum \theta_i$	$\sum \lvert\theta_i\rvert$
1	21.4323	-0.1047	-0.4106	$> 1000.$	$> 1000.$
2	25.1049	-0.2535	-1.0086	$> 1000.$	$> 1000.$
6	29.5986	-0.1013	-0.4044	∞	∞
12	29.9906	-0.0075	-0.0299	∞	∞
24	30.0000	-0.0000	-0.0001	∞	∞
∞	30.0000	0.0000	0.0000	∞	∞
Time	Case 3				
(hours)	θ_0	θ_{den}	θ_{thk}	$\sum \theta_i$	$\sum \lvert\theta_i\rvert$
1	27.6470	-2.2525	-4.9602	∞	∞
2	29.9723	-36.0187	-79.1535	∞	∞
6	30.0000	$< -1000.$	$< -1000.$	∞	∞
12	30.0000	$< -1000.$	$< -1000.$	∞	∞
∞	30.0000	$< -1000.$	$< -1000.$	∞	∞

Table C.32: Uncertainties: density 5%, thickness 10%.

Time	Case 1				
(hours)	θ_0	θ_{den}	θ_{thk}	$\sum \theta_i$	$\sum \lvert\theta_i\rvert$
1	20.0172	-0.0026	-0.0197	0.1748	0.6082
2	20.1009	-0.0140	-0.1070	2.6669	6.2264
6	21.2866	-0.1351	-0.9628	$> 1000.$	$> 1000.$
12	23.4442	-0.2897	-1.8934	$> 1000.$	$> 1000.$
24	26.3645	-0.5033	-3.0873	$> 1000.$	$> 1000.$
120	29.9676	-1.9128	-11.3493	∞	∞
∞	29.9734	-1.9977	-11.8503	∞	∞
Time	Case 2				
(hours)	θ_0	θ_{den}	θ_{thk}	$\sum \theta_i$	$\sum \lvert\theta_i\rvert$
1	21.4323	-0.2077	-1.8943	$> 1000.$	$> 1000.$
2	25.1049	-0.6831	-6.3220	∞	∞
6	29.5986	-2.8108	-26.0824	∞	∞
12	29.9906	-14.8952	-138.2261	∞	∞
24	30.0000	-273.7918	$< -1000.$	∞	∞
∞	30.0000	$< -1000.$	$< -1000.$	∞	∞
Time	Case 3				
(hours)	θ_0	θ_{den}	θ_{thk}	$\sum \theta_i$	$\sum \lvert\theta_i\rvert$
1	27.6470	∞	∞	∞	∞
2	29.9723	∞	∞	∞	∞
6	30.0000	∞	∞	∞	∞
12	30.0000	∞	∞	∞	∞
∞	30.0000	∞	∞	∞	∞

Table C.33: Uncertainties: density 10%, conductivity 1%.

Time	Case 1				
(hours)	θ_0	θ_{den}	θ_{con}	$\sum \theta_i$	$\sum \lvert\theta_i\rvert$
1	20.0172	-0.0042	0.0003	-0.0017	0.0069
2	20.1009	-0.0234	0.0015	-0.0053	0.0421
6	21.2866	-0.2129	0.0117	0.3387	0.7731
12	23.4442	-0.3880	0.0178	5.5218	6.3773
24	26.3645	-0.4652	0.0184	271.2383	275.7828
120	29.9676	-0.0325	0.0011	$> 1000.$	$> 1000.$
∞	29.9734	-0.0281	0.0010	$> 1000.$	$> 1000.$
Time	Case 2				
(hours)	θ_0	θ_{den}	θ_{con}	$\sum \theta_i$	$\sum \lvert\theta_i\rvert$
1	21.4323	-0.1897	0.0167	-0.0710	0.3123
2	25.1049	-0.4453	0.0404	0.0970	1.0011
6	29.5986	-0.1420	0.0130	2.3610	2.7052
12	29.9906	-0.0072	0.0007	6.8071	6.9859
24	30.0000	-0.0000	0.0000	38.2468	39.1642
∞	30.0000	0.0000	0.0000	$> 1000.$	$> 1000.$
Time	Case 3				
(hours)	θ_0	θ_{den}	θ_{con}	$\sum \theta_i$	$\sum \lvert\theta_i\rvert$
1	27.6470	-0.2245	0.0028	12.0114	15.1327
2	29.9723	-0.0156	0.0001	$> 1000.$	$> 1000.$
6	30.0000	0.0000	0.0000	$> 1000.$	$> 1000.$
12	30.0000	0.0000	0.0000	$> 1000.$	$> 1000.$
∞	30.0000	0.0000	0.0000	$> 1000.$	$> 1000.$

Table C.34: Uncertainties: density 10%, thickness 1%, conductivity 1%.

Time	Case 1					
(hours)	θ_0	θ_{den}	θ_{thk}	θ_{con}	$\sum \theta_i$	$\sum \lvert\theta_i\rvert$
1	20.0172	-0.0043	-0.0014	0.0003	-0.0016	0.0110
2	20.1009	-0.0235	-0.0076	0.0015	-0.0020	0.0674
6	21.2866	-0.2143	-0.0664	0.0117	0.6966	1.3726
12	23.4442	-0.3927	-0.1146	0.0180	12.8408	15.2029
24	26.3645	-0.4761	-0.1328	0.0188	$> 1000.$	$> 1000.$
120	29.9676	-0.0369	-0.0099	0.0013	$> 1000.$	$> 1000.$
∞	29.9734	-0.0321	-0.0086	0.0011	$> 1000.$	$> 1000.$
Time	Case 2					
(hours)	θ_0	θ_{den}	θ_{thk}	θ_{con}	$\sum \theta_i$	$\sum \lvert\theta_i\rvert$
1	21.4323	-0.1910	-0.0720	0.0169	0.1340	0.8183
2	25.1049	-0.4496	-0.1718	0.0409	2.2281	4.4106
6	29.5986	-0.1459	-0.0559	0.0134	290.2156	382.8534
12	29.9906	-0.0076	-0.0029	0.0007	$> 1000.$	$> 1000.$
24	30.0000	-0.0000	-0.0000	0.0000	$> 1000.$	$> 1000.$
∞	30.0000	0.0000	0.0000	0.0000	$> 1000.$	$> 1000.$
Time	Case 3					
(hours)	θ_0	θ_{den}	θ_{thk}	θ_{con}	$\sum \theta_i$	$\sum \lvert\theta_i\rvert$
1	27.6470	-0.2376	-0.0535	0.0030	$> 1000.$	$> 1000.$
2	29.9723	-0.0182	-0.0040	0.0002	∞	∞
6	30.0000	0.0000	0.0000	0.0000	∞	∞
12	30.0000	0.0000	0.0000	0.0000	∞	∞
∞	30.0000	0.0000	0.0000	0.0000	∞	∞

Table C.35: Uncertainties: density 10%, thickness 5%, conductivity 1%.

Time	Case 1					
(hours)	θ_0	θ_{den}	θ_{thk}	θ_{con}	$\sum \theta_i$	$\sum \lvert\theta_i\rvert$
1	20.0172	-0.0044	-0.0075	0.0003	0.0122	0.0656
2	20.1009	-0.0245	-0.0411	0.0016	0.1502	0.4533
6	21.2866	-0.2280	-0.3628	0.0128	17.5726	26.0916
12	23.4442	-0.4374	-0.6519	0.0203	$> 1000.$	$> 1000.$
24	26.3645	-0.5865	-0.8317	0.0231	$> 1000.$	$> 1000.$
120	29.9676	-0.1259	-0.1721	0.0043	∞	∞
∞	29.9734	-0.1150	-0.1572	0.0040	∞	∞
Time	Case 2					
(hours)	θ_0	θ_{den}	θ_{thk}	θ_{con}	$\sum \theta_i$	$\sum \lvert\theta_i\rvert$
1	21.4323	-0.2144	-0.4203	0.0197	$> 1000.$	$> 1000.$
2	25.1049	-0.5252	-1.0442	0.0497	$> 1000.$	$> 1000.$
6	29.5986	-0.2269	-0.4527	0.0216	∞	∞
12	29.9906	-0.0193	-0.0385	0.0018	∞	∞
24	30.0000	-0.0001	-0.0002	0.0000	∞	∞
∞	30.0000	0.0000	0.0000	0.0000	∞	∞
Time	Case 3					
(hours)	θ_0	θ_{den}	θ_{thk}	θ_{con}	$\sum \theta_i$	$\sum \lvert\theta_i\rvert$
1	27.6470	-12.9268	-14.1933	0.1098	∞	∞
2	29.9723	-938.8314	$< -1000.$	7.9033	∞	∞
6	30.0000	$< -1000.$	$< -1000.$	$> 1000.$	∞	∞
12	30.0000	$< -1000.$	$< -1000.$	$< -1000.$	∞	∞
∞	30.0000	$< -1000.$	$< -1000.$	$< -1000.$	∞	∞

Table C.36: Uncertainties: density 10%, thickness 10%, conductivity 1%.

Time	Case 1					
(hours)	θ_0	θ_{den}	θ_{thk}	θ_{con}	$\sum \theta_i$	$\sum \lvert\theta_i\rvert$
1	20.0172	-0.0054	-0.0205	0.0004	0.2717	0.8775
2	20.1009	-0.0296	-0.1120	0.0022	4.4543	10.1536
6	21.2866	-0.2982	-1.0483	0.0184	$> 1000.$	$> 1000.$
12	23.4442	-0.7038	-2.2550	0.0340	$> 1000.$	$> 1000.$
24	26.3645	-1.5405	-4.6280	0.0612	$> 1000.$	$> 1000.$
120	29.9676	-70.7631	-207.5482	2.5918	∞	∞
∞	29.9734	-82.5259	-242.0447	3.0225	∞	∞
Time	Case 2					
(hours)	θ_0	θ_{den}	θ_{thk}	θ_{con}	$\sum \theta_i$	$\sum \lvert\theta_i\rvert$
1	21.4323	-0.4584	-2.0857	0.0487	$> 1000.$	$> 1000.$
2	25.1049	-1.6110	-7.4349	0.1758	∞	∞
6	29.5986	-10.6565	-49.2962	1.1679	∞	∞
12	29.9906	-125.2615	-579.4664	13.7286	∞	∞
24	30.0000	$< -1000.$	$< -1000.$	995.1362	∞	∞
∞	30.0000	$< -1000.$	$< -1000.$	$< -1000.$	∞	∞
Time	Case 3					
(hours)	θ_0	θ_{den}	θ_{thk}	θ_{con}	$\sum \theta_i$	$\sum \lvert\theta_i\rvert$
1	27.6470	∞	∞	∞	∞	∞
2	29.9723	∞	∞	∞	∞	∞
6	30.0000	∞	∞	∞	∞	∞
12	30.0000	∞	∞	∞	∞	∞
∞	30.0000	∞	∞	∞	∞	∞

Table C.37: Uncertainties: density 10%, conductivity 5%.

Time	Case 1				
(hours)	θ_0	θ_{den}	θ_{con}	$\sum \theta_i$	$\sum \lvert\theta_i\rvert$
1	20.0172	-0.0043	0.0013	-0.0001	0.0091
2	20.1009	-0.0235	0.0073	0.0050	0.0556
6	21.2866	-0.2140	0.0585	0.6147	1.1002
12	23.4442	-0.3916	0.0898	9.9000	11.3383
24	26.3645	-0.4738	0.0933	785.6683	836.5917
120	29.9676	-0.0360	0.0062	$> 1000.$	$> 1000.$
∞	29.9734	-0.0313	0.0054	$> 1000.$	$> 1000.$
Time	Case 2				
(hours)	θ_0	θ_{den}	θ_{con}	$\sum \theta_i$	$\sum \lvert\theta_i\rvert$
1	21.4323	-0.1902	0.0839	0.0631	0.4711
2	25.1049	-0.4472	0.2029	0.6950	1.6974
6	29.5986	-0.1438	0.0657	9.2259	10.4937
12	29.9906	-0.0074	0.0034	101.1050	111.7560
24	30.0000	-0.0000	0.0000	$> 1000.$	$> 1000.$
∞	30.0000	0.0000	0.0000	$> 1000.$	$> 1000.$
Time	Case 3				
(hours)	θ_0	θ_{den}	θ_{con}	$\sum \theta_i$	$\sum \lvert\theta_i\rvert$
1	27.6470	-0.2347	0.0147	$> 1000.$	$> 1000.$
2	29.9723	-0.0176	0.0008	$> 1000.$	$> 1000.$
6	30.0000	0.0000	0.0000	∞	∞
12	30.0000	0.0000	0.0000	∞	∞
∞	30.0000	0.0000	0.0000	∞	∞

Table C.38: Uncertainties: density 10%, thickness 1%, conductivity 5%.

Time	Case 1					
(hours)	θ_0	θ_{den}	θ_{thk}	θ_{con}	$\sum \theta_i$	$\sum \lvert\theta_i\rvert$
1	20.0172	-0.0043	-0.0014	0.0013	0.0003	0.0141
2	20.1009	-0.0236	-0.0076	0.0073	0.0115	0.0870
6	21.2866	-0.2156	-0.0667	0.0589	1.1538	1.9540
12	23.4442	-0.3972	-0.1158	0.0908	23.5887	28.2090
24	26.3645	-0.4871	-0.1357	0.0956	$> 1000.$	$> 1000.$
120	29.9676	-0.0421	-0.0113	0.0072	$> 1000.$	$> 1000.$
∞	29.9734	-0.0368	-0.0099	0.0063	$> 1000.$	$> 1000.$
Time	Case 2					
(hours)	θ_0	θ_{den}	θ_{thk}	θ_{con}	$\sum \theta_i$	$\sum \lvert\theta_i\rvert$
1	21.4323	-0.1918	-0.0723	0.0847	0.4322	1.2428
2	25.1049	-0.4524	-0.1728	0.2055	4.8864	8.1239
6	29.5986	-0.1488	-0.0570	0.0681	$> 1000.$	$> 1000.$
12	29.9906	-0.0079	-0.0030	0.0036	$> 1000.$	$> 1000.$
24	30.0000	-0.0000	-0.0000	0.0000	$> 1000.$	$> 1000.$
∞	30.0000	0.0000	0.0000	0.0000	$> 1000.$	$> 1000.$
Time	Case 3					
(hours)	θ_0	θ_{den}	θ_{thk}	θ_{con}	$\sum \theta_i$	$\sum \lvert\theta_i\rvert$
1	27.6470	-0.2648	-0.0594	0.0160	∞	∞
2	29.9723	-0.0248	-0.0054	0.0011	∞	∞
6	30.0000	0.0000	0.0000	0.0000	∞	∞
12	30.0000	0.0000	0.0000	0.0000	∞	∞
∞	30.0000	0.0000	0.0000	0.0000	∞	∞

Table C.39: Uncertainties: density 10%, thickness 5%, conductivity 5%.

Time	Case 1					
(hours)	θ_0	θ_{den}	θ_{thk}	θ_{con}	$\sum \theta_i$	$\sum \lvert\theta_i\rvert$
1	20.0172	-0.0045	-0.0075	0.0015	0.0178	0.0798
2	20.1009	-0.0247	-0.0414	0.0079	0.2053	0.5649
6	21.2866	-0.2312	-0.3672	0.0646	26.2146	39.3717
12	23.4442	-0.4490	-0.6676	0.1035	$> 1000.$	$> 1000.$
24	26.3645	-0.6189	-0.8751	0.1208	$> 1000.$	$> 1000.$
120	29.9676	-0.1788	-0.2439	0.0306	∞	∞
∞	29.9734	-0.1657	-0.2260	0.0283	∞	∞
Time	Case 2					
(hours)	θ_0	θ_{den}	θ_{thk}	θ_{con}	$\sum \theta_i$	$\sum \lvert\theta_i\rvert$
1	21.4323	-0.2180	-0.4272	0.1001	$> 1000.$	$> 1000.$
2	25.1049	-0.5383	-1.0698	0.2543	$> 1000.$	$> 1000.$
6	29.5986	-0.2461	-0.4907	0.1171	∞	∞
12	29.9906	-0.0232	-0.0463	0.0111	∞	∞
24	30.0000	-0.0002	-0.0003	0.0001	∞	∞
∞	30.0000	0.0000	0.0000	0.0000	∞	∞
Time	Case 3					
(hours)	θ_0	θ_{den}	θ_{thk}	θ_{con}	$\sum \theta_i$	$\sum \lvert\theta_i\rvert$
1	27.6470	$< -1000.$	$< -1000.$	56.3538	∞	∞
2	29.9723	$< -1000.$	$< -1000.$	$< -1000.$	∞	∞
6	30.0000	$< -1000.$	$< -1000.$	$< -1000.$	∞	∞
12	30.0000	$< -1000.$	$< -1000.$	$< -1000.$	∞	∞
∞	30.0000	$< -1000.$	$< -1000.$	$< -1000.$	∞	∞

Table C.40: Uncertainties: density 10%, thickness 10%, conductivity 5%.

Time	Case 1					
(hours)	θ_0	θ_{den}	θ_{thk}	θ_{con}	$\sum \theta_i$	$\sum \lvert\theta_i\rvert$
1	20.0172	-0.0055	-0.0208	0.0020	0.3519	1.1248
2	20.1009	-0.0302	-0.1140	0.0110	6.1248	14.1610
6	21.2866	-0.3104	-1.0851	0.0945	$> 1000.$	$> 1000.$
12	23.4442	-0.7624	-2.4241	0.1801	$> 1000.$	$> 1000.$
24	26.3645	-1.8408	-5.4894	0.3566	$> 1000.$	$> 1000.$
120	29.9676	-234.2539	-684.0790	42.2521	∞	∞
∞	29.9734	-285.4333	-833.5333	51.4827	∞	∞
Time	Case 2					
(hours)	θ_0	θ_{den}	θ_{thk}	θ_{con}	$\sum \theta_i$	$\sum \lvert\theta_i\rvert$
1	21.4323	-0.5022	-2.2802	0.2660	$> 1000.$	$> 1000.$
2	25.1049	-1.8819	-8.6641	1.0223	∞	∞
6	29.5986	-19.5083	-89.9979	10.6370	∞	∞
12	29.9906	-478.3202	$< -1000.$	260.8132	∞	∞
24	30.0000	$< -1000.$	$< -1000.$	$> 1000.$	∞	∞
∞	30.0000	$< -1000.$	$< -1000.$	$< -1000.$	∞	∞
Time	Case 3					
(hours)	θ_0	θ_{den}	θ_{thk}	θ_{con}	$\sum \theta_i$	$\sum \lvert\theta_i\rvert$
1	27.6470	∞	∞	∞	∞	∞
2	29.9723	∞	∞	∞	∞	∞
6	30.0000	∞	∞	∞	∞	∞
12	30.0000	∞	∞	∞	∞	∞
∞	30.0000	∞	∞	∞	∞	∞

Table C.41: Uncertainties: density 10%, conductivity 10%.

Time	Case 1				
(hours)	θ_0	θ_{den}	θ_{con}	$\sum \theta_i$	$\sum \lvert\theta_i\rvert$
1	20.0172	-0.0043	0.0027	0.0019	0.0121
2	20.1009	-0.0236	0.0146	0.0188	0.0749
6	21.2866	-0.2154	0.1175	1.0611	1.6542
12	23.4442	-0.3966	0.1812	19.6968	22.9230
24	26.3645	-0.4859	0.1905	$> 1000.$	$> 1000.$
120	29.9676	-0.0416	0.0142	$> 1000.$	$> 1000.$
∞	29.9734	-0.0363	0.0124	$> 1000.$	$> 1000.$
Time	Case 2				
(hours)	θ_0	θ_{den}	θ_{con}	$\sum \theta_i$	$\sum \lvert\theta_i\rvert$
1	21.4323	-0.1910	0.1684	0.2668	0.7296
2	25.1049	-0.4500	0.4082	1.8146	3.0857
6	29.5986	-0.1467	0.1340	48.2733	57.5410
12	29.9906	-0.0077	0.0071	$> 1000.$	$> 1000.$
24	30.0000	-0.0000	0.0000	$> 1000.$	$> 1000.$
∞	30.0000	0.0000	0.0000	$> 1000.$	$> 1000.$
Time	Case 3				
(hours)	θ_0	θ_{den}	θ_{con}	$\sum \theta_i$	$\sum \lvert\theta_i\rvert$
1	27.6470	-0.2632	0.0318	∞	∞
2	29.9723	-0.0244	0.0022	∞	∞
6	30.0000	0.0000	-0.0000	∞	∞
12	30.0000	0.0000	-0.0000	∞	∞
∞	30.0000	0.0000	0.0000	∞	∞

Table C.42: Uncertainties: density 10%, thickness 1%, conductivity 10%.

Time	Case 1					
(hours)	θ_0	θ_{den}	θ_{thk}	θ_{con}	$\sum \theta_i$	$\sum \lvert\theta_i\rvert$
1	20.0172	-0.0043	-0.0014	0.0027	0.0027	0.0184
2	20.1009	-0.0237	-0.0077	0.0147	0.0297	0.1152
6	21.2866	-0.2174	-0.0672	0.1185	1.9217	2.9735
12	23.4442	-0.4035	-0.1175	0.1837	49.3508	60.6677
24	26.3645	-0.5028	-0.1398	0.1960	$> 1000.$	$> 1000.$
120	29.9676	-0.0507	-0.0136	0.0172	$> 1000.$	$> 1000.$
∞	29.9734	-0.0446	-0.0120	0.0151	$> 1000.$	$> 1000.$
Time	Case 2					
(hours)	θ_0	θ_{den}	θ_{thk}	θ_{con}	$\sum \theta_i$	$\sum \lvert\theta_i\rvert$
1	21.4323	-0.1931	-0.0728	0.1704	0.9516	2.0191
2	25.1049	-0.4567	-0.1744	0.4148	11.2567	17.3820
6	29.5986	-0.1532	-0.0587	0.1402	$> 1000.$	$> 1000.$
12	29.9906	-0.0084	-0.0032	0.0077	$> 1000.$	$> 1000.$
24	30.0000	-0.0000	-0.0000	0.0000	$> 1000.$	$> 1000.$
∞	30.0000	0.0000	0.0000	0.0000	$> 1000.$	$> 1000.$
Time	Case 3					
(hours)	θ_0	θ_{den}	θ_{thk}	θ_{con}	$\sum \theta_i$	$\sum \lvert\theta_i\rvert$
1	27.6470	-0.3353	-0.0747	0.0381	∞	∞
2	29.9723	-0.0499	-0.0109	0.0044	∞	∞
6	30.0000	-0.0000	-0.0000	0.0000	∞	∞
12	30.0000	0.0000	0.0000	0.0000	∞	∞
∞	30.0000	0.0000	0.0000	0.0000	∞	∞

Table C.43: Uncertainties: density 10%, thickness 5%, conductivity 10%.

Time	Case 1					
(hours)	θ_0	θ_{den}	θ_{thk}	θ_{con}	$\sum \theta_i$	$\sum \lvert\theta_i\rvert$
1	20.0172	-0.0045	-0.0076	0.0029	0.0255	0.1006
2	20.1009	-0.0250	-0.0417	0.0159	0.2869	0.7369
6	21.2866	-0.2355	-0.3733	0.1309	43.1817	66.3765
12	23.4442	-0.4653	-0.6896	0.2123	$> 1000.$	$> 1000.$
24	26.3645	-0.6665	-0.9387	0.2566	$> 1000.$	$> 1000.$
120	29.9676	-0.2931	-0.3989	0.0993	∞	∞
∞	29.9734	-0.2772	-0.3772	0.0939	∞	∞
Time	Case 2					
(hours)	θ_0	θ_{den}	θ_{thk}	θ_{con}	$\sum \theta_i$	$\sum \lvert\theta_i\rvert$
1	21.4323	-0.2231	-0.4370	0.2046	$> 1000.$	$> 1000.$
2	25.1049	-0.5573	-1.1068	0.5258	$> 1000.$	$> 1000.$
6	29.5986	-0.2763	-0.5506	0.2625	∞	∞
12	29.9906	-0.0303	-0.0604	0.0288	∞	∞
24	30.0000	-0.0003	-0.0006	0.0003	∞	∞
∞	30.0000	0.0000	0.0000	0.0000	∞	∞
Time	Case 3					
(hours)	θ_0	θ_{den}	θ_{thk}	θ_{con}	$\sum \theta_i$	$\sum \lvert\theta_i\rvert$
1	27.6470	$< -1000.$	$< -1000.$	$< -1000.$	∞	∞
2	29.9723	$< -1000.$	$< -1000.$	$< -1000.$	∞	∞
6	30.0000	∞	∞	∞	∞	∞
12	30.0000	∞	∞	∞	∞	∞
∞	30.0000	∞	∞	∞	∞	∞

Table C.44: Uncertainties: density 10%, thickness 10%, conductivity 10%.

Time	Case 1					
(hours)	θ_0	θ_{den}	θ_{thk}	θ_{con}	$\sum \theta_i$	$\sum \lvert\theta_i\rvert$
1	20.0172	-0.0056	-0.0213	0.0041	0.4900	1.5551
2	20.1009	-0.0311	-0.1169	0.0224	9.3625	22.1748
6	21.2866	-0.3277	-1.1375	0.1960	$> 1000.$	$> 1000.$
12	23.4442	-0.8508	-2.6781	0.3903	$> 1000.$	$> 1000.$
24	26.3645	-2.3562	-6.9613	0.8847	$> 1000.$	$> 1000.$
120	29.9676	$< -1000.$	$< -1000.$	423.7654	∞	∞
∞	29.9734	$< -1000.$	$< -1000.$	547.7548	∞	∞
Time	Case 2					
(hours)	θ_0	θ_{den}	θ_{thk}	θ_{con}	$\sum \theta_i$	$\sum \lvert\theta_i\rvert$
1	21.4323	-0.5724	-2.5921	0.6033	$> 1000.$	$> 1000.$
2	25.1049	-2.3644	-10.8479	2.5526	∞	∞
6	29.5986	-47.2850	-217.3026	51.2034	∞	∞
12	29.9906	$< -1000.$	$< -1000.$	$> 1000.$	∞	∞
24	30.0000	$< -1000.$	$< -1000.$	$< -1000.$	∞	∞
∞	30.0000	$< -1000.$	$< -1000.$	$< -1000.$	∞	∞
Time	Case 3					
(hours)	θ_0	θ_{den}	θ_{thk}	θ_{con}	$\sum \theta_i$	$\sum \lvert\theta_i\rvert$
1	27.6470	∞	∞	∞	∞	∞
2	29.9723	∞	∞	∞	∞	∞
6	30.0000	∞	∞	∞	∞	∞
12	30.0000	∞	∞	∞	∞	∞
∞	30.0000	∞	∞	∞	∞	∞

Table C.45: Uncertainties: density 10%.

Time	Case 1			
(hours)	θ_0	θ_{den}	$\sum \theta_i$	$\sum \lvert\theta_i\rvert$
1	20.0172	-0.0042	-0.0021	0.0064
2	20.1009	-0.0234	-0.0078	0.0390
6	21.2866	-0.2127	0.2788	0.7042
12	23.4442	-0.3872	4.7348	5.5092
24	26.3645	-0.4631	207.7717	208.6980
120	29.9676	-0.0317	$> 1000.$	$> 1000.$
∞	29.9734	-0.0274	$> 1000.$	$> 1000.$

Time	Case 2			
(hours)	θ_0	θ_{den}	$\sum \theta_i$	$\sum \lvert\theta_i\rvert$
1	21.4323	-0.1896	-0.1012	0.2779
2	25.1049	-0.4449	-0.0235	0.8664
6	29.5986	-0.1416	1.6384	1.9216
12	29.9906	-0.0072	3.4821	3.4964
24	30.0000	-0.0000	10.1916	10.1916
∞	30.0000	0.0000	82.8140	82.8140

Time	Case 3			
(hours)	θ_0	θ_{den}	$\sum \theta_i$	$\sum \lvert\theta_i\rvert$
1	27.6470	-0.2234	0.5803	1.0271
2	29.9723	-0.0154	1.9253	1.9562
6	30.0000	0.0000	7.2806	7.2807
12	30.0000	0.0000	23.2087	23.2087
∞	30.0000	0.0000	33.0713	33.0713

Table C.46: Uncertainties: density 10%, thickness 1%.

Time	Case 1				
(hours)	θ_0	θ_{den}	θ_{thk}	$\sum \theta_i$	$\sum \lvert\theta_i\rvert$
1	20.0172	-0.0043	-0.0014	-0.0021	0.0103
2	20.1009	-0.0235	-0.0076	-0.0052	0.0630
6	21.2866	-0.2140	-0.0663	0.5996	1.2524
12	23.4442	-0.3916	-0.1144	10.9830	13.0103
24	26.3645	-0.4735	-0.1322	891.2002	969.9600
120	29.9676	-0.0358	-0.0096	$> 1000.$	$> 1000.$
∞	29.9734	-0.0311	-0.0084	$> 1000.$	$> 1000.$

Time	Case 2				
(hours)	θ_0	θ_{den}	θ_{thk}	$\sum \theta_i$	$\sum \lvert\theta_i\rvert$
1	21.4323	-0.1908	-0.0719	0.0713	0.7318
2	25.1049	-0.4490	-0.1715	1.7578	3.7705
6	29.5986	-0.1452	-0.0557	191.1622	250.3090
12	29.9906	-0.0076	-0.0029	$> 1000.$	$> 1000.$
24	30.0000	-0.0000	-0.0000	$> 1000.$	$> 1000.$
∞	30.0000	0.0000	0.0000	$> 1000.$	$> 1000.$

Time	Case 3				
(hours)	θ_0	θ_{den}	θ_{thk}	$\sum \theta_i$	$\sum \lvert\theta_i\rvert$
1	27.6470	-0.2333	-0.0525	$> 1000.$	$> 1000.$
2	29.9723	-0.0173	-0.0038	$> 1000.$	$> 1000.$
6	30.0000	0.0000	0.0000	∞	∞
12	30.0000	0.0000	0.0000	∞	∞
∞	30.0000	0.0000	0.0000	∞	∞

Table C.47: Uncertainties: density 10%, thickness 5%.

Time	Case 1				
(hours)	θ_0	θ_{den}	θ_{thk}	$\sum \theta_i$	$\sum \lvert\theta_i\rvert$
1	20.0172	-0.0044	-0.0075	0.0109	0.0623
2	20.1009	-0.0245	-0.0410	0.1376	0.4284
6	21.2866	-0.2273	-0.3617	15.8885	23.5551
12	23.4442	-0.4347	-0.6483	$> 1000.$	$> 1000.$
24	26.3645	-0.5791	-0.8218	$> 1000.$	$> 1000.$
120	29.9676	-0.1160	-0.1587	∞	∞
∞	29.9734	-0.1056	-0.1444	∞	∞
Time	Case 2				
(hours)	θ_0	θ_{den}	θ_{thk}	$\sum \theta_i$	$\sum \lvert\theta_i\rvert$
1	21.4323	-0.2135	-0.4187	$> 1000.$	$> 1000.$
2	25.1049	-0.5222	-1.0383	$> 1000.$	$> 1000.$
6	29.5986	-0.2227	-0.4443	∞	∞
12	29.9906	-0.0185	-0.0369	∞	∞
24	30.0000	-0.0001	-0.0002	∞	∞
∞	30.0000	0.0000	0.0000	∞	∞
Time	Case 3				
(hours)	θ_0	θ_{den}	θ_{thk}	$\sum \theta_i$	$\sum \lvert\theta_i\rvert$
1	27.6470	-6.3723	-7.0089	∞	∞
2	29.9723	-170.6324	-187.4029	∞	∞
6	30.0000	$< -1000.$	$< -1000.$	∞	∞
12	30.0000	$< -1000.$	$< -1000.$	∞	∞
∞	30.0000	$< -1000.$	$< -1000.$	∞	∞

Table C.48: Uncertainties: density 10%, thickness 10%.

Time	Case 1				
(hours)	θ_0	θ_{den}	θ_{thk}	$\sum \theta_i$	$\sum \lvert\theta_i\rvert$
1	20.0172	-0.0053	-0.0204	0.2547	0.8256
2	20.1009	-0.0295	-0.1115	4.1223	9.3706
6	21.2866	-0.2954	-1.0397	$> 1000.$	$> 1000.$
12	23.4442	-0.6905	-2.2168	$> 1000.$	$> 1000.$
24	26.3645	-1.4771	-4.4459	$> 1000.$	$> 1000.$
120	29.9676	-53.2443	-156.3341	∞	∞
∞	29.9734	-61.4465	-180.4140	∞	∞
Time	Case 2				
(hours)	θ_0	θ_{den}	θ_{thk}	$\sum \theta_i$	$\sum \lvert\theta_i\rvert$
1	21.4323	-0.4488	-2.0431	$> 1000.$	$> 1000.$
2	25.1049	-1.5546	-7.1785	∞	∞
6	29.5986	-9.2773	-42.9434	∞	∞
12	29.9906	-91.9198	-425.4991	∞	∞
24	30.0000	$< -1000.$	$< -1000.$	∞	∞
∞	30.0000	$< -1000.$	$< -1000.$	∞	∞
Time	Case 3				
(hours)	θ_0	θ_{den}	θ_{thk}	$\sum \theta_i$	$\sum \lvert\theta_i\rvert$
1	27.6470	∞	∞	∞	∞
2	29.9723	∞	∞	∞	∞
6	30.0000	∞	∞	∞	∞
12	30.0000	∞	∞	∞	∞
∞	30.0000	∞	∞	∞	∞

Table C.49: Uncertainties: conductivity 1%.

Time	Case 1			
(hours)	θ_0	θ_{con}	$\sum \theta_i$	$\sum \lvert\theta_i\rvert$
1	20.0172	0.0003	0.0003	0.0003
2	20.1009	0.0014	0.0014	0.0015
6	21.2866	0.0114	0.0117	0.0118
12	23.4442	0.0172	0.0180	0.0184
24	26.3645	0.0170	0.0187	0.0195
120	29.9676	0.0007	0.0013	0.0015
∞	29.9734	0.0006	0.0011	0.0013
Time	Case 2			
(hours)	θ_0	θ_{con}	$\sum \theta_i$	$\sum \lvert\theta_i\rvert$
1	21.4323	0.0166	0.0169	0.0171
2	25.1049	0.0401	0.0415	0.0421
6	29.5986	0.0126	0.0144	0.0150
12	29.9906	0.0006	0.0008	0.0009
24	30.0000	0.0000	0.0000	0.0000
∞	30.0000	0.0000	0.0000	0.0000
Time	Case 3			
(hours)	θ_0	θ_{con}	$\sum \theta_i$	$\sum \lvert\theta_i\rvert$
1	27.6470	0.0028	0.0060	0.0077
2	29.9723	0.0001	0.0046	0.0068
6	30.0000	0.0000	0.0023	0.0034
12	30.0000	0.0000	0.0006	0.0010
∞	30.0000	0.0000	0.0004	0.0007

Table C.50: Uncertainties: thickness 1%, conductivity 1%.

Time	Case 1				
(hours)	θ_0	θ_{thk}	θ_{con}	$\sum \theta_i$	$\sum \lvert\theta_i\rvert$
1	20.0172	-0.0014	0.0003	-0.0008	0.0022
2	20.1009	-0.0075	0.0014	-0.0043	0.0120
6	21.2866	-0.0644	0.0115	-0.0271	0.1126
12	23.4442	-0.1083	0.0172	-0.0085	0.2409
24	26.3645	-0.1183	0.0170	0.1679	0.5068
120	29.9676	-0.0052	0.0007	556.4725	674.6095
∞	29.9734	-0.0044	0.0006	784.1979	950.5992
Time	Case 2				
(hours)	θ_0	θ_{thk}	θ_{con}	$\sum \theta_i$	$\sum \lvert\theta_i\rvert$
1	21.4323	-0.0713	0.0167	-0.0049	0.1726
2	25.1049	-0.1693	0.0403	0.1262	0.6067
6	29.5986	-0.0535	0.0128	2.3133	3.6344
12	29.9906	-0.0027	0.0006	35.3982	53.6744
24	30.0000	-0.0000	0.0000	$> 1000.$	$> 1000.$
∞	30.0000	0.0000	0.0000	$> 1000.$	$> 1000.$
Time	Case 3				
(hours)	θ_0	θ_{thk}	θ_{con}	$\sum \theta_i$	$\sum \lvert\theta_i\rvert$
1	27.6470	-0.0521	0.0029	$> 1000.$	$> 1000.$
2	29.9723	-0.0037	0.0002	$> 1000.$	$> 1000.$
6	30.0000	0.0000	0.0000	∞	∞
12	30.0000	0.0000	0.0000	∞	∞
∞	30.0000	0.0000	0.0000	∞	∞

Table C.51: Uncertainties: thickness 5%, conductivity 1%.

Time	Case 1				
(hours)	θ_0	θ_{thk}	θ_{con}	$\sum \theta_i$	$\sum \lvert\theta_i\rvert$
1	20.0172	-0.0073	0.0003	0.0021	0.0313
2	20.1009	-0.0397	0.0015	0.0360	0.1913
6	21.2866	-0.3413	0.0122	2.7040	4.7796
12	23.4442	-0.5795	0.0185	84.2380	113.1334
24	26.3645	-0.6497	0.0188	$> 1000.$	$> 1000.$
120	29.9676	-0.0365	0.0010	$> 1000.$	$> 1000.$
∞	29.9734	-0.0313	0.0008	$> 1000.$	$> 1000.$
Time	Case 2				
(hours)	θ_0	θ_{thk}	θ_{con}	$\sum \theta_i$	$\sum \lvert\theta_i\rvert$
1	21.4323	-0.4049	0.0190	$> 1000.$	$> 1000.$
2	25.1049	-0.9882	0.0470	$> 1000.$	$> 1000.$
6	29.5986	-0.3789	0.0181	∞	∞
12	29.9906	-0.0259	0.0012	∞	∞
24	30.0000	-0.0001	0.0000	∞	∞
∞	30.0000	0.0000	0.0000	∞	∞
Time	Case 3				
(hours)	θ_0	θ_{thk}	θ_{con}	$\sum \theta_i$	$\sum \lvert\theta_i\rvert$
1	27.6470	-6.3791	0.0505	∞	∞
2	29.9723	-148.4900	1.1543	∞	∞
6	30.0000	$< -1000.$	$> 1000.$	∞	∞
12	30.0000	$< -1000.$	$< -1000.$	∞	∞
∞	30.0000	$< -1000.$	$< -1000.$	∞	∞

Table C.52: Uncertainties: thickness 10%, conductivity 1%.

Time	Case 1				
(hours)	θ_0	θ_{thk}	θ_{con}	$\sum \theta_i$	$\sum \lvert\theta_i\rvert$
1	20.0172	-0.0192	0.0004	0.1257	0.4737
2	20.1009	-0.1038	0.0020	1.8497	4.4781
6	21.2866	-0.9103	0.0165	$> 1000.$	$> 1000.$
12	23.4442	-1.6921	0.0271	$> 1000.$	$> 1000.$
24	26.3645	-2.3983	0.0342	$> 1000.$	$> 1000.$
120	29.9676	-1.7776	0.0231	∞	∞
∞	29.9734	-1.7128	0.0221	∞	∞
Time	Case 2				
(hours)	θ_0	θ_{thk}	θ_{con}	$\sum \theta_i$	$\sum \lvert\theta_i\rvert$
1	21.4323	-1.7999	0.0422	$> 1000.$	$> 1000.$
2	25.1049	-5.8085	0.1378	∞	∞
6	29.5986	-18.7360	0.4455	∞	∞
12	29.9906	-65.0597	1.5472	∞	∞
24	30.0000	-571.1641	13.5828	∞	∞
∞	30.0000	$< -1000.$	649.3210	∞	∞
Time	Case 3				
(hours)	θ_0	θ_{thk}	θ_{con}	$\sum \theta_i$	$\sum \lvert\theta_i\rvert$
1	27.6470	∞	∞	∞	∞
2	29.9723	∞	∞	∞	∞
6	30.0000	∞	∞	∞	∞
12	30.0000	∞	∞	∞	∞
∞	30.0000	∞	∞	∞	∞

Table C.53: Uncertainties: conductivity 5%.

Time	Case 1			
(hours)	θ_0	θ_{con}	$\sum \theta_i$	$\sum \lvert\theta_i\rvert$
1	20.0172	0.0013	0.0013	0.0014
2	20.1009	0.0072	0.0074	0.0078
6	21.2866	0.0572	0.0639	0.0679
12	23.4442	0.0860	0.1116	0.1245
24	26.3645	0.0849	0.1547	0.1883
120	29.9676	0.0034	0.5485	0.8166
∞	29.9734	0.0029	0.5796	0.8633
Time	Case 2			
(hours)	θ_0	θ_{con}	$\sum \theta_i$	$\sum \lvert\theta_i\rvert$
1	21.4323	0.0832	0.0907	0.0965
2	25.1049	0.2006	0.2393	0.2572
6	29.5986	0.0634	0.1360	0.1638
12	29.9906	0.0031	0.0220	0.0291
24	30.0000	0.0000	0.0006	0.0009
∞	30.0000	0.0000	0.0000	0.0000
Time	Case 3			
(hours)	θ_0	θ_{con}	$\sum \theta_i$	$\sum \lvert\theta_i\rvert$
1	27.6470	0.0144	$> 1000.$	$> 1000.$
2	29.9723	0.0008	$> 1000.$	$> 1000.$
6	30.0000	0.0000	∞	∞
12	30.0000	0.0000	∞	∞
∞	30.0000	0.0000	∞	∞

Table C.54: Uncertainties: thickness 1%, conductivity 5%.

Time	Case 1				
(hours)	θ_0	θ_{thk}	θ_{con}	$\sum \theta_i$	$\sum \lvert\theta_i\rvert$
1	20.0172	-0.0014	0.0013	0.0005	0.0038
2	20.1009	-0.0075	0.0072	0.0032	0.0213
6	21.2866	-0.0645	0.0574	0.0551	0.2131
12	23.4442	-0.1085	0.0863	0.2189	0.5438
24	26.3645	-0.1186	0.0853	1.0716	1.8002
120	29.9676	-0.0053	0.0034	$> 1000.$	$> 1000.$
∞	29.9734	-0.0045	0.0029	$> 1000.$	$> 1000.$
Time	Case 2				
(hours)	θ_0	θ_{thk}	θ_{con}	$\sum \theta_i$	$\sum \lvert\theta_i\rvert$
1	21.4323	-0.0714	0.0837	0.1291	0.3559
2	25.1049	-0.1697	0.2019	0.7180	1.4438
6	29.5986	-0.0538	0.0643	13.9417	21.4301
12	29.9906	-0.0027	0.0032	718.2672	$> 1000.$
24	30.0000	-0.0000	0.0000	$> 1000.$	$> 1000.$
∞	30.0000	0.0000	0.0000	$> 1000.$	$> 1000.$
Time	Case 3				
(hours)	θ_0	θ_{thk}	θ_{con}	$\sum \theta_i$	$\sum \lvert\theta_i\rvert$
1	27.6470	-0.0565	0.0154	∞	∞
2	29.9723	-0.0047	0.0010	∞	∞
6	30.0000	0.0000	0.0000	∞	∞
12	30.0000	0.0000	0.0000	∞	∞
∞	30.0000	0.0000	0.0000	∞	∞

Table C.55: Uncertainties: thickness 5%, conductivity 5%.

Time	Case 1				
(hours)	θ_0	θ_{thk}	θ_{con}	$\sum \theta_i$	$\sum \lvert\theta_i\rvert$
1	20.0172	-0.0073	0.0014	0.0054	0.0394
2	20.1009	-0.0398	0.0077	0.0632	0.2459
6	21.2866	-0.3431	0.0613	4.2447	7.1908
12	23.4442	-0.5854	0.0934	163.1586	226.3923
24	26.3645	-0.6634	0.0955	$> 1000.$	$> 1000.$
120	29.9676	-0.0411	0.0054	$> 1000.$	$> 1000.$
∞	29.9734	-0.0354	0.0046	$> 1000.$	$> 1000.$
Time	Case 2				
(hours)	θ_0	θ_{thk}	θ_{con}	$\sum \theta_i$	$\sum \lvert\theta_i\rvert$
1	21.4323	-0.4098	0.0961	$> 1000.$	$> 1000.$
2	25.1049	-1.0058	0.2393	$> 1000.$	$> 1000.$
6	29.5986	-0.4008	0.0957	∞	∞
12	29.9906	-0.0293	0.0070	∞	∞
24	30.0000	-0.0001	0.0000	∞	∞
∞	30.0000	0.0000	0.0000	∞	∞
Time	Case 3				
(hours)	θ_0	θ_{thk}	θ_{con}	$\sum \theta_i$	$\sum \lvert\theta_i\rvert$
1	27.6470	-281.9321	10.0927	∞	∞
2	29.9723	$< -1000.$	$> 1000.$	∞	∞
6	30.0000	$< -1000.$	$< -1000.$	∞	∞
12	30.0000	$< -1000.$	$< -1000.$	∞	∞
∞	30.0000	$< -1000.$	$< -1000.$	∞	∞

Table C.56: Uncertainties: thickness 10%, conductivity 5%.

Time	Case 1				
(hours)	θ_0	θ_{thk}	θ_{con}	$\sum \theta_i$	$\sum \lvert\theta_i\rvert$
1	20.0172	-0.0194	0.0019	0.1636	0.5986
2	20.1009	-0.1051	0.0103	2.4863	6.0265
6	21.2866	-0.9307	0.0839	$> 1000.$	$> 1000.$
12	23.4442	-1.7686	0.1402	$> 1000.$	$> 1000.$
24	26.3645	-2.6466	0.1865	$> 1000.$	$> 1000.$
120	29.9676	-3.6693	0.2376	∞	∞
∞	29.9734	-3.6553	0.2361	∞	∞
Time	Case 2				
(hours)	θ_0	θ_{thk}	θ_{con}	$\sum \theta_i$	$\sum \lvert\theta_i\rvert$
1	21.4323	-1.9322	0.2261	$> 1000.$	$> 1000.$
2	25.1049	-6.5347	0.7739	∞	∞
6	29.5986	-29.6916	3.5239	∞	∞
12	29.9906	-185.3827	22.0030	∞	∞
24	30.0000	$< -1000.$	537.5000	∞	∞
∞	30.0000	$< -1000.$	$> 1000.$	∞	∞
Time	Case 3				
(hours)	θ_0	θ_{thk}	θ_{con}	$\sum \theta_i$	$\sum \lvert\theta_i\rvert$
1	27.6470	∞	∞	∞	∞
2	29.9723	∞	∞	∞	∞
6	30.0000	∞	∞	∞	∞
12	30.0000	∞	∞	∞	∞
∞	30.0000	∞	∞	∞	∞

Table C.57: Uncertainties: conductivity 10%.

Time	Case 1			
(hours)	θ_0	θ_{con}	$\sum \theta_i$	$\sum \lvert\theta_i\rvert$
1	20.0172	0.0026	0.0027	0.0031
2	20.1009	0.0144	0.0153	0.0169
6	21.2866	0.1145	0.1443	0.1627
12	23.4442	0.1722	0.3073	0.3783
24	26.3645	0.1702	0.7372	1.0273
120	29.9676	0.0069	$> 1000.$	$> 1000.$
∞	29.9734	0.0058	$> 1000.$	$> 1000.$
Time	Case 2			
(hours)	θ_0	θ_{con}	$\sum \theta_i$	$\sum \lvert\theta_i\rvert$
1	21.4323	0.1667	0.1992	0.2251
2	25.1049	0.4019	0.5846	0.6747
6	29.5986	0.1275	0.7716	1.0419
12	29.9906	0.0064	0.7110	1.0044
24	30.0000	0.0000	0.6246	0.8848
∞	30.0000	0.0000	0.4830	0.6841
Time	Case 3			
(hours)	θ_0	θ_{con}	$\sum \theta_i$	$\sum \lvert\theta_i\rvert$
1	27.6470	0.0307	∞	∞
2	29.9723	0.0020	∞	∞
6	30.0000	-0.0000	∞	∞
12	30.0000	-0.0000	∞	∞
∞	30.0000	0.0000	∞	∞

Table C.58: Uncertainties: thickness 1%, conductivity 10%.

Time	Case 1				
(hours)	θ_0	θ_{thk}	θ_{con}	$\sum \theta_i$	$\sum \lvert\theta_i\rvert$
1	20.0172	-0.0014	0.0027	0.0021	0.0062
2	20.1009	-0.0075	0.0144	0.0133	0.0349
6	21.2866	-0.0646	0.1149	0.1875	0.3890
12	23.4442	-0.1088	0.1729	0.7511	1.3133
24	26.3645	-0.1194	0.1714	5.6850	8.7592
120	29.9676	-0.0055	0.0071	$> 1000.$	$> 1000.$
∞	29.9734	-0.0046	0.0060	$> 1000.$	$> 1000.$
Time	Case 2				
(hours)	θ_0	θ_{thk}	θ_{con}	$\sum \theta_i$	$\sum \lvert\theta_i\rvert$
1	21.4323	-0.0716	0.1678	0.3472	0.6785
2	25.1049	-0.1704	0.4054	1.9950	3.3721
6	29.5986	-0.0546	0.1303	115.1295	179.7947
12	29.9906	-0.0028	0.0066	$> 1000.$	$> 1000.$
24	30.0000	-0.0000	0.0000	$> 1000.$	$> 1000.$
∞	30.0000	0.0000	0.0000	$> 1000.$	$> 1000.$
Time	Case 3				
(hours)	θ_0	θ_{thk}	θ_{con}	$\sum \theta_i$	$\sum \lvert\theta_i\rvert$
1	27.6470	-0.0684	0.0356	∞	∞
2	29.9723	-0.0083	0.0034	∞	∞
6	30.0000	0.0000	0.0000	∞	∞
12	30.0000	0.0000	0.0000	∞	∞
∞	30.0000	0.0000	0.0000	∞	∞

Table C.59: Uncertainties: thickness 5%, conductivity 10%.

Time	Case 1				
(hours)	θ_0	θ_{thk}	θ_{con}	$\sum \theta_i$	$\sum \lvert\theta_i\rvert$
1	20.0172	-0.0073	0.0028	0.0099	0.0514
2	20.1009	-0.0400	0.0154	0.1027	0.3296
6	21.2866	-0.3458	0.1234	7.1754	11.9537
12	23.4442	-0.5943	0.1890	390.6725	567.9432
24	26.3645	-0.6843	0.1960	$> 1000.$	$> 1000.$
120	29.9676	-0.0493	0.0128	$> 1000.$	$> 1000.$
∞	29.9734	-0.0428	0.0111	$> 1000.$	$> 1000.$
Time	Case 2				
(hours)	θ_0	θ_{thk}	θ_{con}	$\sum \theta_i$	$\sum \lvert\theta_i\rvert$
1	21.4323	-0.4169	0.1954	$> 1000.$	$> 1000.$
2	25.1049	-1.0315	0.4907	$> 1000.$	$> 1000.$
6	29.5986	-0.4350	0.2077	∞	∞
12	29.9906	-0.0352	0.0168	∞	∞
24	30.0000	-0.0002	0.0001	∞	∞
∞	30.0000	0.0000	0.0000	∞	∞
Time	Case 3				
(hours)	θ_0	θ_{thk}	θ_{con}	$\sum \theta_i$	$\sum \lvert\theta_i\rvert$
1	27.6470	$< -1000.$	$< -1000.$	∞	∞
2	29.9723	$< -1000.$	$< -1000.$	∞	∞
6	30.0000	$< -1000.$	$< -1000.$	∞	∞
12	30.0000	∞	∞	∞	∞
∞	30.0000	∞	∞	∞	∞

Table C.60: Uncertainties: thickness 10%, conductivity 10%.

Time	Case 1				
(hours)	θ_0	θ_{thk}	θ_{con}	$\sum \theta_i$	$\sum \lvert\theta_i\rvert$
1	20.0172	-0.0197	0.0039	0.2256	0.8059
2	20.1009	-0.1068	0.0209	3.6275	8.8847
6	21.2866	-0.9598	0.1719	$> 1000.$	$> 1000.$
12	23.4442	-1.8815	0.2944	$> 1000.$	$> 1000.$
24	26.3645	-3.0436	0.4214	$> 1000.$	$> 1000.$
120	29.9676	-10.2216	1.3132	∞	∞
∞	29.9734	-10.6260	1.3644	∞	∞
Time	Case 2				
(hours)	θ_0	θ_{thk}	θ_{con}	$\sum \theta_i$	$\sum \lvert\theta_i\rvert$
1	21.4323	-2.1373	0.4992	$> 1000.$	$> 1000.$
2	25.1049	-7.7510	1.8318	∞	∞
6	29.5986	-58.0724	13.7496	∞	∞
12	29.9906	-835.2187	197.7559	∞	∞
24	30.0000	$< -1000.$	$> 1000.$	∞	∞
∞	30.0000	$< -1000.$	$< -1000.$	∞	∞
Time	Case 3				
(hours)	θ_0	θ_{thk}	θ_{con}	$\sum \theta_i$	$\sum \lvert\theta_i\rvert$
1	27.6470	∞	∞	∞	∞
2	29.9723	∞	∞	∞	∞
6	30.0000	∞	∞	∞	∞
12	30.0000	∞	∞	∞	∞
∞	30.0000	∞	∞	∞	∞

Table C.61: Uncertainties: thickness 1%.

Time	Case 1			
(hours)	θ_0	θ_{thk}	$\sum \theta_i$	$\sum \lvert\theta_i\rvert$
1	20.0172	-0.0014	-0.0012	0.0018
2	20.1009	-0.0075	-0.0061	0.0099
6	21.2866	-0.0644	-0.0450	0.0917
12	23.4442	-0.1083	-0.0491	0.1900
24	26.3645	-0.1182	0.0633	0.3651
120	29.9676	-0.0052	345.5625	411.8077
∞	29.9734	-0.0044	485.7220	578.8713
Time	Case 2			
(hours)	θ_0	θ_{thk}	$\sum \theta_i$	$\sum \lvert\theta_i\rvert$
1	21.4323	-0.0713	-0.0341	0.1347
2	25.1049	-0.1692	0.0156	0.4573
6	29.5986	-0.0534	1.3807	2.2257
12	29.9906	-0.0027	16.8400	25.5267
24	30.0000	-0.0000	$> 1000.$	$> 1000.$
∞	30.0000	0.0000	$> 1000.$	$> 1000.$
Time	Case 3			
(hours)	θ_0	θ_{thk}	$\sum \theta_i$	$\sum \lvert\theta_i\rvert$
1	27.6470	-0.0514	$> 1000.$	$> 1000.$
2	29.9723	-0.0036	$> 1000.$	$> 1000.$
6	30.0000	0.0000	$> 1000.$	$> 1000.$
12	30.0000	0.0000	∞	∞
∞	30.0000	0.0000	∞	∞

Table C.62: Uncertainties: thickness 5%.

Time	Case 1			
(hours)	θ_0	θ_{thk}	$\sum \theta_i$	$\sum \lvert\theta_i\rvert$
1	20.0172	-0.0073	0.0013	0.0294
2	20.1009	-0.0397	0.0297	0.1791
6	21.2866	-0.3408	2.3984	4.3120
12	23.4442	-0.5781	71.7490	95.6820
24	26.3645	-0.6466	$> 1000.$	$> 1000.$
120	29.9676	-0.0356	$> 1000.$	$> 1000.$
∞	29.9734	-0.0305	$> 1000.$	$> 1000.$
Time	Case 2			
(hours)	θ_0	θ_{thk}	$\sum \theta_i$	$\sum \lvert\theta_i\rvert$
1	21.4323	-0.4038	$> 1000.$	$> 1000.$
2	25.1049	-0.9842	$> 1000.$	$> 1000.$
6	29.5986	-0.3741	∞	∞
12	29.9906	-0.0252	∞	∞
24	30.0000	-0.0001	∞	∞
∞	30.0000	0.0000	∞	∞
Time	Case 3			
(hours)	θ_0	θ_{thk}	$\sum \theta_i$	$\sum \lvert\theta_i\rvert$
1	27.6470	-3.6464	∞	∞
2	29.9723	-36.0971	∞	∞
6	30.0000	$< -1000.$	∞	∞
12	30.0000	$< -1000.$	∞	∞
∞	30.0000	$< -1000.$	∞	∞

Table C.63: Uncertainties: thickness 10%.

Time	Case 1			
(hours)	θ_0	θ_{thk}	$\sum \theta_i$	$\sum \lvert\theta_i\rvert$
1	20.0172	-0.0191	0.1175	0.4469
2	20.1009	-0.1035	1.7183	4.1634
6	21.2866	-0.9056	$> 1000.$	$> 1000.$
12	23.4442	-1.6747	$> 1000.$	$> 1000.$
24	26.3645	-2.3441	$> 1000.$	$> 1000.$
120	29.9676	-1.5048	∞	∞
∞	29.9734	-1.4394	∞	∞

Time	Case 2			
(hours)	θ_0	θ_{thk}	$\sum \theta_i$	$\sum \lvert\theta_i\rvert$
1	21.4323	-1.7704	$> 1000.$	$> 1000.$
2	25.1049	-5.6528	∞	∞
6	29.5986	-16.8566	∞	∞
12	29.9906	-51.0671	∞	∞
24	30.0000	-352.5547	∞	∞
∞	30.0000	$< -1000.$	∞	∞

Time	Case 3			
(hours)	θ_0	θ_{thk}	$\sum \theta_i$	$\sum \lvert\theta_i\rvert$
1	27.6470	∞	∞	∞
2	29.9723	∞	∞	∞
6	30.0000	∞	∞	∞
12	30.0000	∞	∞	∞
∞	30.0000	∞	∞	∞